School of Doctoral Studies in Biological Sciences

University of South Bohemia in České Budějovice

Faculty of Science

Functional analysis of cryoprotectant system in *Chymomyza costata*
Ph.D. Thesis

Mgr. Robert Grgac

Supervisor: prof. Ing. Vladimír Košťál, CSc.

Institute of Entomology, Biology Centre CAS

České Budějovice, Czech Republic

České Budějovice 2023

Annotation

In this study, employing an integrated approach that involves transcriptomics, metabolomics, and other techniques, we aimed to understand the mechanistic roles of the cryoprotective system underlying extreme freeze tolerance in the larvae of the drosophilid fly, *Chymomyza costata*. Metabolomics unveiled the complex composition of the seasonally accumulated larval innate mixture of putative cryoprotectants. This mixture was predominantly composed of proline and trehalose, supplemented by minor components (glutamine, asparagine, betaine, sarcosine, glycerophospho-choline, and ethanolamine). We identified food ingestion as a significant source for the direct assimilation of amino compounds, while glycogen and phospholipids served as the primary internal sources for the biosynthesis of other cryoprotectants.

The utilization of MALDI-MSI to observe cryoprotectants revealed distinct behaviors of proline and trehalose during ecologically relevant, gradual inoculative extracellular freezing of larvae. Trehalose exhibited accumulation in partially dehydrated hemolymph, inducing a transition to the amorphous glass phase. On the other hand, proline migrated to the boundary between extracellular ice and dehydrated hemolymph and tissues, forming a layer of dense viscoelastic liquid.

Finally, through a combination of *in vivo* and *in vitro* assays, we found that cell membranes are likely targets of freezing injury, while their integrity is sustained by accumulated small cryoprotective molecules and proteins in cold-acclimated *C. costata* larvae. Contrary to our expectations, our assays did not provide support for the hypothesis that proteins (soluble enzymes) require *in vivo* stabilization through the accumulation of cryoprotectants.

Declaration

I hereby declare that I am the author of this dissertation and that I have used only those sources and literature detailed in the list of references.

České Budějovice, 20. 11. 2023.

Robert Grgac

Robert Grgac

This thesis originated from a partnership of Faculty of Science, University of South Bohemia, and the Institute of Entomology, Biology Centre of the ASCR, in the field of doctoral studies in Physiology and Developmental Biology.

Acknowledgements

First and foremost, my heartfelt thanks extend to every colleague, both past and present, in our laboratory. Their combined efforts have not just established a supportive work environment but have also sustained an atmosphere where warmth and camaraderie thrive.

I am also sincerely grateful to Prof. Dr. Sc. Marija Heffer and the Department of Medical Biology and Genetics for facilitating my Erasmus+ exchange program. The exposure to diverse research methodologies and perspectives at the Faculty of Medicine Osijek has not only significantly broadened my knowledge but has also forged lasting friendships and provided me with a wealth of new experiences. In addition, I extend my gratitude to Edi Rođak and the Department of Histology and Embryology for their valuable contributions to my academic and personal journey.

I am deeply grateful to my family for their unwavering support. Their steadfast belief in my academic pursuits has been a constant source of motivation.

And finally, most significantly, I want to express my heartfelt gratitude to my supervisor, Prof. Ing. Vladimír Košťál, CSc. Throughout my entire PhD journey, his unwavering support, insightful guidance, and invaluable mentorship, both in the realm of science and life, have been the cornerstone of my academic endeavors. His expertise and passion for science have not only influenced but also profoundly shaped the trajectory of my research.

Thank you all for supporting me throughout these years!

List of papers and author's contribution

The thesis is based on the following papers (listed chronologically):

I.   Moss, M., Korbelová, J., Štětina T., Opekar, S., Šimek, P., **Grgac, R.**, & Koštál, V. (2022). Cryoprotective metabolites are sourced from both external diet and internal macromolecular reserves during metabolic reprogramming for freeze tolerance in Drosophilid fly, *Chymomyza costata*. Metabolites, 12(2). (IF = 5.581)

> RG participated in design of experiments, sample collection and preparation for metabolomics, measured all enzyme activities, participated in dataset analysis, and wrote parts of manuscript. His contribution was 15%.

II.   Kučera, L., Moss, M., Štětina T., Korbelová, J., Vodrážka, P., Des Marteaux, L., **Grgac, R.**, Hůla, P., Rozsypal, J., Faltus, M., Šimek, P., Sedlacek, R., & Koštál, V. (2022). A mixture of innate cryoprotectants is key for freeze tolerance and cryopreservation of a drosophilid fly larva. Journal of Experimental Biology, 225(8). (IF = 2.8)

> RG participated in the design of experiments, sample collection and preparation for metabolomics, participated in dataset analysis, and wrote parts of manuscript. His contribution was 10%.

III. **Grgac, R.**, Rozsypal, J., Des Marteaux, L., Štětina T., & Koštál, V. (2022). Stabilization of insect cell membranes and soluble enzymes by accumulated cryoprotectants during freezing stress. Proceedings of the National Academy of Sciences, 119(41). (IF = 11.1)

> RG was the lead author of this study together with VK. RG helped to develop the experimental design, performed the majority of experiments (including all enzymatic activity assays), provided input for interpreting the results, and importantly contributed to assembling the datasets, and writing the manuscript together with VK. His contribution was 50%.

Co-author agreement

Vladimír Košťál, the supervisor of this Ph.D. thesis and co-author of papers I, II, and III fully acknowledges the stated contribution of Robert Grgac to these manuscripts.

prof. Ing. Vladimír Košťál, CSc.

Table of contents

1. Introduction

1.1 Insect seasonality and diapause

Insects, as ectothermic organisms, are inherently vulnerable to fluctuations in environmental temperature, lacking the ability to regulate their internal heat. Changes in temperature directly impact their survival, fitness, and molecular interactions (Overgaard et al., 2014). Daily and seasonal temperature fluctuations affect insects, with higher latitudes experiencing greater seasonal temperature variations, resulting in better adaptations to withstand temperature extremes (Sunday et al., 2011).

Low seasonal temperatures pose a significant obstacle to the survival and fitness of insects living in temperate and polar regions. Low temperatures limit the viability of cells, tissues, and entire organisms, although the exact mechanisms remain unclear due to the complex effects of low temperatures on living organisms. The effect of low temperatures impacts various structures, processes, activities, and molecules, making it challenging to discern the hierarchy, importance, and causal relationship of individual changes. Therefore, the question of what determines the survival of individual insect species at low temperatures, often below freezing point, remains unresolved (Storey & Storey, 2013). The seasonal plasticity and thermal limits for survival and fitness are crucial factors in determining the geographic distribution of insect species and their response to global climate change (Sunday et al., 2012).

In response to these environmental pressures, insects have evolved complex strategies, with diapause and cold acclimation emerging as two major adaptive complexes, which include diverse mechanisms to adapt to challenging conditions, such as producing antifreeze proteins, accumulating cryoprotectants (CPs), and modifying their metabolism and behavior (Koštál et al., 2010). The significance of cryoprotectants in cold acclimation and mitigating freeze dehydration stresses has been emphasized in numerous studies, revealing various types of cryoprotectants present in different organisms, including insects. Despite these findings, the precise mechanisms governing their biosynthesis, accumulation, and physiological roles still lack comprehensive understanding (Storey & Storey, 2013).

Insects living in polar and temperate regions have life cycles that are highly adapted to seasonality, characterized by active summer phenotypes and dormant winter phenotypes. In response to changing environmental signals, such as photoperiod and thermoperiod, diapause is induced prior to the onset of environmental stressors. Diapause is a form of dormancy that is systemically regulated, whereas quiescence is a type of dormancy that occurs directly in response to environmental factors that fall below a critical threshold. Any developmental stage of an insect can potentially enter quiescence triggered by low temperatures (Lees, 1955; Danks, 1987; Koštál, 2006).

During the diapause induction phase, photoperiod and thermoperiod changes are sensed by specific developmental stages, leading to a deep transformation of the insect's phenotype. Insect brains and/or eyes contain specialized photoperiodic receptors that transduce the short-day signal into changes in the synthesis and secretion of developmental hormones, such as ecdysone and juvenile hormone (JH). The signaling of ecdysone or JH will systematically govern

the phenotypic transformation in all peripheral organs, depending on the stage of development at which diapause is expressed. Insects engage in intensive foraging activity during the preparation phase to build up energy reserves for the harsh period to come (Hahn & Denlinger, 2007). During diapause, the reproductive activity of adult insects ceases, and the proliferation activity in precursor cells stops. As a result, the behavioral activities related to mating, parental care, and partner location are halted (Koštál et al., 2009).

During the early phase of diapause, insects may still be highly active as they migrate to seek out overwintering microhabitats and initiate various protective mechanisms (Willmer, 1982; Masters et al., 1988; Solensky, 2004). These mechanisms include building cocoons (Danks, 1987), increasing the thickness of cuticular hydrocarbon layers (Rinehart et al., 2001; Benoit, 2010), upregulation of heat shock proteins (Rinehart et al., 2006), stimulation of antioxidant mechanisms (Jovanović-Galović et al., 2007), and inhibition of proapoptotic pathways (Villeneuve et al., 2006).

However, during the next phase of diapause, insects become very inactive and experience deep metabolic suppression to avoid prematurely reaching the next developmental stage, which would be unable to survive the winter. The gradual drop in temperature during autumn has two important consequences: the termination of diapause and the induction of cold-acclimation processes. Transcription profiles, protein expression patterns, and metabolic pathways undergo deep restructuring during diapause to support the insect's survival during the winter months (Emerson et al., 2010; Kankare et al., 2010; MacRae, 2010; Ragland et al., 2010; Poelchau et al., 2013; Teets & Denlinger, 2013; Poupardin et al., 2015; Yocum et al., 2015; Koštál et al., 2017).

It takes weeks or months of exposure to low temperatures for diapause to end and for insects to resume their normal activities. The end of diapause typically occurs in December or January for most insect species. Even after diapause has ended, insects remain in a state of low temperature-quiescence until the spring, when the rise in temperature allows them to rapidly resume their behavioral activities and reproduction/development (Tauber et al., 1986; Danks, 1987; Denlinger, 2002).

The topic of the relationship between diapause and cold tolerance in insects has been debated for a long time (Denlinger, 1991). Although cold hardiness generally increases upon entering diapause, the greatest increase in cold hardiness usually occurs during the gradual decrease in ambient temperature during autumn (Šlachta et al., 2002). Insects use an adaptive complex of cold acclimation, which is often linked with diapause, to increase their cold tolerance. Cold acclimation is based on extensive restructuring of the transcriptome, proteome, and metabolic pathways and includes number of interconnected mechanisms (Qin et al., 2005; Sinclair et al., 2007; Zhang et al., 2011; Colinet et al., 2013; Shang et al., 2015; MacMillan et al., 2016; Koštál et al., 2017).

1.2 Mechanisms of insect cold acclimation

The literature on insect cold hardiness reveals a comprehensive framework that categorizes their adaptive responses into three distinct and well-defined strategies. Each strategy is characterized by the state of body water at temperatures below the melting point of body fluids (Zachariassen, 1985). When an insect's body temperature dips below the threshold of fluid melting, three possible outcomes emerge, shaping the fundamental approaches insects adopt to withstand cold stress:

- Freeze avoidance or supercooling strategy: In this strategy, some insects manage to maintain their body water in a liquid state, even at temperatures below the freezing point of their bodily fluids. This remarkable ability to supercool enables them to avoid the formation of ice crystals within their tissues, thus preventing the damaging consequences of ice formation. The intricate mechanisms that underlie this strategy involve the suppression of ice nucleation, often achieved through the presence of high concentrations of various low molecular weight cryoprotectants (LMW CPs) and also specialized proteins or antifreeze compounds (Zachariassen, 1985; Holmstrup et al., 2002; Sinclair & Renault, 2010; Rozsypal, 2022).

- Freeze tolerance strategy: In contrast to supercooling, other insects have evolved to embrace the freezing of their body water, manifesting the remarkable capacity to survive the formation of ice crystals within their tissues. This strategy involves a series of sophisticated adaptations that protect the insects' cellular structures and prevent lethal damage during freezing and subsequent thawing. These adaptations include the accumulation of cryoprotectants, adjustments to cellular physiology, and the stabilization of membranes and macromolecules (Horwath & Duman, 1984; Zachariassen, 1985; Holmstrup et al., 2002; Sinclair & Renault, 2010; Rozsypal, 2022).

- Cryoprotective dehydration strategy: Some insects take a unique route to cold hardiness by allowing their body water to vaporize, effectively undergoing a process of cryoprotective dehydration. This strategy involves the deliberate reduction of body water content to minimize the risk of ice crystal formation. The remaining small amount of liquid solution may undergo vitrification, forming an amorphous solid or "glass" phase, which further contributes to the preservation of cellular integrity and function (Sformo et al., 2009, 2010; Koštál et al., 2011a).

1.2.1   Mechanisms of cold and freeze-induced injuries

Low temperature is defined as any temperature falling below a species-specific threshold, beyond which activity, growth, or developmental processes become constrained. In a more precise context, it can be described as the temperature level that triggers some form of injury, which may ultimately result in mortality or various sub-lethal outcomes (Lee, 1991). It is crucial to emphasize that a substantial differentiation exists between cold and freeze-induced injuries, as these processes are entirely distinct from one another (Rozsypal, 2022).

Low temperature-induced injuries are generally categorized into two distinct types: cold (or chill) injury and freeze injury, as outlined by Storey and Storey (1988). Cold injury occurs when temperatures fall below optimal levels but remain above the crystallization point of bodily fluids, known as the supercooling point (SCP). Cold injury can be further subdivided into acute cold injury, occurring in response to rapid and brief temperature fluctuations, and chronic or cumulative cold injury, arising from prolonged exposures to low temperatures. Freeze injury, on the other hand, ensues due to the formation of ice within the organism, either extracellularly or intracellularly. Evaluating the extent of cold injury commonly involves assessing mortality following cold exposure. It is important to note that cold injury does not invariably lead to immediate fatality; instead, organisms may exhibit varying degrees of tolerance or repair capabilities (e.g., Košťál et al., 2007; Štětina et al., 2018). Depending on the extent of damage and the organism's ability to tolerate or repair it, cold injury may also manifest as sub-lethal effects, such as delayed mortality, impaired development, reduced lifespan, and compromised fitness (Košťál et al., 2019).When organisms experience temperatures below their optimal or "permissive" range (which do not cause immediate injury), it primarily affects chemical reactions at the molecular level. Enzymes, which catalyze these reactions, are highly sensitive to temperature changes. Lower temperatures alter enzyme conformation, affecting their affinity for substrates (Franks & Hatley, 1991). Additionally, temperature impacts the fluidity of biological membranes, influencing membrane permeability and the function of membrane-bound proteins (Quinn, 1988). These alterations in enzyme activity and membrane function can result in an overall decline in organismal activity and may have consequences for various biological processes, including performance, reproduction, development, and distribution (Gilbert & Raworth, 1996; Overgaard & Macmillan, 2017; MacMillan, 2019).

Injury caused by low temperatures primarily involves the disruption of macromolecular structures. This includes the denaturation of proteins, changes in membrane properties, and potential damage to nucleic acids. The hydrophobic effect, a critical force in maintaining protein structure, weakens at lower temperatures, leading to protein denaturation (Privalov, 1990; Dias et al., 2010).

Proteins play a critical role in metabolism and form vital intracellular structures such as the cytoskeleton. While it is generally believed that proteins are particularly vulnerable to damage by low temperatures and require relatively high concentrations of cryoprotectants to protect them against cold denaturation, evidence suggests that such a "rule" may not be universal

(Rozsypal, 2022). Some proteins may be resistant to cold denaturation under physiological conditions, or they may denature reversibly (Kunugi & Tanaka, 2002). Membranes composed of phospholipids undergo phase transitions at different temperatures, affecting their fluidity and barrier function. Lateral phase separation and the formation of pores can result from these transitions, leading to membrane damage (Quinn, 1985; Hazel, 1995). Nucleic acids, such as DNA and RNA, can also be affected by low temperatures, potentially resulting in breaks or degradation (Linfor & Meyers, 2002; Huang et al., 2017). While cold-induced damage to nucleic acids is not fully understood, it may involve changes in the structure of histones and other factors (Tatone et al., 2010; Fraser et al., 2011).

The rate at which temperatures change, both during cooling and warming, plays a significant role in cold injury. Rapid cooling can lead to the formation of small ice crystals, while slow cooling helps prevent intracellular freezing. Rapid warming is used to avoid recrystallization during thawing (Seki & Mazur, 2008).

Freezing injury is a combination of the effects of low temperatures and ice formation. Supercooling can occur when a solution remains in a liquid state below its freezing point, but ice nucleation eventually leads to freezing. The extent of supercooling depends on various factors, including solution volume, solute concentration, and the presence of ice nucleators (Lee, 1991; Lee et al., 1996; Zhao, 1997). This freeze-induced injury is a complex phenomenon associated with the need to withstand a series of challenges. These challenges include exposure to severe cold, mechanical stress caused by the growth of ice crystals, loss of liquid water, elevated osmolality, increased concentrations of protons, metal ions, and other potentially harmful compounds, disruption of vital processes such as anoxia and ischemia, increased compaction of cellular components, and cell shrinkage (Sinclair et al., 2003).

1.2.2   General suppression and specific regulation of metabolic pathways
During cold acclimation, temperature has a direct effect on enzyme kinetics and biological processes leading to metabolic suppression. However, this suppression is often deeper than expected, as many processes are completely inhibited rather than slowed down (Hochachka, 1986). In supercooled insects, protein stability and lifespan are limited in a liquid environment, necessitating a slow continuation of processes such as gene transcription and protein turnover. Regulated metabolism is required to maintain basal cellular homeostasis, including transmembrane ion gradients, which consumes energy in the form of ATP (Koštál et al., 2004a). On the other hand, frozen insects are likely to save energy since they most likely do not continue regulated metabolism, though insects frozen at ecologically relevant temperatures display signs of anaerobic metabolism, such as slow lactate accumulation (Storey & Storey, 1985).

Interestingly, glycogen degradation serves as an example of a specific metabolic pathway paradoxically upregulated at low temperatures, stimulated below +5°C (Storey &

Storey, 1991). The liberated glucose from glycogen contributes to the synthesis and accumulation of diverse cryoprotectants, encompassing glycerol, sorbitol, and ribitol. The reduction of sugars into their corresponding polyols necessitates the involvement of NADPH, which is primarily generated in the pentose cycle—a process that must also undergo upregulation to facilitate this metabolic transformation (Storey & Storey, 1991; Koštál et al., 2004b). Understanding intricate metabolic shifts was highly important, as metabolic restructuring was one of the aims of my study.

1.2.3 Restructuring of biological membranes

Sinensky's (1974) pioneering study elucidated the connection between membrane lipid composition, fluidity, and biological functions, while Cossins (1994) extended this insight to explore the interplay of membrane fluidity and temperature adaptation. Cold acclimation induces significant changes in membrane composition, such as increased fatty acyl unsaturation, enhancing fluidity at low temperatures, coupled with decreased fatty acyl chain length (Hazel, 1995; Koštál, 2010). Moreover, membrane restructuring during cold acclimation involves shifts in phospholipid and sterol ratios; Koštál et al. (2013) observed elevated sterol levels in insects adapted to low temperatures, possibly contributing to membrane stability in cold environments.

Crucial to membrane functionality and integrity in supercooled and frozen insects, membrane restructuring is vital for maintaining protein functionality, including ion transport systems (McElhaney, 1984; Hazel, 1995). While specific fluidity prevents membrane leakiness during supercooling, protection of membrane integrity is pivotal during extracellular ice crystal growth and cell dehydration in frozen insects (Hazel, 1995). Cellular dehydration during extracellular freezing makes the phospholipid bilayer susceptible to unregulated transitions to hexagonal phase compromising the membrane barrier function. In addition, membrane fusions may occur due to closely packed membranes (Uemura et al., 1996; Hincha et al., 1998).

Furthermore, oxidative stress, a notable cause of harm, can also inflict damage upon membranes, particularly as a result of heightened metabolism and the generation of free oxygen radicals during the recovery process (Colinet et al., 2016). Insects enact cellular protective adjustments during diapause and cold acclimation, developing a winter phenotype to counteract oxidative stress (Storey & Storey, 2012). Among supercooling and freeze-tolerant species, adaptive regulation of enzymatic and non-enzymatic systems is observed, including the upregulation of heat shock proteins (HSPs), which stabilize protein complexes, bind hydrophobic domains, and prevent protein aggregation due to cold or freeze-dehydration stress (Rinehart et al., 2006; King & MacRae, 2015; Toxopeus et al., 2019a). Also, HSPs play a pivotal role in repairing damaged proteins and contribute to recovery from cold stress (Richter et al., 2010; Goto & Kimura, 1998; Sinclair et al., 2007; Koštál & Tollarová-Borovanská, 2009; Štětina et al., 2015).

1.2.4 Accumulation of low molecular weight cryoprotectants (CPs)

Organisms have various ways of responding to environmental stress, including the accumulation of small protective molecules known as compatible osmolytes (Yancey, 2005). Although first discovered in organisms that cope with osmotic stress, these molecules have been found to have protective functions in many forms of life (Yancey & Siebenaller, 2015). Insects, in particular, accumulate cryoprotectants in response to cold stress. CPs are often represented by sugars, polyols, and free amino acids (Storey & Storey, 1988; Koštál et al., 2011a). These molecules protect the insects from the effects of low temperatures by affecting the water phase behavior, metabolic protection, and stabilization of macromolecules (protein, nucleic acid, lipid bilayer) (Storey & Storey, 1988).

Freeze-avoiding insects have high concentrations of CPs, which suppress the temperature of supercooling point and stabilize the metastable supercooled phase of water, making the biological solution unfreezable under ecologically-relevant conditions (Zachariassen, 1985). In contrast, freeze-tolerant insects prefer to freeze at relatively high subzero temperatures and accumulate low to medium concentrations of various CPs (Storey and Storey, 1988). This way, accumulated CPs can reduce the amount of ice generated at any given subzero temperature and reduce the osmotic outflow of water from cells, thus reducing cell shrinkage (Meryman, 1971; Rozsypal & Koštál, 2018; Rozsypal et al., 2018). Insects that undergo cryoprotective dehydration or freeze-induced cellular dehydration can transit highly concentrated solutions into an amorphous glass phase, which may be adaptive (Rudolph & Crowe, 1986; Sformo et al., 2010; Koštál et al., 2011a; Rozsypal et al., 2018).

The CP concentrations in insects can reach very high levels, up to 3M or even 5M in some cases of supercooling insects (Gehrken, 1984; Salt, 1961). However, the accumulation of very high concentrations of CPs would be counterproductive for freeze-tolerant insects, whose general role of accumulated CPs is to reduce ice generation and cell shrinkage rather than prevent freezing altogether (Storey & Storey, 1988). The accumulation of CPs can have an impact on the redox balance, as the metabolism of polyols consumes NADPH, which is also required for the re-reduction of oxidized glutathione. However, many CPs, such as trehalose (Reyes-DelaTorre et al., 2012) and proline (Kaul et al., 2008), have antioxidant capacity and can theoretically protect overwintering insects against oxidative damage.

The stability of macromolecules and integrity of macromolecular complexes are directly threatened by low temperature. A number of polymeric proteins will depolymerize already at moderately low temperatures around zero degrees Celsius (Privalov, 1990). While depolymerized proteins lose their activity (enzymes, signaling molecules) or structural function (cytoskeleton), the depolymerization is usually reversible upon return of normal conditions and, therefore, need not negatively affect the viability of cold-stressed insects (Des Marteaux et al., 2018). In liquid environments at very low temperatures (supercooled state), proteins may also denature, i.e., exposed their internal hydrophobic domains. The occurrence of cold and heat denaturation of proteins is similarly probable at extremely low and high, respectively,

temperatures (Dias et al., 2010; Sanfelice & Temussi, 2016). Denatured proteins may aggregate, i.e., tightly interact via their exposed hydrophobic regions. As the aggregation is hardly reversible, it will negatively affect the viability of an insect after cold stress. Phospholipid bilayers undergo a phase transition to a non-functional gel phase at low temperatures. In supercooled insects, the accumulated CPs can protect native protein structures as well as the functional liquid crystalline bilayer phase via a mechanism known as preferential exclusion (Arakawa & Timasheff, 1985; Timasheff, 1992a). Many CPs have been found to behave as kosmotropes in aquatic solutions, i.e., compounds highly soluble in water that prefer interactions with water molecules over interactions with proteins or phospholipid headgroups. Consequently, kosmotropic CPs are preferentially excluded from macromolecular vicinities, rendering the macromolecules preferentially hydrated and thermodynamically more stable (Xie & Timasheff, 1997; Timasheff, 1998; Jensen et al., 2004; Ball, 2008).

When it comes to freeze-tolerant insects, their cells are subjected to not only low temperatures, but also two other stressors: a near lack of liquid bulk water and the presence of ice crystals. Consequently, freezing stress is much riskier than simply supercooling at the same temperature. This stress affects four different levels of biological organization all at once. At the molecular level, freezing stress causes a reduction in the kinetic energy and reactivity of all molecules, such as enzymes and signaling cascades. The reduction in molecular mobility poses a significant threat to the functional conformation, stability, and complex integrity of macromolecules (Carpenter & Crowe, 1988; Franks & Hatley, 1991; Muldrew et al., 2004; Des Marteaux et al., 2018). Low water activity can cause nucleic acids to shift from their biologically relevant B-form to nonfunctional A-form (Brovchenko & Oleinikova, 2008). Furthermore, euchromatin DNA loops may break when subjected to mechanical stress (Lubawy et al., 2019). These molecular dysfunctions can impair metabolic processes and inhibit biochemical and cellular functions, leading to energy depletion and toxic buildup (Storey & Storey, 1985; Joanisse & Storey, 1996).

At the cellular and tissue levels, osmotic fluxes of water and growing ice crystals exert osmotic and direct mechanical stresses on organelles, cells, and extracellular matrices, which may lead to a loss of physical integrity (Lovelock, 1954; Mazur, 1984). Injured molecules, structures, cells, and organs may fail to interact properly during repair of freezing injury and resumption of life functions after freezing stress, leading to organismal collapse or loss of fitness (Pörtner, 2002; MacMillan, 2019). Despite these severe effects, some ectotherm vertebrates and invertebrates have independently evolved freeze tolerance mechanisms (Salt, 1961; Asahina, 1970; Storey & Storey, 1988, 1992). This is a surprising phenomenon given the significant combination of deleterious effects associated with internal freezing.

Several specific cryoprotective proteins have been suggested to provide protection against denaturation and aggregation of native protein structures caused by freeze dehydration (Inoue & Timasheff, 1972; Tamiya et al., 1985; Wang, 1999; Bolen & Baskakov, 2001; Kaushik & Bhat, 2003; Toxopeus & Sinclair, 2018). During freeze dehydration, 50-70% of cellular water is

removed, and the cell interior becomes more viscous, leading to a failure of the mechanism of preferential exclusion. Most kosmotropic (stabilizing) CPs are unable to provide protection beyond a hydration threshold of 0.3 g of water per gram of dry mass (Hoekstra et al., 2001). However, some disaccharides and oligosaccharides, including trehalose, have been shown to stabilize membranes during desiccation by forming hydrogen bonds with polar residues on phospholipid headgroups and replacing the missing water molecules (Crowe et al., 1984; Thompson, 2003). Therefore, this mechanism is known as water replacement (Crowe et al., 2001; Crowe, 2007). Among all amino acids, proline and arginine are very specific in their ability to directly interact with partially denatured proteins resulting from freezing stress and stabilize them in a molted globule phase, thus preventing further denaturation and aggregation (Samuel et al., 1997; Das et al., 2007; Lange & Rudolph, 2009; Schneider et al., 2011). Moreover, proline and arginine are the only two amino acids that display, at high concentrations and low water activities, a high propensity to self-associate and form supramolecular clusters (stacked columns) with hydrophobic surfaces that interact with hydrophobic surfaces of partially unfolded proteins (Rudolph & Crowe, 1986; Das et al., 2007). Notably, proline and arginine are the two most potent cryoprotective compounds in a large screening bioassay of 31 different native amino acids in *Drosophila melanogaster* (Koštál et al., 2016a). Additionally, high concentrations of proline can alter the temperature of bilayer phase transitions and reduce the tendency for fusion in closely packed membranes through hydrophobic interactions of proline imino-groups with the hydrocarbon chains of the bilayer phospholipids (Anchordoguy et al., 1987).

Cellular freeze dehydration can result in crowded cytoplasmic components, close contact between organelles, and possible membrane fusion (Uemura et al., 1996). To prevent unwanted interactions between tightly adjacent phospholipid bilayers or proteins, a variety of CPs have been proposed to act as a molecular shield (Bryant et al., 2001; Hoekstra et al., 2001; Ball, 2008). Furthermore, highly concentrated CPs like trehalose and proline can stimulate the transition of highly concentrated body solutions into the amorphous phase, which can further stabilize structures and protect them against thermomechanical stress (Rudolph & Crowe, 1986; Rubinsky et al., 1980).

1.2.5   Production of high molecular weight cryoprotectants

In preparation for winter, certain insect species accumulate two classes of proteins associated with ice crystal regulation: anti-freeze proteins (AFPs) and protein ice nucleators (PINs) (Zachariassen & Kristiansen, 2000; Duman, 2001; Duman et al., 2010; Duman, 2015). In sub-zero temperatures, AFPs attach to embryonic ice crystals, inhibiting water molecule binding and suppressing crystal growth, lowering freezing points by -2°C to -8°C compared to melting points (thermal hysteresis, magnitude species-dependent). Paradoxically, AFPs also function in some freezing insects with high-temperature initiation, limiting ice recrystallization (Capicciotti et al., 2013). PINs, unlike AFPs, catalyze ice crystallization near freezing points, preventing

supercooling and accelerating ice formation in the extracellular space (Zachariassen & Kristiansen, 2000).

Highly conserved heat shock proteins stabilize protein complexes, e.g., cytoskeleton (Russotti et al., 1997; Des Marteaux et al., 2018), aiding during cold stress or freeze dehydration. Cold-exposed insects regulate HSP gene expression in early diapause/cold acclimatization, adapting for future thermal stress (Rinehart et al., 2006; Toxopeus et al., 2019a). Increased HSP gene expression primarily follows cold/frost shock, associated with protein repair (Goto & Kimura, 1998; Colinet et al., 2010a). However, HSP mRNA may not correlate with protein activity (Feder & Walser, 2005; Nielsen et al., 2005; Tollarová et al., 2005). Silencing small HSP genes (hsp22, hsp23) prolongs *Drosophila* recovery from cold coma (Colinet et al., 2010b). RNAi against hsp70 decreases cold tolerance in *Sarcophaga crassipalpis* (Rinehart et al., 2007) and reduces survival in *Pyrrhocoris apterus* after cold stress (Koštál & Tollarová-Borovanská, 2009). Absence of hsp70 negatively impacts extreme supercooling survival in *Drosophila* (Štětina et al., 2015).

1.2.6   Cold acclimation and recovery after cold stress

The assessment of insect cold hardiness varies among researchers, with survival following cold exposure being a direct and fundamental metric of cold hardiness. Typically, lower lethal temperature (LT50) and lethal time at low temperature (Lt50) are analyzed in population samples to gauge the lethality of various cold exposures. While direct analysis of cold hardiness through lethality seems straightforward, practical limitations arise from the need for large insect populations and the challenge of determining accurate survival criteria that align with ecologically meaningful outcomes (Nedvěd et al., 1998).

Cold acclimation is a crucial strategy employed by insects to enhance their ability to withstand freezing stress. Various physiological changes, such as alterations in membrane composition, metabolic pathways, and gene expression, contribute to the development of enhanced cold hardiness (Hazel, 1995; Koštál et al., 2013). However, the assessment of cold hardiness often neglects the consideration of delayed mortality and sublethal effects that can impact an insect's overall fitness and survival. Delayed mortality, observed in different ontogenetic stages not directly subjected to cold stress, has been reported in various insect species (Turnock et al., 1983, 1985; Pullin & Bale, 1988; Bale et al., 1989; Yocum et al., 1994; Marshall & Sinclair, 2015; Štětina et al., 2018; Koštál et al., 2019). Such sublethal effects, encompassing physiological and behavioral changes, may significantly influence an insect's ability to cope with cold stress and can have profound implications for population dynamics and ecological interactions (Coulson & Bale, 1992; Hutchinson & Bale, 1994; Kelty et al., 1996; Marshall & Sinclair, 2010).

Understanding the complex interplay between resistance and tolerance mechanisms in response to cold stress is essential for a comprehensive grasp of insect cold hardiness.

Resistance mechanisms involve reducing or avoiding cold stress injury to maintain high survival rates and fitness, while tolerance mechanisms focus on an insect's ability to survive or repair injuries incurred during cold stress, albeit potentially at a fitness cost. In this context, analyzing fitness parameters such as reproductive output, developmental transitions, and longevity can shed light on the relative contributions of resistance and tolerance mechanisms in different insect species (Simms & Triplett, 1994; Núñez-Farfán et al., 2007; Råberg et al., 2007).

1.3   Model species

My research focuses on exploring the biosynthesis, physico-chemical properties, and protective functions of low molecular weight CPs in *Chymomyza costata* (Zetterstedt, 1838) (*Diptera*, *Drosophilidae*). This species is an important model for studying the bionomics of the genus *Chymomyza*, which comprises around 60 described species. *Chymomyza costata* is distributed across the Holarctic region and is one of the northernmost species in the *Drosophilidae* family, with a range extending beyond the Arctic Circle (Hackman et al., 1970; Toda, 1985). The *Drosophilidae* family has more than 1,500 species, and they are predominantly distributed in tropical regions. These species typically exhibit limited diapause expression and have low cold tolerance. Only a few species are adapted to polar or temperate regions (Strachan et al., 2011).

Temperate vinegar fly species typically enter adult reproductive dormancy during winter through diapause or quiescence. However, pupal diapause has been observed in one species, *Drosophila alpina* (Lumme, 1978), while *Chymomyza* species (including *C. costata*) and *Scaptodrosophila deflexa* are reported to undergo larval diapause (Basden, 1954).

The taxonomic classification of the species can be found on the following websites:

- NCBI Taxonomy browser, ID 76946:
  https://www.ncbi.nlm.nih.gov/Taxonomy/Browser/wwwtax.cgi?mode=Info&id=76946
- NCBI Life map:
  https://lifemap-ncbi.univ-lyon1.fr/?tid=7271

1.3.1   Larval diapause in *Chymomyza costata*

Overwintering of *C. costata* larvae in a diapause state has been described for both Finnish and Japanese populations (Lakovaara et al., 1972; Enomoto, 1982). In the 1980s, a joint Finnish-Japanese group began to study the mechanism of diapause in more detail. Most of their research was conducted on a fly line that originated from several individuals captured in 1983 near the city of Sapporo, Hokkaido Island, Japan (43.06°N, 141.35°E). The research was stimulated by the isolation of a non-diapausing fly line, which spontaneously appeared in laboratory culture in the first few years after capture in the wild. This line did not respond to the short-day signal that otherwise reliably induces diapause in virtually all wild-type larvae

(Riihimaa & Kimura, 1988). Further genetic analysis suggested that the loss of photoperiod sensitivity in larvae was likely caused by a mutation of a single recessive allele of an unknown gene (locus) located on autosomes. The gene locus was named NPD (Non-Photoperiodic Diapause), reflecting the fact that larvae can enter a dormant (quiescent) state if exposed to low temperatures (<LDT, <11°C), but the photoperiodic signal itself applied at relatively high temperatures (18°C) does not induce diapause (Riihimaa & Kimura, 1989). The NPD line thus became a suitable model for studying the genetic and molecular basis of photoperiodism in insects.

Debates about the nature of the so-called photoperiodic calendar have been ongoing for decades (Pittendrigh, 1960), and recently, the prevailing view is that the photoperiodic calendar (the ability to recognize day length and respond to it with a complex phenotypic change, such as entering diapause) is based on specific interactions in the neural network of so-called "clock neurons" in the insect brain (Saunders, 2002; Koštál, 2011). Research conducted on the NPD *C. costata* model line has contributed to support this view. First, using formal experiments (monitoring the response to photoperiods with a total length of >24 h; experiments with long nights interrupted by short flashes of light, etc.), it was found that the measurement of day (or night) length is attended by a factor with circadian rhythmicity in *C. costata* larvae that is not specified in more detail (Yoshida & Kimura, 1995; Lankinen & Riihimaa, 1997; Koštál et al., 2000). Analysis of the clock gene period revealed that it exhibits daily and circadian rhythms in expression in the wild line of larvae, whereas its expression is low and arrhythmic in the NPD line of larvae (Koštál & Shimada, 2001). Transcripts of another clock gene, timeless (*tim*), were not detectable in the NPD line, whereas in the wild line, they again exhibited the typical daily rhythm of expression. At the same time, disruption of timeless gene expression by RNAi led to a loss of photoperiodic sensitivity in larvae (Pavelka et al., 2003). The protein TIM was localized to two neurons in the larval brain in each hemisphere, where it exhibited a daily rhythm in the wild line. In the NPD line, the TIM protein was not detected at all (Stehlík et al., 2008). These results suggest that the dysfunction of circadian clocks in the brain of NPD larvae may be related to the loss of photoperiodic calendar function. Sequencing of the _tim_ gene locus revealed that the recessive allele of this gene in the NPD line carries a long deletion (1,855 base pairs) in the 5'-UTR region. This deletion removed the transcription start and regulatory elements called E-boxes and TER-boxes (Stehlík et al., 2008). Gradual artificial shortening of the sequence revealed that insect S2 cells transfected with shortened constructs require precisely those promoter regions that are removed by the mutation in the NPD line to express the *tim* gene (Kobelková et al., 2010). It is therefore possible that the NDP locus is occupied by the *tim* gene, and this clock gene may represent a molecular link between clock and calendar functions.

The larvae of *C. costata* have also been used as a model for detailed characterization of factors inducing diapause in insects (Koštál et al., 2016b). It is often incorrectly stated in literature that diapause in insects is induced by low temperature (or primarily by low temperature). However, the main inducing factors are signals from the environment that have a rhythmic character and thus encode calendar time - photoperiod and also thermoperiod. These

rhythmic signals can safely induce diapause in *C. costata* larvae even when applied individually or independently. If both are applied simultaneously, the larvae are governed only by the photoperiodic information. Other factors (temperature, population density, food access) play a secondary role and modify the response to primary rhythmic factors. Furthermore, diapause of *C. costata* larvae has been used as a model for characterizing individual ecophysiological phases of insect diapause development (Poupardin et al., 2015; Koštál et al., 2016b, 2017). The simplified notion of diapause as a static state has been replaced by a model of dynamic changes in gene expression and physiology, which run spontaneously (endogenously, without changing external conditions) while also responding to (exogenous) changes in external conditions, leading to gradual termination of diapause during the winter season.

1.3.2   Cold hardiness in *Chymomyza costata*

The initial investigation into *C. costata* larvae's cold tolerance identified freeze-avoidance as the primary strategy for subzero survival (Enomoto, 1982). This classification relied on supercooling point (SCP) measurements, which were relatively low (around -20°C). However, it's now understood that the same SCP value is also observed in tropical drosophilids, including the vinegar fly larvae, *D. melanogaster*, which possess low cold tolerance and perish rapidly at 0°C exposure (Koštál et al., 2011b). Consequently, the mere presence of a low SCP does not necessarily correlate with high cold tolerance.

Subsequently, the strategy classification shifted to freeze-tolerance (Riihimaa, 1988), when it was recognized that *C. costata* larvae exhibit high sensitivity to surrounding ice inoculation, likely common in their hibernation sites. Inoculative freezing initiates at mild subzero temperatures between -1°C and -3°C (Rozsypal et al., 2018). Early inoculation and slow freezing rates enable survival of frozen larvae down to -100°C (Shimada, 1990). The same authors highlighted another survival condition - prior entry into diapause and cold acclimation (4°C, 1-month, constant darkness). Furthermore, larvae undergoing photoperiodic diapause displayed a slightly heightened freeze-tolerance compared to their quiescing counterparts. Cold acclimation also triggered the accumulation of two potentially cryoprotective substances: proline (up to 175 nmol.mg^{-1} FW) and trehalose (up to 37 nmol.mg^{-1} FW).

In 1996, it was discovered that frozen larvae could endure cooling to the temperature of liquid nitrogen (-196°C) (Moon et al., 1996). This revelation rendered *C. costata* larvae a compelling model for cryopreservation studies involving complex animal organisms. While current cryobiology effectively stores cells and simple embryos in liquid nitrogen, significant challenges arise when dealing with basic tissues (ovaries, kidneys), and cryopreserving entire organs or organisms was long deemed nearly impossible (Fahy & Wowk, 2015). It's important to mention that these organisms, like *C. costata* larvae, are well-hydrated, distinguishing them from anhydrobiotic organisms that experience loss of water before freezing, such as plant seeds, various invertebrate embryos, and tardigrades.

Koštál et al. (2011a) affirmed larvae's resilience to liquid nitrogen exposure and validated proline and trehalose accumulation during cold acclimation of diapausing larvae through metabolomic profiling. Moreover, they established that diapause entry and cold acclimation coincide with an overall rise in hemolymph osmotic concentration up to 700 mOsmol.kg^{-1}, a loss of osmotically active (freezable) water, and heightened susceptibility to traverse the glass transition during freezing. Similar changes were evident in non-diapausing larvae fed a proline-enriched diet. Heat-acclimated, non-diapausing larvae can't withstand freezing or cryopreservation, but proline-enriched diet consumption bestowed this ability. A subsequent study (Koštál et al., 2012) employed relatively simple methods to "transform" *D. melanogaster*, a tropical and cold-sensitive fruit fly larva, into a -5°C freeze-tolerant organism. Survival post-freezing necessitated preliminary cold acclimation, halting development via cold quiescence, proline-enriched diet intake, early ice inoculation, and slow freezing.

Diverse microscopic approaches were employed to unveil micro-morphological alterations arising from the freezing of *C. costata* larvae, pinpointing vulnerable tissues and structures. Employing light and confocal microscopy, cytoskeletal structures like tubulin and actin experienced breakdown, especially in larval fat tissue (Des Marteaux et al. 2018). Simultaneously, the freezing-induced cytosol dehydration led to the pronounced coalescence of lipid droplets. Whether this coalescence instigated the secondary disruption of radial tubulin fiber structures or was enabled by tubulin breakdown remains ambiguous. Additionally, actin microfilaments aggregated within the adipose cell cortical layer. Freeze-tolerant larvae demonstrated less pronounced cytoskeletal damage than their freeze-sensitive counterparts (non-diapausing and warm-acclimated). Remarkably, feeding sensitive larvae a proline-enriched diet significantly mitigated cytoskeletal damage.

The utilization of electron microscopy provided even deeper insights into the micro-morphology of frozen *C. costata* larval tissues (Štětina et al., 2020). Sensitive larvae exhibited a prominent inclination toward pathological mitochondrial changes, ranging from enlargement and rounding to the disruption of cristae structures on the inner membrane. Both inner and outer membrane ruptures occurred, leading to the release of mitochondrial contents into the cytosol. The intensity of these changes exhibited an adverse correlation with larval survival, and these alterations were evident in adipose, hindgut (Štětina et al., 2020), and later also in muscular tissues (Štětina et al., unpublished data). Intriguingly, while respiratory tissue capacity decreased, the activity of the citrate synthase enzyme, typically sensitive to cold and frost damage, paradoxically persisted. As seen in prior research, mitochondria's pathological changes were absent in resistant larvae and notably suppressed in sensitive larvae nourished with a proline-rich diet. Collectively, these experiments highlight the substantial, microscopically discernible influence of proline incorporation into the metabolism of *C. costata* larvae on freezing damage repair and larval tissue development.

1.4 Objectives of the dissertation

According to the doctoral study plan, the main objective of my dissertation was to carry out a functional examination of the cryoprotectant system in *C. costata*. The plan was modified throughout a four-year period in response to the results of specific experiments, and more precise goals were established:

- Diversity and biosynthesis of cryoprotectants (CPs)

  The primary objective of our study was to determine an exhaustive compilation of potential CPs of *C. costata* using global comparative metabolomics of tissues in differently acclimated larvae (GC-LC/MS). Next, we aimed to distinguish whether the CPs are synthesized from internal larval reserves or assimilated from diet. We approached this goal by mapping the metabolomics and gene transcriptomics profiles on CPs' biosynthetic pathways and combined this approach with key enzyme activity assays and feeding assays.

- Physico-chemical behavior of CPs *in vivo* during slow inoculative freezing

  The study's secondary objective was to determine (using differential scanning calorimetry) the thermal phase transition properties of artificial mixtures of CPs mimicking the composition of the hemolymph of cold-acclimated *C. costata* larva. We aimed to test the hypothesis that such mixtures possess physico-chemical properties of NADES (natural deep eutectic systems). Next, using MALDI mass spectrometry imaging, we aimed to track the localization of CPs to larval tissues and, mainly, whether and how this localization changes during the process of extracellular ice formation and cell freeze-dehydration.

- Protective roles of CPs during extracellular freezing and cell freeze dehydration
  The final objective of our study was to test the coupled hypotheses: that irreversible denaturation of proteins and loss of biological membrane integrity are two ultimate molecular mechanisms of freezing injury in freeze-sensitive insects and that seasonally accumulated CPs stabilize proteins and membranes against injury in freeze-tolerant insects. We approached this goal by a combination of *in vivo* and *in vitro* assays of selected enzyme activities and membrane permeability in differently acclimated larvae and tissues incubated in different mixtures of CPs and exposed to different freezing stresses.

2. Results

Paper I

Cryoprotective Metabolites Are Sourced from Both External Diet and Internal Macromolecular Reserves during Metabolic Reprogramming for Freeze Tolerance in Drosophilid Fly, *Chymomyza costata*

Moss, M., Korbelová, J., Štětina T., Opekar, S., Šimek, P., Grgac, R., Koštál, V. (2022)

Cryoprotective Metabolites Are Sourced from Both External Diet and Internal Macromolecular Reserves during Metabolic Reprogramming for Freeze Tolerance in Drosophilid Fly, *Chymomyza costata*

Martin Moos [1], Jaroslava Korbelová [1], Tomáš Štětina [1], Stanislav Opekar [1], Petr Šimek [1], Robert Grgac [1,2] and Vladimír Koštál [1,*

[1] Institute of Entomology, Biology Centre, Czech Academy of Sciences, Branišovská 31, 370 05 České Budějovice, Czech Republic; moos@bclab.eu (M.M.); j.korbelova87@centrum.cz (J.K.); tomas.stetina@seznam.cz (T.Š.); opekar@bclab.eu (S.O.); simek@bclab.eu (P.Š.); robert.grgac@entu.cas.cz (R.G.)
[2] Faculty of Science, University of South Bohemia, 370 05 České Budějovice, Czech Republic
*   Correspondence: author: kostal@entu.cas.cz; Tel.: +42-038-777-5324

Abstract: Many cold-acclimated insects accumulate high concentrations of low molecular weight cryoprotectants (CPs) in order to tolerate low subzero temperatures or internal freezing. The sources from which carbon skeletons for CP biosynthesis are driven, and the metabolic reprogramming linked to cold acclimation, are not sufficiently understood. Here we aim to resolve the metabolism of putative CPs by mapping relative changes in concentration of 56 metabolites and expression of 95 relevant genes as larvae of the drosophilid fly, *Chymomyza costata* transition from a freeze sensitive to a freeze tolerant phenotype during gradual cold acclimation. We found that *C. costata* larvae may directly assimilate amino acids proline and glutamate from diet to acquire at least half of their large proline stocks (up to 55 µg per average 2 mg larva). Metabolic conversion of internal glutamine reserves that build up in early diapause may explain the second half of proline accumulation, while the metabolic conversion of ornithine and the degradation of larval collagens and other proteins might be two additional minor sources. Next, we confirm that glycogen reserves represent the major source of glucose units for trehalose synthesis and accumulation (up to 27 µg per larva), while the diet may serve as an additional source. Finally, we suggest that interconversions of phospholipids may release accumulated glycero-phosphocholine (GPC) and -ethanolamine (GPE). Choline is a source of accumulated methylamines: glycine-betaine and sarcosine. The sum of methylamines together with GPE and GPC represents approximately 2 µg per larva. In conclusion, we found that food ingestion may be an important source of carbon skeletons for direct assimilation of, and/or metabolic conversions to, CPs in a diapausing and cold-acclimated insect. So far, the cold-acclimation- linked accumulation of CPs in insects was considered to be sourced mainly from internal macromolecular reserves.

Keywords: cryoprotectant metabolites; metabolic pathways; transcriptomics; metabolomics; proline; trehalose; betaine

1. Introduction

Convergent evolution repeatedly 'discovered' benefits of accumulation of a stereotypic family of cytoprotectant molecules (sugars and polyols, amino acids and derivatives, methylamines) in various organisms from archaea and bacteria to animals responding to different environmental stressors such as heat, cold, freezing, drought, hypersalinity, or high hydrostatic pressure [1–4]. For instance, the insects that invaded temperate and polar habitats have evolved accumulation of low molecular weight cryoprotectants (CPs) as one of principal tenets of their complex adaptive strategies for survival at subzero temperatures [5–8]. Some insects avoid internal freezing by extensive supercooling of their

body liquids, others tolerate extracellular ice formation, and still others avoid freezing by losing most of their body water [5,9–12]. Whatever strategy the insect uses, the accumulation of CPs is considered to be one of the major mechanisms that protects insect cells against damage exerted by low temperatures (supercooling), growing ice crystals and freeze-dehydration (freeze tolerance), or evaporative loss of body water (cryoprotective dehydration) [5–8]. The metabolic origin of insect CPs is relatively well understood for the class of sugars and polyols [13–18] but was not sufficiently studied for the classes of amino acids and methylamines. Here we contribute by tracing the sources of carbon skeletons and the pathways for biosynthesis of all three CP classes in the extremely freeze-tolerant drosophilid fly, *Chymomyza costata*. The larvae of this fly survive winter in cold-temperate and sub-arctic climate zones in a state of deep dormancy (diapause), during which they acquire extremely high levels of freeze tolerance. In the laboratory, the diapause cold acclimated larvae can even survive long-term cryopreservation in liquid nitrogen (LN_2), which makes them an interesting model for cryobiology [19–22].

Most insects accumulate CPs seasonally. Their metabolic pathways are hormonally diverted from support of active life toward preparation for winter dormancy during the relatively warm end of summer or autumn [23–26]. In autumn, insects start to accumulate macromolecular substrates such as glycogen, proteins and lipids [27]. Later in the season, usually upon cold acclimation during the coming winter, the macromolecular substrates may serve as sources for CP biosynthesis [28,29]. This general mechanism is best exemplified by degrading glycogen reserves in order to produce various sugars and polyols such as glucose, trehalose, glycerol, sorbitol and ribitol in different cold-hardy animals, including insects [13–18]. Primary control over this process is at the level of glycogen breakdown via direct triggering of glycogen phosphorylase activity by a drop of temperature below 5 °C [28,30]. Cold-activation of glycogen phosphorylase goes hand in hand with concerted changes in expression and allosteric modulation of activity in many other enzymes of intermediary metabolism, which finally results in accumulation of sugars and polyols [31–34]. Similarly to animals, cold-hardy plants also accumulate soluble sugars [35] by degrading their macromolecular reserves of starch [36].

Some insects seasonally accumulate high concentrations of free amino acids, especially proline [37–40]. The cryoprotective effects of proline are well documented [19,20,41–45] but the metabolic origin of proline in cold-hardy insects was not previously studied. We speculated that collagens in the extracellular matrix (ECM) may represent macromolecular depots of relatively 'dispensable' proteins from which proline, and other amino acids, can be obtained upon need [20,40]. Collagens are known to make up a large part of total proteins in animals, and are characterized by a high content of proline and hydroxyproline in their structure [46,47]. For example, massive degradation of ECM collagens is known to supply proline as an alternative energy source for rapid metabolism of proliferating or cancerous animal cells [48]. Proline appears to be one of the most widely distributed cytoprotectants accumulated under various stress conditions not only in insects and marine invertebrates [3] but also in eubacteria, protozoa, algae and plants [49,50]. The strong evidence for the role of proline in plant freeze tolerance comes from genetic manipulations of *Arabidopsis* [51]. Plants and eubacteria synthesize proline from glutamate and ornithine precursors in response to stress [49].

In addition, we found recently that cold-acclimated larvae of *C. costata* accumulate glycerophosphocholine (GPC), glycerophosphoethanolamine (GPE) and methylamines such as glycine betaine (betaine henceforth), and sarcosine [22]. Accumulation of betaine is well documented in plants and halophilic prokaryotes under various types of environmental stress [52,53], and genetic proofs for betaine contributing to freeze tolerance exist [54,55]. Betaine and GPC also provide osmoprotection of mammalian kidney cells exposed to high salt concentrations [56,57]. Animals, plants, and bacteria synthesize betaine from choline via a two-step oxidation pathway [56,58] and may further convert betaine to DMG (dimethylglycine) and sarcosine. Some halophilic prokaryotes, however, can synthesize

betaine from glycine via a three-step methylation, which requires activity of two specific methyltransferases [59].

Here, we explore adaptive adjustments in metabolism as the larvae of *C. costata* transit from freeze-sensitive to freeze-tolerant phenotype during entry into winter diapause and subsequent cold acclimation. We map onto metabolic pathways the changes in relative quantities of 56 metabolites (analyzed using liquid chromatography and high resolution mass spectrometry, LC-HRMS), and relative expression of 95 key genes coding key metabolic enzymes and transport systems (analyzed using reverse transcription quantitative PCR, RT-qPCR). We cover metabolic pathways representing all three major chemical groups of putative CPs. We focus on distinguishing between alternative sources of carbon skeletons for the CPs' biosynthesis, as follows. (i) Proline (and also other amino acids): is it derived from stored macromolecular reserves such as collagens and total proteins or from metabolic precursors such as glutamine, glutamate and ornithine, or rather assimilated from diet as an external source? (ii) Trehalose (and other sugars and polyols): derived from glycogen reserves or dietary starch and glucose? (iii) Methylamines: choline coming from interconversions of phospholipids or glycine which can be massively released during the breakdown of collagens?

2. Results and Discussion

We conducted experiments using four acclimation/phenotypic variants of 3rd instar *C. costata* larvae that were generated according to previously published acclimation protocols [19–21] and widely differed in freeze tolerance and cryopreservability in LN_2. All acclimation variants are described in detail in the Materials and Methods and presented in Table 1. Briefly, the variants SD3, SD6, and SD11 represent successive stages of diapause maintenance (3, 6, and 11 weeks old larvae, respectively) under constant warm conditions (18 °C). During diapause maintenance, relatively weak freeze tolerance gradually develops. The variant SDA represents the 11 weeks old larvae that undergo a gradual cold-acclimation process (11 °C for 1 week, followed by 4 °C for 4 weeks), which results in development of a maximal level of freeze tolerance.

Table 1. Freeze-tolerance phenotypes of *Chymomyza costata* larvae.

Phenotype	Acclimation Variant/ Phenotype	Freeze Tolerance at −30 °C * [% Larvae Surviving to Adulthood]	Survival in LN_2 * [% Larvae Surviving to Adulthood]
SD3	Diapause entry	0	0
SD6	Early diapause maintenance	65.0	7.7
SD11	Late diapause maintenance	41.5	10.1
SDA	Diapause, cold-acclimated	75.9	42.5

* Data taken from [19–21].

We restricted analyses to changes occurring *within* diapause larval phenotypes, focusing on the transition from freeze sensitivity (SD3) to extreme freeze tolerance including the ability to survive long-term cryopreservation in LN_2 (SDA). We omit metabolic reconstructions for non-diapause larvae as they exhibit intense locomotive activity, voracious feeding, and rapid growth and development; a stark contrast to diapausing larvae which are characterized by metabolic suppression and hormonally arrested development [26,60]. Such deep phenotypic differences between non-diapause and diapause could overwhelm or obscure the metabolic changes associated with cold acclimation and the acquisition of freeze tolerance. We mapped changes in 56 metabolites (Table S1) and 95 genes (Table S2) onto three schematic pathways (proline, trehalose, betaine) and will discuss them one by one. It is important to note that our schematic maps do not represent any specific cell type though they show plasmatic membranes and distinguish between cytosolic and extracellular spaces. As the metabolomic analyses were conducted using whole larvae, resolution to tissue level is not possible. The metabolomics results presented in this study are based on relative quantification (comparing chromatographic peak areas). We will refer to our earlier studies [20,22] for absolute quantities of select metabolites.

2.1. Proline and Other Amino Acids

Complete results of metabolomics and transcript analysis are presented in Table S3 while the differences between diapause maintenance (transition from SD6 to SD11) and cold acclimation-linked metabolisms (transition from SD6 to SDA) are graphically presented in Figure 1.
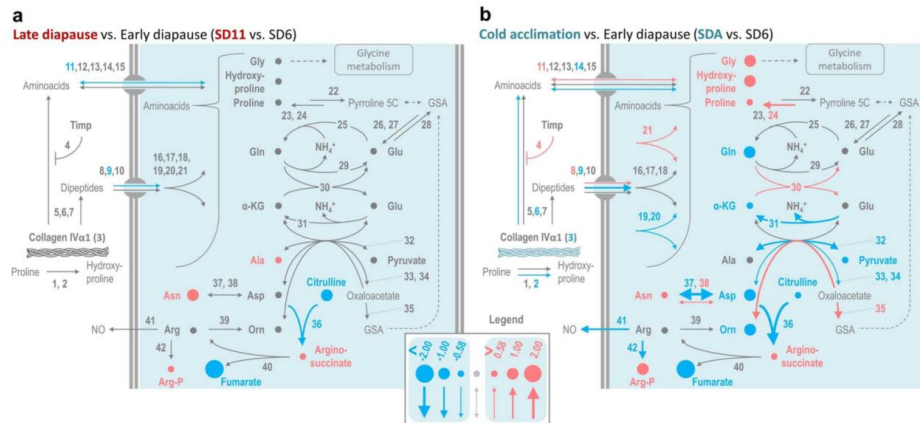

Figure 1. Changes in metabolism of proline during diapause maintenance vs. cold acclimation in *C. costata* larvae. The maps show $\log_2$-fold changes in relative concentrations of metabolites (circles) and gene expression (arrows) according to numerical results (Table S4) during diapause maintenance (**a**) and gradual cold acclimation (**b**). Three different thresholds for change were reflected in the size of symbols used (circles and arrows): absolute $\log_2$-fold change >0.58 (1.5-fold change); >1.00 (2-fold change); and >2.00 (4-fold change). Red indicates upregulation, blue indicates downregulation, grey indicates $\log_2$-fold changes between -0.58 to 0.58. Genes are coded by numbers (see Table S3). Thick grey double lines symbolize the plasma membrane with embedded transport systems. α-KG, ketoglutarate; GSA (glutamate-5-semialdehyde) and pyrroline 5C are tautomers and their interconversions are spontaneous.

Larvae undergoing cold acclimation exhibited more intense up- or down-regulations of proline-associated metabolites and transcripts compared to those in diapause maintenance (compare Figure 1a vs. Figure 1b). The chromatographic peak area of proline increased 1.6-fold during cold acclimation, and we observed concomitant peak area increases for glycine (2.2-fold) and hydroxyproline (2.1-fold) (Figure 1b, Table S3). The synchronous accumulation of glycine, proline, and hydroxyproline suggests that degradation of collagens—which are characterized by a high content of just these three amino acids [46]—is a potential source of accumulated proline. For example, the *C. costata* collagen IVα1 (Seq33535, Table S2) contains approximately twice as many glycine residues as proline residues (it has 1782 aa-residues and a molecular mass of 174,993 kDa; 497 residues (27.9%) are glycines; 244 residues (13.7%) are prolines and hydroxyprolines in an unknown ratio). Hydroxyproline is synthesized by proline hydroxylases (genes no. 1 and 2 in Figure 1) as a post-translational modification of proline residues bound to nascent collagen chains [61], so it is unlikely that the accumulated hydroxyproline originated from sources other than collagen-like proteins. However, other pieces of evidence speak clearly against the probability that collagens are the major source of accumulated proline, which we discuss in detail below.

First, the absolute concentration of glycine in SDA larvae is at least two orders lower than the concentration of proline [20,22]. Degradation of collagens, however, should release approximately twice as many glycine residues as proline residues. Should the proline be released from collagens, the massive flow of concomitantly released glycine would have

to be catabolized or, potentially, converted to betaine (we discuss this possibility later). Second, a stoichiometric calculation shows that *C. costata* larvae do not carry stores of degradable protein sufficient to account for the amount of free proline accumulated by the SDA phenotype. We may consider that: (i) the average SDA-larva accumulates proline at a concentration of 339 mmol.kg^{-1} of body water while an average SD11-larva has only 162 mmol.kg^{-1} of proline [20], which corresponds to a total pool of 475 nmoles (54.6 µg) or 227 nmoles (26.1 µg) of proline per larva, respectively (considering larval FM as 2 mg and water content as 1.4 mg); (ii) in order to produce $475 - 227 = 248$ nmoles of proline, the average larva would need to degrade at least 178 µg of collagen IVα1 (considering that degradation of 1 mole, i.e., almost 175 kg, of collagen IVα1 produces 244 moles of proline and hydroxyproline residues); (iii) the average SD6-larva, however, carries only ca. 270 µg of total protein (450 µg mg^{-1} DM), and only 38 µg of total protein is depleted during cold acclimation (Figure 2a). Third, the overall content of collagens increased during cold acclimation (Figure 2b), while a decrease would be expected if proline was released by degradation of collagens. Paradoxically, the activity of collagen-degradation enzymes (matrix metalloproteinases; MMPs) increased significantly (albeit slightly) during cold acclimation as well (Figure 2c). Fourth, using analysis of total proteins on PAGE, we verified that dominant protein bands show stable patterns across phenotypic variants suggesting that proteins are not massively degraded (Figure S1). Fifth, transcriptomic analysis suggested that proline transport is bolstered in SDA larvae as we observed significant (1.9-fold) increase in the relative expression of the gene coding for amino acid nutrient transporter NAAT1 (no. 11, Figure 1b, Table S3) which shows high specificity for proline [62]. Nevertheless, the origin of proline from collagen was not supported by transcriptomics as there were: (i) 3.3-fold decrease in relative expression of the gene coding for collagen IVα1 (no. 3, Figure 1b, Table S3); (ii) 1.8-fold decrease in one of two genes coding for MMPs (*MMP2*, no. 6, Figure 1b, Table S3); countered by (iii) 1.7-fold increase in Timp (no. 4, Figure 1b, Table S3) which is coding for an inhibitor of MMPs [63].
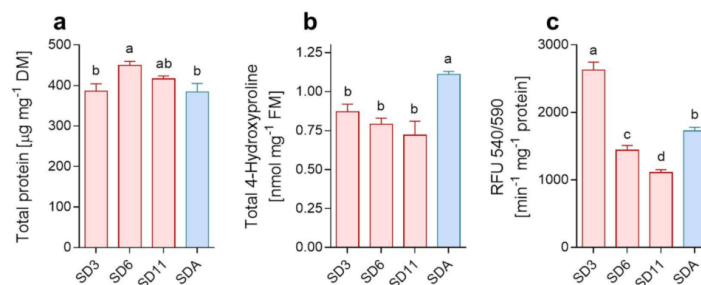

Figure 2. Total protein, collagens and MMPs. Changes in (**a**) total protein content, (**b**) total content of collagens estimated based on 4-hydroxyproline released upon acidic hydrolysis of larval total proteins, and (**c**) activity of general metalloproteinases (MMPs, collagenases). All analyses were performed on extracts of whole body larvae of different variants (diapause maintenance: SD3, SD6, SD1 (red columns); cold acclimation: SDA (blue column); see Table 1)) and each column is a mean of 3 biological replicates. Means were compared using one-way ANOVAs followed by Bonnferoni's multiple comparison tests (different letters indicate significantly different means). Note that nanomolar amounts of hydroxyproline were released from collagens upon acidic hydrolysis (**c**), while the total pool of free hydroxyproline in larval tissues is three orders lower—approximately 4–8 femtomoles [22].

Similarly as in plants under stress [49], proline in *C. costata* may be sourced from its nearest metabolic precursors, glutamine, glutamate and ornithine. We found that relatively large reserves of glutamine build up in early diapause (transition from SD3 to SD6), while they are partially depleted during subsequent cold acclimation (Figure 1b,

Table S3). In absolute terms, total glutamine content may reach up to 180 nmoles in the average SD11-larva while only 38 nmoles are found in the average SDA-larva [20]. Hence, the conversion of $180 - 38 = 142$ nmoles of glutamine may help to explain the origin of almost one half of the proline molecules accumulated in SDA-larvae, while the second half remains unexplained. The activation of glutamine conversion via the glutamate pathway is supported by upregulated glutamate synthetase (no. 30) and P5C reductase (no. 24) expressions during cold acclimation (Figure 1b). The glutamate synthetase activity, however, requires a supply of additional carbon skeletons from ketoglutarate, which might be limited due to general suppression of glycolysis and TCA metabolism in diapausing, cold-acclimated larvae (see discussion on trehalose metabolism). Stimulation of ornithine conversion via upregulated expression of ornithine aminotransferase (no. 35) may also contribute to accumulation of proline (Figure 1b). However, the total pools of glutamate (ca. 8 nmoles) and ornithine (ca. 0.5 nmoles) are relatively low throughout the acclimation variants [20], which suggests that these compounds are metabolic intermediates rather than sources from which the accumulation of proline would drive the carbon skeletons.

Since internal sources (either proteins or metabolic precursors) are obviously not sufficient to fully explain a massive accumulation of proline, the larval diet should be another source. Previously, we had not considered the diet as a source of proline because diapausing insects are known to drastically suppress their feeding, digestion, and metabolic rates [27,64]. The larvae of *C. costata*, for instance, gradually lose weight during diapause [65]. However, examining the feeding activity of diapausing *C. costata* larvae, we found that they consume food not only during diapause maintenance at a relatively high temperature of 18 °C but also during cold acclimation to 4 °C (Figure 3).
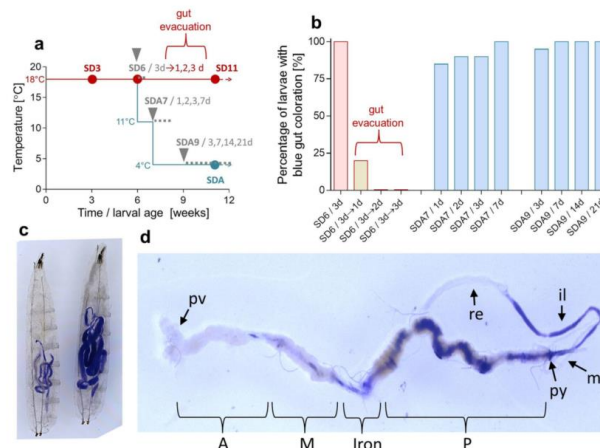

Figure 3. Diet consumption in diapause, of cold-acclimated larvae of *C. costata*. (**a**) shows the times when larvae were transferred to BB-augmented diets (grey triangles) and for how many days (grey font). Each column in (**b**) shows the percentage of larvae (*n* = 20 each) with blue gut contents. SD6 larvae exposed to BB diet for 3 d (all guts blue-colored) were returned to a standard diet to show that the blue coloration disappears in 80% of individuals within 1 d, and in all individuals within 2 d (gut evacuation). Most of the diapausing, cold-acclimated larvae (SDA7 and SDA9) exhibit blue guts within a few days of exposure to the BB diet. (**c**) shows examples of BB diet-fed larvae: left, an SDA9 larva exposed to BB diet for 14 d at 4 °C; right, a non-diapause (LD) larva exposed to BB diet for 1 h at 18 °C. (**d**) shows a gut dissected from an SDA larva exposed to the BB diet. Gut segments are described according to the gut morphology of *D. melanogaster* larvae: pv, proventriculus; A, M, P, anterior, middle, and posterior midgut; Iron, iron cells segment; py, pylorus; mt, Malpighian tubules; il, ileum; re, rectum.

Next, we analyzed the composition of the larval diet (Table S4) and found that proline was the highest in concentration of all the amino acids (2.7 mmol.kg^{-1} FM or 25.6 mmol.kg^{-1} DM). The amount of dietary proline that is directly 'assimilated' from food depends on the amount of food ingested and the food assimilation efficiency, both unknown for *C. costata* larvae. At 100% assimilation efficiency, the average larva of *C. costata* would need to ingest 37 mg of diet FM in order to accumulate 100 nmoles of proline. At a more realistic assimilation efficiency of 16% as demonstrated for larvae of the black soldier fly *Hermetia illucens* [66] this amount would increase to 231 mg of diet FM. Because the fresh mass of *C. costata* larvae gradually decreases during diapause at low temperatures [65], the calculations suggest that larvae must be able to absorb proline from the ingested diet without assimilating many of the other nutrients. The high ability of *C. costata* larvae to 'harvest' dietary proline is supported by two earlier observations: (i) the non-diapause larvae were able to increase their whole body concentration of proline almost 7-fold (from 39 to 268 mmol.kg^{-1} FM) within just three days of feeding on proline augmented diet [22]; (ii) when feeding *Drosophila melanogaster* larvae the same proline-augmented diet as *C. costata*, we found that *D. melanogaster* accumulated about one order less proline relative to *C. costata* [41]. In addition, glutamate is the second most concentrated amino acid in larval food (2.6 mmol.kg^{-1} FM or 24.9 mmol.kg^{-1} DM) (Table S4) and, hence, may serve as additional dietary precursor for biosynthesis of proline.

Overall, our results suggest that high concentrations of proline in SDA larvae of *C. costata* originate from different sources: (i) direct assimilation of ingested dietary proline, together with metabolic conversion of dietary glutamate (a proline precursor), can explain about one half of the proline accumulation; (ii) metabolic conversion of larval glutamine reserves formed in early diapause can explain the second half of proline accumulation; (iii) two other minor sources can be the metabolic conversion of ornithine and the degradation of larval ECM collagens and other proteins.

2.2. Trehalose and Other Sugars and Polyols

Complete results of metabolomics and transcript analysis are presented in Table S5, while the differences between diapause maintenance and cold-acclimation-linked metabolisms are graphically presented in Figure 4. Trehalose consists of two glucose molecules [67] and its non-reducing nature allows for safe 'storage' in large amounts in larval hemolymph. No trehalose accumulation was observed in *C. costata* during diapause maintenance (Figure 4a, Table S5) but the chromatographic peak area of trehalose increased 2.2-fold during cold acclimation (Figure 4b, Table S5). In support of upregulated trehalose biosynthesis in SDA larvae, the expression of a gene coding for two synthetic enzymes, *trehalose 6-phosphate synthase* (gene no. 20) and *phosphatase* (no. 21) increased substantially (4.1- and 10.1-fold, respectively), while the expression of a gene coding for the catabolic enzyme *trehalase* (no. 23) decreased 4.1-fold during cold acclimation (Table S5).

The metabolic map of trehalose further suggests that the glycolytic flux toward TCA was suppressed during late diapause maintenance and especially during cold acclimation (Figure 4, Table S5). In SDA-larvae, the genes coding for glycolytic enzymes nos. 5, 6, 7, and 8 were downregulated as were intermediates of the fermentation and TCA cycle: pyruvate, lactate, citrate, ketoglutarate, and fumarate. In addition, ATP concentrations increased whereas the concentrations of ADP and AMP decreased (Figure 4b), which is consistent with a relatively low demand for energy turnover during diapause and even less at low temperatures [27,64]. Glucose metabolism was redirected from glycolysis to: (i) trehalose biosynthesis (discussed above); (ii) sorbitol biosynthesis (no. 9 aldoketoreductase was upregulated 4.2-fold, resulting in a 2.1-fold increase in sorbitol); (iii) conversion to gluconolactone (no. 11 glucose 6-phosphate dehydrogenase was upregulated 3.5-fold, resulting in a 5.1-fold higher accumulation of 6-P gluconate). The conversion in (iii) is associated with the production of reducing equivalents in the form of NADPH. This reducing power is required, for example, for syntheses of proline from P5C and sorbitol from glucose.
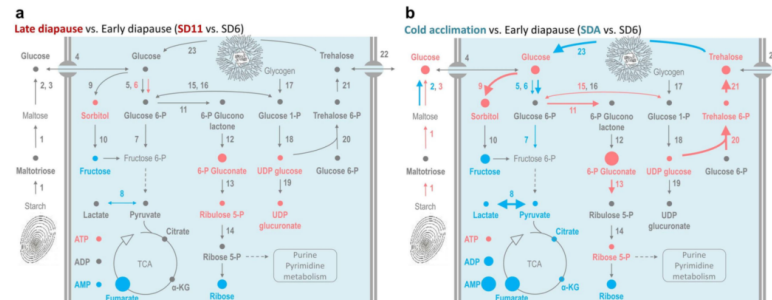
Figure 4. Changes in metabolism of trehalose during diapause maintenance vs. cold acclimation in *C. costata* larvae. The maps show $\log_2$-fold changes in relative concentrations of metabolites (circles) and gene expressions (arrows) during diapause maintenance (**a**) and gradual cold acclimation (**b**) (see Table S5). Other descriptions are as in Figure 2. TCA, tricarboxylic acid cycle; α-KG, ketoglutarate.

The map of trehalose metabolism shows that glucose was also accumulated during cold acclimation (Figure 4b). Note, however, that glucose reached absolute molar concentrations two orders lower than trehalose [20]. Glycogen might be an important source of glucose units as suggested by a trend of total glycogen accumulation during early diapause, followed by its partial depletion during cold acclimation (Figure 5a). A similar depletion trend has been stereotypically observed in many diapausing insects, and glycogen is thought to be the major source for accumulation of various sugar-derived CPs in insects [13,28,30]. The total pool of trehalose is approximately 79 nmoles (27 µg) in an average SDA-larva, while only 34 nmoles 9 (11.6 µg) are found in an SD11-larva [20]. The accumulation of $79 - 34 = 45$ nmoles of trehalose can be explained if only breakdown of glycogen is considered. We may assume that: (i) the cold-acclimation-linked depletion of glycogen represents 34.3 µg.mg^{-1} DM (Figure 5a i.e., 17.1 µg per larva); (ii) this amount of glycogen can release about 145 nmoles of glucose, from which about 72 nmoles of trehalose can be synthesized. The gene coding for a key enzyme of glycogen degradation, *glycogen phosphorylase* (no. 17) showed little change in expression upon cold acclimation (a 1.3-fold decrease, Table S5) and the total enzymatic activity of glycogen phosphorylase was significantly lower in SDA-larvae compared to other phenotypes. At least, we observed a relatively high contribution of the active 'a' form to total glycogen phosphorylase activity in cold-acclimated SDA larvae (Figure 5b). This is in accordance with the well-described process of cold activation of glycogen phosphorylase that initiates synthesis of sugar-derived CPs in insects [32].

In addition to the internal source of glucose units (glycogen), large amounts of glucose are available in the larval diet (11.6 mmol.kg^{-1} FM or 109.9 mmol.kg^{-1} DM; Table S4). Thus, the ingested diet may serve as an additional source of glucose for diapausing, cold-acclimated larvae. The diet also contains starch and maltose (maltose in concentration of 3.6 mmol.kg^{-1} FM or 33.9 mmol.kg^{-1} DM; Table S4), and the transcriptomic data suggest that digestion of starch and maltose might be enhanced in SDA larvae (see the increasing expression of amylases and maltase, nos. 1 and 3 in Figure 4b). However, this was not confirmed by direct assay of enzyme activities; the combined activity of general amylases and maltases decreased sharply during cold acclimation (Figure 5c). Overall, our results suggest that glycogen is the main source of glucose units for trehalose synthesis and accumulation, whereas the diet may serve as an additional source.
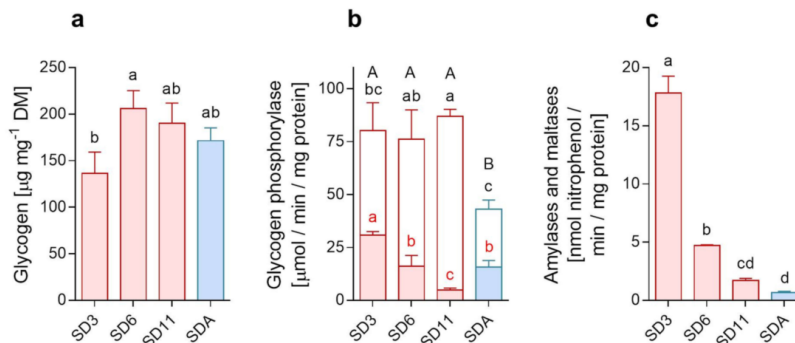
Figure 5. Glycogen, glycogen phosphorylase, amylases and maltases. Changes in (**a**) the total glycogen content, and the activities of (**b**) glycogen phosphorylase (white portions of the columns represent active form 'a' and colored portions inactive form 'b'), and (**c**) amylases and maltases. All analyses were performed in extracts of whole body larvae of different acclimation variants (diapause maintenance: SD3, SD6, SD1 (red columns); cold acclimation: SDA (blue column); see Table 1)). Each column is a mean of 3 biological replicates. Means were compared using one-way ANOVAs followed by Bonnferoni's multiple comparison tests (different letters indicate significantly different means; in panel b: the capital letters show differences between total activities, while the lower-case letters show differences between activities of the inactive (red font) and active (black font) forms of the glycogen phosphorylase).

2.3. Betaine, Other Methylamines and Related Compounds

Complete results of metabolomics and transcript analysis are presented in Table S6, while the differences between diapause maintenance and cold acclimation-linked metabolisms are graphically presented in Figure 6. During cold acclimation, the chromatographic peak area of betaine increased 1.6-fold and the gene coding for betaine transporter (no. 12) was upregulated 2-fold (Figure 6b, Table S6). In contrast, betaine decreased slightly (by 1.3-fold) and no change in transporter expression was observed during diapause maintenance (Figure 6a, Table S6). The absolute concentration of betaine in hemolymph of SDA-larvae (6 mmol.L^{-1}, [22]) was relatively low compared to that observed in plants under various types of environmental stress: tens to hundreds of mmol.kg^{-1} [52]; or halophilic prokaryotes: over 1 mol.kg^{-1} [53]. Nevertheless, genetic manipulations of *Arabidopsis* metabolism show that accumulations of just millimolar concentrations of betaine significantly improve plant tolerance to various stresses including cold and freezing [54,55].

Animals, plants, and bacteria synthesize betaine from choline via a two-step oxidation pathway [56,58] and may further convert betaine to DMG (dimethylglycine) and sarcosine (methylglycine) by activities of BHMT and DMGDH enzymes (see Figure 6 for more details). Only some halophilic prokaryotes can synthesize betaine from glycine via a three-step methylation, which requires specific activity of two methyltransferases (EC 2.1.1.156 and EC 2.1.1.161) [57]. Because the potential degradation of collagens would produce a large excess of glycine (discussed above) and because cold acclimation is accompanied by concerted increases in sarcosine (methylglycine), dimethylglycine, and betaine (trimethylglycine) concentrations (Figure 6b), we investigated whether a 'halophile-like' three-step methylation pathway contributes to betaine biosynthesis in *C. costata* larvae. Using fluxomics LC-HRMS analysis of ^{13}C-labelled compounds, we found no support for a halophile pathway in *C. costata* i.e., conversion of ^{13}C-glycine beyond sarcosine was not possible in whole non-diapause (LD) larvae (Figure 7) or in isolated fat body and muscle dissected from non-diapause and diapause (SDA) larvae (Figure S2). In contrast, we found good support for the classical animal pathway; i.e., ^{13}C-choline was converted not only to betaine but also to DMG, sarcosine, and glycine (Figure 7 and Figure S2).
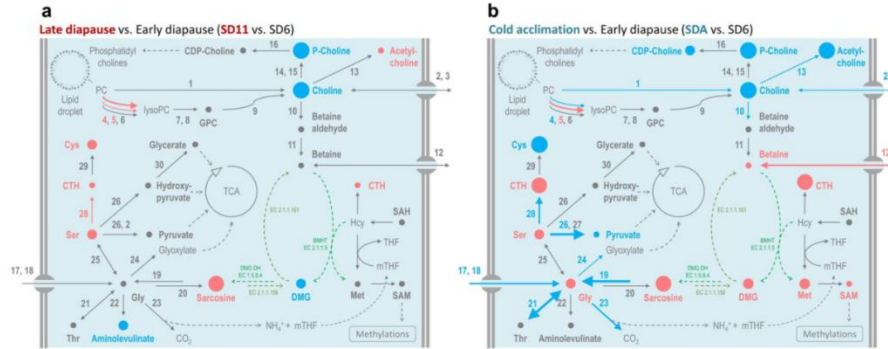
Figure 6. Changes in metabolism of betaine during diapause maintenance and cold acclimation. The maps show log2-fold changes in relative concentrations of metabolites (circles) and gene expressions (arrows) during diapause maintenance (**a**) and gradual cold acclimation (**b**) (see Table S6). Other descriptions are as in Figure 2. TCA, tricarboxylic acid cycle; DMG, dimethylglycine; SAM, S-adenosylmethionine; SAH, S-adenosylhomocysteine; (m)THF, (methyl-) tetrahydrofolate; (lyso)PC, (lyso) phosphatidylcholine; GPC, glycerol 3-phosphocholine; BHMT (EC 2.1.1.5), betaine homocysteine methyltransferase; DMGDH (EC 1.5.8.4), DMG dehydrogenase; EC 2.1.1.156, sarcosine DMG methyltransferase; EC 2.1.1.161, DMG betaine methyltransferase.
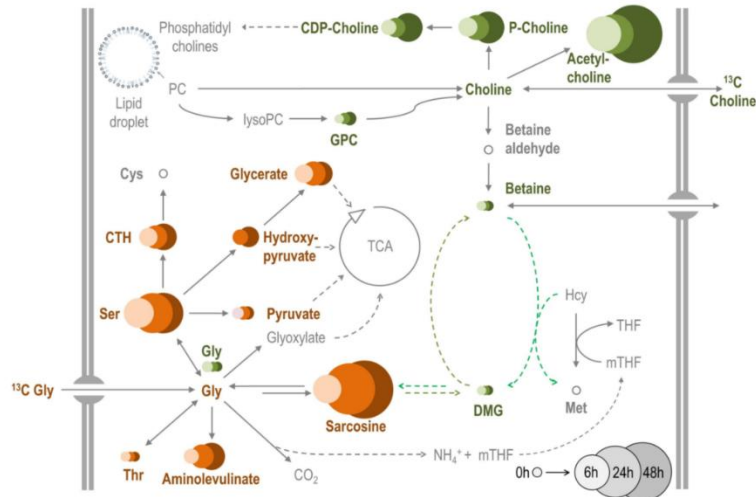
Figure 7. Fluxomics of potential metabolic precursors of betain in *C. costata* larvae. The map shows the metabolic destiny of two ^{13}C-labelled compounds (^{13}C-glycine, brown circles; 1,2-[13]C2 choline chloride, green circles) added to the diet of 15 d-old non-diapause (LD) larvae. The larvae were fed on these diets for 6 h, 24 h, or 48 h (6 h is the smallest and lightest circle on the left of the triplet) after which they were processed and analyzed using LC-HRMS metabolomic platform (for more detail, see Materials and Methods). The results are expressed for each metabolite as a percentage of the peak area of ^{13}C-form (subtracting the native occurrence of ^{13}C-carbon) relative to ^{12}C-form (100% is the 0 h small circle in the legend). The size of circles is proportional to the percentage of the ^{13}C-form. For reference to enzymes (arrows), see Figure 6.

The origin of choline itself, however, remains unclear. It was shown that insects cannot synthesize choline and this must be supplied by the diet [68,69]. Nevertheless, the presence of an ortholog of *GPC phosphodiesterase* gene in genomes of *D. melanogaster* (CG2818) or *C. costata* (no. 9 in Figure 6, Table S6) suggests that flies can release choline from GPC, similarly to its release in mammals [70].

The consistently increasing concentrations of GPC and GPE during diapause maintenance and cold acclimation (Table S6) are likely related to the remodeling of membrane phospholipids that accompanies the entry into diapause and cold acclimation of *C. costata* larvae [71]. The increases in GPC an d GPE concentrations were consistent during transition from SD3 to SDA but often <0.58 $\log_2$-fold (Table S6) during each step of acclimation, which is why they do not appear in red symbols in the metabolic map (Figure 6b). GPC together with sorbitol, betaine, and myo-inositol are believed to play a role as compatible osmolytes in kidney medulla cells, counteracting the high interstitial concentrations of perturbing Na^+ ions and urea [70,72,73]. The GPC concentrations in the inner kidney medulla of various mammals reach tens of $mmol.kg^{-1}$ FM [74]. The absolute concentrations of GPC (2.9 $mmol.L^{-1}$) and GPE (4.0 $mmol.L^{-1}$) in SDA-larval hemolymph [22] are much lower than in mammalian kidney.

We have not measured the absolute concentrations of GPC, GPE and methylamines in larval whole body in our earlier work [20]. Based on hemolymph and tissue concentrations, however, we can estimate sum mass of accumulated GPC, GPE, betaine, and sarcosine as representing approximately 10 moles per SDA larva (corresponding to approximately 2 µg). Though these absolute amounts are relatively low compared to proline or trehalose, the role of GPC, GPE and methylamines in cryoprotective mixtures deserves further investigation in future. Collectively, our results suggest that GPC and GPE are metabolized and accumulated in *C. costata* larvae in association with membrane phospholipid conversions. Betaine is synthesized, as in other animals, from choline via a two-step oxidation pathway.

3. Materials and Methods

3.1. Insects

A colony of *C. costata*, Sapporo strain (Riihimaa and Kimura, 1988) was reared on an artificial diet in MIR 154 incubators (Sanyo Electric, Osaka, Japan) as described previously [75,76]. Four phenotypic variants (SD3, SD6, SD11, and SDA, Table 1) of the 3rd instar larvae were generated according to our earlier acclimation protocols [19,20] as described in Figure 8.

3.2. Extraction of Metabolites and LC-HRMS Platform

Analyses were performed for whole *C. costata* larvae (pools of 5 larvae taken in 4 replicates). The larvae were weighed to obtain fresh mass, plunged into LN_2, and stored at -80 °C until analysis. Frozen samples were melted on ice and homogenized in 400 µL of extraction buffer: methanol:acetonitrile:deionized water mixture (2:2:1, *v/v/v*). The methanol and acetonitrile (Optima™ LC/MS) were purchased from Fisher Scientific (Pardubice, Czech Republic) and the deionized water was prepared using Direct Q 3UV (Merck, Prague, Czech Republic). Internal standards, *p*-fluoro-DL-phenylalanine, methyl α-D-glucopyranoside (both from Sigma-Aldrich, Saint Luis, MI, USA) were added to the extraction buffer, both at a final concentration of 200 $nmol.mL^{-1}$. Samples were homogenized using a TissueLyser LT (Qiagen, Hilden, Germany) set to 50 Hz for 5 min (with a rotor pre-chilled to -20 °C). Homogenization and centrifugation (at 20,000× *g* for 5 min at 4 °C) was repeated twice and the two supernatants were combined.
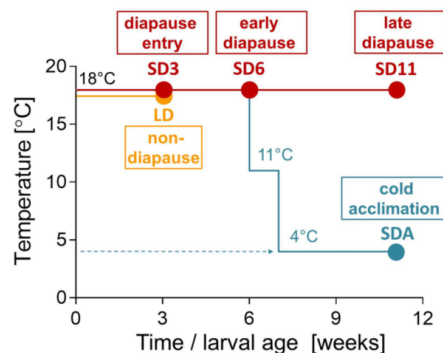
Figure 8. Phenotypic/acclimation variants of *Chymomyza costata*. *C. costata* flies were reared from eggs (time 0) to 3rd larval instars (time 3 weeks) at 18 °C under long-day photoperiod (LD; L16h:D8h, which allows direct non-diapause development to pupa and adult; orange line) or short-day photoperiod (SD; L12h:D12h, which induces diapause). Diapausing larvae then either remained at 18 °C and SD to maintain diapause (SD3, SD6, SD11; red line) or were transferred to constant darkness and progressively cold acclimated over five weeks (SDA; blue line). Note that non-diapause larvae (LD) were not used in this study except as controls for BB-food intake experiments and for ^{13}C-precursor fluxomics. Filled circles indicate sample points for LC-HRMS metabolomics analyses and RNA extraction for RT-qPCR analysis of relative gene expression.

In the whole-body extracts, we performed relative quantification analyses of 56 select metabolites (listed in Table S1) using the LC-HRMS platform on the Q Exactive Plus high resolution Orbitrap mass spectrometer coupled to a Dionex Ultimate 3000 liquid chromatograph and a Dionex open autosampler (all from ThermoFisher Scientific, Waltham, MA, USA). Full scan LC-HRMS positive and negative ion mass spectra were recorded in separate runs with a mass range of 70–1000 Da at 70,000 resolution (at mass m/z 200). The LC-HRMS settings were: scan rate at ±3 Hz, 3×106 automatic gain control (AGC) target, and maximum ion injection time (IT) 100 ms. Source ionization parameters were as follows: ($\pm$) 3000 kV spray voltage, 350 °C capillary temperature, sheath gas at 60 au, aux gas at 20 au, spare gas at 1 au, probe temperature 350 °C, and S-Lens level at 60 au. For accurate mass identification, we used lock masses of 622.0290 Da for the positive ion mode and 301.9981 Da for the negative ion mode. Chromatographic separation of metabolites was carried out on the SeQuant ZIC-pHILIC (150 mm × 4.6 mm i.d., 5 μm, Merck, Darmstadt, Germany), the mobile phase flow rate was 450 μL/min; the injection volume, 5 μL; column temperature, 35 °C. The mobile phase: A = acetonitrile (ThermoFisher Scientific, Waltham, MA, USA). B = 20 mM aqueous ammonium carbonate (pH = 9.2 adjusted by NH_4OH, Sigma-Aldrich); gradient: 0 min, 20% B; 20 min, 80% B; 20.1 min, 95% B; 23.3 min, 95% B; 23.4 min, 20% B; 30.0 min 20% B. Data were acquired and metabolites identified using an in-house Metabolite Mapper platform equipped with an internal metabolite database in conjunction with Xcalibur™ software (v2.1, ThermoFisher Scientific, Waltham, MA, USA). All 56 metabolites were quantified relatively using the areas under respective chromatographic peaks normalized to fresh mass of larval samples.

3.3. Target Gene Sequences and Gene Expression Analysis

Sequences putatively coding for 95 target genes (listed in Table S2) involved in CP metabolism, and five reference genes, were retrieved from a *C. costata* Illumina RNAseq database (ArrayExpress accession E-MTAB-3620) published earlier [77]. Using the Geneious R9.1.8 platform (Biomatters Ltd., Auckland, New Zealand), we used the BLASTn tool to align the *C. costata* target gene sequences with those most similar to sequences of *D. melanogaster* (Table S2). Next, we designed optimal oligonucleotide PCR primer pairs for

all sequences using Geneious, observing uniform criteria such as small PCR product size (70–200 bp), optimal size of primer (20 bp), optimal primer T_m (61 °C), optimal percentage of GC (50%), etc. (all primer pairs given Table S2).

We used RT-qPCR to compare the relative gene expressions of four diapause larval phenotypes (SD3, SD6, SD11, SDA) as described earlier [77]. LD larvae were excluded from these comparisons, as substantial differences in their gene expression relative to SD larvae [26] would obscure our ability to detect differences among SD variants. We extracted total RNA from larvae (pools of 30 larvae were taken in 3 biological replicates) using RNA Blue (Top-Bio, Vestec, Czech Republic), levelled to exactly 1 $\mu g.\mu L^{-1}$ sterile water and treated with DNase I (Invitrogen, ThermoFisher Sci., Prague, Czech Republic). We then converted 5 µg of total RNA to cDNA using Superscript III (Invitrogen, Carlsbad, CA, USA). The cDNA products (20 µL) were diluted 25 times with sterile water. We performed qPCR with a CFX Connect PCR Cycler (BioRad, Philadelphia, PA, USA), using the oligonucleotide primers shown in Table S3 [21]. Relative ratios of the target gene mRNA to the geometric mean of the levels of five reference gene mRNAs were calculated as ddC_T [26,78].

3.4. Supplementary Assays to Clarify the Metabolism of CPs
3.4.1. A Brilliant Blue Larval Food Intake Assay

A Brilliant Blue Larval Food Intake Assay [79] was used to assess whether larvae in diapause ingest food. In a preliminary assay, we verified that 100% of non-diapause (LD) larvae (n = 25) will intake larval diet mixed with 0.1% Brilliant Blue R dye (Sigma) (BB diet). The LD larvae were transferred to BB diet for 1 h at constant 18 °C, after which they were observed and photographed under a dissecting microscope. Food intake was apparent as blue coloration of the gut. Next, the larvae of different diapause acclimation variants (SD6, SDA7, and SDA9) were used for the BB assay as shown in Figure 3a.

3.4.2. Total Proteins

Whole *C. costata* larvae (pools of 5 larvae taken in 3 replicates) were homogenized and total proteins were extracted twice in 400 µL of 50 mM Tris buffer, pH 7.2, containing 100 mM NaCl, 1% deoxycholate, 0.2% SDS, and 1% Nonidet. Total proteins were determined by bicinchoninic acid assay (BCA) [80].

3.4.3. PAGE

The extracts of total proteins (see above) were levelled to equal protein concentration of 1 mg.mL^{-1}, mixed with 4× Loading buffer (LB) in a volume ratio 1:3, and heated at 95 °C for 10 min (the LB contained: 2 mL 1M Tris-HCl, pH 6.8; 4 mL 1M dithiothreitol; 0.8 g sodium dodecylsulphate (SDS); 40 mg bromphenol blue (BPB); and 3.2 mL glycerol in 10 mL of distilled water). Aliquots were loaded (20 µL per lane) onto precast 12% MiniProtean TGX gels (BioRad, Hercules, CA, USA) and separated by polyacrylamide gel electrophoresis (PAGE) using Mini-Protean Tetra Cell apparatus (Biorad). The gels were run in a classical Tris-Glycine-SDS buffer, pH 8.3 at a constant voltage of 150 V until BPB left the gel. Protein bands were stained with Coommassie Brilliant Blue and band densities were measured using Gel Analyzer function of ImageJ software (https://imagej.nih.gov/ij/; accessed on 15 November 2021) (for more information, see Figure S1).

3.4.4. Total Collagen

Total collagen in larvae was estimated based on the release of 4-hydroxyproline upon acidic hydrolysis of total larval proteins according to [81]. Whole *C. costata* larvae (pools of 5 larvae taken in 3 replicates) were homogenized in 100 µL of distilled water. Next, 100 µL of concentrated HCl (12 M) was added to the homogenate in a glass tube caped tightly with a Teflon insert. The sample was hydrolyzed at 120 °C for 3 h, after which 5 mg of activated charcoal was added and the sample was centrifuged at 3000 g for 5 min. Then, 50 µL of supernatant was moved to a clean vial and dried at 60 °C under stream nitrogen and stored at −80 °C until LC-HRMS analysis of 4-hydroxyproline was performed.

3.4.5. Collagenase

Collagenase activity was assayed using the fluorimetric MMP Activity Assay Kit (ab112147, Abcam, Cambridge, UK) according to the manufacturer's manual. Whole *C. costata* larvae (pools of 5 larvae taken in 3 replicates) were homogenized and total proteins were extracted in 500 μL of 100 mM Tris buffer, pH 7.2. A 25 μL aliquot of supernatant was used as a source of enzymatic activity. We measured the increase in fluorescence over time (15 min at constant 25 °C) at 540/590 nm (Ex/Em) using the microplate reader Infinite 200Pro (Tecan) and normalized the slopes of linear regressions to mg of total protein (BCA assay, see above) in the sample aliquot.

3.4.6. Glycogen

Whole *C. costata* larvae (pools of 5 larvae taken in 3 replicates) were homogenized twice in 400 μL of a methanol:acetonitrile:water mixture. After centrifugation at $20,000 \times g$ for 10 min at 4 °C, glycogen was extracted from the pellet in hot alkali [82] and quantified by colorimetric assay with phenol and concentrated sulphuric acid [83].

3.4.7. Glycogen Phosphorylase

Whole *C. costata* larvae (pools of 10 larvae taken in 3 replicates) were homogenized in 600 μL of 100 mM Tris-HCl buffer, pH 8.0 containing 15 mM mercaptoethanol and 1 mM EDTA. The activity of active ('a') and inactive forms ('b') of the enzyme were measured in 70 μL aliquots of supernatant as described by [84] and normalized to mg of total protein (BCA assay, see above) in the sample aliquot. The reaction mixture contained 50 mM potassium phosphate buffer, pH 6.8; 5 mg mL^{-1} glycogen (omitted from control), 5 μM glucose-1,6-diphosphate, 0.6 mM NADP, 2 mM 5′AMP, 15 mM MgCl$_2$, 2 U mL^{-1} phosphoglucomutase, and 2 U mL^{-1} glucose 6-P dehydrogenase. The active form of the enzyme was measured in the absence of 5′AMP.

3.4.8. Amylases and Maltases

Whole *C. costata* larvae (pools of 10 larvae taken in 3 replicates) were homogenized in 1 mL of Assay Buffer supplied in the Amylase Assay Kit (ab102523, Abcam, Cambridge, UK) and 50 μL aliquots of supernatant were used as sources of enzymatic activity. We measured the increase of absorbance over time (15 min at constant 25 °C) at 405 nm using the microplate reader Infinite 200Pro (Tecan, Männedorf, Switzerland), converted this to nmoles of released nitrophenol (using the calibration nitrophenol standards), and normalized the results to mg of total protein (BCA assay, see above) in the sample aliquot.

3.4.9. Fluxomics of ^{13}C-Labelled Metabolic Precursors of Betaine

We performed assays for (i) whole non-diapause (LD) larvae fed a standard diet augmented with ^{13}C-labelled metabolic precursors and (ii) tissues dissected from non-diapause (LD) and diapause (SDA) larvae. The examination of the tissues allowed us to rule out possible contribution of microbes to metabolic conversions in the larval diet or inside the larval gut. The tissues were incubated in Schneider's *Drosophila* medium (Biosera, Nuaille, France) augmented with ^{13}C-labelled metabolic precursors purchased from Cambridge Isotope Laboratories (Tewksbury, MA, USA). The ^{13}C-glycine had both carbons labelled (item no. CLM-1017, m.w. 77.05) and the ^{13}C-choline chloride had two carbons labelled (1,2-^{13}C2 choline chloride, item no. CLM-548, m.w. 141.61).

(i) Whole larvae: suitable doses of ^{13}C-labelled precursors in larval diets (^{13}C-glycine, 15 mg per g of diet; ^{13}C-choline chloride, 20 mg per g of diet) were derived from preliminary experiments showing that lower doses have no effect on the timing of larval development, a 'suitable' dose causes a small (2–3 d) delay in timing of pupariation but no mortality, and higher doses cause longer developmental delays and mortality. Third instar LD larvae (15–16 d old) were transferred from a standard diet to a ^{13}C-precursor-augmented diet for 6, 24, or 48 h at constant 18 °C (20 larvae per vial with 1 g of diet). Next, larvae were processed for LC-HRMS analysis.

(ii) Dissected tissues: larval fat body and muscle tissues were dissected from a group of 50 larvae (either LD- or SDA-larvae) into the wells of a 12-well tissue culture plate (TRP, Switzerland) containing 650 μL of Schneider's medium supplemented with 100 mM of either ^{13}C-glycine or ^{13}C-choline chloride. After 3 h (LD) or 6 h (SDA) incubation at 22 °C, the tissues were rinsed in Schneider's medium and processed for LC-HRMS analysis. Results of LC-HRMS analyses were expressed for each target metabolite as a percentage of the peak area of ^{13}C-form (subtracting the native occurrence of ^{13}C-carbon) relative to the ^{12}C-form.

4. Conclusions

Here we show that diapausing and cold-acclimated larvae of *C. costata* continue with food ingestion and the diet serves as important source of direct assimilation of, and/or metabolic conversions to, cryoprotective molecules. We show that even the complete degradation of larval reserves of total protein, including collagens, would not suffice to explain accumulation of proline. Moreover, total protein or collagen reserves are depleted only moderately or not at all, respectively, during cold acclimation. We identified direct assimilation of dietary amino acids proline and glutamate, plus metabolic conversion of glutamine reserves, as two major sources of proline accumulation. In agreement with general consensus on metabolic origin of sugar-based CPs, we show that trehalose is sourced mainly from internal glycogen depots that are filled during early diapause and partially depleted during subsequent cold acclimation. Lastly, we suggest that the accumulations of GPC and GPE result from cold-acclimation-linked remodeling of phospholipids. Choline, either released from GPC or assimilated from diet, serves as a source for accumulation of methylamines betaine and sarcosine.

References

1. Somero, G. Protons, osmolytes, and fitness of internal milieu for protein function. *Am. J. Physiol. Regul. Integr. Comp. Physiol.* **1986**, *251*, R197–R213. [CrossRef] [PubMed]
2. Yancey, P.H. Organic osmolytes as compatible, metabolic and counteracting cytoprotectants in high osmolarity and other stresses. *J. Exp. Biol.* **2005**, *208*, 2819–2830. [CrossRef]

3. Yancey, P.H.; Siebenaller, J.F. Co-evolution of proteins and solutions: Protein adaptation versus cytoprotective micromolecules and their roles in marine organisms. *J. Exp. Biol.* **2015**, *218*, 1880–1896. [CrossRef] [PubMed]

4. Hochachka, P.; Somero, G. *Biochemical Adaptation. Mechanism and Process in Physiological Evolution*; Oxford University Press: Oxford, UK, 2002; p. 478.

5. Lee, R.E.J. A primer on insect cold-tolerance. In *Low Temperature Biology of Insects*; Denlinger, D.L., Lee, R.E.J., Eds.; Cambridge University Press: Cambridge, UK, 2010.

6. Toxopeus, J.; Sinclair, B.J. Mechanisms underlying insect freeze tolerance. *Biol. Rev.* **2018**, *93*, 1891–1914. [CrossRef]

7. Teets, N.M.; Denlinger, D.L. Physiological mechanisms of seasonal and rapid cold-hardening in insects. *Physiol. Entomol.* **2013**, *38*, 105–116. [CrossRef]

8. Storey, K.B. Organic solutes in freezing tolerance. *Comp. Biochem. Physiol. A* **1997**, *117*, 319–326. [CrossRef]

9. Salt, R. Principles of insect cold-hardiness. *Annu. Rev. Entomol.* **1961**, *6*, 55–74. [CrossRef]

10. Lee, R.E. Principles of insect low temperature tolerance. In *Insects at Low Temperature*; Springer: Berlin/Heidelberg, Germany, 1991; pp. 17–46.

11. Zachariassen, K.E. Physiology of cold tolerance in insects. *Physiol. Rev.* **1985**, *65*, 799–832. [CrossRef]

12. Holmstrup, M.; Westh, P. Dehydration of earthworm cocoons exposed to cold: A novel cold hardiness mechanism. *J. Comp. Physiol. B* **1994**, *164*, 312–315. [CrossRef]

13. Hayakawa, Y.; Chino, H. Temperature-dependent interconversion between glycogen and trehalose in diapausing pupae of *Philosamia cynthia ricini* and *pryeri*. *Insect Biochem.* **1981**, *11*, 43–47. [CrossRef]

14. Storey, J.M.; Storey, K.B. Winter survival of the gall fly larva, *Eurosta solidaginis*: Profiles of fuel reserves and cryoprotectants in a natural population. *J. Insect Physiol.* **1986**, *32*, 549–556. [CrossRef]

15. Rickards, J.; Kelleher, M.J.; Storey, K.B. Strategies of freeze avoidance in larvae of the goldenrod gall moth, *Epiblema scudderiana*: Winter profiles of a natural population. *J. Insect Physiol.* **1987**, *33*, 443–450. [CrossRef]

16. Koštál, V.; Tollarova, M.; Šula, J. Adjustments of the enzymatic complement for polyol biosynthesis and accumulation in diapausing cold-acclimated adults of *Pyrrhocoris apterus*. *J. Insect Physiol.* **2004**, *50*, 303–313. [CrossRef] [PubMed]

17. Storey, J.M.; Storey, K.B. Triggering of cryoprotectant synthesis by the initiation of ice nucleation in the freeze tolerant frog, *Rana sylvatica*. *J. Comp. Physiol. B* **1985**, *156*, 191–195. [CrossRef]

18. Calderon, S.; Holmstrup, M.; Westh, P.; Overgaard, J. Dual roles of glucose in the freeze-tolerant earthworm *Dendrobaena octaedra*: Cryoprotection and fuel for metabolism. *J. Exp. Biol.* **2009**, *212*, 859–866. [CrossRef]

19. Koštál, V.; Zahradníčková, H.; Šimek, P. Hyperprolinemic larvae of the drosophilid fly, *Chymomyza costata*, survive cryopreservation in liquid nitrogen. *Proc. Natl. Acad. Sci. USA* **2011**, *108*, 13041–13046. [CrossRef]

20. Rozsypal, J.; Moos, M.; Šimek, P.; Koštál, V. Thermal analysis of ice and glass transitions in insects that do and do not survive freezing. *J. Exp. Biol.* **2018**, *221*, 170464. [CrossRef]

21. Des Marteaux, L.E.; Hůla, P.; Koštál, V. Transcriptional analysis of insect extreme freeze tolerance. *Proc. R. Soc. B* **2019**, *286*, 20192019. [CrossRef]

22. Kučera, L.; Moos, M.; Štetina, T.; Korbelová, J.; Vodrážka, P.; Marteaux, L.D.; Grgac, R.; Hula, P.; Rozsypal, J.; Faltus, M.; et al. A mixture of innate cryoprotectants is key for freeze tolerance and cryopreservation of a drosophilid fly larva. *bioRxiv* **2022**.

23. Denlinger, D.L. Relationship between cold hardiness and diapause. In *Insects at Low Temperature*; Lee, R.E., Denlinger, D.L., Eds.; Chapmann and Hall: New York, NY, USA, 1991; pp. 174–198.

24. MacRae, T.H. Gene expression, metabolic regulation and stress tolerance during diapause. *Cell. Mol. Life Sci.* **2010**, *67*, 2405–2424. [CrossRef]

25. Ragland, G.J.; Denlinger, D.L.; Hahn, D.A. Mechanisms of suspended animation are revealed by transcript profiling of diapause in the flesh fly. *Proc. Natl. Acad. Sci. USA* **2010**, *107*, 14909–14914. [CrossRef] [PubMed]

26. Koštál, V.; Štětina, T.; Poupardin, R.; Korbelová, J.; Bruce, A.W. Conceptual framework of the eco-physiological phases of insect diapause development justified by transcriptomic profiling. *Proc. Natl. Acad. Sci. USA* **2017**, *114*, 8532–8537. [CrossRef] [PubMed]

27. Hahn, D.A.; Denlinger, D.L. Energetics of insect diapause. *Annu. Rev. Entomol.* **2011**, *56*, 103–121. [CrossRef] [PubMed]

28. Storey, K.B.; Storey, J.M. Biochemistry of cryoprotectants. In *Insects at Low Temperature*; Springer: Berlin/Heidelberg, Germany, 1991; pp. 64–93.

29. Šlachta, M.; Vambera, J.; Zahradníčková, H.; Košťál, V. Entering diapause is a prerequisite for successful cold-acclimation in adult *Graphosoma lineatum* (Heteroptera: Pentatomidae). *J. Insect Physiol.* **2002**, *48*, 1031–1039. [CrossRef]

30. Hayakawa, Y. Activation mechanism of insect fat body phosphorylase by cold phosphorylase kinase, phosphatase and ATP level. *Insect Biochem.* **1985**, *15*, 123–128. [CrossRef]

31. Storey, K.B.; Storey, J.M. Biochemical strategies of overwintering in the gall gly larva, *Eurosta solidaginis*: Effect of low temperature acclimation on the activities of enzymes of intermediary metabolism. *J. Comp. Physiol.* **1981**, *144*, 191–199. [CrossRef]

32. Storey, K.B.; Storey, J.M. Insect cold hardiness: Metabolic, gene, and protein adaptation. *Can. J. Zool.* **2012**, *90*, 456–475. [CrossRef]

33. Storey, K.B.; Storey, J.M. Molecular biology of freezing tolerance. *Compr. Physiol.* **2013**, *3*, 1283–1308.

34. Pfister, T.D.; Storey, K.B. Insect freeze tolerance: Roles of protein phosphatases and protein kinase A. *Insect Biochem. Mol. Biol.* **2006**, *36*, 18–24. [CrossRef]

35. Wanner, L.A.; Junttila, O. Cold-induced freezing tolerance in Arabidopsis. *Plant Physiol.* **1999**, *120*, 391–400. [CrossRef]

36. Nagao, M.; Minami, A.; Arakawa, K.; Fujikawa, S.; Takezawa, D. Rapid degradation of starch in chloroplasts and concomitant accumulation of soluble sugars associated with ABA-induced freezing tolerance in the moss *Physcomitrella patens*. *J. Plant Physiol.* **2005**, *162*, 169–180. [CrossRef]

37. Morgan, T.; Chippendale, G. Free amino acids of the haemolymph of the southwestern corn borer and the European corn borer in relation to their diapause. *J. Insect Physiol.* **1983**, *29*, 735–740. [CrossRef]

38. Fields, P.G.; Fleurat-Lessard, F.; Lavenseau, L.; Febvay, G.; Peypelut, L.; Bonnot, G. The effect of cold acclimation and deacclimation on cold tolerance, trehalose and free amino acid levels in *Sitophilus granarius* and *Cryptolestes ferrugineus* (Coleoptera). *J. Insect Physiol.* **1998**, *44*, 955–965. [CrossRef]

39. Shimada, K.; Riihimaa, A. Cold acclimation, inoculative freezing and slow cooling: Essential factors contributing to the freezing-tolerance in diapausing larvae of *Chymomyza costata* (Diptera: Drosophilidae). *Cryo Lett.* **1988**, *9*, 5–10.

40. Koštál, V.; Renault, D.; Rozsypal, J. Seasonal changes of free amino acids and thermal hysteresis in overwintering heteropteran insect, *Pyrrhocoris apterus*. *Comp. Biochem. Physiol. Part A Mol. Integr. Physiol.* **2011**, *160*, 245–251. [CrossRef]

41. Koštál, V.; Korbelová, J.; Poupardin, R.; Moos, M.; Šimek, P. Arginine and proline applied as food additives stimulate high freeze tolerance in larvae of *Drosophila melanogaster*. *J. Exp. Biol.* **2016**, *219*, 2358–2367. [CrossRef]

42. Koštál, V.; Šimek, P.; Zahradníčková, H.; Cimlová, J.; Štětina, T. Conversion of the chill susceptible fruit fly larva (*Drosophila melanogaster*) to a freeze tolerant organism. *Proc. Natl. Acad. Sci. USA* **2012**, *109*, 3270–3274. [CrossRef]

43. Li, Y.; Zhang, L.; Chen, H.; Koštál, V.; Simek, P.; Moos, M.; Denlinger, D.L. Shifts in metabolomic profiles of the parasitoid Nasonia vitripennis associated with elevated cold tolerance induced by the parasitoid's diapause, host diapause and host diet augmented with proline. *Insect Biochem. Mol. Biol.* **2015**, *63*, 34–46. [CrossRef]

44. Zhang, L.; Xue, X.; Yan, J.; Yan, L.-Y.; Jin, X.-H.; Zhu, X.-H.; He, Z.-Z.; Liu, J.; Li, R.; Qiao, J. L-proline: A highly effective cryoprotectant for mouse oocyte vitrification. *Sci. Rep.* **2016**, *6*, 1–8. [CrossRef]

45. Dou, M.; Li, Y.; Sun, Z.; Li, L.; Rao, W. L-proline feeding for augmented freeze tolerance of *Camponotus japonicus* Mayr. *Sci. Bull.* **2019**, *64*, 1795–1804. [CrossRef]

46. Li, P.; Wu, G. Roles of dietary glycine, proline, and hydroxyproline in collagen synthesis and animal growth. *Amino Acids* **2018**, *50*, 29–38. [CrossRef]

47. Shoulders, M.D.; Raines, R.T. Collagen structure and stability. *Annu. Rev. Biochem.* **2009**, *78*, 929–958. [CrossRef]

48. Phang, J.M.; Liu, W.; Hancock, C.N.; Fischer, J.W. Proline metabolism and cancer: Emerging links to glutamine and collagen. *Curr. Opin. Clin. Nutr. Metab. Care* **2015**, *18*, 71. [CrossRef]

49. Delauney, A.J.; Verma, D.P.S. Proline biosynthesis and osmoregulation in plants. *Plant J.* **1993**, *4*, 215–223. [CrossRef]

50. Szabados, L.; Savouré, A. Proline: A multifunctional amino acid. *Trends Plant Sci.* **2010**, *15*, 89–97. [CrossRef] [PubMed]

51. Xin, Z. Eskimo1 mutants of Arabidopsis are constitutively freezing-tolerant. *Proc. Natl. Acad. Sci. USA* **1998**, *95*, 7799–7804. [CrossRef] [PubMed]

52. Sakamoto, A.; Murata, N. The role of glycine betaine in the protection of plants from stress: Clues from transgenic plants. *Plant Cell Environ.* **2002**, *25*, 163–171. [CrossRef]

53. Trüper, H.G.; Galinski, E.A. Biosynthesis and fate of compatible solutes in extremely halophilic phototrophic eubacteria. *FEMS Microbiol. Rev.* **1990**, *6*, 247–254. [CrossRef]

54. Sakamoto, A.; Valverde, R.; Chen, T.H.; Murata, N. Transformation of Arabidopsis with the codA gene for choline oxidase enhances freezing tolerance of plants. *Plant J.* **2000**, *22*, 449–453. [CrossRef]

55. Chen, T.H.; Murata, N. Glycinebetaine: An effective protectant against abiotic stress in plants. *Trends Plant Sci.* **2008**, *13*, 499–505. [CrossRef]

56. Figueroa-Soto, C.G.; Valenzuela-Soto, E.M. Glycine betaine rather than acting only as an osmolyte also plays a role as regulator in cellular metabolism. *Biochimie* **2018**, *147*, 89–97. [CrossRef]

57. Sizeland, P.C.; Chambers, S.T.; Lever, M.; Bason, L.M.; Robson, R.A. Organic osmolytes in human and other mammalian kidneys. *Kidney Int.* **1993**, *43*, 448–453. [CrossRef]

58. Pajares, M.A.; Pérez-Sala, D. Betaine homocysteine S-methyltransferase: Just a regulator of homocysteine metabolism? *Cell. Mol. Life Sci. CMLS* **2006**, *63*, 2792–2803. [CrossRef]

59. Nyyssölä, A.; Kerovuo, J.; Kaukinen, P.; von Weymarn, N.; Reinikainen, T. Extreme halophiles synthesize betaine from glycine by methylation. *J. Biol. Chem.* **2000**, *275*, 22196–22201. [CrossRef]

60. Denlinger, D.L. Regulation of diapause. *Annu. Rev. Entomol.* **2002**, *47*, 93–122. [CrossRef]

61. Kivirikko, K.I.; Kishida, Y.; Sakakibara, S.; Prockop, D.J. Hydroxylation of (X-Pro-Gly) n by protocollagen proline hydroxylase Effect of chain length, helical conformation and amino acid sequence in the substrate. *Biochim. Biophys. Acta (BBA) Protein Struct.* **1972**, *271*, 347–356. [CrossRef]

62. Miller, M.M.; Popova, L.B.; Meleshkevitch, E.A.; Tran, P.V.; Boudko, D.Y. The invertebrate B0 system transporter, D. melanogaster NAT1, has unique D-amino acid affinity and mediates gut and brain functions. *Insect Biochem. Mol. Biol.* **2008**, *38*, 923–931. [CrossRef]

63. LaFever, K.S.; Wang, X.; Page-McCaw, P.; Bhave, G.; Page-McCaw, A. Both Drosophila matrix metalloproteinases have released and membrane-tethered forms but have different substrates. *Sci. Rep.* **2017**, *7*, 44560. [CrossRef]

64. Hahn, D.A.; Denlinger, D.L. Meeting the energetic demands of insect diapause: Nutrient storage and utilization. *J. Insect Physiol.* **2007**, *53*, 760–773. [CrossRef]

65. Kostal, V.; Shimada, K.; Hayakawa, Y. Induction and development of winter larval diapause in a drosophilid fly, *Chymomyza costata*. *J. Insect Physiol.* **2000**, *46*, 417–428. [CrossRef]

66. Diener, S.; Zurbrügg, C.; Tockner, K. Conversion of organic material by black soldier fly larvae: Establishing optimal feeding rates. *Waste Manag. Res.* **2009**, *27*, 603–610. [CrossRef]

67. Thompson, S.N. Trehalose—The insect 'blood'sugar. *Adv. Insect Physiol.* **2003**, *31* (Suppl. SC), 205–285.

68. Fraenkel, G.; Friedman, S.; Hinton, T.; Laszlo, S.; Noland, J.L. The effect of substituting carnitine for choline in the nutrition of several organisms. *Arch. Biochem. Biophys.* **1955**, *54*, 432–439. [CrossRef]

69. Geer, B.; Vovis, G.; Yund, M. Choline activity during the development of *Drosophila melanogaster*. *Physiol. Zool.* **1968**, *41*, 280–292. [CrossRef]

70. Gallazzini, M.; Burg, M.B. What's new about osmotic regulation of glycerophosphocholine. *Physiology* **2009**, *24*, 245–249. [CrossRef] [PubMed]

71. Koštál, V.R.; Berková, P.; Šimek, P. Remodelling of membrane phospholipids during transition to diapause and cold-acclimation in the larvae of *Chymomyza costata* (Drosophilidae). *Comp. Biochem. Physiol. B* **2003**, *135*, 407–419. [CrossRef]

72. Burg, M.B.; Ferraris, J.D. Intracellular organic osmolytes: Function and regulation. *J. Biol. Chem.* **2008**, *283*, 7309–7313. [CrossRef] [PubMed]

73. Burg, M.B.; Kwon, E.D.; Peters, E.M. Glycerophosphocholine and betaine counteract the effect of urea on pyruvate kinase. *Kidney Int. Suppl.* **1996**, *57*, 100–104.

74. Garcia-Perez, A.; Burg, M.B. Renal medullary organic osmolytes. *Physiol. Rev.* **1991**, *71*, 1081–1115. [CrossRef]

75. Kostal, V.; Noguchi, H.; Shimada, K.; Hayakawa, Y. Developmental changes in dopamine levels in larvae of the fly *Chymomyza costata*: Comparison between wild-type and mutant-nondiapause strains. *J. Insect Physiol.* **1998**, *44*, 605–614. [CrossRef]

76. Lakovaara, S. Malt as a culture medium for Drosophila species. *Drosoph. Inf. Serv.* **1969**, *44*, 128.

77. Poupardin, R.; Schöttner, K.; Korbelová, J.; Provazník, J.; Doležel, D.; Pavlinic, D.; Beneš, V.; Koštál, V. Early transcriptional events linked to induction of diapause revealed by RNAseq in larvae of drosophilid fly, *Chymomyza costata*. *BMC Genom.* **2015**, *16*, 720. [CrossRef]

78. Pfaffl, M.W. A new mathematical model for relative quantification in real-time RT–PCR. *Nucleic Acids Res.* **2001**, *29*, e45. [CrossRef]

79. Kaun, K.R.; Riedl, C.A.; Chakaborty-Chatterjee, M.; Belay, A.T.; Douglas, S.J.; Gibbs, A.G.; Sokolowski, M.B. Natural variation in food acquisition mediated via a Drosophila cGMP-dependent protein kinase. *J. Exp. Biol.* **2007**, *210*, 3547–3558. [CrossRef]

80. Smith, P.e.; Krohn, R.I.; Hermanson, G.; Mallia, A.; Gartner, F.; Provenzano, M.; Fujimoto, E.; Goeke, N.; Olson, B.; Klenk, D. Measurement of protein using bicinchoninic acid. *Anal. Biochem.* **1985**, *150*, 76–85. [CrossRef]

81. Cross, H.; Carpenter, Z.; Smith, G. Effects of intramuscular collagen and elastin on bovine muscle tenderness. *J. Food Sci.* **1973**, *38*, 998–1003. [CrossRef]

82. Bueding, E.; Orrell, S.A. A mild procedure for the isolation of polydisperse glycogen from animal tissues. *J. Biol. Chem.* **1964**, *239*, 4018–4020. [CrossRef]

83. Dubois, M.; Gilles, K.A.; Hamilton, J.K.; Rebers, P.T.; Smith, F. Colorimetric method for determination of sugars and related substances. *Anal. Chem.* **1956**, *28*, 350–356. [CrossRef]

84. Koštál, V.; Tamura, M.; Tollarová, M.; Zahradníčková, H. Enzymatic capacity for accumulation of polyol cryoprotectants changes during diapause development in the adult red firebug, *Pyrrhocoris apterus*. *Physiol. Entomol.* **2004**, *29*, 344–355. [CrossRef]

Supplementary Figures for:

Accumulation of innate cryoprotective metabolites in a freeze-tolerant insect: internal macromolecular reserves or diet as alternative sources of carbon skeletons.

Martin Moos, Jaroslava Korbelová, Robert Grgac, Tomáš Štětina, Stanislav Opekar, Petr Šimek, Vladimír Koštál

Figure S1   PAGE analysis of total proteins.

Figure S2   Fluxomics of ^{13}C-labelled metabolic precursors of betain.
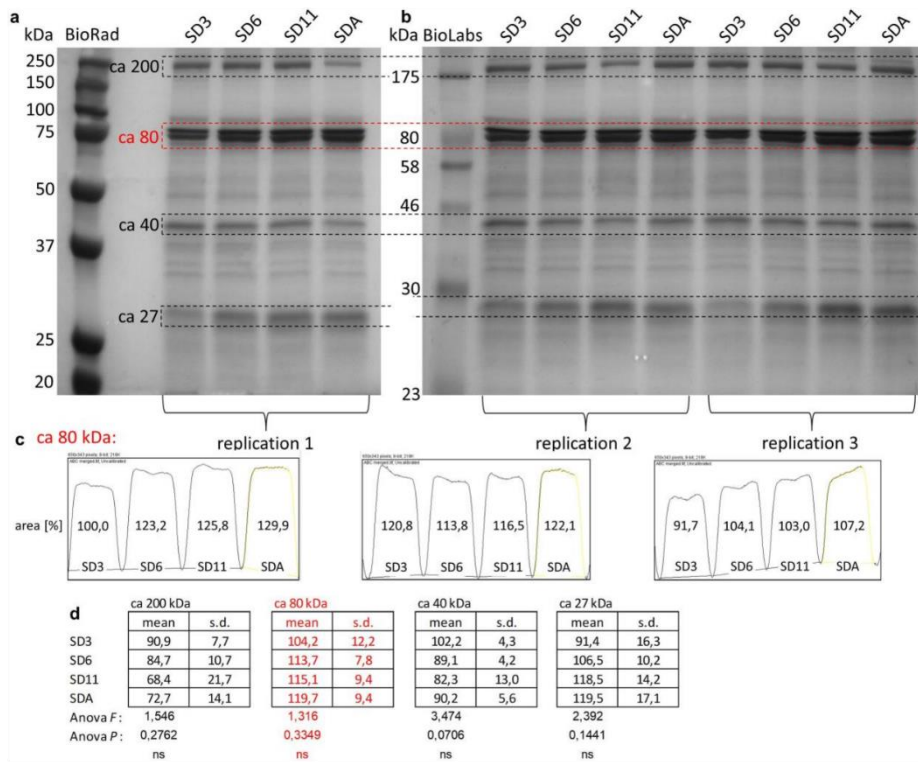
Figure S1: PAGE analysis of total proteins.
Total proteins were extracted from different acclimation variants of larvae of *C. costata* (SD3, SD6, SD11, SDA; for description, see Fig. 8). Protein extracts were loaded onto precast 7.5% MiniProtean TGX gels and separated by polyacrylamide gel electrophoresis (PAGE). Protein bands were stained with Coommassie Brilliant Blue and band densities in selected areas (ca 200, ca 80, ca 40, and ca 27 kDa as delimited by broken rectangles) were compared using ImageJ software. **(a)** First replicate of total protein extracts. BioRad, Precision Plus Protein Dual Color Standards. **(b)** Second and third replicates. BioLabs, ColorPlus Prestained Protein Marker, Broad Range. **(c)** Example of ImageJ analysis for the protein area of ca 80 kDa (red rectangle). Two dense bands are most likely corresponding to Larval serum proteins Lsp1 and Lsp2, which are the most adundant proteins in drosophilid larval hemolymph [1]. The area under density peak of the first band of replication 1 is set to 100% and all other bands are normalized to it. **(d)** Results of statistical analysis using one way Anova (the result for protein area of ca 80 kDa is highlighted in red font). No significant influence of phenotypic variant on density of protein bands was detected (Anova *P* > 0.05; ns, non-significant).

2

38
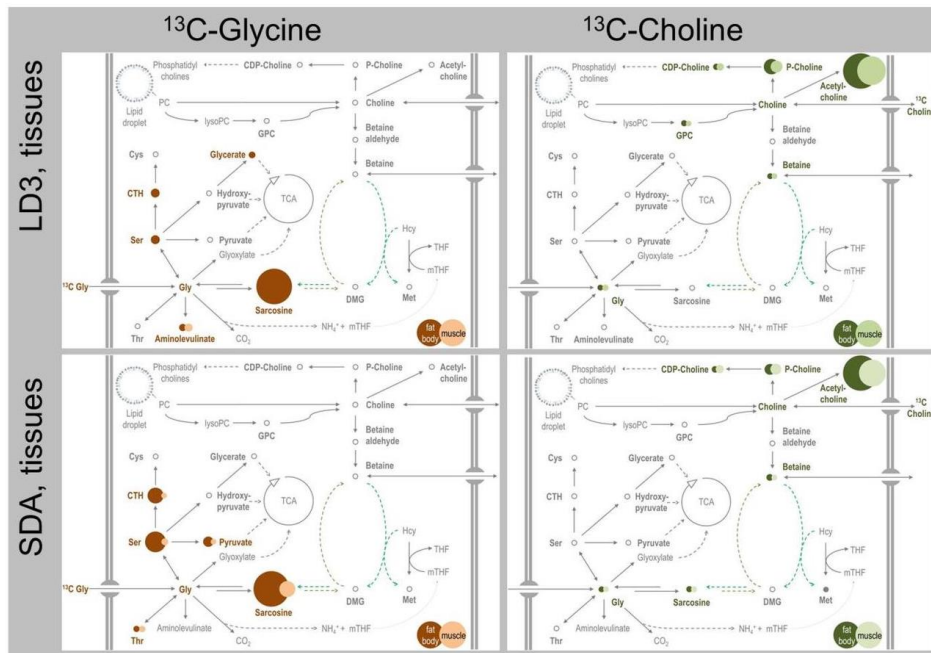
Figure S2: Fluxomics of ¹³C-labelled metabolic precursors of betain.
The maps show metabolic destiny of two ¹³C-labelled compounds (¹³C-glycine, left maps; and 1,2-¹³C2 choline chloride, right maps) added to the medium (Schneider's Drosophila Medium, Biosera), in which fat body and muscle tissues (distinguised by shade as indicated) dissected from LD (3-w-old, upper row) and SDA (11-w-old, lower row) larvae were incubated for 3 h (LD) or 6 h (SDA) and then processed and analyzed using HRMS metabolomics platform (for more detail, see Materials and Methods). The results are expressed for each metabolite as a percentage of the peak area of ¹³C-form (subtracting the native occurrence of ¹³C-carbon) relative to ¹²C-form (100% is a small circle in the Legend, at 0h). The size of circles is proportional to the percentage of ¹³C-form. For reference to enzymes (arrows), see Fig. 6.

Note: Fig. S2 brings basically the same general message as Fig. 6: The ¹³C glycine can be methylated only once, forming sarcosine. Di- and tri-methylation-conversions of glycine to DMG and betaine, respectively, were not observed, which suggests that these conversions, characteristic for microbial halophiles, do not exist in *C. costata* larval tissues. The ¹³C choline chloride can be converted to betaine and also to sarcosine and glycine, which suggests that this classical animal pathway is operational also in *C. costata* larval tissues.

References in Supporting materials

1.   Powell, D.; Sato, J. D.; Brock, H. W.; Roberts, D. B., Regulation of synthesis of the larval serum proteins of Drosophila melanogaster. *Dev. Biol.* **1984,** 102, (1), 206-215.

3

Paper II

A mixture of innate cryoprotectants is key for freeze tolerance and cryopreservation of a drosophilid fly larva

Kučera, L., Moss, M., Štětina T., Korbelová, J., Vodrážka, P., Des Marteaux, L., Grgac, R., Hůla, P., Rozsypal, J., Faltus, M., Šimek, P., Sedlacek, R., & Koštál, V. (2022)

The Company of **Biologists**

RESEARCH ARTICLE

A mixture of innate cryoprotectants is key for freeze tolerance and cryopreservation of a drosophilid fly larva

Lukáš Kučera[1,‡], Martin Moos[2,‡], Tomáš Štětina[2], Jaroslava Korbelová[2], Petr Vodrážka[2], Lauren Des Marteaux[2,*], Robert Grgac[2,3], Petr Hůla[2,3], Jan Rozsypal[2], Miloš Faltus[4], Petr Šimek[2], Radislav Sedlacek[1] and Vladimír Koštál[2,§]

ABSTRACT

Insects that naturally tolerate internal freezing produce complex mixtures of multiple cryoprotectants (CPs). Better knowledge on composition of these mixtures, and on the mechanisms of individual CP interactions, could inspire development of laboratory CP formulations optimized for cryopreservation of cells and other biological material. Here, we identify and quantify (using high resolution mass spectrometry) a range of putative CPs in larval tissues of a subarctic fly, *Chymomyza costata*, which survives long-term cryopreservation in liquid nitrogen. The CPs proline, trehalose, glutamine, asparagine, glycine betaine, glycerophosphoethanolamine, glycerophosphocholine and sarcosine accumulate in hemolymph in a ratio of 313:108:55:26:6:4:2.9:0.5 mmol l^{-1}. Using calorimetry, we show that artificial mixtures, mimicking the concentrations of major CPs in hemolymph of freeze-tolerant larvae, suppress the melting point of water and significantly reduce the ice fraction. We demonstrate in a bioassay that mixtures of CPs administered through the diet act synergistically rather than additively to enable cryopreservation of otherwise freeze-sensitive larvae. Using matrix-assisted laser desorption/ionization mass spectrometry imaging (MALDI-MSI), we show that during slow extracellular freezing trehalose becomes concentrated in partially dehydrated hemolymph where it stimulates transition to the amorphous glass phase. In contrast, proline moves to the boundary between extracellular ice and dehydrated hemolymph and tissues where it probably forms a layer of dense viscoelastic liquid. We propose that amorphous glass and viscoelastic liquids may protect macromolecules and cells from thermomechanical shocks associated with freezing and transfer into and out of liquid nitrogen.

KEY WORDS: Freeze tolerance, Cryoprotection, Insects, Metabolites, Natural deep eutectic systems

[1]Czech Centre of Phenogenomics, Institute of Molecular Genetics, Czech Academy of Sciences, 25250 Vestec, Czech Republic. [2]Institute of Entomology, Biology Centre, Czech Academy of Sciences, 37005 České Budějovice, Czech Republic. [3]Faculty of Science, University of South Bohemia, 37005 České Budějovice, Czech Republic. [4]Crop Research Institute, 16106 Praha, Czech Republic.
*Present address: Agriculture and Agri-Food Canada, Harrow Research and Development Centre, Harrow, ON, Canada, N0R 1G0.
‡These authors contributed equally to this work

§Author for correspondence (kostal@entu.cas.cz)

L.K., 0000-0002-0009-5105; M.M., 0000-0003-3930-3132; T.Štětina, 0000-0001-7289-5534; P.V., 0000-0001-9875-668X; L.D., 0000-0002-0461-2704; P.H., 0000-0002-5797-010X; J.R., 0000-0002-7925-7401; M.F., 0000-0003-2217-5226; P.Šimek, 0000-0003-2754-6372; R.S., 0000-0002-3352-392X; V.K., 0000-0002-4994-5123

INTRODUCTION

Various organisms from bacteria to animals respond to environmental stressors such as heat, cold, freezing, drought, hypersalinity and high hydrostatic pressure by accumulating a stereotypic set of cytoprotective compounds including amino acids, sugars, polyols and methylamines (Somero, 1986; Yancey, 2005). This is also true for insects that naturally tolerate extracellular freezing during overwintering in temperate and polar habitats (Lee, 2010; Storey and Storey, 1988). In such insects, the accumulation of low molecular weight carbohydrate and free amino acid cryoprotectants (CPs) is considered a fundamental tenet of their freeze tolerance (Storey, 1997; Storey and Storey, 1988; Storey and Storey, 1991; Toxopeus and Sinclair, 2018). Extensive knowledge has accumulated over many decades about which CPs are present in many different species (Asahina, 1970; Salt, 1961; Sømme, 1982; Storey and Storey, 1991), but our understanding of how they protect the insect tissues and cells is far from complete (Toxopeus and Sinclair, 2018).

Here, we focus on an important but previously neglected aspect of natural freeze tolerance: the components of complex mixtures of multiple CPs may contribute to freeze tolerance via additive or even synergistic mechanisms (Storey and Storey, 1986; Storey and Storey, 1988; Toxopeus et al., 2019). It is well known from practice in clinical medicine and biotechnology that combinations of CPs protect the viability of cryopreserved cells or materials better than single substances (Elliott et al., 2017). The mixtures may even have emergent properties, i.e. those beyond the summation of properties of the individual components. Relatively recently, the existence of specific mixtures, so-called NADES (natural deep eutectic systems) in various organisms was proposed (Dai et al., 2013; Choi et al., 2011). These mixtures consist of stereotypic sets of natural primary metabolites such as sugars, sugar alcohols, organic acids, amino acids and amines, and are characterized by a much lower melting point than that of the individual components, mainly because of the formation of intermolecular hydrogen bonds (Dai et al., 2015). These mixtures have been proposed to serve various physiological functions, including survival of organisms in extreme drought and cold (Castro et al., 2018; Gertrudes et al., 2017; Liu et al., 2018), and have also been proposed as new agents for cell cryopreservation (Hornberger et al., 2021). We believe that there may be major practical consequences of exploring the complex composition of insect CP mixtures, as they could aid in the development of applicable cryogenic techniques. Freeze-tolerant insects also offer the potential for the discovery of novel components, for the study of interactions between individual components, and for the analysis of the principles underlying survival after freezing in a complex organism composed of different cell types and tissues; a complexity that still poses a challenge for medical cryopreservation (Fahy et al., 2006; Pegg, 2001).

It is reasonable to first analyze the suite of CPs accumulated by the most freeze-tolerant model species, and larvae of the malt fly, *Chymomyza costata* (Diptera: Drosophilidae), are among the most cold-hardy animals known (Des Marteaux et al., 2019). Overwintering cold-acclimated larvae in diapause can survive freezing of all osmotically active water (68% of total body water), down to −75°C, with survival rates similar to those in unfrozen controls, and they can even survive long-term (18 month) cryopreservation in liquid N$_2$ (Moon et al., 1996; Rozsypal et al., 2018; Shimada and Riihimaa, 1988). We have previously shown that high concentrations of the free amino acid proline acquired by diapausing *C. costata* larvae during cold acclimation are essential for the survival of freezing and cryopreservation stress (Koštál et al., 2011b; Rozsypal et al., 2018).

Here, we extend our previous results to include a whole complex of CPs accumulated by these freeze-tolerant larvae. Using a combination of four chromatographic mass spectrometric (MS) analytical platforms, we established metabolite profiles of four different *C. costata* tissues in two contrasting larval phenotypes that differ greatly in freeze tolerance and cryopreservability in liquid N$_2$. By combining the results of the analytical chromatographic MS analysis with matrix-assisted laser desorption/ionization (MALDI) mass spectrometry imaging (MSI), we show that freeze-tolerant larvae accumulate putative CPs in all tissues, but especially in hemolymph. Using the same technique, we observed changes in CP localization during slow extracellular freezing associated with partial dehydration of hemolymph and tissues. We then used differential scanning calorimetry (DSC) to determine the thermal phase transition properties of artificial aqueous CP mixtures mimicking the concentrations of the five most abundant metabolites in the hemolymph. Finally, we show in a bioassay that mixtures of CPs administered through the diet work in a synergistic rather than an additive way to induce strong freeze tolerance and cryopreservability in otherwise freeze-sensitive larvae.

MATERIALS AND METHODS
Fly rearing and acclimations

A colony of *C. costata*, Sapporo strain (Riihimaa and Kimura, 1988), was reared on artificial diet in MIR 154 incubators (Sanyo Electric, Osaka, Japan) as described previously (Kostal et al., 1998; Lakovaara, 1969). Two phenotypic variants (LD and SDA) of the 3rd larval instar were generated according to our earlier acclimation protocols (Des Marteaux et al., 2019; Koštál et al., 2011b; Rozsypal et al., 2018) (Fig. S1a). The LD larvae (warm acclimated, active larvae reared at long-day conditions) have limited survival after freezing (35% survive to −5°C, 10% to −10°C, and none survive freezing to −20°C or below). In contrast, practically all SDA larvae (diapause larvae reared at short-day conditions and gradually acclimated to cold) survive deep freezing to −30°C or even −75°C, and 42.5% survive at least 18 months of cryopreservation in liquid N$_2$ (Rozsypal et al., 2018). In addition, SDA larvae were frozen (variant SDA-frozen) according to a previously developed optimal freezing protocol (Rozsypal et al., 2018) schematically presented in Fig. S1b. Survival after freezing and cryopreservation in liquid N$_2$ was assessed as the ability to pupate and metamorphose into the adult stage within 42 days of thawing (at a constant 18°C, LD).

To collect the hemolymph, 30 larvae were gently pierced and torn on a piece of Parafilm, creating a large droplet of pooled hemolymph. This droplet was then extracted using a calibrated glass capillary (Drummond Sci., Broomall, PA, USA). Collection of hemolymph in a single group of 30 larvae took less than 2 min. To obtain fat body, muscle and midgut tissues, the larvae were

quickly dissected under binocular microscope in ice-cold phosphate-buffered saline. Dissected tissues were collected in ice-cold extraction buffer (see below) and stored at −80°C until analysis. Dissection of a single larva took less than 2 min, and we took care to sample a similar part of the respective tissue from each individual. This allowed us to express each metabolite concentration as a 'pool per tissue'. Only in hemolymph samples where we could measure the exact sample volume, could we also calculate the concentration in mmol l^{-1}.

Extraction of metabolites and analytical MS platforms

Analyses were performed for whole *C. costata* larvae (pools of five larvae taken in four replicates) or dissected tissues (pools of 30 tissues in four replicates). Whole larvae were weighed to obtain fresh mass, immersed in liquid N$_2$, and stored at −80°C until analysis. Frozen samples of whole larvae/tissues were melted on ice and homogenized in 400 µl of extraction buffer (methanol: acetonitrile:deionized water in a volume ratio of 2:2:1). The methanol and acetonitrile (Optima LC/MS) were purchased from Fisher Scientific (Pardubice, Czech Republic) and the deionized water was prepared using Direct Q 3UV (Merck, Prague, Czech Republic). Internal standards, *p*-fluoro-DL-phenylalanine, methyl α-D-glucopyranoside (both from Sigma-Aldrich, St Louis, MI, USA) were added to the extraction buffer, both at a final concentration of 200 nmol ml^{-1}. Samples were homogenized using a TissueLyser LT (Qiagen, Hilden, Germany) set to 50 Hz for 5 min (with a rotor pre-chilled to −20°C). Homogenization and centrifugation (at 20,000 *g* for 5 min at 4°C) were repeated twice and the two supernatants were combined.

We performed targeted analyses of 49 select metabolites (Table S1) using a combination of four different mass spectrometry-based (MS) analytical platforms that were described previously: ECF-LC/MS and ECF-GC/MS (Štětina et al., 2018), SILYL-GC/MS (Škodová-Sveráková et al., 2020) and HILIC-LC/MS (Škodová-Sveráková et al., 2021). More details on instrumentation and chromatographic columns are in Table S1. All 49 metabolites were identified against relevant standards (Sigma-Aldrich) and subjected to quantitative analysis using a standard calibration curve method. The analytical results were validated by simultaneously running blank samples (no larvae in the sample), standard biological quality control samples (the periodic analysis of a standardized larva/tissue sample – the pool of all samples) and quality control mixtures of amino acids (AAS18, Sigma-Aldrich).

Matrix-assisted laser desorption/ionization mass spectrometry imaging (MALDI-MSI)

The MALDI-MSI (Khalil et al., 2017; Tuthill et al., 2020; Yang et al., 2020) was conducted in LD and SDA larvae and also on SDA frozen larvae (Fig. S1); the LD frozen variant was not considered relevant as all LD larvae die when exposed to freezing to −30°C. Larvae were rinsed in water, incubated for 3 min in 2% gelatin, and then submerged into 5 ml of 10% gelatin in a plastic mold (Tissue-Tek Cryomold, Sakura, Mdesa, Czech Republic) placed on an ice-cold stage. The molds with solid gelatin were then immersed in isopentane pre-cooled to −140°C in liquid N$_2$ vapors for 3 min and transferred to −80°C for storage until further processing. Preparation of the SDA frozen larvae was modified as shown in Fig. S2.

For cryo-sectioning, the frozen molds were placed into a cryostat chamber (Leica CM1950, Germany) pre-cooled to −20°C. Sections of 10 µm thickness were mounted on indium tin oxide coated glass slides (ITO, Bruker, Czech Republic), previously washed with hexane and then with 2-propanol. Sections of the LD and SDA

larval variants were thaw-mounted on warm glass (standard procedure MALDI-TOF/MSI) (TOF, time of flight), while sections of the SDA frozen larval variant were mounted on a gold-coated ITO glass pre-cooled to −20°C in order to preserve the tissue organization as it formed during slow pre-freezing (extracellular ice formation and tissue freeze-dehydration). The sections were dried for 15 min in a desiccator at low air pressure (at room temperature for the LD and SDA variants, while at −20°C for the SDA frozen variant), then sealed in plastic foil inside a plastic mailer, evacuated, and stored at −80°C until further processing. The ITO glasses with sections were transferred to room temperature, left to temper for 15 min, and dried in a desiccator for 15 min. Samples were then sprayed with a matrix solution of 9-aminoacridine hydrochloride, 7 mg ml⁻¹ in 70% ethanol (v/v). A TM-Sprayer 3 (HTX-Technologies, USA) was used to cover the tissue with the matrix solution using the following settings: nozzle temperature, 50°C; 12 passes; flow, 0.035 ml min⁻¹; nozzle velocity, 1000 mm min⁻¹; track spacing, 2 mm, HH pattern; gas pressure, 10 psi; gas flow rate, 2 l min⁻¹; drying time, 0 s; nozzle height, 40 mm; and propelled with 50% methanol (v/v). After spraying, the samples were dried in a desiccator for 15 min.

Spectral images were acquired using a rapifleX MALDI-TOF/TOF spectrometer (Bruker, Germany) in reflector negative mode with a 355 nm smartbeam™ 3D laser with a spatial resolution of 10×10 μm (pixel) in an m/z range of 20–1000, at a constant laser fluence of 72% and laser frequency of 5 kHz. Two hundred images were accumulated from every position. The instruments were set up with: ion source 1, 19.973 kV; PIE, 2.664 kV; lens, 11.353 kV; reflector 1, 20.810 kV; reflector 2, 1.034 kV; reflector 3, 8.577 kV. The pulsed ion extraction time was set to 90 ns and detector gain was 2302 V. Data were acquired with digitizer speed, 2.5 GS s⁻¹. Samples were measured in random order. Calibration was done externally using red phosphorus, achieving precision up to 5 p.p.m. (Kolářová et al., 2016).

After MALDI-MSI, tissues on ITO glass were washed three times for 2 min with 70% ethanol and afterwards washed with water. The samples were then stained with Hematoxylin and Eosin (H&E, a general staining method, which allows to visualize the shape, and structure of cells in a tissue sample; Hematoxylin stains mainly heterochromatin and nucleoli, while Eosin stains cytoplasmic components including collagen and elastic fibers) and scanned with Axio Scan.Z1 (Zeiss, Germany) operated by Zen 2 software (blue edition; Zeiss, Germany). Single raw data files on the intensities of the MALDI-TOF signals of individual m/z peaks were processed using SCiLS Lab software (v.2021c, SCiLS, Bruker, Germany). The raw data were smoothed with a convolution algorithm (width 20) and all subsequent computations and images rendering were done with total ion count square normalization. We collected MALDI-TOF signal-intensity datasets for 5 transverse sections of LD and SDA larvae and for 6 sections of SDA frozen larvae, plus one longitudinal section of an SDA larva. For relative quantification of signal intensities and statistical analyses, the transversal sections were used. Galleries showing the complete results for all transversal sections are available in figshare (https://figshare.com/articles/figure/Appendice_MALDI_MSI_images_pdf/19590694).

Regions (or tissues) of interest in the sections were manually delimited using H&E-stained images in QuPath software (v.0.2.3, University of Edinburgh, UK) (Bankhead et al., 2017) and imported into SCiLS software. The summary spectrum was exported into mMass software (v.5.5.0) (Niedermeyer and Strohalm, 2012), internally re-calibrated, and annotated based on m/z values with 50 ppm tolerance using an in-house modified database based on the HMDB metabolite database considering [M-H]⁻ and [M+Cl]⁻ adducts (Wishart et al., 2018). Selected peaks were then analyzed using SCiLS software with mean spectral intensity scaled in arbitrary units (A.U.) for each region and treatment. These spectral intensity data were then statistically compared using ANOVA followed by Bonferroni's multiple comparison test (Prism, v.6.07, GraphPad Software, San Diego, USA). In addition, we verified the identities of m/z peaks for trehalose and proline in the experiment where LD larvae were fed diet augmented by ¹³C6 glucose (for details, see Figs S13 and S14). The ¹³C6 glucose was purchased from Sigma-Aldrich (product ID 389374).

Differential scanning calorimetry (DSC)

Thermal analysis was performed using the Q2000 calorimeter (TA Instruments, New Castle, DE, USA) as previously described (Pokorna et al., 2020). The analyzed solutions (see Table S2 for a complete list) were loaded and hermetically sealed into aluminium pans. The amount of loaded solution (∼5 μl) was controlled by weighing with precision to 0.01 mg using a Sartorius CP 225 D balance (Sartorius AG, Goettingen, Germany). The solutions were frozen and thawed according to the following protocol: (i) start at 25°C, (ii) cool to −90°C at 10°C min⁻¹, (iii) hold for 5 min at −90°C, and (iv) warm to 25°C at 10°C min⁻¹. An empty pan was used as a reference, and samples were run in technical triplicates (same solution analyzed three times). DSC results were analyzed using TA Universal Analysis 2000 software (v.4.5A Build 4.5.0.5). The onset of exotherm on the cooling scan was taken as the supercooling point (temperature of ice crystallization). Two major thermal events were analyzed on heating scans above −60°C. (1) Glass transition: an inflection point of the second-order phase transition was read as the temperature of vitrification (T_g). The change in specific heat capacity (ΔC_p) was derived from the difference in heat flow between the onset and the end of the glass transition. (2) Melting of bulk water: an onset of melting endotherm (first-order phase transition) was read as the melting point (m.p.), while the enthalpy of melting (ΔH, calculated from the area under the endothermic peak) served to estimate the fraction of melted (i.e. crystallized) water using the standard heat of fusion for the ice/water transition of 334 J g⁻¹. The remaining fraction of unfrozen water was considered osmotically inactive (%OIW).

Larval feeding on CP-augmented diets

Seventeen-day-old freeze sensitive (LD) larvae (i.e. roughly mid-3rd instar, voracious feeding stage) were extracted from the standard diet and groups of 20 individuals were moved to one of a variety of specific diets: (i) fresh standard diet (control); (ii) 'CP mix 508' diet – a standard diet augmented with five select CPs (proline, product ID P0380; trehalose, T9449; glutamine, G3126; asparagine, A0884; and betaine, 61962; all from Sigma-Aldrich) in concentrations corresponding to those observed in SDA larval hemolymph (i.e. 508 mmol kg⁻¹ water in total, see Table S3); (iii) five different standard diets augmented with the select CPs individually; (iv) 'CP mix minus Pro 313' diet – a mixture of the four select CPs but without the 313 mmol kg⁻¹ proline [because proline was the only metabolite capable of supporting freeze tolerance in a previous experiment (iii)]. After exposure to these diets for 3 days, the larvae were removed and used for the liquid N₂ survival bioassay (Fig. S1b).

RESULTS
Characterization of the CP mixture from *C. costata* larvae
Results of targeted quantitative analysis of 49 metabolites are summarized in Table S1 and plotted in Fig. 1A (hemolymph) and
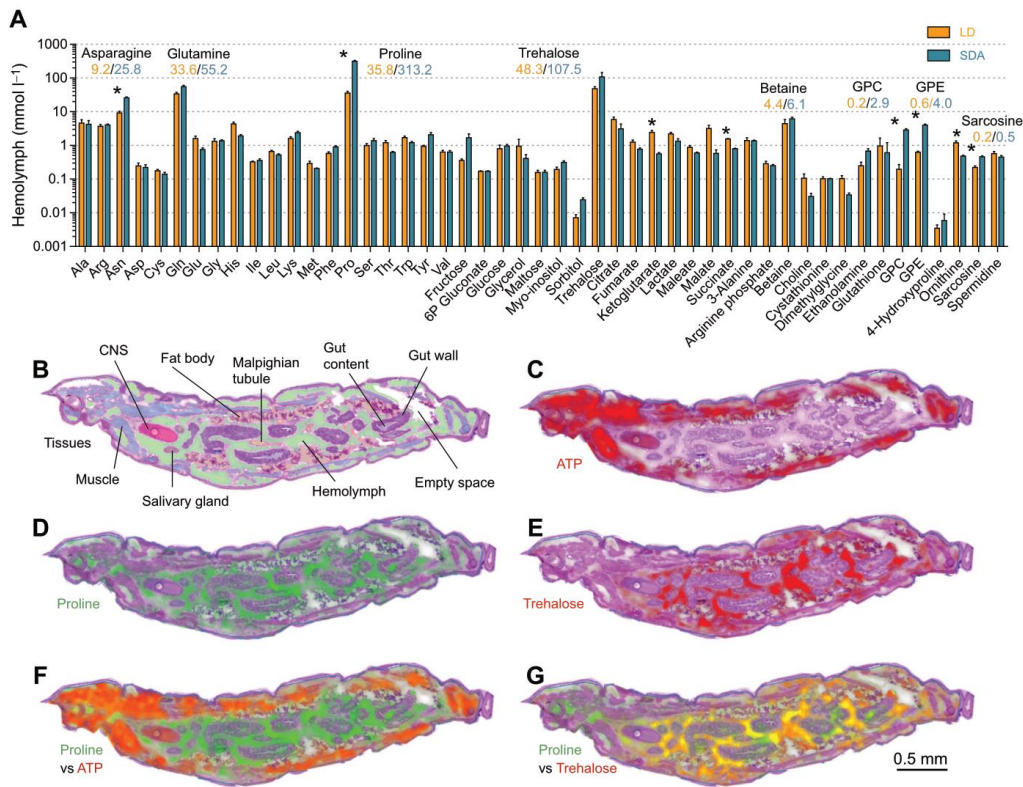
3

Fig. 1. Metabolite profiles and localization in hemolymph and tissues of *Chymomyza costata* larvae. (A) Forty-nine target metabolites were absolutely quantified in the hemolymph of freeze-sensitive (LD) and freeze-tolerant (SDA) larvae using four MS-based analytical platforms. Each column represents a metabolite concentration (means±s.d.; *n*=4 biological replicates, each containing hemolymph from 30 larvae). Differences between the means of LD and SDA were assessed by unpaired *t*-tests corrected for multiple comparisons using the Holm–Sidak method with α=0.01. Asterisks indicate significantly different means and the concentrations are shown for all metabolites that were considered in this paper as putative CPs (GPC, glycerophosphocholine; GPE, glycerophosphoethanolamine). (B) Longitudinal section of a SDA larva stained with Hematoxylin and Eosin, with tissues highlighted by different colors. (C–E) Intensities of the MALDI-TOF signals corresponding to the three analyzed compounds: ATP (C); proline (D); trehalose (E). (F) While proline (green signal) is most evident in hemolymph, ATP (red signal) is mainly found in muscles. (G) Proline (green) and trehalose (red) colocalize in hemolymph (a yellow color results from the mixing of green and red). See Fig. S3 for MALDI-MSI images of other compounds.

Fig. S3 (other tissues). For most metabolites, the pool in the hemolymph was significantly larger than the pools in other tissues (Fig. S4). The volume of hemolymph in one larva is approximately 200 nl (see Table S1) representing only 10% of the total body volume or body mass (∼2 mg). Nevertheless, the hemolymph contained approximately 50% of the total metabolite pool in both LD and SDA larvae (Table S1). Entry into diapause and cold acclimation (associated with the acquisition of extreme freeze tolerance) induced accumulation of specific metabolites (putative CPs) in SDA larvae (Fig. S1). The sum of the molar concentrations of the 49 metabolites in LD hemolymph was 182 mmol l^{-1}, but this increased to 554 mmol l^{-1} in SDA hemolymph (Table S1). Four compounds that contributed most to this increase were: proline (increase of 277 mmol l^{-1}), trehalose (increase of 59 mmol l^{-1}), glutamine (increase of 22 mmol l^{-1}) and asparagine (increase of 17 mmol l^{-1}). The same four compounds also ranked first in order of concentration in SDA hemolymph: proline (313 mmol l^{-1}),

trehalose (108 mmol l^{-1}), glutamine (55 mmol l^{-1}) and asparagine (26 mmol l^{-1}). Glycine-betaine (hereafter 'betaine', 6.1 mmol l^{-1}) was fifth in concentration, although it increased only moderately (by 1.7 mmol l^{-1}) in SDA compared with LD larvae. In addition, three other compounds had statistically higher hemolymph concentrations in SDA than in LD larvae, although their concentrations in SDA hemolymph were relatively low in absolute terms: glycerophosphoethanolamine (GPE, 4.0 mmol l^{-1}), glycerophosphocholine (GPC, 2.9 mmol l^{-1}) and sarcosine (0.5 mmol l^{-1}). For the purposes of this article, we consider the above compounds as putative CPs.

Localization of CP mixture components in larval tissues

Using MALDI-MSI, we localized select metabolites in larval sections. A longitudinal section through the SDA larva provides the best overview of tissue structure (Fig. 1B). The highest intensity of the MALDI-TOF signal for ATP is localized predominantly in

muscle tissue (corresponding to its role as the most important intracellular phosphagen) (Fig. 1C). In contrast, the highest intensities of proline and trehalose signals are localized in the hemolymph (Fig. 1D,E), where they are also colocalized with the high-intensity signals of glutamine, asparagine and GPE (Fig. S5).

As it was difficult to obtain enough high-quality longitudinal sections, we used transverse sections through the middle region of the larvae for the statistical analysis of the relative intensities of the MALDI-TOF signals. Quantitative analysis of these signals is technically difficult for small metabolite molecules freely dissolved in biological aqueous solutions (Fig. S6). Nevertheless, our analysis suggests that there are no differences in the overall localization patterns of the five putative CPs (proline, trehalose, glutamine, asparagine and GPE) between LD and SDA larvae. However, the

signal intensities for all five CPs were much stronger in SDA than in LD larvae (compare the *y*-axes of Fig. S7 with Fig. S8). The MALDI-MSI thus confirms the results of the quantitative MS analysis (Fig. 1A) that the putative CPs are accumulated in all tissues, but especially in the hemolymph, of SDA larvae (for details, see MALDI-MSI images in figshare (https://figshare.com/articles/figure/Appendice_MALDI_MSI_images_pdf/19590694).

During slow inoculative freezing to $-30°C$ (rate of $0.1°C\,min^{-1}$ see Fig. S1b for the freezing protocol) large masses of extracellular ice crystals developed in between partially dehydrated pools of larval hemolymph and tissues (Fig. 2A–D). We observed a striking difference in the 'behavior' of two major components of the CP mixture during slow extracellular freezing: whereas trehalose was concentrated in the pool of dehydrated hemolymph of SDA larvae, a
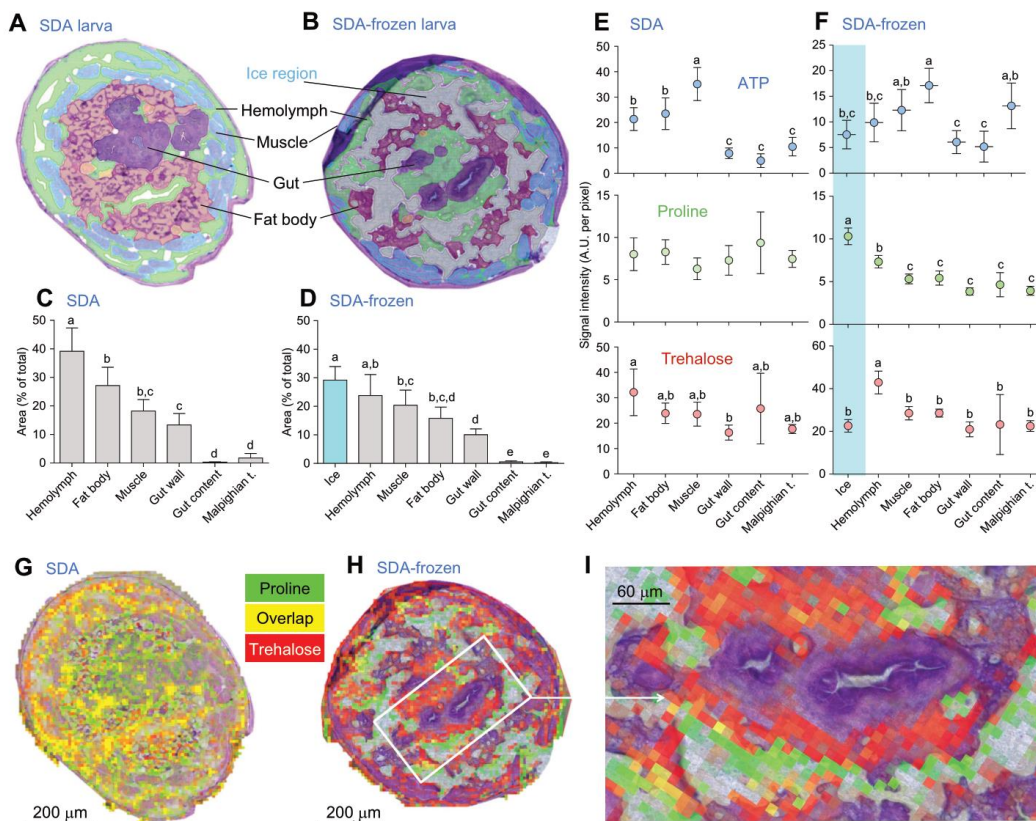
Fig. 2. Localization of proline and trehalose in *C. costata* SDA larvae before and after slow freezing. (A,B) Examples of transverse sections through the middle region of SDA larva (A) and SDA-frozen larva (B). The tissues are highlighted in different colors. Note the large masses of extracellular ice between the partially dehydrated tissues of SDA-frozen larva. (C,D) Relative proportions of total area occupied by different tissues or ice. Each column is mean±s.d. of five or six sections (SDA or SDA-frozen larvae, respectively). Means flanked by different letters are significantly different (one-way ANOVA followed by Bonferroni's multiple comparison test). (E,F) Results of MALDI-TOF signal intensity quantification (arbitrary units, A.U. per pixel of 10×10 µm) for three select metabolites (ATP, proline, trehalose). Each point is the mean±s.d. of five or six sections (SDA or SDA-frozen larvae, respectively). Mean values flanked by different letters are significantly different (one way ANOVA followed by Bonferroni's multiple comparison test). (G,H,I) Examples of MALDI-TOF signal intensities for proline (green) and trehalose (red). Note that proline and trehalose signals markedly overlap (yellow color) in the hemolymph of SDA larva (G), while they apparently delocalize in SDA-frozen larva (H,I). Trehalose concentrates in the partially dehydrated hemolymph, while proline migrates to the border between extracellular ice and partially dehydrated tissues of the SDA-frozen larva.

large quantity of proline apparently 'migrated' from the hemolymph toward the ice region (Fig. 2E,F) and formed thin 'layers' of concentrated proline at the boundary between the extracellular ice and the dehydrated hemolymph and tissues (Fig. 2G–I). In these layers, proline colocalized with high-intensity signals from glutamine and asparagine, while trehalose colocalized with GPE in the dehydrated hemolymph (Fig. S9; for details, see figshare (https://figshare.com/articles/figure/Appendice_MALDI_MSI_images_pdf/19590694).

Thermal phase transitions in artificial CP mixtures

To assess the influence of different CP mixture components on water binding and thermal phase transitions, we compared heating curves from DSC scans of aqueous solutions containing single components or different CP mixtures with real SDA hemolymph. We focused on melting of bulk water (Fig. 3A) and glass transition (Fig. 3B). The full DSC analysis results can be found in Table S2.

We designed the CP mixtures according to the concentrations of the five most abundant (and commercially available/affordable) compounds in the SDA larval hemolymph. CP mix 508 mimics the composition of the major CPs in the hemolymph of SDA larvae prior to freezing, while CP mix 1588 takes into account a 3.125-fold increase in the concentration of all components resulting from extracellular freezing of osmotically active water (and, this way, it mimics the composition in the SDA-frozen variant). In addition, we tested all components individually at concentrations equivalent to those estimated in SDA hemolymph after extracellular freezing, and we also designed two reduced-composition mixes: Pro-Tre 1316 (proline 978+trehalose 338) and Pro-Gln-Asn 1231 (proline 978+glutamine 172+asparagine 81) (see Table S2 for details).

We found that depression of the bulk water melting point, as well as the fraction of 'bound' water (unfrozen, osmotically inactive water, %OIW), correlated linearly with the molal concentration of a
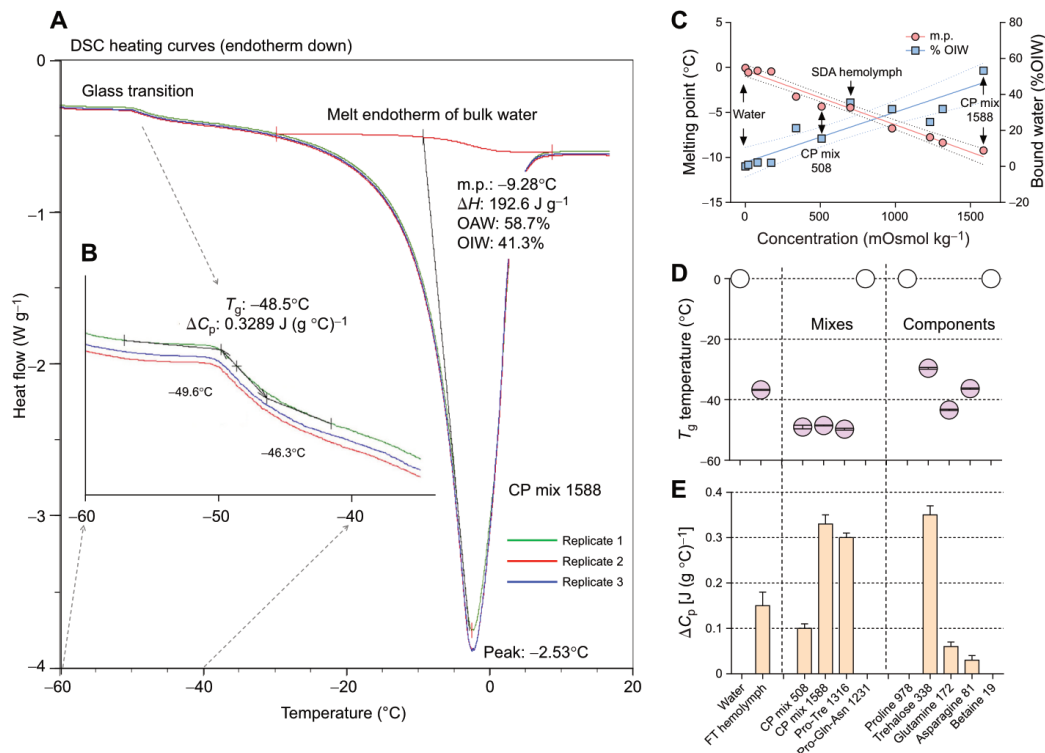
Fig. 3. Thermal phase transitions in the aqueous solutions of artificial CP mixtures and individual components. (A) Example of a heating curve recorded by differential scanning calorimetry (DSC) of the artificial CP mix 1588. Three technical replicates are shown in different colors. Results calculated by TA Universal Analysis 2000 software are shown for the 1st replicate only (green line). The analysis of melting endotherm shows that melting of bulk water starts at a melting point m.p.) of −9.28°C, while only 58.7% of the total water in the sample is osmotically active (OAW), i.e. melts (the enthalpy of melting transition of ΔH of 334 J g^{-1} would correspond to melting of 100% total water) while 41.3% of total water is osmotically inactive (OIW) or 'bound'. (B) A glass transition was observed at −48.5°C (T_g, inflection point) associated with change in specific thermal capacity ΔC_p of 0.3289 J (g °C)$^{-1}$. (C) Linear associations of the melting point (m.p., red line) or the fraction of bound water (%OIW, blue line) with the osmolality of the solution. Each point represents a specific solution and all solutions are shown in detail in Table S2. Points corresponding to water, SDA hemolymph, and CP mixes 508 and 1588 are identified for clarity. The broken lines show 95% confidence intervals of the linear regressions. (D,E) Temperatures of the glass transition, T_g (D) and changes in thermal capacity, ΔC_p (E) of the different solutions. Empty points in D or a missing column in E indicate that no glass transition was observed, while the violet points and orange columns show mean±s.d. values of T_g or ΔC_p, respectively, for solutions where a glass transition was observed (see Table S2 for the full dataset).

solution, regardless of whether it was a single component solution or a mixture. Even the values for real hemolymph collected from SDA larvae fitted well to a linear relationship (Fig. 3C).

A clear glass transition was observed whenever trehalose was present in a mixture (Fig. S10). The temperatures of glass transition (T_g) in different trehalose-containing solutions varied from $-29.6°C$ (trehalose 338) to $-49.7°C$ (Pro-Tre 1316) (Fig. 3D). The change of thermal capacity (ΔC_p) during de-glassing was slightly above 0.3 J $(g \, °C)^{-1}$ in the solutions containing a relatively high concentration of trehalose (338 mmol kg^{-1}) but lower, ~0.1 J $(g \, °C)^{-1}$, in the solution containing a relatively low concentration of trehalose (CP mix 508 contains 108 mmol kg^{-1} of trehalose) and in real SDA hemolymph (which also contains 108 mmol kg^{-1} of trehalose) (Fig. 3E). No glass transition was observed in the concentrated proline 978 solution (Fig. S11). The presence of proline in a mixture with glutamine and asparagine (Pro-Gln-Asn 1231) resulted in the elimination of small glass transitions observed in single-component mixtures of glutamine or asparagine (Fig. 3D,E). We also observed minor exotherms in heating curves of glutamine and asparagine at $-22.8°C$ and $-14.6°C$, respectively (Fig. S12). The presence of such exotherms was also eliminated by the addition of proline in the Pro-Gln-Asn 1231 mix (Table S2).

CPs in mixture protect larvae from cryopreservation stress better than individual CPs

To evaluate the ability of a complex cryoprotective mixture to increase freeze tolerance compared with individual components of the CP mix, we fed LD larvae with CP-augmented diets and then performed freezing survival assays. We prepared the CP mix 508 diet by augmenting the standard larval diet with a CP mix 508 solution (see Table S3). When LD larvae were fed with the CP mix 508 diet from hatching, more than 90% died (often as 1st instars). We therefore exposed only 3rd instar LD larvae to this diet and for only 3 days (at ages 17–19 days), which reduced larval mortality to 20%. The surviving larvae were significantly smaller at day 19 and pupariation was delayed by 2 days (Table S4), indicating that even short-term exposure to CP mix 508 appears to have some toxic effects.

A 3 day exposure to the CP mix 508 diet significantly increased whole-body concentrations of most CP mix components: proline increased 6.8-fold, trehalose 1.7-fold, glutamine 5.4-fold and asparagine 19.9-fold (see Table S5 for more details). In the hemolymph, the concentrations of proline, glutamine and asparagine reached high levels of 289, 80 and 49 mmol l^{-1}, respectively, while trehalose and betaine remained relatively low at 29 and 7 mmol l^{-1}, respectively (Fig. 4A, see Table S5 for more details). The sum molarity of the five CPs in hemolymph reached 454 mmol l^{-1} in LD larvae fed with the CP mix 508 diet, which is broadly similar to the sum of 508 mmol l^{-1} seen in SDA larvae.

No LD larvae that fed exclusively on the standard diet survived cryopreservation in liquid N_2. In striking contrast, 58% of the LD larvae survived cryopreservation after only 3 days of feeding with the CP mix 508 diet; 24.5% went on to pupate and 18.3% successfully metamorphosed to the adult stage (Fig. 4B). The components of the CP mix 508 administered via the diet had much less (or no) effect on larval freeze tolerance when they acted in isolation: betaine and asparagine had absolutely no effect; glutamine and trehalose resulted in 1 and 2 larvae surviving (out of 100), respectively, but these larvae did not pupate; proline augmentation was most effective, resulting in 37.7%, 10.3% and 7.2% survival for larvae, pupae and adults, respectively. When proline was excluded from the CP mix, the remaining components allowed only 4 larvae (out of 100) to survive liquid N_2 exposure, demonstrating that proline is the most important component of the mixture, or even the requisite for survival in liquid N_2. Nevertheless, the complete CP mix 508 was approximately 2-fold more effective at bolstering liquid N_2 survival than proline alone. This result was consistent at all three levels of survival (see t-tests in Fig. 4B) and also across five different generations of assayed insects (Table S6). Simple addition of the individual effects of the three components (proline+trehalose+glutamine) was not sufficient to explain the effect of the complete CP mix 508. These results suggest a synergy between CP mix 508 components that should be investigated in the future.

DISCUSSION

Components of the fly's innate CP mixture behave differently during slow extracellular freezing

We identified the composition of the innate putative CP mixture which bathes the tissues of extremely freeze-tolerant *C. costata*
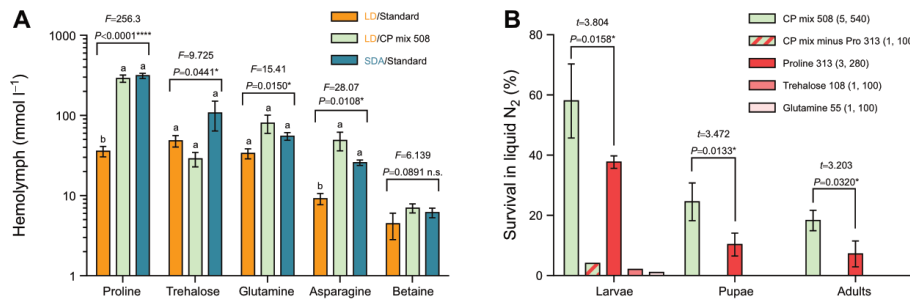
Fig. 4. Effects of CP-augmented diets on *C. costata* larvae. (A) Change in the hemolymph concentration of five CPs in response to feeding 17-day-old LD larvae a CP mix 508 diet for 3 days. Concentrations are compared with LD and SDA larvae fed on a standard diet, using one-way ANOVAs followed by Bonferroni's multiple comparison tests (columns flanked by different letters differ significantly). (B) Percentage survival of larvae cryopreserved in liquid N_2 (note: only diets where at least one larva survived are shown). The 17-day-old LD larvae were fed different diets for 3 days, then exposed to liquid N_2 for 1 h, returned to the standard diet at a constant 18°C, and their survival to larval (movements 24 h later), pupal (formation of puparium) and adult stage (emergence of adult fly) were observed over the next 14 days. The two numbers in parentheses (*n*, *N*) show: *n*=the number of fly generations, and *N*=the total number of larvae in all replicates. The mean survival for larvae fed a CP mix 508 diet versus a proline diet (Pro 313) were directly compared using a two-tailed Student's *t*-test. Asterisk indicates a significant difference; n.s., not significant.

larvae: proline, trehalose, glutamine, asparagine, betaine, GPE, GPC and sarcosine, which occur in hemolymph in a stoichiometric ratio of 313:108:55:26:6:4:2.9:0.5 mmol l^{-1}, respectively. It may not be surprising that the mixture is broadly similar to the cocktails known from other organisms exposed to various environmental stressors (Gertrudes et al., 2017; Choi et al., 2011; Somero, 1986; Yancey, 2005). The occurrence of the same classes of organic cytoprotectants and compatible osmolytes in different organisms is likely based on convergent evolution which favors accumulation of polar molecules with high solubility in water (high accumulation capacity) countered by low tendency to interact with charged groups of macromolecules and membranes (low toxicity) (Hochachka and Somero, 2002).

We performed a bioassay showing that supplementation of the larval diet with major components of the CP mixture in their native stoichiometric ratio changes freeze-sensitive larvae into freeze-tolerant/cryopreservable larvae within just 3 days. This result convincingly demonstrates that the accumulation of CPs has a strong functional (adaptive) significance in *C. costata*. However, this adaptation has probably evolved to cope with conditions typical for larvae overwintering in thermally buffered microhabitats under the bark of fallen trees, often under a blanket of snow (Band and Band, 1982; Grimaldi, 1986). Therefore, there may be different functional explanations for the roles of CPs in ecologically relevant situation in the field and for deep freezing and cryopreservation in liquid N$_2$ in the laboratory. Here, we avoid discussion of the eco-physiological aspects of CP-based freeze tolerance in animals and insects in the field, as these have already been covered for animals (Sinclair, 1999; Storey and Storey, 1988; Toxopeus and Sinclair, 2018; Zachariassen, 1985) and also specifically for *C. costata* (Rozsypal et al., 2018) elsewhere. Instead, we limit further discussion to the potential relevance of our results for deep freezing and cryopreservation in the laboratory.

We applied the MALDI-MSI technique to localize CPs in larval tissues and, for the first time in cryobiology literature, to determine how this localization changes during slow extracellular freezing, i.e. under conditions that allow larvae to survive deep freezing and subsequent cryopreservation in liquid N$_2$. So far, concentrations of CPs in insects have mostly been reported in whole body samples for two general reasons: first, insect tissues are small, making it technically difficult to estimate precise concentrations; and second, native CPs – being standard products of metabolism – have been considered to move freely across membranes (Somero, 1986). In cases where CP analyses were performed on separate tissues (Koštál et al., 2011a; Rozsypal et al., 2013; Toxopeus et al., 2019), the CPs were generally found in all examined tissues. Here, we have confirmed that SDA larvae of *C. costata* accumulate putative CPs in all examined tissues but that the highest concentrations occur in the hemolymph.

One of the most salient findings of this study is the observation that the two major components of the CP mixture, proline and trehalose, 'behave' differently during slow extracellular freezing. The MALDI-MSI analysis suggests that the bulk of trehalose molecules remain in their original location (before freezing) and concentrate in partially freeze-dehydrated hemolymph and tissues. In contrast, some of proline molecules appear to move out of the hemolymph and concentrate in thin layers separating the extracellular ice crystals from freeze-dehydrated tissues and hemolymph. At this stage of research, we can only offer hypothetical/speculative explanations for the physico-chemical mechanisms responsible for delocalization of proline and trehalose and for its possible functional significance in a cryopreserved insect. We suggest that the mechanism behind the de-localization could be explained by differences between trehalose and proline in water solubility, propensity to induce glass transition, and mobility in highly viscous freeze-concentrated solutions.

Trehalose stimulates glass transition in partially freeze-dehydrated hemolymph and tissues

We have previously shown that in gradually frozen SDA larvae a glass transition of the residual solution occurs between −20°C and −30°C. Moreover, only larvae pre-frozen to temperatures below −30°C (i.e. below the temperature of glass transition) were able to survive abrupt submersion and cryopreservation in liquid N$_2$ and successfully develop into adults (Rozsypal et al., 2018). This result clearly demonstrated the importance of the glass transition for survival in liquid N$_2$. In our earlier work (Rozsypal et al., 2018), we attributed glass formation to high concentrations of proline in accordance with results of the DSC analysis performed by Rudolph and Crowe (1986). However, this observation was challenged in later DSC studies (Liu et al., 2020; Rasmussen et al., 1997) and our own analysis confirms that proline at a concentration of 978 mmol kg^{-1} does not induce glass transition, at least not at temperatures above −60°C. Instead, trehalose is known in physical chemistry as one of the strongest glass transition inducers in aqueous systems (Cesaro et al., 2008; Green and Angell, 1989; Chen et al., 2000). Nicolajsen and Hvidt (1994) reported that a water:trehalose mixture (%weight, 89.7:10.3) de-glasses at −30.5°C with a ΔC_p of 0.38 J (g °C)$^{-1}$. These values agree well with our DSC analysis results showing de-glassing at −29.6°C with a ΔC_p of 0.33 J (g °C)$^{-1}$ for the trehalose 338 solution (which is 88.7:11.3%weight of water:trehalose). Accurate interpretation of the thermal behavior and glass transition parameters is a challenge for physical chemistry of simple binary mixtures such as trehalose: water (Cesaro et al., 2008; Chen et al., 2000; Nicolajsen and Hvidt, 1994; Olgenblum et al., 2020; Weng and Elliott, 2014). This limitation becomes almost insurmountable for more complex mixtures and, especially, for biological solutions. Nevertheless, our DSC analysis suggests that trehalose rather than proline may be the component mainly responsible for the glass transition in larval body fluids: (i) all artificial CP mixtures containing trehalose showed clear glass transitions with broadly similar T_g and ΔC_p parameters; (ii) the parameters were similar for real hemolymph collected from SDA larvae (containing 108 mmol l^{-1} trehalose) and for the artificial CP mix 508 (simulating composition of major CPs in SDA hemolymph and also containing 108 mmol kg^{-1} trehalose); (iii) no glass transition was observed in the concentrated proline 978 solution.

During glass transition, the viscosity of the supercooled liquid increases rapidly as the frequency, strength and lifetime of hydrogen bonds in a system increases. In dilute systems, most hydrogen bonds are formed between water molecules, but as the concentration of solute molecules increases the interactions between water–trehalose and trehalose–trehalose become more frequent until trehalose molecules form large hydrogen-bonded clusters that exclude water (Olgenblum et al., 2020; Weng and Elliott, 2014). The increase in viscosity slows the molecular dynamics and macromolecules become trapped in an amorphous hydrogen-bonded matrix, which probably prevents undesirable transitions such as protein unfolding. In addition, trehalose can directly form hydrogen bonds with macromolecules, which probably further increases their stability in the amorphous glass (Crowe et al., 1998; Olgenblum et al., 2020). Trehalose molecules involved in glass formation are relative immobile. Moreover, large proportions of water molecules are

'bound', i.e. osmotically inactive in SDA larval hemolymph (35.5%) or in whole-body *C. costata* (42%; Rozsypal et al., 2018) and therefore do not contribute much to trehalose solvation. As a result, trehalose can even locally reach the solubility limit ($\sim$1.7 mol kg^{-1} according to ALOGPS, http://www.vcclab.org/lab/alogps/), partly crystallize and form a eutectic system with ice crystals. Both crystallization and glass formation would make trehalose molecules immobile, i.e. gradually concentrated in dehydrated tissues and hemolymph, which we observed.

Proline-rich viscoelastic liquid forms at the boundary between extracellular ice and dehydrated tissues

In contrast to trehalose, proline does not induce a glass transition (Liu et al., 2020; Rasmussen et al., 1997) and its solubility in water is enormous (it may reach over 15 mol kg^{-1}; Held et al., 2014; Qiu et al., 2019). Nevertheless, physical chemistry shows that proline in high concentration also extensively hydrogen bonds with water and together they form a viscoelastic liquid (de Molina et al., 2017; McLain et al., 2007; Troitzsch et al., 2008). The formation of dense, viscoelastic liquids is a guiding principle underlying the theory of NADES systems (Choi et al., 2011). The components in a complex mixture forming NADES are connected to one another through a well-organized tridimensional system with optimum interactions via inter- and intramolecular hydrogen bonding (Dai et al., 2013; Dai et al., 2015). Through these interactions, NADES systems exhibit emergent properties: (i) the melting point is deeply suppressed (usually below −30°C); (ii) ice crystallization is completely (or at least strongly) inhibited; whereas (iii) the tendency to transition to amorphous glasses is enhanced (Castro et al., 2018; Liu et al., 2018; Martins et al., 2019). However, work with NADES has also shown that the interactions between the NADES components are weakened with water dilution and even broken with water content exceeding 50% weight, when each component recovers its own specific properties (Castro et al., 2018; Dai et al., 2015; Durand et al., 2016). Our artificial CP mixtures have relatively high water content (between 79 and 99%weight), as do the SDA larval hemolymph (74.4%weight) and whole larvae (69.3%weight). Using DSC analysis, we show that these solutions exhibit significant suppression of the melting point (e.g. to −9.2°C in CP mix 1588, and to −4.5°C in SDA hemolymph) and significant water-binding capacity (41.1%OIW in CP mix 1588, and 35.5%OIW in SDA hemolymph). Both parameters (the decrease in melting point and the increase in OIW fraction) were linearly dependent on the osmolality of a solution (from 0 for water to 1588 mmol kg^{-1} for CP mix 1588). These results suggest that neither the CP mixes 508 and 1588 nor the SDA hemolymph are 'deep eutectic systems' (DES, in the strict sense of Martins et al., 2019), but regular aqueous solutions with relatively low transition temperature from liquid to solid phase [LTTM, in the sense of Durand et al. (2016)].

We suggest that a proline-dominated viscoelastic solution with NADES-like properties may form on a microscale level, locally, in slowly freeze-dehydrating larvae. As water molecules are osmotically driven from the gradually dehydrating hemolymph and tissues and migrate toward the extracellular ice during extracellular freezing, the highly soluble and relatively mobile proline molecules could move together with water until they reach a barrier of ice where they form a thin layer of concentrated proline, which we observed in MALDI-MSI. Such a viscoelastic liquid could contribute to the stabilization of deeply frozen *C. costata* larvae by forming a rubber-like zone between extracellular ice crystals and freeze-dehydrated tissues, thus reducing the thermo-mechanical stresses associated with

temperature fluctuations during immersion in liquid N_2 and rewarming (Rubinsky et al., 1980).

Conclusion

Overall, our study reveals the composition of a specific mixture of putative cryoprotectants accumulated by the freeze-tolerant larvae of *C. costata*. We demonstrate in a bioassay that as little as 3 days of exposure to a diet enriched with an artificial mixture of CPs allows an otherwise freeze-sensitive larva to survive not only deep freezing but also cryopreservation in liquid N_2. The components of CP mixture act synergistically rather than additively to improve the freeze tolerance. These findings open avenues for functional experiments to better understand the mechanisms underlying cryoprotection and cryopreservation of complex multicellular organisms. Toward this goal, we demonstrate that the accumulated CPs suppress the melting point of body water, increase the fraction of osmotically inactive water and significantly reduce the ice fraction. During slow extracellular freezing of whole larvae, trehalose becomes concentrated in the partially dehydrated hemolymph and tissues and stimulates glass transition, whereas proline moves to the boundary between extracellular ice and dehydrated tissues where it probably creates a layer of dense viscoelastic liquid. We suggest that these mechanisms contribute to larval extreme freeze tolerance and enable their cryopreservation by protecting their cells against thermomechanical shocks associated with freezing and transfers into and out of liquid N_2.

References
Asahina, E. (1970). Frost resistance in insects. In *Advances in Insect Physiology* (ed. R. Jurenka), Vol. 6, pp. 1-49: Elsevier. doi:10.1016/S0065-2806(08)60109-5
Band, H. T. and Band, R. N. (1982). Multiple overwintering mechanisms in Chymomyza amoena larvae (Diptera: Drosophilidae) and laboratory induction of freeze tolerance. *Experientia* **38**, 1448-1449. doi:10.1007/BF01955762
Bankhead, P., Loughrey, M. B., Fernández, J. A., Dombrowski, Y., McArt, D. G., Dunne, P. D., McQuaid, S., Gray, R. T., Murray, L. J. and Coleman, H. G. (2017). QuPath: open source software for digital pathology image analysis. *Sci. Rep.* **7**, 1-7. doi:10.1038/s41598-017-17204-5
Castro, V. I. B., Craveiro, R., Silva, J. M., Reis, R. L., Paiva, A. and C. Duarte, A. R. (2018). Natural deep eutectic systems as alternative

nontoxic cryoprotective agents. *Cryobiology* **83**, 15-26. doi:10.1016/j.cryobiol.2018.06.010

Cesaro, A., De Giacomo, O. and Sussich, F. (2008). Water interplay in trehalose polymorphism. *Food Chem.* **106**, 1318-1328. doi:10.1016/j.foodchem.2007.01.082

Crowe, J. H., Carpenter, J. F. and Crowe, L. M. (1998). The role of vitrification in anhydrobiosis. *Annu. Rev. Physiol.* **60**, 73-103. doi:10.1146/annurev.physiol.60.1.73

Dai, Y., van Spronsen, J., Witkamp, G.-J., Verpoorte, R. and Choi, Y. H. (2013). Ionic liquids and deep eutectic solvents in natural products research: mixtures of solids as extraction solvents. *J. Nat. Pro.* **76**, 2162-2173. doi:10.1021/np400051w

Dai, Y., Witkamp, G.-J., Verpoorte, R. and Choi, Y. H. (2015). Tailoring properties of natural deep eutectic solvents with water to facilitate their applications. *Food Chem.* **187**, 14-19. doi:10.1016/j.foodchem.2015.03.123

de Molina, P. M., Alvarez, F., Frick, B., Wildes, A., Arbe, A. and Colmenero, J. (2017). Investigation of the dynamics of aqueous proline solutions using neutron scattering and molecular dynamics simulations. *Phys. Chem. Chem. Phys.* **19**, 27739-27754. doi:10.1039/C7CP05474B

Des Marteaux, L. E., Hůla, P. and Koštál, V. (2019). Transcriptional analysis of insect extreme freeze tolerance. *Proc. R. Soc. B* **286**, 20192019. doi:10.1098/rspb.2019.2019

Durand, E., Lecomte, J. and Villeneuve, P. (2016). From green chemistry to nature: the versatile role of low transition temperature mixtures. *Biochimie* **120**, 119-123. doi:10.1016/j.biochi.2015.09.019

Elliott, G. D., Wang, S. and Fuller, B. J. (2017). Cryoprotectants: a review of the actions and applications of cryoprotective solutes that modulate cell recovery from ultra-low temperatures. *Cryobiology* **76**, 74-91. doi:10.1016/j.cryobiol.2017.04.004

Fahy, G. M., Wowk, B. and Wu, J. (2006). Cryopreservation of complex systems: the missing link in the regenerative medicine supply chain. *Rejuvenation Res.* **9**, 279-291. doi:10.1089/rej.2006.9.279

Gertrudes, A., Craveiro, R., Eltayari, Z., Reis, R. L., Paiva, A. and Duarte, A. R. C. (2017). How do animals survive extreme temperature amplitudes? the role of natural deep eutectic solvents. *ACS Sustain Chem. Eng.* **5**, 9542-9553. doi:10.1021/acssuschemeng.7b01707

Green, J. L. and Angell, C. A. (1989). Phase relations and vitrification in saccharide-water solutions and the trehalose anomaly. *J. Phys. Chem.* **93**, 2880-2882. doi:10.1021/j100345a006

Grimaldi, D. (1986). The chymomyza aldrichii species-group (Diptera: Drosophilidae); relationships, new neotropical species, and the evolution of some sexual traits. *J. N. Y. Entomol. Soc.* **94**, 342-371.

Held, C., Reschke, T., Müller, R., Kunz, W. and Sadowski, G. (2014). Measuring and modeling aqueous electrolyte/amino-acid solutions with ePC-SAFT. *J. Chem. Thermodyn.* **68**, 1-12. doi:10.1016/j.jct.2013.08.018

Hochachka, P. and Somero, G. (2002). *Biochemical Adaptation. Mechanism and Process in Physiological Evolution*: Oxford University Press.

Hornberger, K., Li, R., Duarte, A. R. C. and Hubel, A. (2021). Natural deep eutectic systems for nature-inspired cryopreservation of cells. *AIChE J.* **67**, e17085. doi:10.1002/aic.17085

Chen, T., Fowler, A. and Toner, M. (2000). Literature review: supplemented phase diagram of the trehalose-water binary mixture. *Cryobiology* **40**, 277-282. doi:10.1006/cryo.2000.2244

Choi, Y. H., van Spronsen, J., Dai, Y., Verberne, M., Hollmann, F., Arends, I. W., Witkamp, G.-J. and Verpoorte, R. (2011). Are natural deep eutectic solvents the missing link in understanding cellular metabolism and physiology? *Plant Physiol.* **156**, 1701-1705. doi:10.1104/pp.111.178426

Khalil, S., Pretzel, J., Becker, K. and Spengler, B. (2017). High-resolution AP-SMALDI mass spectrometry imaging of Drosophila melanogaster. *Int. J. Mass Spectrom.* **416**, 1-19. doi:10.1016/j.ijms.2017.04.001

Kolářová, L., Prokeš, L., Kučera, L., Hampl, A., Peňa-Méndez, E., Vaňhara, P. and Havel, J. (2016). Clusters of monoisotopic elements for calibration in (TOF) mass spectrometry. *J. Am. Soc. Mass Spectrom.* **28**, 419-427. doi:10.1007/s13361-016-1567-x

Kostal, V., Noguchi, H., Shimada, K. and Hayakawa, Y. (1998). Developmental changes in dopamine levels in larvae of the fly Chymomyza costata: comparison between wild-type and mutant-nondiapause strains. *J. Insect Physiol.* **44**, 605-614. doi:10.1016/S0022-1910(98)00043-2

Koštál, V., Renault, D. and Rozsypal, J. (2011a). Seasonal changes of free amino acids and thermal hysteresis in overwintering heteropteran insect, Pyrrhocoris apterus. *CBPA* **160**, 245-251.

Koštál, V., Zahradníčková, H. and Šimek, P. (2011b). Hyperprolinemic larvae of the drosophilid fly, Chymomyza costata, survive cryopreservation in liquid nitrogen. *Proc. Natl. Acad. Sci. USA* **108**, 13041-13046. doi:10.1073/pnas.1107060108

Lakovaara, S. (1969). Malt as a culture medium for Drosophila species. *Drosophila Inf. Serv.* **44**, 128.

Lee, R. E. J. (2010). A primer on insect cold-tolerance. In *Low Temperature Biology of Insects* (ed. D. L. Denlinger and R. E. J. Lee), pp. 3-34. Cambridge University Press.

Liu, Y., Friesen, J. B., McAlpine, J. B., Lankin, D. C., Chen, S.-N. and Pauli, G. F. (2018). Natural deep eutectic solvents: properties, applications, and perspectives. *J. Nat. Prod.* **81**, 679-690. doi:10.1021/acs.jnatprod.7b00945

Liu, W., Huang, Z., He, X., Jiang, P., Huo, X., Lu, Z. and Liu, B. (2020). Impacts of trehalose and l-proline on the thermodynamic nonequilibrium phase change and thermal properties of normal saline. *Cryobiology* **96**, 92-98. doi:10.1016/j.cryobiol.2020.07.011

Martins, M. A. R., Pinho, S. P. and Coutinho, J. A. P. (2019). Insights into the nature of eutectic and deep eutectic mixtures. *J. Solution Chem.* **48**, 962-982. doi:10.1007/s10953-018-0793-1

McLain, S. E., Soper, A. K., Terry, A. E. and Watts, A. (2007). Structure and hydration of L-proline in aqueous solutions. *J. Phys. Chem. B* **111**, 4568-4580. doi:10.1021/jp068340f

Moon, I., Fujikawa, S. and Shimada, K. (1996). Cryopreservation of *Chymomyza* larvae (Diptera: Drosophilidae) at-196°C with extracellular freezing. *Cryo. Lett.* **17**, 105-110.

Nicolajsen, H. and Hvidt, A. (1994). Phase behavior of the system trehalose-NaCl-water. *Cryobiology* **31**, 199-205. doi:10.1006/cryo.1994.1024

Niedermeyer, T. H. J. and Strohalm, M. (2012). mMass as a software tool for the annotation of cyclic peptide tandem mass spectra. *PLoS One* **7**, e44913. doi:10.1371/journal.pone.0044913

Olgenblum, G. I., Sapir, L. and Harries, D. (2020). Properties of aqueous trehalose mixtures: Glass transition and hydrogen bonding. *J. Chem. Theory Comput.* **16**, 1249-1262. doi:10.1021/acs.jctc.9b01071

Pegg, D. (2001). The current status of tissue cryopreservation. *Cryo. Lett.* **22**, 105-114.

Pokorna, E., Faltus, M., Machova, P., Zamecnik, J. and Fulin, M. (2020). Grey poplar explant acclimation to improve the dehydration tolerance and cryopreservation. *Biol. Plant.* **64**, 119-128. doi:10.32615/bp.2019.148

Qiu, J., Huang, H., He, H., Liu, H., Hu, S., Han, J., Yi, D., An, M. and Wang, P. (2019). Solubility behavior and data modeling of l-proline in different neat and binary solvent systems. *J. Chem. Eng. Data* **64**, 5920-5928. doi:10.1021/acs.jced.9b00802

Rasmussen, P. H., Jørgensen, B. and Nielsen, J. (1997). Aqueous solutions of proline and NaCl studied by differential scanning calorimetry at subzero temperatures. *Thermochim Acta.* **303**, 23-30. doi:10.1016/S0040-6031(97)00241-4

Riihimaa, A. J. and Kimura, M. T. (1988). A mutant strain of *Chymomyza costata* (Diptera: Drosophilidae) insensitive to diapause–inducing action of photoperiod. *Physiol. Entomol.* **13**, 441-445. doi:10.1111/j.1365-3032.1988.tb01128.x

Rozsypal, J., Koštál, V., Zahradníčková, H. and Šimek, P. (2013). Overwintering strategy and mechanisms of cold tolerance in the codling moth (Cydia pomonella). *PLoS One* **8**, e61745. doi:10.1371/journal.pone.0061745

Rozsypal, J., Moos, M., Šimek, P. and Koštál, V. (2018). Thermal analysis of ice and glass transitions in insects that do and do not survive freezing. *J. Exp. Biol.* **221**, 170464. doi:10.1242/jeb.170464

Rubinsky, B., Cravalho, E. G. and Mikic, B. (1980). Thermal stresses in frozen organs. *Cryobiology* **17**, 66-73. doi:10.1016/0011-2240(80)90009-7

Rudolph, A. S. and Crowe, J. H. (1986). A calorimetric and infrared spectroscopic study of the stabilizing solute proline. *Biophys. J.* **50**, 423-430. doi:10.1016/S0006-3495(86)83478-6

Salt, R. (1961). Principles of insect cold-hardiness. *Annu. Rev. Entomol.* **6**, 55-74. doi:10.1146/annurev.en.06.010161.000415

Shimada, K. and Riihimaa, A. (1988). Cold acclimation, inoculative freezing and slow cooling: essential factors contributing to the freezing-tolerance in diapausing larvae of *Chymomyza costata* (Diptera: Drosophilidae). *Cryo. Lett.* **9**, 5-10.

Sinclair, B. J. (1999). Insect cold tolerance: how many kinds of frozen? *Eur. J. Entomol.* **96**, 157-164.

Somero, G. (1986). Protons, osmolytes, and fitness of internal milieu for protein function. *Am. J. Physiol. Regul. Integr. Comp. Physiol.* **251**, R197-R213. doi:10.1152/ajpregu.1986.251.2.R197

Sømme, L. (1982). Supercooling and winter survival in terrestrial arthropods. *CBPA* **73**, 519-543. doi:10.1016/0300-9629(82)90260-2

Storey, K. B. (1997). Organic solutes in freezing tolerance. *Comp. Biochem. Physiol. A* **117**, 319-326. doi:10.1016/S0300-9629(96)00270-8

Storey, J. M. and Storey, K. B. (1986). Winter survival of the gall fly larva, Eurosta solidaginis: profiles of fuel reserves and cryoprotectants in a natural population. *J. Insect Physiol.* **32**, 549-556. doi:10.1016/0022-1910(86)90070-3

Storey, K. B. and Storey, J. M. (1988). Freeze tolerance in animals. *Physiol. Rev.* **68**, 27-84. doi:10.1152/physrev.1988.68.1.27

Storey, K. B. and Storey, J. M. (1991). Biochemistry of cryoprotectants. In *Insects at Low Temperature*, pp. 64-93: Springer.

Škodová-Sveráková, I., Prokopchuk, G., Peña-Diaz, P., Záhonová, K., Moos, M., Horváth, A., Šimek, P. and Lukeš, J. (2020). Unique dynamics of paramylon storage in the marine euglenozoan Diplonema papillatum. *Protist* **171**, 125717. doi:10.1016/j.protis.2020.125717

Škodová-Sveráková, I., Záhonová, K., Juricová, V., Danchenko, M., Moos, M., Baráth, P., Prokopchuk, G., Butenko, A., Lukáčová, V., Kohútová, L. et al. (2021). Highly flexible metabolism of the marine euglenozoan protist Diplonema papillatum. *BMC Biol.* **19**, 251. doi:10.1186/s12915-021-01186-y

Journal of Experimental Biology

10

Štětina, T., Hůla, P., Moos, M., Šimek, P., Šmilauer, P. Koštál, V. (2018). Recovery from supercooling, freezing, and cryopreservation stress in larvae of the drosophilid fly, *Chymomyza costata. Sci. Rep.* **8**, 4414. doi:10.1038/s41598-018-22757-0

Toxopeus, J. and Sinclair, B. J. (2018). Mechanisms underlying insect freeze tolerance. *Biol. Rev.* **93**, 1891-1914. doi:10.1111/brv.12425

Toxopeus, J., Koštál, V. and Sinclair, B. J. (2019). Evidence for non-colligative function of small cryoprotectants in a freeze-tolerant insect. *Proc. R. Soc. B.* **286**, 20190050. doi:10.1098/rspb.2019.0050

Troitzsch, R. Z., Vass, H., Hossack, W. J., Martyna, G. J. and Crain, J. (2008). Molecular mechanisms of cryoprotection in aqueous proline: light scattering and molecular dynamics simulations. *J. Phys. Chem.* **112**, 4290-4297. doi:10.1021/jp076713m

Tuthill, B. F., , II, Searcy, L. A., Yost, R. A. and Musselman, L. P. (2020). Tissue-specific analysis of lipid species in Drosophila during overnutrition by UHPLC-MS/MS and MALDI-MSI. *J. Lip. Res.* **61**, 275-290. doi:10.1194/jlr.RA119000198

Weng, L. and Elliott, G. D. (2014). Dynamic and thermodynamic characteristics associated with the glass transition of amorphous trehalose–water mixtures. *Phys. Chem. Chem. Phys.* **16**, 11555-11565. doi:10.1039/C3CP55418J

Wishart, D. S., Feunang, Y. D., Marcu, A., Guo, A. C., Liang, K., Vázquez-Fresno, R., Sajed, T., Johnson, D., Li, C. and Karu, N. (2018). HMDB 4.0: the human metabolome database for 2018. *Nucleic Acids Res.* **46**, D608-D617. doi:10.1093/nar/gkx1089

Yancey, P. H. (2005). Organic osmolytes as compatible, metabolic and counteracting cytoprotectants in high osmolarity and other stresses. *J. Exp. Biol.* **208**, 2819-2830. doi:10.1242/jeb.01730

Yang, F. Y., Chen, J. H., Ruan, Q. Q., Saqib, H. S., He, W. Y. and You, M. S. (2020). Mass spectrometry imaging: an emerging technology for the analysis of metabolites in insects. *Arch. Insect Biochem. Physiol.* **103**, e21643. doi:10.1002/arch.21643

Zachariassen, K. E. (1985). Physiology of cold tolerance in insects. *Physiol. Rev.* **65**, 799-832. doi:10.1152/physrev.1985.65.4.799

51

Table S1. Tissue metabolomics results.

Table S2. Results of DSC analysis

Table S3. CP mix 508 diet recipe

Table S4. Effect of CP mix 508 diet on larval survival and pupariation time

Table S5. Effect of CP Mix 508 diet on larval metabolite composition

Table S6. Effect of CP mix 508 and Pro 313 diets on LN2 survival (replicates shown separately)

Click here to download Tables S1-S6
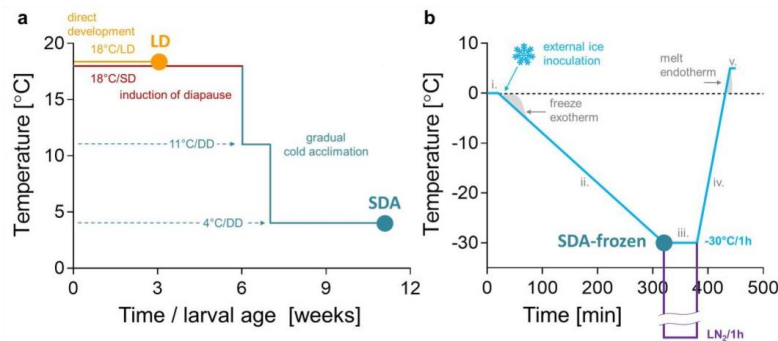
Fig. S1. Phenotypic/acclimation variants and freeze tolerance bioassay.
(a) Acclimation: *Chymomyza costata* flies were reared from eggs (time 0) to 3rd larval instars (time 3 weeks) at constant 18°C under one of two photoperiods: long-day (LD, 16 h light:8 h dark) or short day (SD, 12 h light:12 h dark). The LD conditions promote direct development from larva to pupa. The LD larvae are freeze sensitive and do not survive cryopreservation in LN$_2$. The SD conditions induce entry into developmental arrest (diapause). Larvae reach their final weight aSDAer 6 weeks and are then transferred to constant darkness (DD) and low temperatures of 11°C followed by 4°C. Cold acclimation induces acquisition of freeze tolerance (phenotype SDA) including the ability to survive in LN$_2$. **(b)** Optimal protocols for freezing and LN$_2$ cryopreservation according to (Rozsypal et al., 2018). The protocol consisted of five steps set in a Ministat 240 programmable cryostat (Huber, Offenburg, Germany). The addition of a small ice crystal at the beginning of step (ii.) induces inoculative internal freezing in larvae. The SDA-frozen larvae underwent slow pre-freezing to -30°C associated with freeze dehydration of their tissues.
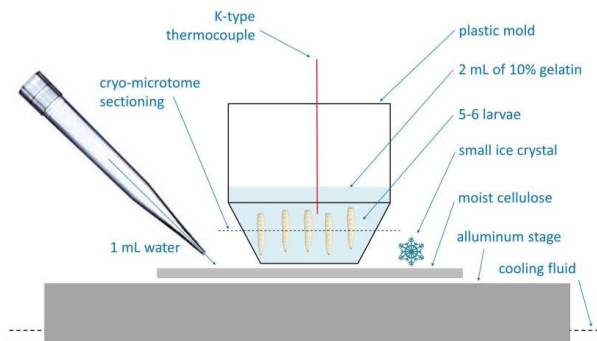
Fig. S2. Preparation of SDA-frozen larvae for MALDI-TOF/MS analysis.
SDA larvae were embedded in gelatin in a plastic mold a top a layer of moist cellulose to which a small ice crystal was added to initiate freezing. The mold had a hole in the bottom (0.5 cm in diameter) to allow ice crystal spreading from the moist cellulose to the gelatin. The whole setup was placed on an aluminum stage pre-cooled to 0°C in the programmable thermostat F32-ME (Julabo, Seelbach, Germany) and the optimal freezing protocol (Fig. A1b) was started. As soon as the temperature inside the gelatin reached -30°C, we immersed the mold into isopentane at -140°C. Using a K-type thermocouple attached to the PicoLog TC-08 datalogger (Pico technology, St. Neots, UK), we verified that the gelatin inside plastic mold was inoculated by external ice crystals at relatively mild subzero temperatures of -1°C to -2°C. We also verified that SDA-frozen larvae survive this treatment and are able to move after re-warming.

Fig. S3. Metabolomic profiles in *C. costata* tissues.
Forty-nine target metabolites were quantified in absolute terms using four different MS analytical platforms. Total pools in four tissues are shown for larvae of two contrasting phenotypes: LD, the non-diapause, warm-acclimated, freeze-sensitive larvae; SDA, the diapausing, cold-acclimated, extremely freeze-tolerant larvae (see Fig. S1 for further explanation). Each column is a mean ± SD (*n* = 4 biological replicates, each containing tissues from 30 larvae). Differences between LD and SDA means were tested with unpaired t-tests corrected for multiple comparison using the Holm-Sidak method with α = 0.01. Asterisks indicate significantly different means. Bright blue columns highlight five metabolites that are most concentrated in the SDA hemolymph.

Fig. S4. Sizes of metabolite pools in *C. costata* tissues.
The sizes of metabolite pools (see Supplementary Fig. 1) in freeze-sensitive (LD) and freeze-tolerant (SDA) larvae were compared as Log_2-fold differences between tissue and hemolymph pools. The hemolymph pool was set to 1 (i.e. Log_2 = 0, baseline). A negative Log_2-fold difference means that the tissue pool is smaller than the hemolymph pool (and *vice versa*).

Notes:
Insect hemolymph it is known to contain relatively high concentrations of various metabolites (Mullins, 1985), including the insect 'blood sugar' trehalose (Thompson, 2003). Accordingly, the trehalose pool in SDA larval hemolymph was approximately 16 times larger than the pools in the fat body or midgut, and 64 times larger than the pool in muscle. Some metabolites predominated in the tissues rather than in the hemolymph. For example, maltose was found mainly in the midgut, reflecting the digestion of dietary starch to maltose (Applebaum, 1985); arginine and arginine phosphate were specifically enriched in muscle, reflecting the phosphagen role of arginine phosphate in insect muscle (Beis and Newsholme, 1975); aspartate and glutamate were prevalent in all tissues, reflecting their role as central sinks for ammonia groups during the metabolic conversions of amino acids (Champe and Harvey, 1994); glutathione was also prevalent in tissues due to its central role in cellular redox balance (Sies, 1999). We assume that our MS analysis has probably captured the majority of prominent (most abundant) metabolites. We base our assumption on the following arguments: (i) the total osmolarity of the SDA hemolymph is approximately 700 mOsmol.kg^{-1} (Rozsypal et al., 2018) of which 554 mmol.L^{-1} is explained by our MS analysis of 49 metabolites; (ii) the metal cations of the hemolymph (dominated by Na^+ and K^+) occupy approximately 80 mmol.L^{-1} (Olsson et al., 2016; Štětina et al., 2018); (iii) a similar concentration (70 mmol.L^-) must be reserved for anions (represented by Cl^-, HCO_3^-, and proteins, with 10 mmol.L^{-1} excluded to account for the negatively charged metabolites aspartate, glutamate, TCA intermediates, etc.); (iv) a calculation [700 − 554 − (80 + 70) = -4] suggests that no unexplained 'osmotic gap' remains between the sum of the molar concentrations of the 49 metabolites analyzed and the hemolymph osmolality.
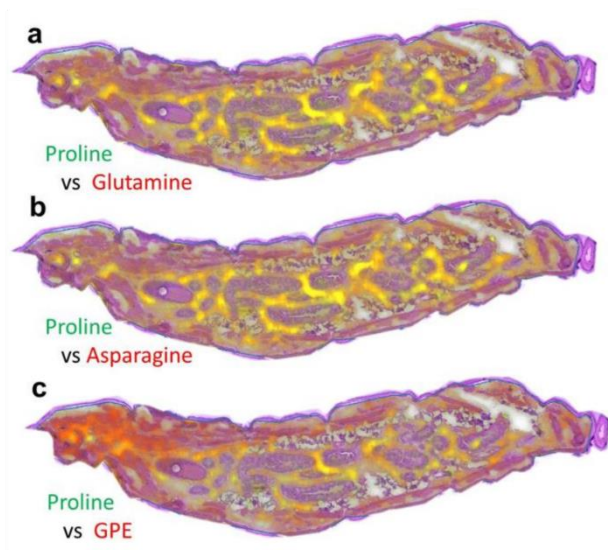
Fig. S5. MALDI-MSI of proline colocalized with Gln, Asn, and GPE in a longitudinal section of an SDA larva.
Colocalizations of select signals shown in color mixing code. Colocalizations were observed in hemolymph for proline (green signal) and three other metabolites: **(a)** glutamine (red signal); **(b)** asparagine (red signal); and **(c)** and GPE (red signal). Medium denoising (SCiLS tool) of signal intensities between adjacent pixels of 10x10 μm was performed.

Note:
The amino acids glutamine and proline are predominantly co-localized with proline in the hemolymph (the yellow colour results from the mixture of the green and red signals). The high intensity GPE signal is present in the hemolymph and in muscle tissue.
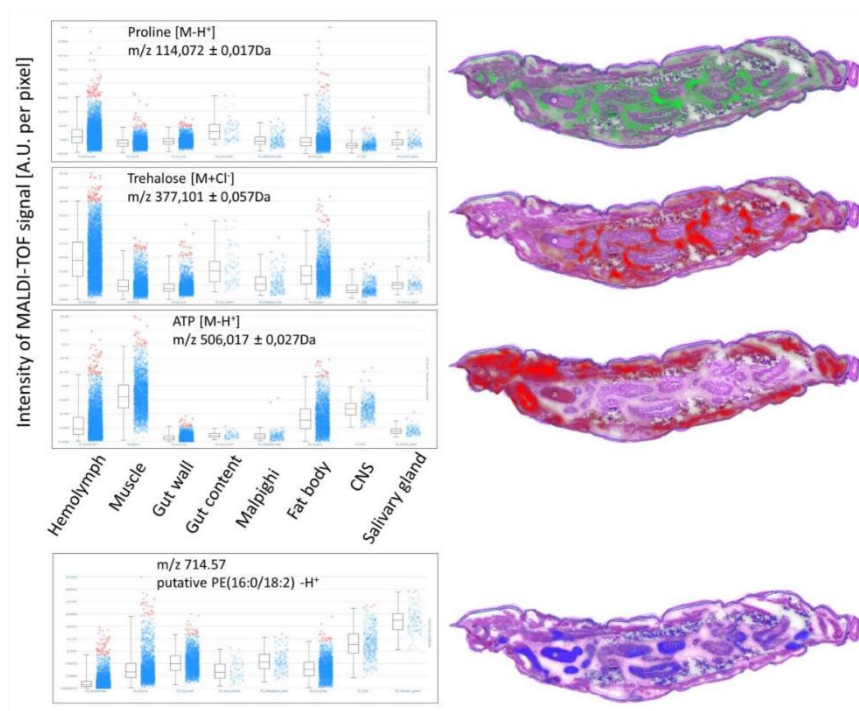
Fig. S6. Relative quantification of MALDI-TOF signals: method and limitations.
Examples of the tissue-specific intensities of the MALDI-TOF signals for three compounds shown in Fig. 1 (proline, trehalose, and ATP). For comparison, we show the signal of a putative phospholipid (m/z 714.57). Each coloured dot in the diagram is the signal intensity per pixel of 10x10 μm (expressed in arbitrary units, A.U.). Boxes show the median, upper, and lower quartiles; whiskers show the 0% and 99% quantiles. Orange data points are those above the 99% quantile.

Note:
The signal intensities per pixel vary greatly in all tissues. This is at least partly because the MALDI-MSI analysis of small molecules (smaller than m/z 700) freely dissolved in biological solutions is technically difficult (Fujimura and Miura, 2014). Diffusion of small metabolites within the tissue during matrix application and other steps of sample preparation can limit spatial resolution. In general, some analytes may delocalize from their original positions into adjacent tissues (Fujimura and Miura, 2014). An example of this problem is shown in analysis of the ATP signal, whose highest intensity is expected in tissues. Although our analysis localizes the ATP mainly in muscle, fat body, and CNS tissues, a relatively high signal intensity is also detected in hemolymph. As ATP leaks from the tissues into the hemolymph during sample preparation, the same can happen in reverse with hemolymph-specific metabolites (such as trehalose). For this reason, the MALDI-MSI is most successfully used for larger molecules such as proteins, peptides, and lipids, which are less mobile (Tuthill II et al., 2020). The analysis of the compound with m/z 714.57 (probably phosphatidylethanolamine) is such an example of a larger and less mobile molecule allowing better tissue resolution.
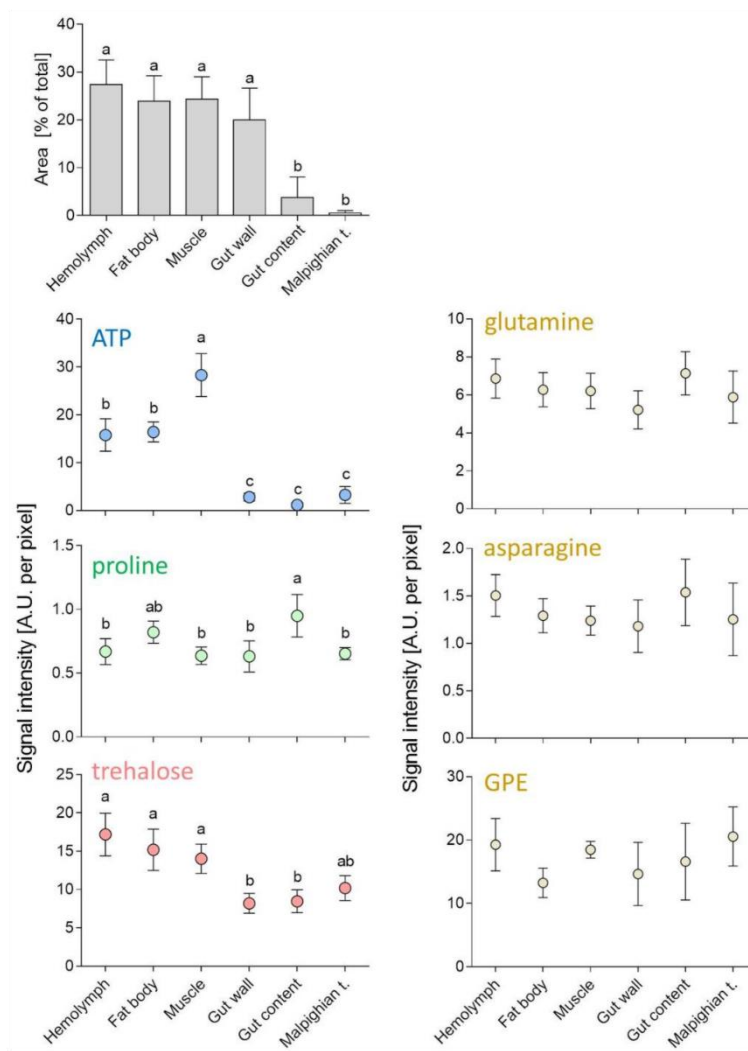
Fig. S7.Relative quantification of MALDI-TOF signals in LD larvae.
Results of the MALDI-TOF signal intensity analysis on transversal sections through the middle part of the larva (five larvae were sectioned). The upper leSDA figure shows the relative proportions of the different tissues on five sections (each column is a mean ± S.D. % of total area). Shown are the signal intensities of five selected putative CPs plus ATP. Each point is a mean ± S.D of five tissue-median intensities (for explanation, see Fig. S6). The relative intensities are expressed in arbitrary units, A.U. Differences between means were statistically analyzed using a one-way ANOVA followed by a Bonferroni's multiple comparison test. Means flanked by different letters (within each subpanel) are statistically different. GPE, glycerophosphoethanolamine. For details, see Appendice containing all MALDI-MSI images.
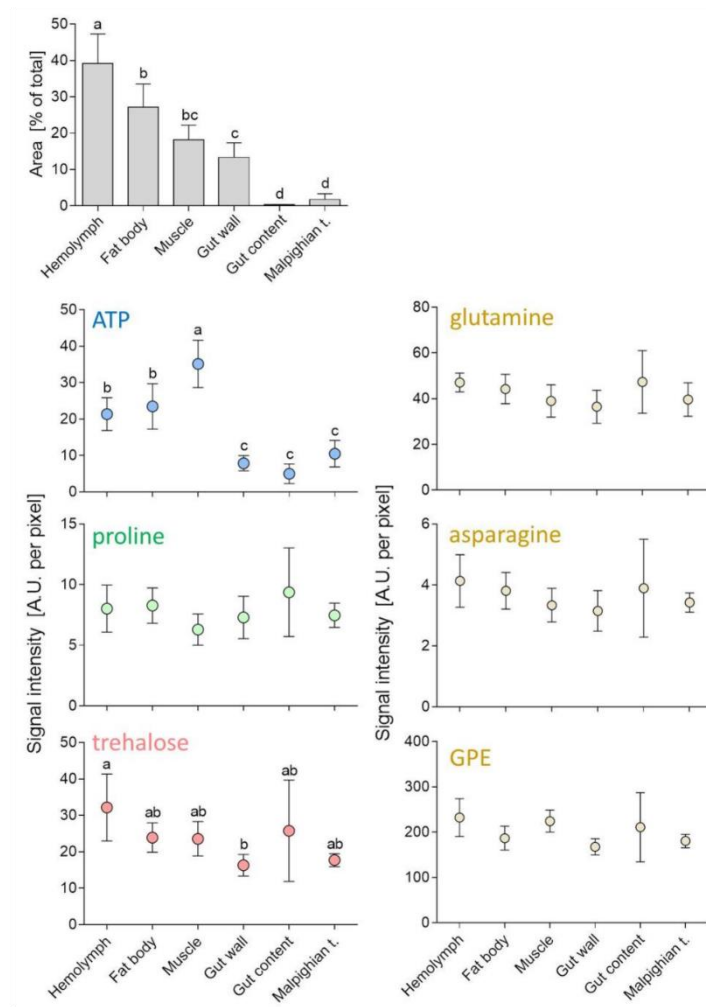
Fig. S8. Relative quantification of MALDI-TOF signals in SDA larvae. All descriptions as in Fig. S7. For details, see MALDI-MSI images.
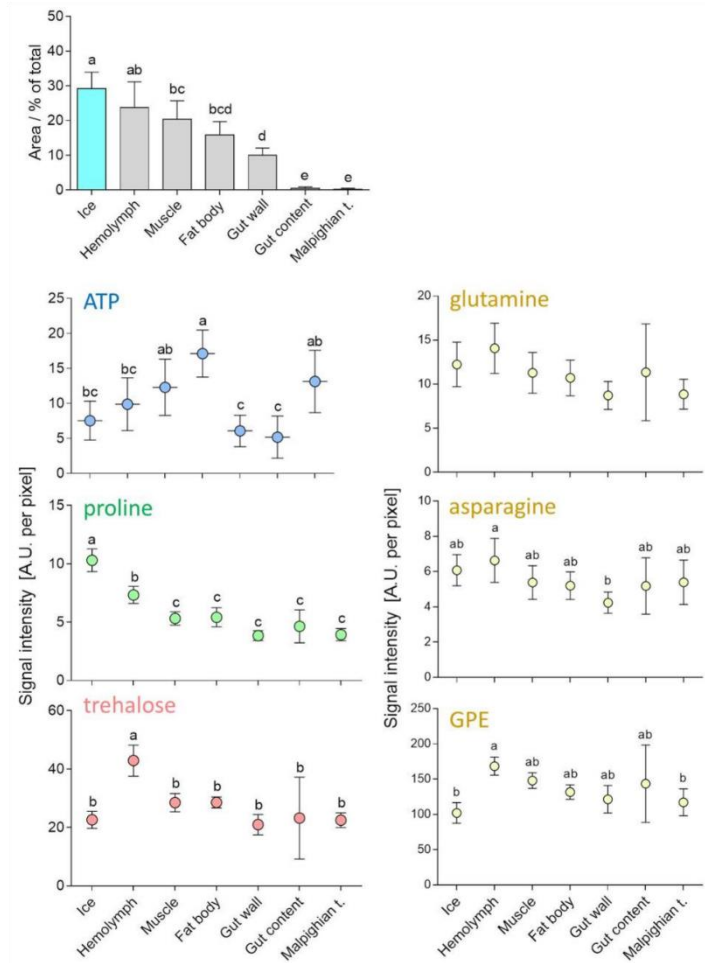
Fig. S9. Relative quantification of MALDI-TOF signals in SDA-frozen larvae.
All descriptions as in Supplementary Fig. S7 except that six larvae were sectioned in the SDA-frozen group. For details, see MALDI-MSI images.
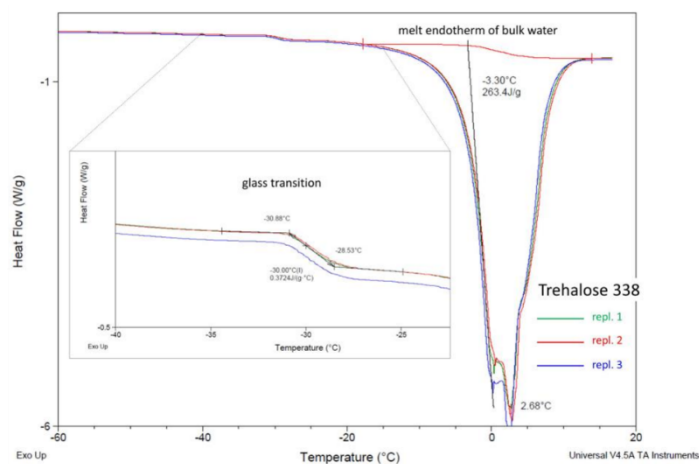
Fig. S10. Analysis of DSC heating curves of trehalose solution (338 mmol.kg^{-1}) in water. Three technical replicates of the same solution are shown in different colours. Replicate 1 (green line) is quantified using TA Universal Analysis 2000 soSDAware as an example. The complete dataset of DSC analysis results can be found in Table S2.
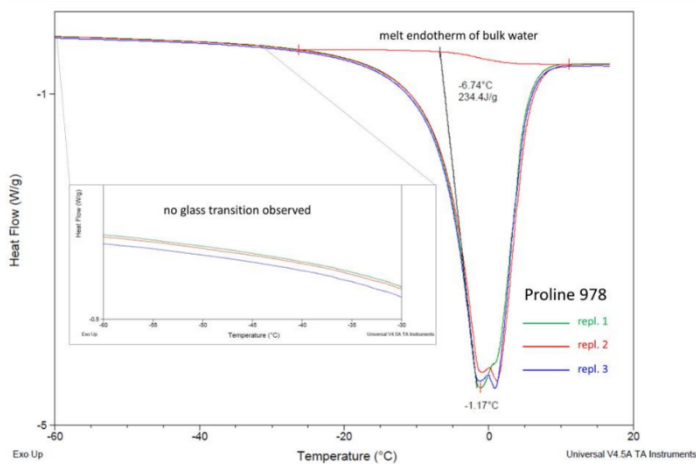
Fig. S11. Analysis of DSC heating curves of proline solution (978 mmol.kg^{-1}) in water.
Three technical replicates of the same solution are shown in different colours. Replicate 1 (green line) is quantified as an example. The complete dataset of DSC analysis results can be found in Table S2.
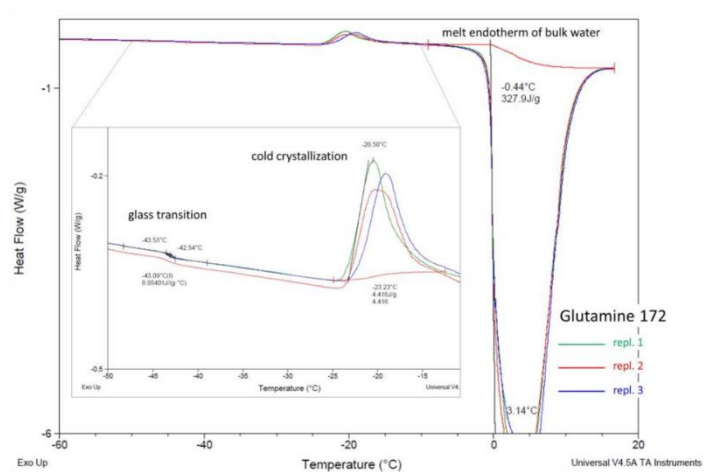
Fig. S12. Analysis of DSC heating curves of glutamine solution (172 mmol.kg^{-1}) in water. Three technical replicates of the same solution are shown in different colours. Replicate 1 (green line) is quantified as an example. The complete dataset of DSC analysis results can be found in Table S2.
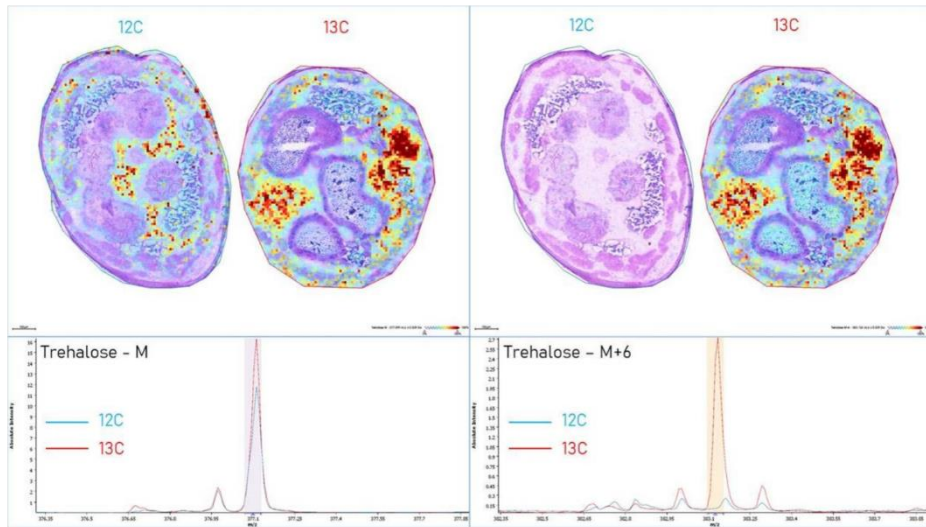
Fig. S13. Validation of trehalose m/z peak identity using a ^{13}C6 experiment.
LD larvae at 17 days of age were fed a ^{13}C6-labelled glucose enriched diet (13C, red font) for 24 hours, while the control group was fed standard diet (12C, blue font). The larvae were then processed for MALDI-MS/TOF analysis as described in Materials and Methods. The left pair of sections shows the signal of trehalose (M, m/z 337.101), the right pair of sections shows the signal of the trehalose molecules with one ^{13}C6-labelled glucose incorporated into its structure (M+6, m/z 383.1).

Notes:

Larvae fed a standard 12C diet show a distinct signal from trehalose (M) in hemolymph and no signal from ^{13}C6 labelled trehalose (M+6).

Larvae fed a ^{13}C6 glucose-enriched diet (13C) show that the signal from M and M+6 are co-localized at exactly the same positions (mainly in hemolymph).
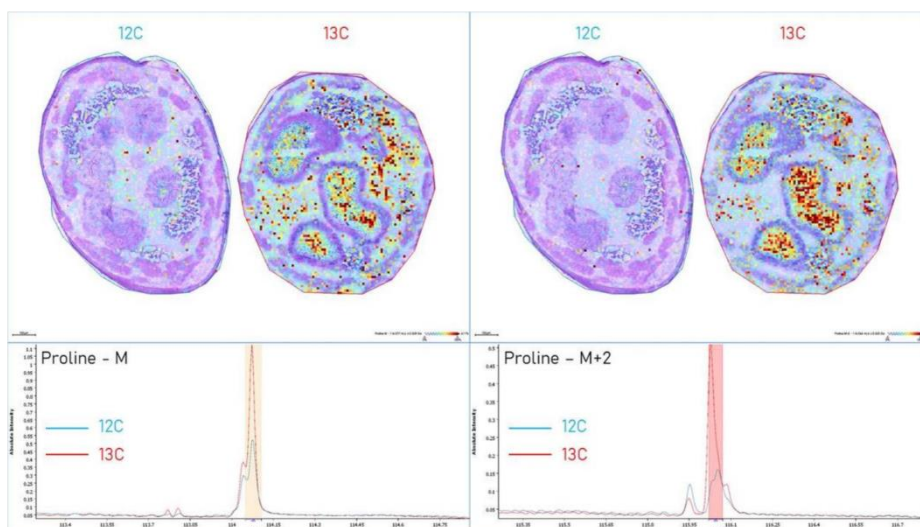
Fig. S14. Validation of proline m/z peak identity using a [13]C6 experiment.
LD larvae at 17 days of age were fed [13]C6-labelled glucose enriched diet (13C, red font) for 24 hours, while the control group was fed standard diet (12C, blue font). The larvae were then processed for MALDI-MS/TOF analysis as described in Materials and Methods. The left pair of sections shows the signal of the proline molecule (M, m/z 114.072), the right pair of sections shows the signal of the proline molecule containing two ^{13}C-labelled atoms in its structure (M+2, m/z 116.1). Only two ^{13}C-labelled atoms are transferred from [13]C6 glucose to the proline structure as it undergoes glycolysis, TCA, and proline biosynthetic pathways.

Notes:
Larvae fed standard 12C diet show signal of proline (M) in the gut content, hemolymph, and fat body, while the signal of [13]C6 labelled proline (M+2) is weaker or absent.

Larvae fed [13]C6 glucose-enriched diet (13C) show the signal of M and M+2 co-localized at the same positions. The proline (M) signal is very abundant in the gut content of other LD larvae (Fig. S7 and Appendice), as the diet contains a relatively high concentration of proline (unpublished data).

References

Applebaum, S. W. (1985). Biochemistry of digestion. In *Comprehensive insect physiology, biochemistry and pharmacology*, vol. 4, pp. 279-311.

Beis, I. and Newsholme, E. A. (1975). The contents of adenine nucleotides, phosphagens and some glycolytic intermediates in resting muscles from vertebrates and invertebrates. *Biochem J.* **152**, 23-32.

Fujimura, Y. and Miura, D. (2014). MALDI Mass Spectrometry Imaging for Visualizing In Situ Metabolism of Endogenous Metabolites and Dietary Phytochemicals. *Metabolites* **4**, 319-346.

Champe, P. and Harvey, R. (1994). Lippincott's illustrated reviews: biochemistry 2nd ed: Philadelphia: JB Lippincott.

Mullins, D. (1985). Chemistry and physiology of the hemolymph. In *Comprehensive insect physiology, biochemistry and pharmacology*, vol. 3, pp. 355-400.

Olsson, T., MacMillan, H. A., Nyberg, N., Staerk, D., Malmendal, A. and Overgaard, J. (2016). Hemolymph metabolites and osmolality are tightly linked to cold tolerance of Drosophila species: a comparative study. *J Exp Biol.* **219**, 2504-2513.

Rozsypal, J., Moos, M., Šimek, P. and Koštál, V. (2018). Thermal analysis of ice and glass transitions in insects that do and do not survive freezing. *J Exp Biol.* **221**, 170464.

Sies, H. (1999). Glutathione and its role in cellular functions. *Free Radic Biol Med.* **27**, 916-921.

Štětina, T., Hůla, P., Moos, M., Šimek, P., Šmilauer, P. and Koštál, V. (2018). Recovery from supercooling, freezing, and cryopreservation stress in larvae of the drosophilid fly, *Chymomyza costata.* *Sci Rep.* **8**, 4414.

Thompson, S. N. (2003). Trehalose—the insect 'blood'sugar. *Adv In Insect Phys.* **31**, 205-285.

Tuthill II, B. F., Searcy, L. A., Yost, R. A. and Musselman, L. P. (2020). Tissue-specific analysis of lipid species in Drosophila during overnutrition by UHPLC-MS/MS and MALDI-MSI. *J Lip Res* **61**, 275-290.

Paper III

Stabilization of insect cell membranes and soluble enzymes by accumulated cryoprotectants during freezing stress

Grgac, R., Rozsypal, J., Des Marteaux, L., Štětina T., & Koštál, V. (2022)

Stabilization of insect cell membranes and soluble enzymes by accumulated cryoprotectants during freezing stress

Robert Grgac[a,b] ![ORCID], Jan Rozsypal[a] ![ORCID], Lauren Des Marteaux[a,1] ![ORCID], Tomáš Štětina[b] ![ORCID], and Vladimír Koštál[a,2] ![ORCID]

Most multicellular organisms are freeze sensitive, but the ability to survive freezing of the extracellular fluids evolved in several vertebrate ectotherms, some plants, and many insects. Here, we test the coupled hypotheses that are perpetuated in the literature: that irreversible denaturation of proteins and loss of biological membrane integrity are two ultimate molecular mechanisms of freezing injury in freeze-sensitive insects and that seasonally accumulated small cryoprotective molecules (CPs) stabilize proteins and membranes against injury in freeze-tolerant insects. Using the drosophilid fly, *Chymomyza costata*, we show that seven different soluble enzymes exhibit no or only partial loss of activity upon lethal freezing stress applied in vivo to whole freeze-sensitive larvae. In contrast, the enzymes lost activity when extracted and frozen in vitro in a diluted buffer solution. This loss of activity was fully prevented by adding low concentrations of a wide array of different compounds to the buffer, including *C. costata* native CPs, other metabolites, bovine serum albumin (BSA), and even the biologically inert artificial compounds HistoDenz and Ficoll. Next, we show that fat body plasma membranes lose integrity when frozen in vivo in freeze-sensitive but not in freeze-tolerant larvae. Freezing fat body cells in vitro, however, resulted in loss of membrane integrity in both freeze-sensitive and freeze-tolerant larvae. Different additives showed widely different capacities to protect membrane integrity when added to in vitro freezing media. A complete rescue of membrane integrity in freeze-tolerant larvae was observed with a mixture of proline, trehalose, and BSA.

cryopreservation | freeze tolerance | protein stabilization | enzyme activity | biological membrane integrity

Freezing of the body fluids is lethal for most multicellular organisms, but many plants, invertebrates, and also a few amphibians and reptiles evolved the capacity to survive internal ice formation (i.e., freeze tolerance) (1–3). Freeze tolerance is particularly widespread among insects (4). All freeze-tolerant organisms rely on extracellular ice formation, while formation of ice inside their cells is (with exceptions) lethal (5). Extracellular ice causes osmotic outflow of water from cells, which results in cell shrinkage and concentration of cytosolic solutions (6). Consequently, the freeze-dehydrated cells are exposed to a combination of mechanical stress, low temperatures, decreasing activity of liquid water, and increasing levels of protons, metal ions, or other chemical perturbants, which altogether threaten conformational stability of proteins, lipid bilayers, and other macromolecular complexes (7).

A widely accepted consensus among environmental physiologists and low-temperature biologists is that irreversible denaturation of proteins and loss of biological membrane integrity are two important mechanisms of lethal freezing injury for various organisms (6, 8–11). Another, almost unanimous agreement exists about the role of low molecular mass cryoprotective molecules (CPs), such as sugars, polyols, amino acids, and their derivatives, that are accumulated by naturally freeze-tolerant organisms: that CPs protect proteins and membranes against freezing injury (1, 12–15). Accordingly, in the insect cold hardiness literature, proteins and membranes are often mentioned simultaneously as the two most likely targets of cold and freezing injury, and their stabilization by seasonally accumulated CPs is accepted as a highly plausible hypothesis (1, 16–19).

CPs are believed to help primarily by affecting the colligative properties of biological solutions, specifically by increasing osmolarity and thereby reducing the amount of ice formed at any given subzero temperature, which, in turn, alleviates all mechanical, freeze-dehydration, and solute concentration stresses (6, 20–23). In addition, various noncolligative mechanisms of cryoprotection were hypothetically ascribed to insect CPs (1, 16, 23) and were also supported by indirect experimental evidence (24–26). The noncolligative mechanisms are theoretically based on noncovalent interactions between water molecules, destabilizing solutes (perturbants), stabilizing solutes (CPs), and stabilized proteins and

Significance

Here, we suggest that soluble enzymes are not primary targets of insect freezing injury. We demonstrate that various enzymes are not inactivated in freeze-sensitive insects exposed to lethal freezing stress, as they are sufficiently protected from loss of activity by the complex composition of native biological solutions. Next, we confirm that cell membranes are likely targets of freezing injury. We show that cell membranes lose integrity in freeze-sensitive insects exposed to freezing stress, while their integrity is maintained by accumulated small cryoprotective molecules, and also by proteins, in freeze-tolerant insects.

lipid bilayers [reviewed in (27–29)]. The protective effects of CPs were empirically demonstrated to occur in numerous in vitro experiments when isolated proteins or lipid bilayers were exposed to freezing or other stresses (30–38). It has always been a challenge, however, to demonstrate that these in vitro–observed stabilizing effects of CPs also participate in cryoprotection in vivo, during the extracellular freezing of a freeze-tolerant organism. Here we aim to fill this gap in knowledge by using the drosophilid fly, *Chymomyza costata*, as a model.

The larvae of *C. costata* have two distinct seasonal phenotypes: active, warm acclimated (in summer) and diapause, cold acclimated (in winter) (39). While active larvae are freeze sensitive, diapause larvae belong to the most cold-hardy animals known; they survive freezing of all osmotically active water in their body (68% water turned to ice crystals) down to −75 °C and survive even after long-term (18 mo) cryopreservation in liquid nitrogen (25, 40–43). In our previous work (26), we identified potential components of the native mixture of CPs that seasonally accumulate in the hemolymph of diapause larvae (proline, trehalose, glutamine, asparagine, and betaine, to name the five most abundant molecules). We described the colligative effects of accumulated CPs on temperature-driven dynamism of the water/ice transition (25) and demonstrated the existence of synergies between effects of different CPs (26).

Here we test the hypothesis that seasonally accumulated CPs act as noncolligative stabilizers of soluble enzymes and plasma membranes in *C. costata* during freezing stress. We show that the soluble enzymes residing in their native biological solutions are well protected against freezing injury even in the freeze-sensitive phenotype and, consequently, do not need additional protection by seasonally accumulated CPs. In contrast, we found that the fat body cell plasma membrane is highly sensitive to freezing injury in both larval phenotypes, but its integrity during freezing stress is protected by CPs (specifically proline and trehalose) and also by proteins that seasonally accumulate in the hemolymph of the freeze-tolerant phenotype.

Results

Freezing Stress Kills Freeze-Sensitive Larvae but Does Not Inactivate Their Soluble Enzymes. In the first series of experiments, we killed freeze-sensitive *C. costata* larvae by exposing them to SLOW inoculative freezing to –30 °C (for a schematic outline of the experiment, see *SI Appendix*, Fig. S1*A*). Immediately upon thawing, we assessed the postfreezing activities of

select soluble enzymes extracted from different tissues. In these experiments, enzymes were frozen in vivo, and unfrozen larvae of the same phenotype served as controls.

Fig. 1 shows enzyme activities for glucose 6-P dehydrogenase (G6PDH), citrate synthase (CS), and lactate dehydrogenase (LDH), while those of four additional enzymes are shown in *SI Appendix*, Fig. S2. Lethal freezing stress never caused complete loss of enzyme activity. Statistically significant decreases in activity were observed only in two cases: G6PDH in muscle (Fig. 1*A*, decrease by 32%) and amylases and maltases in the midgut (*SI Appendix*, Fig. S2*C*, decrease by 28%). In contrast, the activity of prophenoloxidase in the hemolymph was stimulated by freezing stress (*SI Appendix*, Fig. S2*A*).

In order to demonstrate that *C. costata* is not exceptional in its ability to stabilize its soluble enzymes in vivo, we subjected two other insects to the same slow inoculative freezing as applied to *C. costata* larvae: the larvae of the vinegar fly, *Drosophila melanogaster*, and the tibial levator muscle dissected from the femur of the hind leg of the adult locust, *Locusta migratoria*. Immediately after thawing the specimens, we extracted total proteins from muscle tissue and assessed the activity of LDH. The activity was 41% higher in the muscle of frozen compared to that of control *Drosophila* larvae (*SI Appendix*, Fig. S3*A*), while no loss of LDH activity was observed in frozen muscle of the locust (*SI Appendix*, Fig. S3*B*).

Freezing Stress Inactivates Enzymes In Vitro. In a second series of experiments, we froze the total protein extracts of fat body or muscle tissue of freeze-sensitive *C. costata* larvae. The enzymes in these experiments underwent freezing stress in a diluted aqueous solution of 20 mM imidazole buffer (i.e., in vitro). The protein extracts were divided into aliquots: One aliquot served as a control (no additive, unfrozen), and the other aliquots were exposed to freezing stress in the presence of different concentrations of various additives. We used two freezing protocols: FAST, which simulates routine laboratory practice when a protein extract in an Eppendorf tube is simply moved to a deep freezer set to −75 °C; and SLOW, which simulates ecologically relevant, slow inoculative freezing (to compare FAST and SLOW in vitro freezing protocols, see *SI Appendix*, Fig S1*B*). In both FAST and SLOW protocols, we invariably observed complete (or almost complete) loss of activity for three different enzymes: G6PDH, CS, and LDH. We are not presenting these results in an independent figure as this would only show a difference between 100% enzymatic activity in unfrozen control versus 0% (or close to 0%) activity in
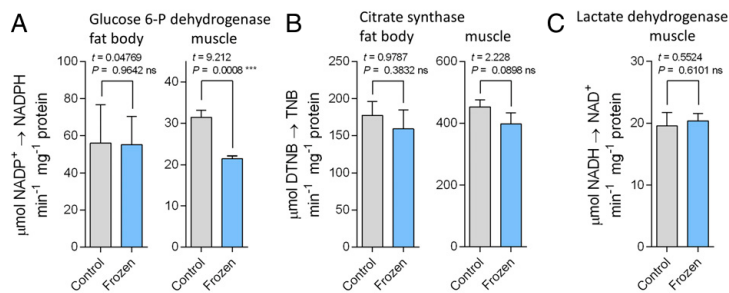
Fig. 1. Enzyme activities persist after lethal freezing stress. *C. costata* larvae of the freeze-sensitive phenotype were killed by freezing to −30 °C, while control larvae were not frozen. The activities of three different enzymes, (*A*) glucose 6-phosphate dehydrogenase, (*B*) citrate synthase, and (*C*) lactate dehydrogenase, were measured in total protein extracts of the fat body and muscle tissues dissected from control and frozen larvae right upon melting. Each column shows the mean + SD of the enzyme activity (*n* = 3, each replicate represents a pool of tissues from 30 larvae). The enzyme activities in control versus frozen larvae were compared via unpaired, two-tailed *t* tests (*t* statistics and *P* values are shown: ns, not significant; *** significant difference; GraphPad Prism v. 6.07). For examples of other enzymes, see *SI Appendix*, Figs. S2 and S3.

68
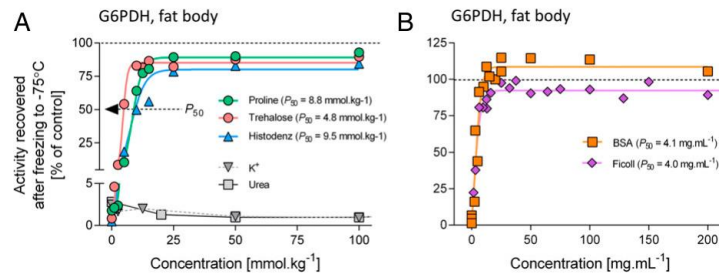
Fig. 2. Enzyme activity is protected by low concentrations of various additives to the in vitro freezing solution. Total protein was extracted from the fat body tissues of freeze-sensitive *C. costata* larvae, and the activity of G6PDH was measured before (control) and after (test) FAST freezing to $-75\,°C$ (see *SI Appendix*, Fig. S1B for protocol). The test aliquots were augmented with different additives: (*A*) proline, trehalose, HistoDenz, K^+, and urea; and (*B*) BSA and Ficoll administered at different concentrations (see *x* axes). Enzyme activity in the unfrozen aliquot (100% active) served as control. Freezing without additive (concentration = 0) caused complete loss of enzyme activity. Different additives protected the enzyme from loss of activity upon freezing at low concentrations (P_{50} is a cryoprotective concentration that allows 50% recovery of control, prefreezing activity). K^+ and urea showed no cryoprotective effects. For other additives and enzymes, see *SI Appendix*, Fig. S5.

frozen extract. Instead, these results are presented as initial points (concentration of additive = 0 on the *x* axis) in Figs. 2 and 3 and in related supplementary figures.

Low CP Concentrations Are Sufficient to Protect Activity of Enzymes Frozen In Vitro. Next, we applied different additives to 20 mM imidazole buffer to assess whether this change in in vitro freezing solution composition can protect *C. costata* enzymes against loss of activity upon freezing stress. We searched for the additive concentration (P_{50}) that ensures 50% recovery of initial (unfrozen control) enzyme activity after freezing stress. In preliminary experiments, we verified that the incubation of protein extract at $0\,°C$ (without freezing) for 1 h, with or without CP additives, had no or little effect on

G6PDH activity (*SI Appendix*, Fig. S4 *A* and *B*). The incubation with potential chemical perturbants was also tested, and a loss of G6PDH activity was seen only with urea administered at concentrations higher than 500 mmol/kg (*SI Appendix*, Fig. S4C).

We found that very low concentrations of various additives were sufficient to protect fat body G6PDH from loss of activity upon FAST in vitro freezing (Fig. 2 and *SI Appendix*, Fig. S5). Five components of the *C. costata* native cryoprotectant mixture showed P_{50} values ranging from 4.8 mmol/kg (trehalose, Fig. 2A) to 13.9 mmol/kg (asparagine, *SI Appendix*, Fig. S5A). The general-use cryoprotectant glycerol (P_{50}, 13.1 mmol/kg, *SI Appendix*, Fig. S5A) and even the biologically inert low-molecular-weight additive HistoDenz (P_{50}, 9.5 mmol/kg, Fig. 2A) showed
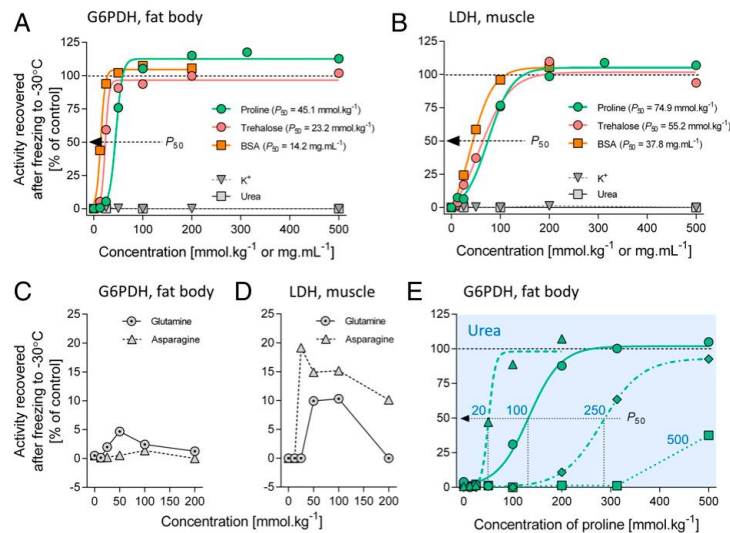
Fig. 3. Slow rate of in vitro freezing and the effect of urea as chemical perturbant. Total protein was extracted from the fat body or muscle tissues of freeze-sensitive *C. costata* larvae, and the activities of G6PDH and LDH were measured before (control) and after (test) SLOW inoculative freezing to $-30\,°C$ (see *SI Appendix*, Fig. S1B for the protocol). The test aliquots were augmented with different additives administered at different concentrations (see *x* axes). Enzyme activity in the unfrozen aliquot (100% active) served as control. Freezing without additive (concentration = 0) caused complete loss of enzyme activity. Some additives protected the enzyme from loss of activity upon freezing (P_{50} is a cryoprotective concentration that allows 50% recovery of control, prefreezing activity). (*A*, *B*) Proline, trehalose, and BSA protected the enzymes from loss of activity at low P_{50} concentrations. K^+ and urea showed no cryoprotective effects. For other additives, see *SI Appendix*, Fig. S6A. (*C*, *D*) Glutamine and asparagine showed no or only weak ability to protect the enzymes. (*E*) Simultaneous presence of urea (perturbant) and proline (CP) during SLOW freezing resulted in shifting the P_{50} values for proline toward higher concentrations (for other combinations of CPs and potential chemical perturbants, see *SI Appendix*, Fig. S6 *B–D*).

similar cryoprotective abilities. The macromolecules BSA (P_{50}, 4.1 mg/mL) and Ficoll (biologically inert high-molecular-weight additive; P_{50}, 4.0 mg/mL) also protected G6PDH at very low concentrations (Fig. 2B). In contrast, urea and K$^+$ failed to protect G6PDH at any concentration assessed (Fig. 2A). Despite being perfect cryoprotectants, neither proline nor Ficoll were able to protect G6PDH from almost complete loss of activity upon heat stress (*SI Appendix*, Fig. S5B).

We conducted similar experiments as described above (although less extensive) for two other enzymes with basically similar results: CS extracted from fat body and LDH extracted from muscle of *C. costata* larvae lost their activities completely upon FAST in vitro freezing stress without additives. However, very low concentrations of proline (P_{50}, 7.2 and 8.0 mmol/kg), trehalose (P_{50}, 7.3 and 4.6 mmol/kg), or bovine serum albumin (BSA) (P_{50}, 4.9 and 1.5 mg/mL) were sufficient to protect the CS and LDH, respectively, from loss of activity upon FAST in vitro freezing (*SI Appendix*, Fig. S5 C and D).

Higher CP Concentrations Are Required during Slow Freezing and Presence of Chemical Perturbants. Next, we exposed G6PDH and LDH in vitro to a more ecologically relevant, SLOW inoculative freezing protocol (*SI Appendix*, Fig S1B). The P_{50} concentrations for all protective additives (proline, trehalose, betaine, glycerol, HistoDenz, BSA, and Ficoll) were invariably higher in the SLOW than in the FAST protocol. For instance, 45.1 mmol/kg of proline was needed to protect 50% G6PDH activity in the SLOW protocol, while only 8.8 mmol/kg was sufficient in the FAST protocol. Urea and K$^+$ failed to protect the G6PDH from loss of activity (Fig. 3 A and B and *SI Appendix*, Fig S6A). Glutamine and asparagine, though behaving as perfect cryoprotectants in the FAST protocol, showed only negligible (G6PDH, Fig. 3C) or weak (LDH, Fig. 3D) ability to protect the enzymes in the SLOW protocol.

Furthermore, we assessed the capacity of proline and trehalose to stabilize G6PDH during SLOW inoculative freezing stress in the presence of chemical perturbants of enzyme activity, such as urea and K$^+$ (glutamine was also tested as a potential perturbant, as it failed to protect the enzyme). When high concentrations of urea (>100 mmol/kg) were present in the in vitro freezing medium, higher P_{50} concentrations of proline (Fig. 3E) or trehalose (*SI Appendix*, Fig. S6B) were needed to protect the enzyme from loss of activity than in the absence of urea. Presence of K$^+$ or glutamine had no effect on proline P_{50} concentration (*SI Appendix*, Fig. S6 C and D). We used differential scanning calorimetry to measure the ice fraction, which allowed us to estimate the increase in urea concentration caused by freezing of osmotically active water in solutions combining urea plus CPs (proline or trehalose) (*SI Appendix*, Fig. S7A). This analysis showed that the cryoprotective effect of CPs in the presence of urea can be explained partially by decreasing the freeze concentration of urea and partially by counteracting the chemical perturbance caused by high concentrations of urea (see *SI Appendix*, Fig. S7 for more details).

Unprotected Plasma Membrane Loses Integrity upon Freezing Stress Both In Vivo and In Vitro. Using the Trypan blue assay, we assessed the plasma membrane integrity of *C. costata* larval fat body cells exposed to SLOW inoculative freezing stress either in vivo (whole larvae frozen) or in vitro (the dissected fat body tissue exposed to freezing in Schneider's *Drosophila* medium) (for a schematic outline of the experiment, see *SI Appendix*, Fig. S1C). The results for active (freeze-sensitive) versus diapause (freeze-tolerant) larvae were different. In active larvae, 64% of fat body cells stained blue (indicating that the plasma membrane lost integrity) after freezing in vivo, and 94% stained blue after freezing in vitro (Fig. 4A). In diapause larvae, only 2.6% of fat body cells stained blue after freezing
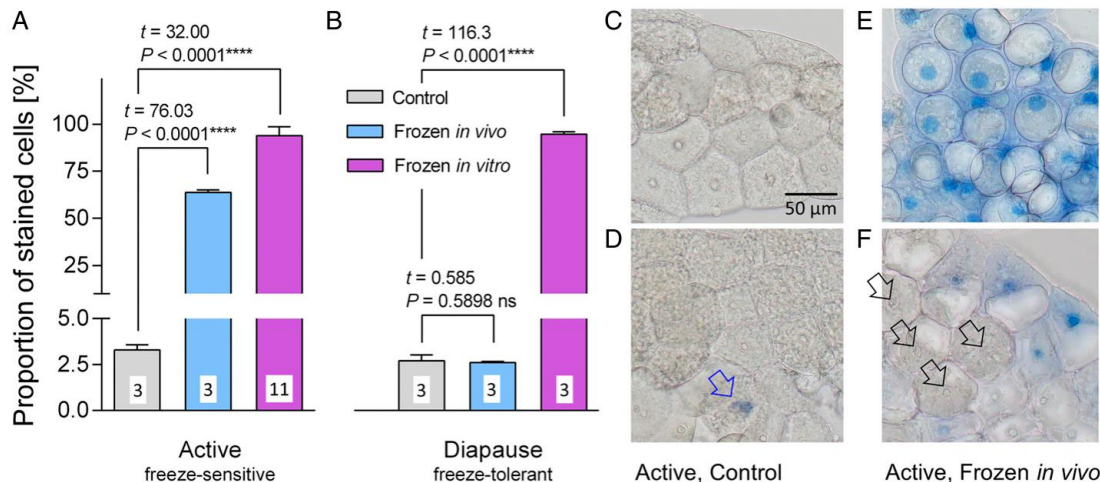
Fig. 4. The integrity of unprotected fat body cell plasma membrane is compromised by freezing stress. (*A*) Active, freeze-sensitive and (*B*) diapause, freeze-tolerant *C. costata* larval phenotypes were used for experiments on fat body cell membrane integrity upon SLOW inoculative freezing to −30 °C. Unfrozen larvae (gray columns) served as controls. Either whole larvae were exposed to freezing stress (in vivo, blue columns; see *SI Appendix*, Fig. S1A for the protocol) or the dissected fat body tissues were frozen in Schneider's *Drosophila* medium (in vitro, violet columns; see *SI Appendix*, Fig. S1C for the protocol). After rewarming, fat body cell plasma membrane integrity was assessed via trypan blue assay (cells with compromised membrane integrity stain blue). Each column shows the mean ± SD of blue staining (*n* = 3 or 11, each replicate represents a pool of 10 larval tissues). The differences in staining proportion were compared via unpaired, two-tailed *t* tests (*t* statistics and *P* values are shown: ns, not significant; **** significant difference; GraphPad Prism v. 6.07). Examples of staining patterns in active, freeze-sensitive larvae are shown in (*C*) control, unfrozen larva, no staining visible; (*D*) another control, unfrozen larva, one cell nucleus stained (blue arrow); (*E*) in vivo frozen larva, all cells stained; and (*F*) another in vivo frozen larva, most cells stained, but there is an island of unstained cells (white arrows). The micrographs were taken with an Olympus SZX12 binocular microscope; the 50 μm bar shown in *C* applies to all four micrographs.

in vivo, while 95% stained blue after freezing in vitro (Fig. 4*B*). These results suggest that the hemolymph of diapause larvae contains components necessary and sufficient for protection of the diapause cell plasma membrane integrity upon freezing stress.

Proline, Trehalose, and BSA Protect Membrane Integrity upon Freezing Stress In Vitro. Next, we assessed whether different additives to the Schneider's medium can protect fat body cell plasma membranes of freeze-sensitive larvae from loss of integrity when freezing stress is applied to dissected tissue in vitro. Before this experiment, we verified that the additives themselves (without freezing stress) do not compromise membrane integrity (*SI Appendix*, Fig. S8*A*). We found that only two of five tested components of the *C. costata* native cryoprotectant mixture were partially effective at membrane cryoprotection. Proline decreased the ratio of blue-stained cells from 94% (control) to 78%, 74%, and 85% when applied at concentrations of 313, 500, and 750 mmol/kg, respectively; and trehalose decreased the ratio of blue-stained cells to 85% and 78% when applied at concentrations of 250 and 500 mmol/kg, respectively (Fig. 5*A*). Three other components of the *C. costata* native cryoprotectant mixture (glutamine, asparagine, and betaine) were ineffective at membrane protection (*SI Appendix*, Fig. S8*C*), as were saccharose, HistoDenz, and Na$^+$ (Fig. 5*A*). Glycerol, which is not natively

accumulated by *C. costata* larvae, was even more effective in membrane cryoprotection than proline and trehalose (*SI Appendix*, Fig. S8*B*). The macromolecular additive BSA showed a cryoprotective effect at concentrations ranging from 25 to 200 mg/mL, while Ficoll was marginally effective only at the highest concentration applied (200 mg/mL, ANOVA $P = 0.0477$) (Fig. 5*B*). The cryoprotective effects of different CPs applied at the same osmotic concentration (500 mOsmol/kg) differed drastically (*SI Appendix*, Fig. S8*D*), which demonstrates that the effect is not explained simply by colligative properties of the augmented Schneider's medium. Examples of blue staining for in vitro frozen fat body cells are shown in *SI Appendix*, Fig. S9.

Looking at interactions between CPs, we compared the cryoprotective effects of different CPs applied singly with those of various mixtures. We prepared an artificial mixture of five putative CPs (CPmix 508), simulating the physiological concentrations of individual components as they were detected in the hemolymph of the freeze-tolerant *C. costata* larval phenotype (i.e., proline, 313 mmol/kg; trehalose, 108 mmol/kg; glutamine, 55 mmol/kg; asparagine, 26 mmol/kg; and betaine, 6 mmol/kg; in total 508 mmol/kg). After freezing in the CPmix 508-augmented Schneider's medium, the ratio of blue-stained cells decreased to 68.5% (Fig. 5*C*). The same cryoprotective effect (68.5%),
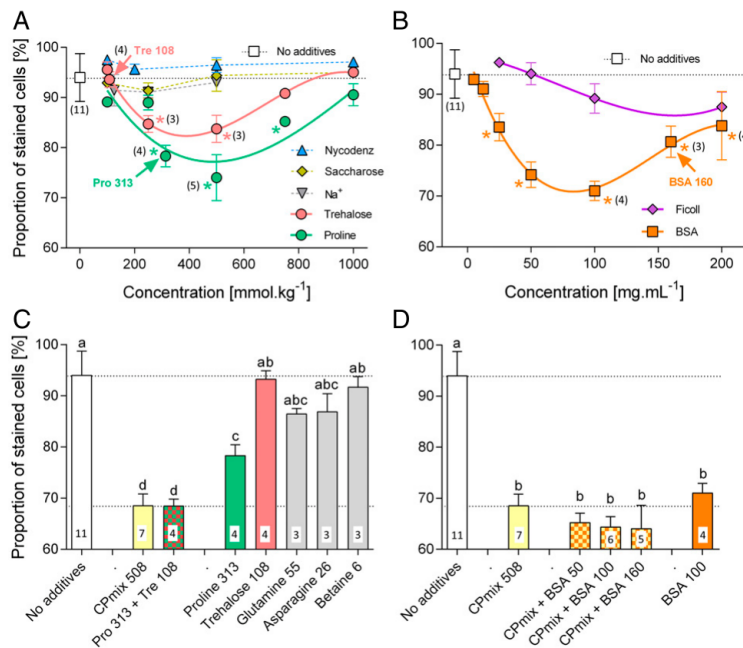
Fig. 5. Membrane integrity upon freezing stress is partially protected by high concentrations of proline, trehalose, and BSA. Dissected fat body tissues of freeze-sensitive *C. costata* larvae were exposed to freezing stress in vitro in Schneider's solution augmented with different additives at different concentrations. Control tissues (empty squares in *A* and *B* or empty columns in *C* and *D*) were exposed to freezing stress without additive. After melting, fat body cell plasma membrane integrity was assessed via trypan blue assay (see *y* axes). *A* and *B* compare the cryoprotective effects of different concentrations (see *x* axes) of different additives (for other additives, see *SI Appendix*, Fig. S8 *B* and *C*). The concentrations corresponding to physiological levels observed in the hemolymph of freeze-tolerant larvae are indicated by arrows flanked by numbers (the concentrations). Third-order polynomial curves or dashed lines are used to visually connect different concentrations of an additive. Panels *C* and *D* compare the cryoprotective effects of different additives added singly or in various mixtures (for other combinations, see *SI Appendix*, Fig. S8 *D* and *E*). Additive concentrations are indicated (313, 108, 55, 26, and 6 mmol/kg for CPs; 50, 100, and 160 mg/mL for BSA; 508 mmol/kg for CPmix of five CPs). Each point or column shows the mean ± SD of blue staining in at least two replicates, while treatments replicated three or more times are indicated by numbers ($n = 3$–11, each replicate represents mean staining in a pool of 10 larval tissues). The differences in staining proportions were compared via one-way ANOVA tests followed by Bonferroni's multiple comparison tests (GraphPad Prism v. 6.07). In *A* and *B*, additive-augmented media were compared with controls, and statistically significant differences are flanked by asterisks; in *C* and *D*, each column was compared with every other column, and the columns flanked by different letters are statistically different.

71

however, was observed for a mixture combining just two major CPs: proline (313 mmol/kg) and trehalose (108 mmol/kg). Comparing these results to the cryoprotective effects of different CPs applied singly, we can conclude that proline was the only component that significantly decreased the ratio of blue-stained cells when applied at its physiological concentration corresponding to freeze-tolerant hemolymph, and there was a synergism between proline and trehalose in their cryoprotective effects (simple addition of the individual effects of two components does not explain the cryoprotective effect observed in their mixture) (Fig. 5C). We further confirmed the synergism between proline and trehalose by removing individual components from the CPmix 508 one by one. Removing glutamine, asparagine, or betaine had practically no impact on the cryoprotective effect of the reduced CPmix. Removing proline or trehalose, however, significantly decreased the cryoprotective effect of the reduced CP mix (*SI Appendix,* Fig. S8E). We can also conclude that when the CPmix 508 was combined with BSA at different concentrations, no synergy was achieved, but a weak, statistically insignificant additive effect was observed (Fig. 5D).

Complete Rescue of Membrane Integrity by CPs and BSA in Freeze-Tolerant Larvae. Experiments described in the preceding section show that fat body cell membranes of freeze-sensitive larvae are only partially protected by CPs against loss of integrity during freezing stress. Now, we move to fat body cell membranes of freeze-tolerant larvae, which also lose integrity when the tissue is frozen in plain Schneider's medium in vitro (Fig. 4B and *SI Appendix,* Fig. S8F). The CPs proline or trehalose, when added singly to Schneider's medium at their respective physiological concentrations, reduced the blue staining in freeze-tolerant phenotype cells significantly from 95% to 66% or 73%, respectively. An additive effect, or a weak synergism, was observed for a mixture of proline and trehalose (reduction of staining to 31%), which was practically the same cryoprotective effect as observed for the complete CPmix 508 (reduction of staining to 33%). BSA appeared to be a highly potent cryoprotective agent as it reduced staining to 10% when applied at a physiological concentration (corresponding to the total hemolymph protein concentration of 160 mg/mL). We achieved a complete rescue of plasma membrane integrity upon freezing stress (reduction of staining below 3%) when a mixture of proline, trehalose, and BSA was added to freeze-tolerant phenotype cells incubated in Schneider's medium (*SI Appendix,* Fig. S8F).

Discussion

Here we provide an experimental test of the widely accepted hypothesis that sees irreversible protein denaturation and loss of integrity of biological membranes as the two most important molecular mechanisms of freezing injury in freeze-sensitive insects, while freeze-tolerant insects are hypothesized to prevent this injury by using accumulated cryoprotective solutes [(1, 16–18); for exact quotations, see *SI Appendix, SI Discussion*]. We believe that the high sensitivity of enzymes exposed to freezing stress in vitro might be the major source of misinterpretation and discrepancy between hypothesis and empirical results.

Insect Soluble Enzymes In Vivo Are Probably Not the Primary Targets of Freezing Injury and Do Not Need Protection by Accumulated CPs. To our best knowledge, the insect cold hardiness literature describes only a single direct experiment on insect enzyme activity measured before and after freezing stress:

citrate synthase in the fat body cells of lethally frozen *C. costata* larvae, which was not inactivated (44). This isolated observation prompted us to extend the assays on in vivo freeze inactivation or stability to other insect enzymes. Here, we show that seven different soluble enzymes representing various biological solutions (hemolymph, alimentary canal, extracellular matrix, cytosol, and mitochondrial matrix of muscle and fat body cells) were not inactivated during organismally lethal freezing stress in *C. costata*, and verified this lack of inactivation for LDH in two other freeze-sensitive insect species (i.e., insects not protected by any accumulated CPs).

Soluble Enzymes Are Prone to Loss of Activity upon Freezing In Vitro in a Dilute Aqueous Solution. We observed complete loss of G6PDH, LDH, and CS activities in *C. costata* larvae when these enzymes were frozen in vitro in tissue extracts diluted in 20 mM imidazole buffer. This observation is in agreement with the rich literature on vertebrate (30, 36, 45) and insect enzymes (35). Our experiments, however, show that the loss of enzyme activity is preventable if low concentrations of various CPs and other microsolutes (including the artificial compound HistoDenz) are added to the freezing medium; concentrations as low as a few mM were sufficient to perfectly protect the enzymes from loss of activity upon freezing. This protective effect also agrees with an earlier study by Storey et al. (35), who found almost exactly the same low P_{50} values (7–25 mM) for a range of sugars, polyols, and amino acids protecting G6PDH from freeze inactivation in a fly (*Eurosta solidaginis*), a moth (*Epiblema scudderiana*), and yeast. Such low concentrations of various microsolutes (regular metabolites), however, occur in almost every organism or cell type, which may help to explain why the enzymes of freeze-sensitive insects "survived" organismally lethal freezing in vivo. In addition to various microsolutes, the native biological solutions contain macromolecules at total concentrations in a range of 50–400 mg/mL (46). Here we observed that macromolecules (BSA or Ficoll) added into the in vitro freezing medium at concentrations as low as 4–40 mg/mL were sufficient to perfectly protect the insect enzymes from loss of activity upon freezing.

Compared to insect enzymes, higher concentrations of CP microsolutes (in the range of hundreds of mM) were needed to protect purified mammalian enzymes from loss of activity upon in vitro freezing (30, 45). However, even the mammalian enzymes were well protected by very low concentrations (in a range of 0.02–0.25 mg/mL) of macromolecular compounds such as polyethylene glycol or BSA or by an increase in the concentration of the enzyme itself (self-protection) (30, 45). Other vertebrate enzymes were observed to survive the freeze–thaw cycle when frozen in situ, inside the tissue, such as succinate dehydrogenase and cytochrome oxidase in rat heart (47) or sarcoplasmic ATPase and aldolase in fish meat, which lost activity significantly only upon prolonged frozen storage (48, 49).

All of these results point to an important difference between typical enzymatic assays conducted at low enzyme concentrations in dilute in vitro solutions, and assays performed either in vivo or under conditions simulating "molecular crowding," which is a hallmark of all living matter (46). Thus, microsolutes and macromolecules ubiquitous in biological solutions of all organisms may be sufficient to stabilize various soluble enzymes during freezing stress. The microsolutes probably act via the mechanism of "preferential exclusion" suggested by Timasheff and colleagues [reviewed in (27–29)], while macromolecules, either natural (such as BSA) or synthetic (such as Ficoll), may stabilize the compact native state of enzymes via the mechanism

72

of nonspecific steric repulsion ("excluded volume effect"), which is caused by mutual impenetrability of solute molecules (50, 51).

Collectively, we suggest that soluble enzymes in insects are sufficiently protected against loss of activity when frozen in their native biochemical environment, a biological solution that is crowded by various microsolutes and macromolecules. Of course, this statement is open to scientific falsification as we can hardly exclude that some other enzymes, not included in this study, are more sensitive to freezing stress. Moreover, there are several reasons for caution when extending the validity of our hypothesis from soluble enzymes to all proteins. We corroborate these reasons in the *SI Appendix, Do Proteins in General Need Stabilization by CPs during Freezing Stress?*

Plasma Membranes Need Protection by CPs and Proteins to Maintain Integrity during Freezing Stress. In agreement with the widely accepted hypothesis on molecular mechanisms of freezing injury, here we confirmed experimentally that fat body plasma membranes of the freeze-sensitive *C. costata* larval phenotype lose their barrier function upon in vivo lethal freezing stress, while almost no loss of membrane integrity is observed in the freeze-tolerant phenotype. The plasma membrane is considered a primary target of cold and freezing injury also in plants (11) and mammalian cells (6, 52).

One salient observation of this work points to the hemolymph of freeze-tolerant *C. costata* larvae, which apparently contains components both necessary and sufficient for protection of the plasma membrane integrity upon freezing stress. In an earlier study (26) we identified the micromolecular components of the freeze-tolerant phenotype hemolymph, and in this study, we tested their cryoprotective abilities in combination with macromolecular BSA. A combination of three additives to Schneider's medium (proline, trehalose, and BSA) appeared sufficient to completely rescue membrane integrity upon freezing stress applied in vitro to fat body cells of freeze-tolerant larvae (reducing the incidence of freezing injury from 95 to 3% of cells). The same three additives were also effective in partially reducing the freezing injury (from 94 to 64–68%) in freeze-sensitive phenotype cells. These results point to the existence of an interactive effect between cell phenotype and the composition of the freezing medium on membrane integrity. What exactly is driving this interaction is currently unclear, although acclimation-linked restructuring of the lipid composition of the cell membrane could play an important role (53).

Of the three additives (proline, trehalose, and BSA), BSA was the most effective in membrane cryoprotection for both freeze-sensitive and freeze-tolerant phenotypes. We used BSA to simulate high concentrations of serum proteins accumulated by many insects late in their larval ontogeny (before metamorphosis) (54–56). Also, *C. costata* larvae in the late third instar (used in this study) show high concentrations of serum proteins and, consequently, total proteins in the hemolymph: 100 and 160 mg/mL for freeze-sensitive and -tolerant phenotypes, respectively. BSA and other membrane-nonpermeable compounds such as saccharose, Ficoll, polyethylene glycol, and hydroxyethyl starch are often added to cryopreservation solutions for mammalian sperm (57), where they probably help to maintain membrane integrity indirectly by affecting thermal transitions in the extracellular medium (including kinetics of growth and morphology of ice crystals and glass transition temperatures) (58, 59), or by reducing the membrane lipid peroxidation by reactive oxygen species (60). The exact mechanism behind the high effectiveness of BSA as *C. costata*'s membrane integrity protectant remains unknown,

however. Other two-cell-membrane nonpermeable compounds (saccharose and Ficoll) showed no or negligible cryoprotective effects toward *C. costata* fat body cell membranes. Additional research is required to determine how plasma membrane permeability for different additives impacts their effectiveness as cryoprotectants.

Our functional assays further corroborate results of earlier studies where insect fat body cells were exposed to freezing in vitro and the integrity of their plasma membrane was then checked with vital dyes. Fat body cells of the larvae of *E. solidaginis* were frozen to –25 °C in Grace's insect medium, and augmentation of that medium with 1 M glycerol increased the proportion of cells with intact plasma membrane from less than 20% to 80% (61). Also, fat body cells of the cricket *Gryllus veletis* were frozen to –12 °C (warm-acclimated crickets) or –16 °C (cold-acclimated crickets) in Grace's medium, plain or augmented with different CPs; the augmentations with myo-inositol, trehalose, and glycerol significantly increased the proportions of cells that survived freezing with intact plasma membrane (24). The later study also suggested that individual CPs differentially impact survival in the frozen state, are not interchangeable, and probably function non-colligatively in insect freeze tolerance. As in the present study, no CP or combination of CPs was sufficient to confer high freeze tolerance to cells of warm-acclimated crickets, whereas in cold-acclimated crickets the proportion of cells with intact membranes after freezing stress increased to ∼75% after the combination of myo-inositol plus trehalose or glycerol alone was added (24).

Collectively, both the literature and our results provide compelling evidence that the loss of cell membrane integrity often occurs in different freeze-sensitive organisms or cells exposed to freezing stress. Here we contribute evidence that accumulated CPs and proteins can stabilize the cell membrane during freezing stress in vivo. Although the loss of cell membrane integrity is considered almost synonymous with the loss of cell viability, we argue that the downstream effects of the loss of cell membrane integrity merit further study in order to make an unambiguous causal connection to cell and organismal death. Taken from the opposite perspective, the fact that the CP-protected cell can retain an intact plasma membrane during freezing stress does not necessarily mean that this cell is viable; rather, it needs rigorous further examination.

Conclusions

We have experimentally attested the roles of seasonally accumulated small CPs in the stabilization of insect enzymes and membranes during freezing stress. Our results confirm the hypothesis that the CPs protect, at least partially, the plasma cell membranes against the loss of integrity. In addition, accumulated hemolymph proteins also appear to support membrane integrity. In contrast, our results do not support the hypothesis that the stability of insect soluble enzymes would be endangered by freezing stress. Although the enzymes are highly sensitive to freezing stress in diluted aqueous solutions in vitro, they show high stability when exposed to freezing in vivo, that is, in their native biological solutions crowded by different microsolutes and macromolecules.

Materials and Methods

For a more detailed description of the materials and methods, see *SI Appendix, SI Methods.*

Insects. Two phenotypic variants of *C. costata* larvae were generated according to our earlier acclimation protocols (26): active, warm-acclimated larvae and diapause, cold-acclimated larvae. The active larvae have limited survival after freezing stress (none survive when frozen below −10 °C), while practically all

73

diapause larvae survive freezing to −75 °C, and 42.5% survive and metamorphose into fit adults even after 18 mo of cryopreservation in LN_2 (25). Because we focused on the nature of damage caused by freezing stress, we used active, freeze-sensitive larvae for most experiments. Diapause, freeze-tolerant larvae were used for the experiments on plasma membrane integrity upon freezing stress.

General Outline of Experiments. The general rationale of all experiments was to expose either whole active, freeze-sensitive larvae (in vivo), or their dissected tissues (in vitro), or protein extracts from their tissues (in vitro) to lethal freezing stress of −30 °C and, upon melting, assess whether their soluble enzymes lost activity, whether the plasma membranes of their fat body cell lost integrity, and whether these losses of activity or integrity can be prevented by different additives in the freezing medium. The general outline of all experiments is presented in *SI Appendix*, Fig. S1.

Enzyme Activity and Plasma Cell Membrane Integrity Assays. The activities of seven different enzymes were measured (as specified in *SI Appendix*, *SI Methods*) before and after the freezing stress. Similarly, plasma membrane integrity before and after the freezing stress was assessed with trypan blue dye, which stains the interior of cells with compromised membrane barrier function. The in vitro experiments allowed us to manipulate the composition of the freezing medium. For enzyme assays, 20 mM imidazole was used as the base in vitro

freezing medium, while Schneider's *Drosophila* medium (Biosera, Nuaillé, France) was used for in vitro incubation and freezing of dissected tissues. The freezing media were augmented by additives in different concentrations. We sought to find the additives, their combinations, and their effective concentrations, which either significantly protected the enzyme from loss of activity, or reduced the proportion of cells with compromised cell membrane integrity (staining blue), during the freezing stress. The additives included the components of native cryoprotective mixture accumulated in the diapause, freeze-tolerant *C. costata* larval phenotype (i.e., proline, trehalose, glutamine, asparagine, and betaine) (26); other additives widely used in cryobiology practice (i.e., glycerol and saccharose); inorganic salts NaCl and KCl; BSA; and biologically inert compounds HistoDenz (with high molecular weight of 70,000 g/mol) and Ficoll (with low molecular weight of 821 g/mol). In addition, urea was used as a chemical perturbant of native protein structure in some experiments (see *SI Appendix*, Table S1 for complete list of additives).

Data, Materials, and Software Availability. All study data are included in the article and/or *SI Appendix*.

1. K. B. Storey, J. M. Storey, Freeze tolerance in animals. *Physiol. Rev.* **68**, 27–84 (1988).
2. E. Asahina, Frost resistance in insects in Advances in Insect Physiology, J. W. L. Beament, J. E. Treherne, V. B. Wigglesworth, Eds. (Elsevier, 1970), vol. 6, pp. 1–49.
3. R. S. Pearce, Plant freezing and damage. *Ann. Bot.* **87**, 417–424 (2001).
4. B. J. Sinclair, Insect cold tolerance: How many kinds of frozen? *Eur. J. Entomol.* **96**, 157–164 (1999).
5. B. J. Sinclair, D. Renault, Intracellular ice formation in insects: Unresolved after 50 years? *Comp. Biochem. Physiol. A Mol. Integr. Physiol.* **155**, 14–18 (2010).
6. P. Mazur, Freezing of living cells: Mechanisms and implications. *Am. J. Physiol.* **247**, C125–C142 (1984).
7. K. Muldrew, J. P. Acker, J. A. Elliott, L. E. McGann, *The Water to Ice Transition: Implications for Living Cells. Life in the Frozen State* (CRC Press, 2004), pp. 93–134.
8. F. Franks, R. H. Hatley, Stability of proteins at subzero temperatures: Thermodynamics and some ecological consequences. *Pure Appl. Chem.* **63**, 1367–1380 (1991).
9. C. L. Dias *et al.*, The hydrophobic effect and its role in cold denaturation. *Cryobiology* **60**, 91–99 (2010).
10. H. Ramløv, Aspects of natural cold tolerance in ectothermic animals. *Hum. Reprod.* **15** (suppl. 5), 26–46 (2000).
11. P. L. Steponkus, Role of the plasma membrane in freezing injury and cold acclimation. *Annu. Rev. Plant Physiol.* **35**, 543–584 (1984).
12. P. H. Yancey, J. F. Siebenaller, Co-evolution of proteins and solutions: Protein adaptation versus cytoprotective micromolecules and their roles in marine organisms. *J. Exp. Biol.* **218**, 1880–1896 (2015).
13. P. H. Yancey, Organic osmolytes as compatible, metabolic and counteracting cytoprotectants in high osmolarity and other stresses. *J. Exp. Biol.* **208**, 2819–2830 (2005).
14. P. W. Hochachka, G. N. Somero, *Biochemical Adaptation: Mechanism and Process in Physiological Evolution* (Oxford University Press, 2002).
15. G. N. Somero, Protons, osmolytes, and fitness of internal milieu for protein function. *Am. J. Physiol.* **251**, R197–R213 (1986).
16. R. E. J. Lee, "A primer on insect cold-tolerance" in *Low Temperature Biology of Insects*, D. L. Denlinger, R. E. J. Lee, Eds. (Cambridge University Press, 2010), pp. 3–34.
17. N. M. Teets, D. L. Denlinger, Physiological mechanisms of seasonal and rapid cold-hardening in insects. *Physiol. Entomol.* **38**, 105–116 (2013).
18. J. Toxopeus, B. J. Sinclair, Mechanisms underlying insect freeze tolerance. *Biol. Rev. Camb. Philos. Soc.* **93**, 1891–1914 (2018).
19. J. Rozsypal, Cold and freezing injury in insects: An overview of molecular mechanisms. *Eur. J. Entomol.* **119**, 43–57 (2022).
20. H. T. Meryman, Cryoprotective agents. *Cryobiology* **8**, 173–183 (1971).
21. J. E. Lovelock, The protective action of neutral solutes against haemolysis by freezing and thawing. *Biochem. J.* **56**, 265–270 (1954).
22. K. E. Zachariassen, Physiology of cold tolerance in insects. *Physiol. Rev.* **65**, 799–832 (1985).
23. K. B. Storey, Organic solutes in freezing tolerance. *Comp Biochem Physiol A Physiol* **117**, 319–326 (1997).
24. J. Toxopeus, V. Koštál, B. J. Sinclair, Evidence for non-colligative function of small cryoprotectants in a freeze-tolerant insect. *Proc. Biol. Sci.* **286**, 20190050 (2019).
25. J. Rozsypal, M. Moos, P. Šimek, V. Koštál, Thermal analysis of ice and glass transitions in insects that do and do not survive freezing. *J. Exp. Biol.* **221**, 170464 (2018).
26. L. Kučera *et al.*, A mixture of innate cryoprotectants is key for freeze tolerance and cryopreservation of a drosophilid fly larva. *J. Exp. Biol.* **225**, jeb243934 (2022).
27. S. Timasheff, *A Physicochemical Basis for the Selection of Osmolytes by Nature. Water and Life* (Springer, 1992), pp. 70–84.
28. S. N. Timasheff, Protein-solvent preferential interactions, protein hydration, and the modulation of biochemical reactions by solvent components. *Proc. Natl. Acad. Sci. U.S.A.* **99**, 9721–9726 (2002).
29. S. N. Timasheff, The control of protein stability and association by weak interactions with water: How do solvents affect these processes? *Annu. Rev. Biophys. Biomol. Struct.* **22**, 67–97 (1993).
30. J. F. Carpenter, J. H. Crowe, The mechanism of cryoprotection of proteins by solutes. *Cryobiology* **25**, 244–255 (1988).
31. T. Arakawa, S. N. Timasheff, Stabilization of protein structure by sugars. *Biochemistry* **21**, 6536–6544 (1982).
32. T. J. Anchordoguy, A. S. Rudolph, J. F. Carpenter, J. H. Crowe, Modes of interaction of cryoprotectants with membrane phospholipids during freezing. *Cryobiology* **24**, 324–331 (1987).
33. L. M. Crowe, R. Mouradian, J. H. Crowe, S. A. Jackson, C. Womersley, Effects of carbohydrates on membrane stability at low water activities. *Biochim. Biophys. Acta* **769**, 141–150 (1984).
34. T. Arakawa, S. N. Timasheff, The stabilization of proteins by osmolytes. *Biophys. J.* **47**, 411–414 (1985).
35. K. B. Storey, D. Keefe, L. Kourtz, J. M. Storey, Glucose-6-phosphate dehydrogenase in cold hardy insects: Kinetic properties, freezing stabilization, and control of hexose monophosphate shunt activity. *Insect Biochem.* **21**, 157–164 (1991).
36. K. Lippert, E. A. Galinski, Enzyme stabilization by ectoine-type compatible solutes: Protection against heating, freezing and drying. *Appl. Microbiol. Biotechnol.* **37**, 61–65 (1992).
37. C. H. Fabrie, B. de Kruijff, J. de Gier, Protection by sugars against phase transition-induced leak in hydrated dimyristoylphosphatidylcholine liposomes. *Biochim. Biophys. Acta* **1024**, 380–384 (1990).
38. A. S. Rudolph, J. H. Crowe, L. M. Crowe, Effects of three stabilizing agents–proline, betaine, and trehalose–on membrane phospholipids. *Arch. Biochem. Biophys.* **245**, 134–143 (1986).
39. V. Koštál, M. Mollaei, K. Schöttner, Diapause induction as an interplay between seasonal token stimuli, and modifying and directly limiting factors: Hibernation in *Chymomyza costata. Physiol. Entomol.* **41**, 344–357 (2016).
40. I. Moon, S. Fujikawa, K. Shimada, Cryopreservation of *Chymomyza* larvae (Diptera: Drosophilidae) at -196°C with extracellular freezing. *Cryo Lett.* **17**, 105–110 (1996).
41. K. Shimada, A. Riihimaa, Cold acclimation, inoculative freezing and slow cooling: Essential factors contributing to the freezing-tolerance in diapausing larvae of *Chymomyza costata* (Diptera: Drosophilidae). *Cryo Lett.* **9**, 5–10 (1988).
42. V. Koštál, H. Zahradníčková, P. Šimek, Hyperprolinemic larvae of the drosophilid fly, *Chymomyza costata*, survive cryopreservation in liquid nitrogen. *Proc. Natl. Acad. Sci. U.S.A.* **108**, 13041–13046 (2011).
43. L. E. Des Marteaux, P. Hůla, V. Koštál, Transcriptional analysis of insect extreme freeze tolerance. *Proc. Biol. Sci.* **286**, 20192019 (2019).
44. T. Štětina, L. E. Des Marteaux, V. Koštál, Insect mitochondria as targets of freezing-induced injury. *Proc. Biol. Sci.* **287**, 20201273 (2020).
45. T. Tamiya *et al.*, Freeze denaturation of enzymes and its prevention with additives. *Cryobiology* **22**, 446–456 (1985).
46. N. A. Chebotareva, B. I. Kurganov, N. B. Livanova, Biochemical effects of molecular crowding. *Biochemistry (Mosc.)* **69**, 1239–1251 (2004).
47. R. Hart, L. J. Ramazzotto, R. Engstrom, Cryoprotection of some rat heart enzymes. *Cryobiology* **9**, 461–464 (1972).
48. H. Yamanaka, I. M. Mackie, Changes in activity of a sarcoplasmic adenosinetriphosphatase during iced-storage and frozen-storage of cod. *Bull. Jpn. Soc. Sci. Fish.* **37**, 1105 (1971).
49. J. Connell, Changes in aldolase activity in cod and haddock during frozen storage. *J. Food Sci.* **31**, 313–316 (1966).
50. A. P. Minton, Implications of macromolecular crowding for protein assembly. *Curr. Opin. Struct. Biol.* **10**, 34–39 (2000).
51. E. Fiorini, R. Börner, R. K. Sigel, Mimicking the in vivo environment–The effect of crowding on RNA and biomacromolecular folding and activity. *Chimia (Aarau)* **69**, 207–212 (2015).
52. E. Z. Drobnis *et al.*, Cold shock damage is due to lipid phase transitions in cell membranes: A demonstration using sperm as a model. *J. Exp. Zool.* **265**, 432–437 (1993).
53. V. Koštál, P. Berková, P. Šimek, Remodelling of membrane phospholipids during transition to diapause and cold-acclimation in the larvae of *Chymomyza costata* (Drosophilidae). *Comp. Biochem. Physiol. B Biochem. Mol. Biol.* **135**, 407–419 (2003).
54. D. Powell, J. D. Sato, H. W. Brock, D. B. Roberts, Regulation of synthesis of the larval serum proteins of *Drosophila melanogaster. Dev. Biol.* **102**, 206–215 (1984).
55. W. H. Telfer, J. G. Kunkel, The function and evolution of insect storage hexamers. *Annu. Rev. Entomol.* **36**, 205–228 (1991).

74

56. M. Moos *et al.*, Cryoprotective metabolites are sourced from both external diet and internal macromolecular reserves during metabolic reprogramming for freeze tolerance in drosophilid fly, *Chymomyza costata*. *Metabolites* **12**, 163 (2022).

57. M. Hidalgo *et al.*, Concentrations of non-permeable cryoprotectants and equilibration temperatures are key factors for stallion sperm vitrification success. *Anim. Reprod. Sci.* **196**, 91–98 (2018).

58. H. Oldenhof *et al.*, Osmotic stress and membrane phase changes during freezing of stallion sperm: Mode of action of cryoprotective agents. *Biol. Reprod.* **88**, 68 (2013).

59. K. Hornberger, R. Li, A. R. C. Duarte, A. Hubel, Natural deep eutectic systems for nature-inspired cryopreservation of cells. *AIChE J.* **67**, e17085 (2021).

60. E. Cabrita, L. Anel, M. P. Herraéz, Effect of external cryoprotectants as membrane stabilizers on cryopreserved rainbow trout sperm. *Theriogenology* **56**, 623–635 (2001).

61. R. E. Lee, J. J. McGrath, R. T. Morason, R. M. Taddeo, Survival of intracellular freezing, lipid coalescence and osmotic fragility in fat body cells of the freeze-tolerant gall fly *Eurosta solidaginis*. *J. Insect Physiol.* **39**, 445–450 (1993).

75

On stabilization of insect cell membranes and soluble enzymes by accumulated cryoprotectants during freezing stress.

Grgac R., Rozsypal J., Des Marteaux L., Štětina T., Koštál V.

Supplementary Information

SI Supplementary Methods

Rearing and acclimation of experimental insects

A colony of *C. costata*, Sapporo strain (1), was reared on artificial diet in MIR 154 incubators (Sanyo Electric, Osaka, Japan) as described previously (2). Two phenotypic variants were generated according to our earlier acclimation protocols (3): (i) active, warm-acclimated, freeze-sensitive larvae (abbreviated as LD in earlier papers); (ii) diapause, cold-acclimated, freeze-tolerant larvae (abbreviated as SDA in earlier papers). Briefly, the active larvae were reared from eggs to 3rd larval instars (age of three weeks) at 18°C under long-day photoperiod (16h light:8h dark), which allows direct non-diapause development to pupa and adult. The diapause larvae were reared until age of six weeks at 18°C under short-day photoperiod (12h light:12h dark) – which induces larval diapause – and were then transferred to constant darkness and progressively cold acclimated over five weeks (one week at 11°C, followed by four weeks at 4°C).

The active larvae of *C. costata* have limited survival after freezing stress (35% survive slow inoculative freezing to -5°C, 10% survive to -10°C, and none survive freezing to -20°C or below). In contrast, practically all diapause larvae survive freezing to -30°C or even -75°C, and 42.5% survive and metamorphose into fit adults after 18 months of cryopreservation in LN$_2$ (4). Because we focus on the nature of damage caused by freezing stress, the freeze-sensitive, active larvae were used for most experiments. Diapause larvae were used for the experiments on integrity of plasma membrane upon freezing stress.

For supplementary experiments, we used larvae of the vinegar fly, *Drososphila melanogaster* (Oregon R strain) and adult locusts, *Locusta migratoria* from insect cultures routinely maintained at the Biology Centre CAS, České Budějovice, Czech Republic. The vinegar flies were reared at constant 18°C, while locusts were maintained at constant 30°C; both species kept under a photoperiodic regime of 12h light:12h dark. Both species represented warm-adapted and warm-acclimated animals with relatively low cold tolerance, killed by chilling to temperatures around 0°C for minutes or hours (i.e. without freezing) (5, 6).

General outline of experiments

1

The general outline of all experiments is presented in Fig. S1. The experiments were performed in two different ways: *in vivo* and *in vitro*.
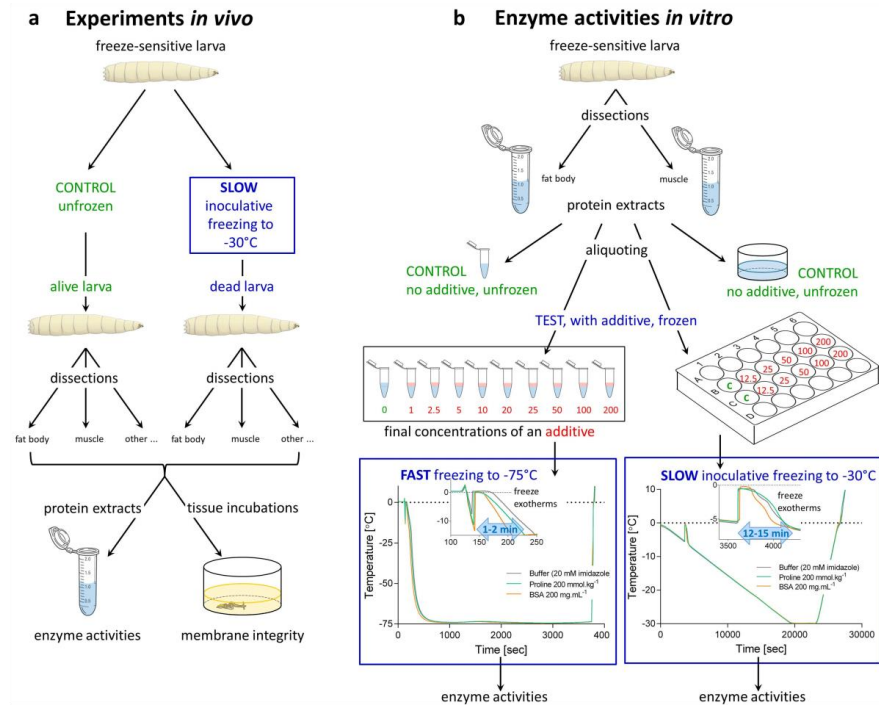
Fig. S1: The schematic outline of experiments.

(a) Experiments *in vivo*. Whole larvae of the freeze-sensitive phenotype of *Chymomyza costata* were exposed to lethal slow inoculative freezing to -30°C using the protocol described earlier (4). Unfrozen larvae served as controls. Upon melting, (i) different larval tissues were rapidly dissected and crude total proteins were extracted, which served as source for analysis of enzyme activities, or (ii) whole 'intestine blobs' with attached fat body were rapidly dissected, incubated in Trypan Blue stain, and membrane integrity was assessed. For more explanations, see text (section *In vivo* experiments).

(b) Enzyme activities *in vitro*. The fat body or muscle tissues were dissected from freeze-sensitive larvae and total proteins were extracted in 20 mM imidazole buffer, pH 7.2. The extract was aliquoted and the aliquots were exposed to freezing in the absence or presence of different additives. One aliquot served as control – no additive and not frozen. Enzyme activities were measured upon melting. We used two different freezing protocols: (i) FAST freezing to -75°C and (ii) SLOW inoculative freezing to -30°C (the same protocol as used for whole larvae in the *in vivo* experiments). Example temperature courses in the FAST and SLOW protocols are shown in blue frames for plain buffer (20 mM imidazole), buffer augmented with proline (20 mmol.kg^{-1}), and buffer augmented with BSA (200 mg.mL^{-1}). The records were obtained using K-type thermocouples attached to a PicoLog TC-08 datalogger (Pico Technology, St. Neots, UK). Note that additives had a relatively small influence on the temperature course and that the durations of freeze-exotherms were longer in the SLOW than in the FAST protocol (blue arrows in the insets). For more explanations, see text (section: *In vitro* enzyme activity assays).

2
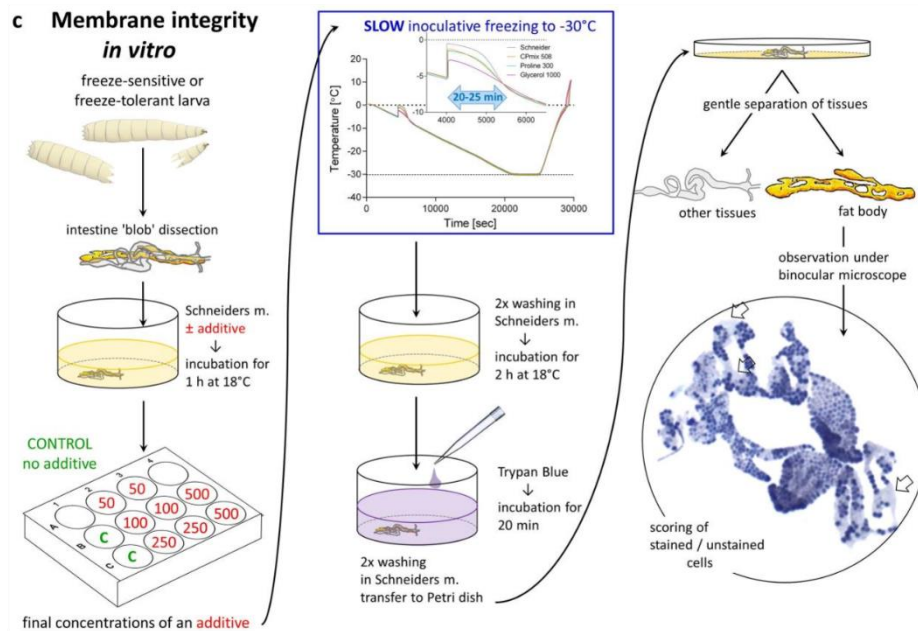
Fig. S1 - continued: The schematic outline of experiments.
(c) Membrane integrity *in vitro*. The 'intestine blobs' were dissected from larvae of the freeze-sensitive or freeze-tolerant phenotypes of *Chymomyza costata* and pre-incubated for 1h in Schneider's medium in the absence or presence of different additives. Next, the intestines were exposed to SLOW inoculative freezing to -30°C (same protocol as used for whole larvae in the *in vivo* experiments). Upon melting, the additives were washed out and the intestines were incubated in Trypan Blue solution. Next, the fat body tissues were gently separated from 'intestine blobs', observed under binocular microscope, and the proportion of blue-stained cells was estimated. The examples of temperature courses during SLOW freezing are shown in the blue frame for plain Schneider's medium, and for Schneider's medium augmented by CPmix 508 (a mixture of *C. costata* native cryoprotectants at concentrations corresponding to that in the hemolymph of freeze-tolerant larvae, sum concentration of 508 mmol.kg^{-1}), proline (300 mmol.kg^{-1}), or glycerol (1,000 mmol.kg^{-1}). Temperature was recorded using K-type thermocouples attached to PicoLog TC-08 datalogger (Pico technology, St. Neots, UK). Note that additives had a relatively small influence on the temperature course and that the durations of freeze-exotherms were approximately 20-25 min. For more explanations, see text (section: *In vitro* membrane integrity assays).

3

Table S1: The list of additives

Additive	Sigma-Aldrich product		m.w.	Medium	Concentration in plain medium [mg/mL] *	Amount in mg added to 1 mL of plain medium to produce given concentration **	
	Name	Number					
Proline	L-Proline	P0380	115.13	20 mM imidazole	0	11.5	100 mmol.kg^{-1}
				Schneider's	1.70	9.8	100 mmol.kg^{-1}
Trehalose	D(+) Trehalose dihydrate	T9449	378.33	20 mM imidazole	0	37.8	100 mmol.kg^{-1}
				Schneider's	2.0	35.8	100 mmol.kg^{-1}
Glutamine	L-Glutamine	G3126	146.14	20 mM imidazole	0	14.6	100 mmol.kg^{-1}
				Schneider's	1.8	12.8	100 mmol.kg^{-1}
Asparagine	L-Asparagine	A0884	132.12	20 mM imidazole	0	13.2	100 mmol.kg^{-1}
				Schneider's	0	13.2	100 mmol.kg^{-1}
Betaine	Betaine	61962	117.15	20 mM imidazole	0	11.7	100 mmol.kg^{-1}
				Schneider's	0	11.7	100 mmol.kg^{-1}
Glycerol	Glycerol	G5516	92.09	20 mM imidazole	0	9.2	100 mmol.kg^{-1}
Saccharose	Sucrose	S1888	342.30	Schneider's	0	34.2	100 mmol.kg^{-1}
Histodenz	Histodenz	1D2158	821.14	20 mM imidazole	0	82.1	100 mmol.kg^{-1}
				Schneider's	0	82.1	100 mmol.kg^{-1}
Urea	Urea	U5378	60.06	20 mM imidazole	0	6.0	100 mmol.kg^{-1}
K^{+}	Potassium chloride	P5405	74.56	20 mM imidazole	0	7.5	100 mmol.kg^{-1}
Na^{+}	Sodium chloride	S5886	58.44	Schneider's £	1.16	1.14 (Na^{+}) 2.87 (NaCl)	100 mmol.kg^{-1}
BSA	Bovine Serum Albumin	A7030	66 430	20 mM imidazole	0	100.0	100 mg.mL^{-1}
				Schneider's $	0	100.0	100 mg.mL^{-1}
Ficoll	Ficoll PM 70	F2878	ca. 70 000	20 mM imidazole	0	100.0	100 mg.mL^{-1}
				Schneider's	0	100.0	100 mg.mL^{-1}

* no 'additives' were present in 20 mM imidazole buffer, while some 'additives' are present in the Schneider's *Drosophila* medium and those were taken into account when preparing the augmented media. The concentration data are according to Biosera formulation of 21/07/2017.

** this is an example showing amounts of additives used to prepare augmented imidazole buffer (for Enzyme experiments) or Schneider's medium (for Membrane experiments) of a given concentration. For simplicity, we considered the mass of 1 mL of 20 mM imidazole or 1 mL of Schneider's medium to be 1 g.

£ the sodium ion (Na^{+}) is present in the Schneider's medium in three forms (NaCl, NaHCO$_3$, and Na$_2$HPO$_4$), which in sum contribute 1.16 mg of sodium ion per mL. We used NaCl to augment the Schneiders's medium by sodium ions.

$ the Schneider's solution contains yeast extract (2 g.L^{-1}) which contributes some additional protein (not taken into account).

4

In vivo experiments

In the *in vivo* experiments (Fig. S1a), whole larvae were exposed to slow inoculative freezing to -30°C using the protocol described earlier (4). The protocol consisted of five steps set in a Ministat 240 programmable cryostat (Huber, Offenburg, Germany): (i) 20 min of larval manipulation at 0°C (washing larvae out of the diet, dividing into groups of 20 specimens, and placing them into 3 mL plastic tubes between two layers of moist cellulose); (ii) slow pre-freezing to -30°C (with a small ice crystal added on top of the moist cellulose) for 300 min (cooling rate, $0.1°C$ min^{-1}); (iii) keeping larvae at -30°C for 60 min; (iv) heating from -30°C to +5°C over 60 min (heating rate, $0.6°C$ min^{-1}); and (v) melting at constant +5°C for 10 min. Adding a small ice crystal at the beginning of step (ii) induces inoculative internal freezing in larvae, which starts between -1 and -2°C, the formation of ice fraction (76% of total body water is freezable in active larvae) is completed at -5.9°C (i.e. takes approximately 59 min) (4). Unfrozen larvae served as controls. Upon melting (end of step v): either different tissues of larvae were rapidly dissected, crude total proteins were extracted (which served as source for analysis of enzyme activities), or 'intestine blobs' were rapidly dissected, incubated in Trypan Blue stain, and fat body plasma membrane integrity was assessed. The enzyme activity and membrane integrity assays are described later in the text.

In vitro enzyme activity assays

To conduct *in vitro* assays of enzyme activities (Fig. S1b), fat body or muscle tissues were rapidly dissected (ca. 30 sec per one larva) from 30 freeze-sensitive larvae and pooled in 1,200 µL of ice cold 20 mM imidazole buffer, pH 7.2. Extracting 30 tissues in 1200 uL of buffer, we estimate that the tissue solutions were diluted approximately 200-fold, which means that they could contribute an additional 2.3 mOsm concentration of tissue solutes to the sample [the larval hemolymph has an osmotic concentration of 465 mOsm according to (7)].

The pools of dissected tissues were homogenized for 6 x 3 sec using X120 homogenizer with metal blades (CAT, Germany), centrifuged at 21,000 g for 10 min at 4°C, and the supernatant was used as the source of enzymes. The supernatant was aliquoted; one aliquot served as control ─ no additive and not frozen ─ and was used for enzyme activity assays after incubation on ice for 1 h (control = 100% activity). The other aliquots were exposed to freezing in the absence or presence of different additives (see Table S1 a for complete list of additives) and the enzyme activities were measured upon melting. We used two different freezing protocols: (i) FAST, which simulates routine laboratory practice when a protein extract in a plastic micro-vial is simply moved to a deep freezer set to -75°C; and (ii) SLOW, which simulates ecologically relevant, slow inoculative freezing as used for whole larvae (*in vivo* experiments).

For the FAST freezing, we used 50 uL aliquots of protein extract mixed with 20 uL volume of additive solution 20 mM imidazole (when no additive was used, 20 uL of plain 20 mM imidazole was added). We mixed the extract and additive solution in 200 uL PCR tubes to produce different concentrations of additives ranging between 0 and 200 mmol.kg^{-1} (or 0 and 200 mg.mL^{-1} for macromolecular compounds BSA and Ficoll). The PCR tubes were moved to a deep freezer (Platinum 370H, Angelantoni, Italy) for 1 h, then melted on ice and immediately used for enzyme activity assays. The freeze exotherms started after spontaneous formation of ice nuclei (at

5

temperatures close to -10°C) and were relatively short (1-2 min) (see inset in FAST freezing protocol in Fig. S1b).

For the SLOW inoculative freezing, we used 100 uL aliquots of protein extract mixed with 100 uL of 20 mM imidazole in wells of a 24-well polysterene Costar plate with untreated surface (Corning, Kennebunk, ME, USA). In this total volume of 200 uL, given amount of additives were dissolved to produce concentrations ranging between 0 and 500 mmol.kg^{-1} (or 0 and 200 mg.mL^{-1} for macromolecular compounds BSA and Ficoll). The plate was moved to the Ministat 240 (Huber) and the same protocol as used for whole larvae was started. Upon melting, the enzyme activities were assessed. Ice formation was initiated by adding an external ice crystal (a frozen 25 uL droplet of 20 mM imidazole) at exactly -5°C and the freeze exotherms lasted for 12-15 min (see inset in SLOW freezing protocol in Fig. S1b). Exact methods to measure the enzyme activities are described below (section: Enzyme activity assays).

In vitro membrane integrity assays

To conduct *in vitro* assays on plasma membrane integrity (Fig. S1c), we dissected whole 'intestine blobs' from larvae under Schneider's *Drosophila* medium (Biosera, Nuaillé, France), which is widely used to support viability of incubated insect tissues. The blobs were obtained by cutting off the front tip of the larval body and gently squeezing the intestines (with attached fat body) out of the integument. No further attempt was made to separate individual tissues from the blob as this would damage many cells. The whole intestine blobs were moved to 650 µL of Schneider's medium in the wells of a 12-well tissue-culture plate (TRP, Switzerland). Typically, ten blobs were placed in one well though this number varied between six and twelve according to availability of larvae. Schneider's medium has a complex composition including different metabolites, salts, and buffers (total osmolarity of 330 mOsm). We changed this composition by adding additives (Table S1) at different concentrations ranging between 0 and 1000 mmol.kg^{-1} (or 0 and 200 mg.mL^{-1} for macromolecular compounds BSA and Ficoll). The final concentrations were prepared by dissolving the given amount of additive in a known small volume of Schneider's medium. That is why we express the concentrations in molal units. For simplicity, we considered the mass of 1 L of the Schneider's solution to be 1 kg. All concentrations we refer to are the final concentrations in the augmented medium taking into account the concentrations of respective compound in the original Schneider's medium. No additives were used in controls.

The intestines were pre-incubated in their respective medium at 18°C for 1 h prior to the freezing stress. The 12-well design of the plate allowed various combinations of controls, treatments, and their replicates. Two wells were always reserved for temperature recording (no tissues). One well was taken as one replication, i.e. the proportion of blue-stained cells was estimated for all fat body tissues in the well (six to twelve fat body sheets) and the mean blue staining of the group was taken for calculation. Each treatment (i.e. a combination of the additive and concentration) was replicated at least twice (two wells) but some treatments were replicated three to seven times and the control was replicated 11 times (the exact numbers of replicates are shown in respective Figures). After pre-incubation, the whole plate was housed in the Ministat 240 (Huber) and the same protocol as used for whole larvae was started. Ice formation was initiated by adding an external ice crystal (a frozen 50 uL droplet of Schneider's medium) at exactly -5°C and the freeze

6

exotherms lasted for 20-25 min (see inset in SLOW freezing protocol in Fig. S1c). Further processing of intestine blobs after melting is described below (section: Trypan Blue assay of plasma membrane integrity).

Enzyme activity assays
The activities of seven different enzymes were measured according to protocols specified below. Activities were measured colorimetrically (most enzymes) or fluorimetrically (matrix metalloproteinases) using either: (i) Quartz glass cuvettes housed in a Cary50 UV-Vis spectrophotometer (Varian, USA) attached to a circulating water bath BC4 (Julabo, Germany) for controlling the constant 25°C in cuvettes, or (ii) 96-well Optical Btm PolymerBase plates (ThermoScientific, USA) housed in the Infinite 200Pro plate reader (Tecan, Austria) equilibrated to constant 25°C (most enzymes) or 30°C (phenoloxidase). All activities were measured in a kinetic mode during the initial (linear) part of enzyme kinetics. We continuously monitored changes in the absorbance/fluorescence intensity over time, which is linked to consumption/production of a specific substrate/product. All chemicals used for enzyme activity assays were either included in the respective enzyme assay kit, or were purchased from Sigma-Aldrich.

For the *in vivo* experiments, three replicates of unfrozen control larvae vs. three replicates of slowly frozen larvae were compared and each replicate was a pool of a group of larvae or tissues (as specified below). The composition of extraction buffers and reaction mixtures are specified below for each enzyme. Enzyme activities were expressed in micromoles of enzymatically converted substrates per min per mg of total protein (except for phenoloxidase and matrix metalloproteinases, see below). The total proteins were measured by bicinchoninic acid assay (BCA) according to (8).

For *in vitro* experiments, a single large-volume extract of 30 larval tissues was prepared by homogenization in 20 mM imidazole, pH 7.2. This extract was divided into equal aliquots, the aliquots exposed to freezing (except controls), and enzyme activities were measured: (i) the activity in unfrozen control was taken as 100%; (ii) the other aliquots were frozen in the presence of various additives at concentrations ranging between 0 and 500 mmol.kg^{-1}. Enzyme activities were expressed as a fraction (in percentage) of enzyme activity that recovers after freezing stress: we searched for the additive concentration (P_{50}) that ensures 50% recovery of initial (unfrozen control) enzyme activity.

Glucose 6-phosphate dehydrogenase (G6PDH) activity was measured in total protein extracts from larval fat body or larval muscles using a Cary50 UV-Vis spectrophotometer. Pools of 30 tissues larvae per replicate were homogenized in 400 µL of ice cold 100 mM Tris-HCl buffer, pH 8.0, containing 15 mM mercaptoethanol and 1 mM EDTA (600 µL of 20 mM imidazole buffer was used for *in vitro* assays). The composition of the reaction mixture for the G6PDH assay was the same as described earlier (9): 20 mM imidazole-HCl buffer, pH 7.2; 5 mM MgSO$_4$; 0.6 mM NADP$^+$; 1 mM glucose 6-phosphate; larval protein extract (50 uL in a total of 500 uL of reaction mixture). The reaction was initiated by adding glucose 6-phosphate solution into the reaction

7

mixture and its conversion to 6-phosphate gluconolactone by G6PDH activity was followed by measuring the increase of 340 nm absorbance (NADP$^+$ → NADPH).

Citrate synthase (CS) activity was measured in total protein extracts from larval fat body or larval muscles using a Cary50 UV-Vis spectrophotometer. Pools of 30 tissues per replicate were homogenized in 400 µL of ice cold 50 mM Tris buffer, pH 8.0, containing 0.2 M sucrose, 1 mM EDTA, and 1% Triton X (600 µL of 20 mM imidazole buffer was used for *in vitro* assays). In addition to standardized homogenization of the tissues using a CAT homogenizer, we sonicated the samples 5 times for 1 sec (4710 Series Ultrasonic Homogenizer, Cole Parmer, Chicago. IL, USA) in order to solubilize the enzyme from mitochondrial matrix. The composition of the reaction mixture for the CS assay was the same as described earlier (10): 50 mM imidazole-HCl buffer, pH 8.0; 0.05 mM DTNB reagent (5,5'-dithiobis-2-nitrobenzoic acid); 0.15 mM acetyl CoA; 0.25 mM oxaloacetate; larval protein extract (10 uL in a total of 500 uL of reaction mixture). The reaction was initiated by the addition of 25 µL of oxaloacetate solution into 475 µL of reaction mixture and the mercaptid ion formation from CoA-SH (that was released upon synthesis of citrate) was followed by measuring the increase of 412 nm absorbance (DTNB → TNB).

Lactate dehydrogenase (LDH) activity was measured in total protein extracts from larval muscles of *C. costata* using a Cary50 UV-Vis spectrophotometer. Pools of 30 muscle tissues per replicate were homogenized in 400 µL of ice cold 100 mM Tris-HCl buffer, pH 8.0, containing 15 mM mercaptoethanol and 1 mM EDTA (600 µL of 20 mM imidazole buffer was used for *in vitro* assays). In addition to *C. costata*, we measured the activity of LDH (using the same method) in the muscles of the 3rd instar larvae of *Drosophila melanogaster* (pool of 30 tissues per replicate), and in the tibial levator muscle dissected from femur of the hind leg of the adult locust, *Locusta migratoria* (single muscle per replicate). Both insects were taken from our routine cultures at the Biology Centre, České Budějovice, and were acclimated to warm conditions (*D. melanogaster* is reared at constant 18°C, while *L. migratoria* at constant 30°C). The composition of the reaction mixture for the CS assay was the same as described earlier (11): 80 mM Tris-HCl, pH 7.5; 100 mM KCl; 0.2 mM NADH; 2 mM pyruvate. The reaction was initiated by the addition of 10 µL of protein extract into 490 µL of reaction mixture and the LDH activity was followed by measuring the decrease of 340 nm absorbance (NADH → NAD$^+$).

Phenoloxidase (PO) activity was measured in hemolymph using an Infinite 200Pro plate reader. The hemolymph was obtained by gently tearing larvae on a piece of Parafilm, creating a large droplet of pooled hemolymph (pool of 30 larvae were bled per replicate). This droplet was then extracted using a calibrated glass capillary (Drummond Sci., Broomall, PA, USA). The PO activity was assayed through its catalytic conversion of L-dopa (3,4-dihydroxy-L-phenylalanine, colourless) to dopachrome (red-brown colour) according to (12): the following components were mixed in wells of a 96-well plate: 5 µL of hemolymph; 35 µL of water; 5 µL of PBS; 20 µL of 5 mM L-DOPA solution. The plate was moved to a plate reader equilibrated to 30°C, briefly shaken (10 sec), and darkening of the sample was continuously followed as the increase of 490 nm absorbance (L-DOPA → dopachrome).

8

General activity of matrix metalloproteinases (MMPs, collagenases) was measured in total protein extracts from whole larval homogenates using an Infinite 200Pro plate reader according to instructions for the MMP Activity Assay Kit (ab112147, Abcam, Cambridge, UK). Pools of 10 larvae per replicate were homogenized in 500 µL of ice cold 100 mM Tris-HCl buffer, pH 7.2. The 25 µL aliquot of supernatant from centrifugation was used as a source of enzyme, combined with 25 µL of 2 mM APMA (4-aminophenylmercuric acetate) in the well of a 96-well plate, and incubated for 15 min at room temperature. Next, 50 µL of artificial Red MMP Substrate (FRET peptide) diluted in Assay Buffer (1:100) was added to the well and the whole plate was moved to the plate reader. Upon cleavage of the FRET peptide by MMPs, the intensity of fluorescence at 540/590 nm (Ex/Em) increases, which was monitored over time (RFU, relative fluorescence units).

General activity of amylases and maltases was measured in total protein extracts from larval midguts using an Infinite 200Pro plate reader according to instructions for use of the Amylase Assay Kit (ab102523, Abcam). Pools of 10 larval midguts per replicate were homogenized in 400 µL of the Assay Buffer. The 50 µL aliquot of supernatant from centrifugation was used as a source of enzyme and combined with 100 µL of artificial substrate ethylidene-pNP-G7 diluted in Assay Buffer (1:1) in the well of a 96-well plate. The plate was then moved to the plate reader. The α-amylase cleaves the artificial substrate to produce smaller fragments that are eventually modified by maltases, causing the release of a chromophore (nitrophenol) that was measured as the increase of 405 nm absorbance. The enzyme activity was converted to $\mu mol.min^{-1}.mg^{-1}$ total protein using a calibration curve produced by measuring absorbance at 405 nm for different concentrations of nitrophenol.

Glycogen phosphorylase activity was measured in total protein extracts from larval muscles using a Cary50 UV-Vis spectrophotometer. Pools of 20 larval muscles per replicate were homogenized in 400 µL of 100 mM Tris-HCl buffer, pH 8.0, containing 15 mM mercaptoethanol and 1 mM EDTA. The composition of reaction mixture was the same as described earlier (13): 50 mM potassium phosphate (KH_2PO_4) buffer, pH 6.8; 5 mg mL^{-1} glycogen; 5 µM glucose-1,6-diphosphate; 0.6 mM $NADP^+$; 2 mM 5'AMP; 15 mM $MgCl_2$; 2 U mL^{-1} phosphoglucomutase (PGM); 2 U mL^{-1} glucose 6-P dehydrogenase (G6PDH). First, the activity of the *active* ('a') form of the enzyme was measured in the absence of 5'AMP. The reaction was initiated by the addition of 70 µL of protein extract into 420 µL of reaction mixture. Glucose units released from glycogen by glycogen phosphorylase activity are converted by coupling enzymes (PGM and G6PDH) to gluconolactone, while $NADP^+$ is oxidized. This conversion was followed by measuring the increase of 340 nm absorbance ($NADP^+ \rightarrow NADPH$). Next, 10 uL of 5'AMP solution was added, which activates the *inactive* ('b') form of the enzyme (14), and the combined activity of ('a+b') forms was measured.

Trypan Blue assay of plasma membrane integrity
The integrity of fat body cell plasma membrane was assessed using the Trypan Blue assay (15). Trypan Blue is a negatively charged and large molecule that is cell membrane impermeable and therefore only enters cells with damaged or compromised membranes. Upon entry into the cell, Trypan Blue binds to intracellular proteins and DNA thereby rendering the cells a bluish color.

9

Upon melting of the medium in wells of a 12-well plate (see Fig. S1c), intestine blobs were immediately washed twice using Schneider's medium in order to remove the additives, and the intestines were then incubated in Schneider's medium for 2 h at 18°C. Next, the Trypan Blue solution was added (400 µL of 1% solution per well) and blobs were incubated in it for 20 min. The blobs were then washed twice with Schneider's medium (in order to remove excess Trypan Blue) and moved to a plastic Petri dish (3 cm diam.) with a thin layer of Schneider's medium covering the bottom. The tissues were gently pushed apart to make fat body lobes visible. The cells of fat body tissues were inspected under binocular microscope at 25x magnification and the percentage of blue-stained cells was estimated. One example of fat body tissue (frozen without additives) is shown in Fig. S1c (estimation: 95% cells blue-stained; the arrows indicate areas with unstained cells).

In a preliminary experiment, we verified that various additives themselves (without freezing stress) have practically no effect on membrane integrity (weak blue-staining) when tissues are incubated for a long time (18 h) at 18°C in the augmented Schneider's medium, while incubation of tissues for short time (2 h) at relatively low concentrations of digitonin ($0.01 - 1.0$ mmol.kg^{-1}) caused severe blue staining in fat body cells (Fig. S8a). Digitonin is a mild detergent that is routinely used to permeabilize plasma membranes of different cells (16).

Differential scanning calorimetry (DSC)
We analyzed thermal transitions in the freezing solutions combining CP (proline or trehalose) and perturbant (urea) that were used for SLOW inoculative freezing in the *in vitro* experiments on enzyme stability. The solution (10 µL) was pipetted into the aluminum DSC pan (volume of 50 µL) and its exact amount was checked by weighing the sample with precision to 0.01 mg using a Metler Toledo NewClassic MS balance. Hermetically sealed pans were then loaded into a Differential Scanning Calorimeter DSC4000 (Perkin Elmer, Waltham, MA, USA) and frozen and thawed according the following protocol: (i) hold for 1 min at 0°C, (ii) cool to -30°C at 2°C.min^{-1}, (iii) hold for 5 min at -30°C, and (iv) warm to 25°C at 10°C min^{-1}. An empty pan was used as a reference. The resulting heating curves (see Fig. S7a for examples) were analyzed using Pyris Software (Perkin Elmer). The fraction of freezable, i.e. osmotically active water (OAW) was derived from the area under the melting endotherm of water using the standard heat of fusion for the ice/water transition of 334.5 J.g^{-1}. The OAW fraction served for estimation of the freeze-concentration of urea in different solutions as follows: if the initial concentrations were, for example, 500 mmol.kg^{-1} of urea and 500 mmol.kg^{-1} of proline, the OAW fraction was 81.81% after freezing to -30°C, meaning that the urea was freeze-concentrated 5.5-fold, and reached the concentration of 2749.5 mmol.kg^{-1} in the remaining unfrozen solution (see Table S2 for all results of DSC analyses and calculations of the freeze-concentrations of urea).

10

SI Supplementary Results
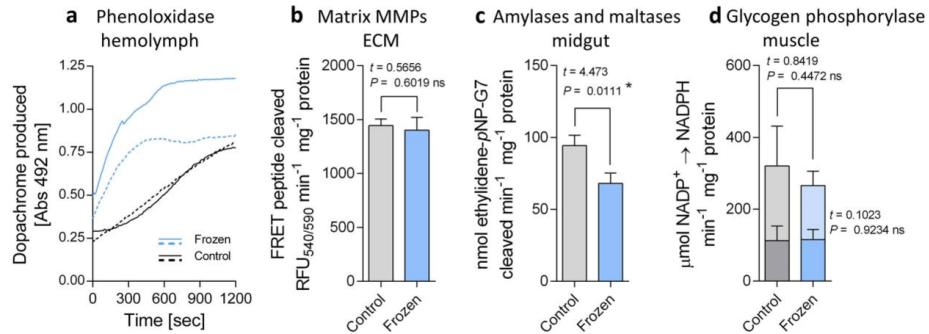
Fig. S2: Enzyme activities persist after organismally-lethal freezing stress – supplement to Fig. 1.
Larvae of the freeze-sensitive phenotype were killed by freezing to -30°C ('Frozen'), while 'Control' larvae were not frozen. The activities of four different enzymes: (**a**) phenoloxidase; (**b**) matrix metalloproteinases (MMPs); (**c**) amylases and maltases; (**d**) glycogen phosphorylase, were measured in total protein extracts of the respective tissues dissected from Control and Frozen larvae right upon melting. For phenoloxidase (a), we show the time records of the changes in absorbance in two independent replicates (distinguished as solid and broken lines); each replicate represents a pool of hemolymph sampled from 30 larvae. In both replicates, the activity of phenoloxidase in the hemolymph of Frozen larvae was relatively high during first 10 min of analysis and then ceased (no further increase of Abs492 was observed), while it was relatively low in Control larvae and a tendency to cessation was seen in one of two replicates (black, solid line). For glycogen phosphorylase (d), we distinguished between the active form ('a', lower portions of bars) and inactive form ('b', upper portions of bars) that was activated by 5'AMP. In (b, c, d), each column shows the mean + S.D. of enzyme activity (n = 3, each replicate represents a pool of tissues from 30 larvae). The enzyme activities in Control vs Frozen larvae were compared using unpaired, two-tailed t tests (t statistics and P values are shown: ns, not significant; * significant difference; GraphPad Prism v. 6.07).

11
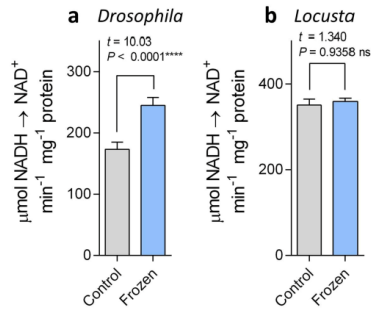
Fig. S3: LDH activity after *in vivo* freezing of larval *Drosophila melanogaster* and femoral muscle of adult *Locusta migratoria*.

The larvae of *D. melanogaster* (**a**) and femoral muscle of *L. migratoria* (**b**) were frozen to -30°C ('Frozen'). The 'Control' specimens were not frozen. The activity of lactate dehydrogenase (LDH) was measured in total protein extracts from muscles obtained right upon melting. Each column shows the mean + S.D. of the enzyme activity [n = 3, each replicate represents a pool of tissues from 30 larvae (a) or single femoral muscle (b)]. The enzyme activities in Control vs Frozen larvae were compared using unpaired, two-tailed t tests (t statistics and P values are shown: ns, not significant; **** significant difference; GraphPad Prism v. 6.07).

12
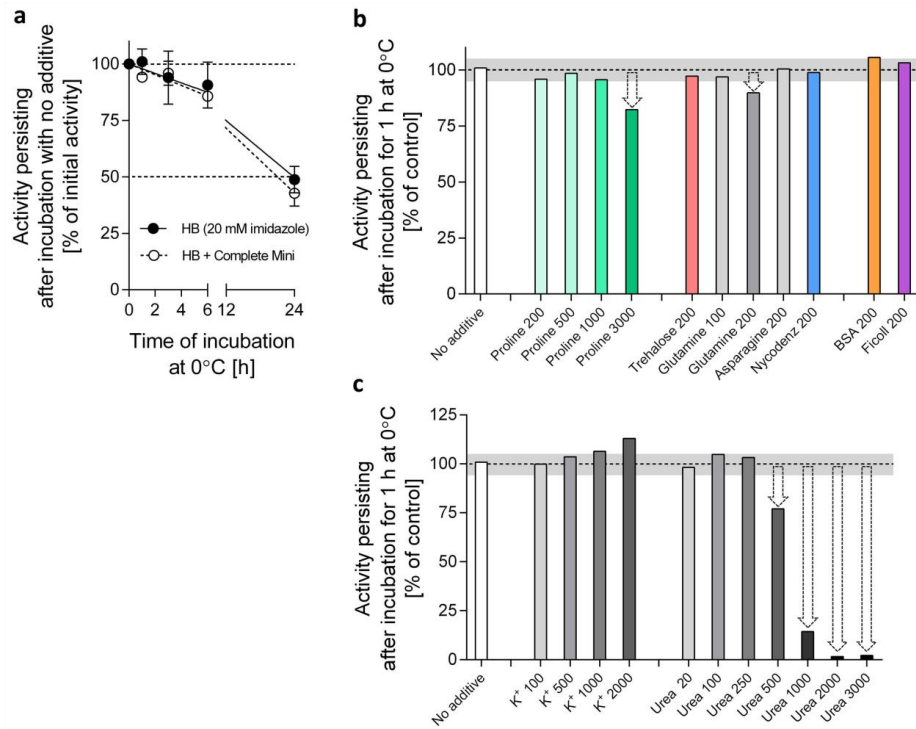
Fig. S4: The effect of incubation at 0°C with different additives on activity of G6PDH extracted from larval fat body tissue of *Chymomyza costata*.

Total proteins were extracted in homogenization buffer (HB, 20 mM imidazole) from the fat body tissue of freeze-sensitive phenotype of *Chymomyza costata* larvae and the activity of glucose 6-phosphate dehydrogenase (G6PDH) was measured. (**a**) The extract aliquots were incubated at 0°C for 0–24 h and the gradual loss of activity over time of incubation was registered. Note that the extraction of proteins with or without the proteinase inhibitor cocktail (Complete Mini, EDTA free, Roche, Mannheim, Germany) had no effect on enzyme activity. Each point is a mean ± SD of five replicates. The lines are linear regressions: HB, $y = -2.096*x+100$; HB+Complete Mini, $y = -2.377*x+100$. (**b, c**) Different additives were added to HB at concentrations indicated and their effect on G6PDH activity after 1h-incubation at 0°C was assessed. High concentrations of proline (3000 mmol.kg^{-1}) and glutamine (200 mmol.kg^{-1}) suggested moderate decrease of enzyme activity (arrows) below the control level [dashed line is a mean and grey field delimits ± SD of enzyme activity in the control without additives, see panel (a)]. Urea administered at concentrations > 500 mmol.kg^{-1} caused drastic decrease of the enzyme activity. Each column is one replicate except for control [see panel (a)].

13

88
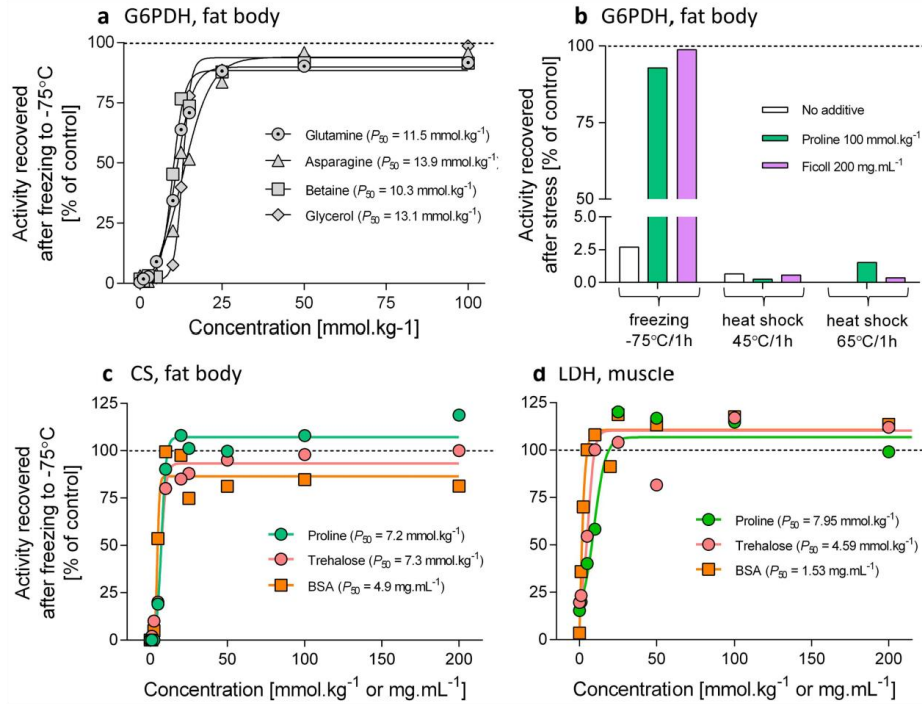
Fig. S5: Enzyme activity is protected by low concentrations of various additives to the *in vitro* freezing solution – supplement to Fig 2.

Total proteins were extracted from the fat body or muscle tissues of the freeze-sensitive phenotype of *Chymomyza costata* larvae and the activity of glucose 6-phosphate dehydrogenase (G6PDH), lactate dehydrogenase (LDH), and citrate synthase (CS) were measured prior to (control) and after (test) FAST freezing to -75°C (see Fig. S1b for protocol). (**a, c, d**) The test aliquots were augmented with different additives administered at different concentrations (see *x* axes). The activity in the unfrozen aliquot served as control = 100%. Freezing without additive (concentration = 0) caused complete loss of the enzyme activity. Different additives protected the enzymes from loss of activity upon freezing at relatively low concentrations (P_{50} is a cryoprotective concentration that allows recovering 50% of control, pre-freezing activity). (**b**) The extract aliquots augmented with proline or Ficoll were exposed to heat shocks. Neither proline nor Ficoll were able to protect the enzyme from almost complete loss of activity upon the heat shock.

14

89
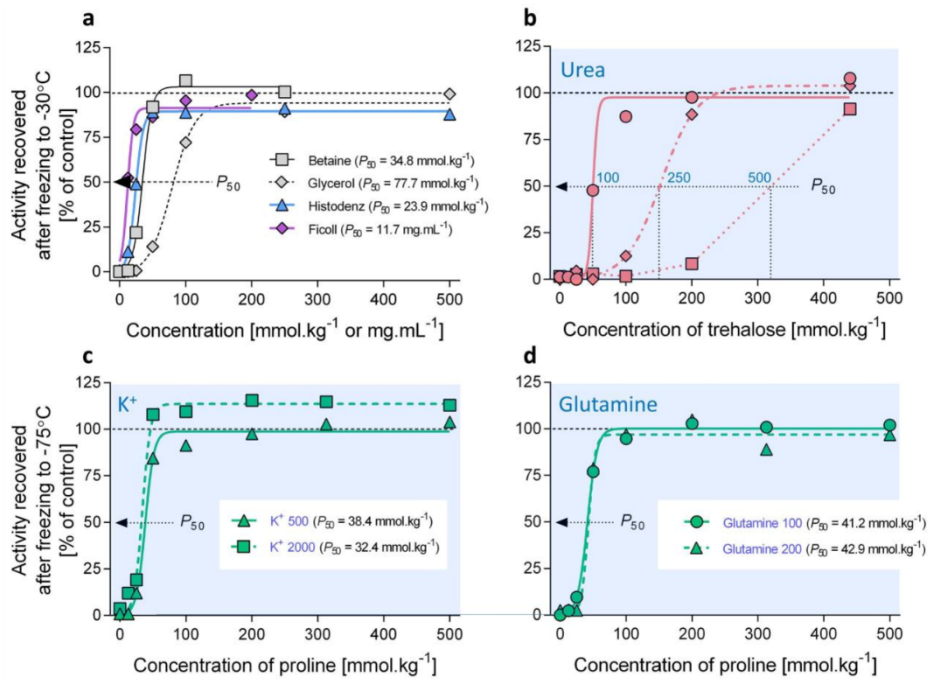
Fig. S6: Slow rate of *in vitro* freezing in the absence or presence of chemical perturbants – supplement to Fig. 3.

Total proteins were extracted from the fat body tissue of the freeze-sensitive phenotype of *Chymomyza costata* larvae and the activity of glucose 6-phosphate dehydrogenase (G6PDH) was measured prior to (control) and after (test) SLOW inoculative freezing to -30°C (see Fig. S1b for the protocol). (**a**) The test aliquots were augmented with different additives administered at different concentrations (see *x* axes). The activity in the unfrozen aliquot served as control = 100%. Freezing without additive (concentration = 0) caused complete loss of enzyme activity. Different additives protected the enzyme from loss of activity upon freezing at relatively low concentrations (P_{50} is a cryoprotective concentration that allows recovering 50% of control, pre-freezing activity). (**b, c, d**) Simultaneous presence of potential perturbants (urea, K^+, or glutamine) and cryoprotectants (trehalose or proline) during SLOW freezing either resulted in shifting the P_{50} values for trehalose toward higher concentrations (b) or had a negligible effect on P_{50} values for proline (c, d).

Note that the results presented in Fig. S6b-d and also in Fig. S4b, c suggest that urea at concentrations higher than approximately 500 mmol·kg^{-1} shows perturbing effects on G6PDH activity. Neither K^+ nor glutamine applied at very high concentrations (close to solubility limits) showed clear perturbing effects on G6PDH activity.

15

90

Table S2: The results of DSC analysis – part 1: Urea + Proline

Urea 100 +Proline

Urea	Proline	water mass	melt endotherm*	delta H	frozen water (OAW fraction)		Freeze-concentration of urea
mmol.kg^{-1}	mmol.kg^{-1}	mg	mJ	J/g	%	linear regression	mmol.kg^{-1}
100	0	10,00	3227,42	322,74	96,48	95,13	2054,1
100	12,5	9,82	3035,56	309,22	92,44	94,92	1970,4
100	25	10,14	3244,40	319,96	95,65	94,72	1893,3
100	50	10,12	3149,88	311,24	93,04	94,30	1755,8
100	100	10,07	3090,04	306,75	91,70	93,48	1533,1
100	200	10,08	3244,46	321,96	96,25	91,82	1222,9
100	313	9,84	2967,85	301,73	90,20	89,95	995,3
100	500	9,89	2826,57	285,77	85,43	86,86	760,9

Urea 250 +Proline

Urea	Proline	water mass	melt endotherm*	delta H	frozen water (OAW fraction)		Freeze-concentration of urea
mmol.kg^{-1}	mmol.kg^{-1}	mg	mJ	J/g	%	linear regression	mmol.kg^{-1}
250	0	10,10	3167,77	313,69	93,78	93,85	4063,3
250	12,5	10,05	3175,45	315,83	94,42	93,64	3932,7
250	25	10,29	3284,67	319,33	95,46	93,44	3810,3
250	50	10,08	3077,01	305,25	91,26	93,03	3586,9
250	100	9,88	2960,98	299,76	89,61	92,21	3210,5
250	200	9,96	3044,94	305,69	91,39	90,58	2653,6
250	313	9,94	3002,32	301,98	90,28	88,73	2218,7
250	500	9,85	2797,80	284,18	84,96	85,68	1745,3

Urea 500 +Proline

Urea	Proline	water mass	melt endotherm*	delta H	frozen water (OAW fraction)		Freeze-concentration of urea
mmol.kg^{-1}	mmol.kg^{-1}	mg	mJ	J/g	%	linear regression	mmol.kg^{-1}
500	0	9,81	3022,95	308,28	92,16	92,24	6446,4
500	12,5	9,91	2997,07	302,48	90,43	91,98	6236,7
500	25	10,06	3093,06	307,48	91,92	91,72	6040,3
500	50	9,91	2995,44	302,41	90,41	91,20	5682,3
500	100	9,74	2960,98	304,14	90,92	90,16	5080,2
500	200	9,54	2912,99	305,23	91,25	88,07	4191,9
500	313	9,74	2757,31	283,19	84,66	85,72	3500,2
500	500	9,42	2558,67	271,49	81,16	81,81	2749,5
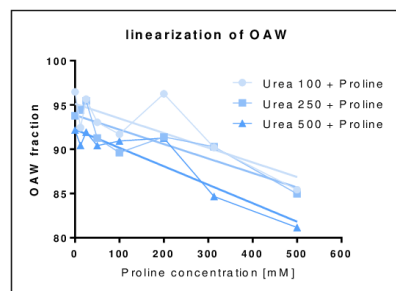
* the analysis of melt endotherm of bulk water is sensitive to the setting of baseline, which must be done manually – this causes fluctuations in the estimated OAW fraction and, consequently, in the estimated freeze-concentration of urea. In order to mitigate the effect of manually setting the baseline, we used OAW fractions interpolated from linear regressions (see figure).

16

Table S2 - continued: The results of DSC analysis – part 2: Urea + Trehalose

Urea 100 + Trehalose

Urea	Trehalose	water mass	melt endotherm*	delta H	frozen water (OAW fraction)		Freeze-concentration of urea
mmol.kg^{-1}	mmol.kg^{-1}	mg	mJ	J/g	%	linear regression	mmol.kg^{-1}
100	0	9,90	3180,34	321,23	96,03	94,85	1943,4
100	12,5	9,99	3228,96	323,15	96,61	94,61	1854,6
100	25	9,99	3071,75	307,63	91,97	94,36	1773,6
100	50	10,00	2983,69	298,34	89,19	93,87	1631,0
100	100	9,81	3128,40	318,92	95,34	92,88	1405,2
100	200	9,97	3107,89	311,86	93,23	90,91	1100,5
100	500	9,13	2568,51	281,38	84,12	85,00	666,7

Urea 250 + Trehalose

Urea	Trehalose	water mass	melt endotherm*	delta H	frozen water (OAW fraction)		Freeze-concentration of urea
mmol.kg^{-1}	mmol.kg^{-1}	mg	mJ	J/g	%	linear regression	mmol.kg^{-1}
250	0	10,08	3261,05	323,56	96,73	95,46	5504,8
250	12,5	9,77	3084,92	315,86	94,43	95,10	5099,0
250	25	9,88	3016,07	305,33	91,28	94,74	4749,0
250	50	9,88	3184,59	322,48	96,41	94,01	4175,7
250	100	9,81	3150,38	321,11	96,00	92,57	3363,5
250	200	9,58	2754,28	287,47	85,94	89,68	2421,6
250	500	9,07	2480,08	273,49	81,76	81,00	1316,0

Urea 500 + Trehalose

Urea	Trehalose	water mass	melt endotherm*	delta H	frozen water (OAW fraction)		Freeze-concentration of urea
mmol.kg^{-1}	mmol.kg^{-1}	mg	mJ	J/g	%	linear regression	mmol.kg^{-1}
500	0	10,00	3196,04	319,60	95,55	93,13	7273,8
500	12,5	9,91	3008,42	303,42	90,71	92,85	6988,2
500	25	9,89	3154,92	319,02	95,37	92,56	6724,3
500	50	9,88	3037,95	307,58	91,95	92,00	6252,0
500	100	9,76	2951,19	302,45	90,42	90,88	5481,9
500	200	9,60	2708,83	282,03	84,31	88,63	4398,3
500	500	8,76	2450,40	279,73	83,63	81,89	2761,1

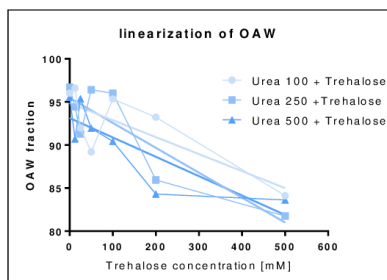* the analysis of melt endotherm of bulk water is sensitive to the setting of baseline, which must be done manually – this causes fluctuations in the estimated OAW fraction and, consequently, in the estimated freeze-concentration of urea. In order to mitigate the effect of manually setting the baseline, we used OAW fractions interpolated from linear regressions (see figure).

17
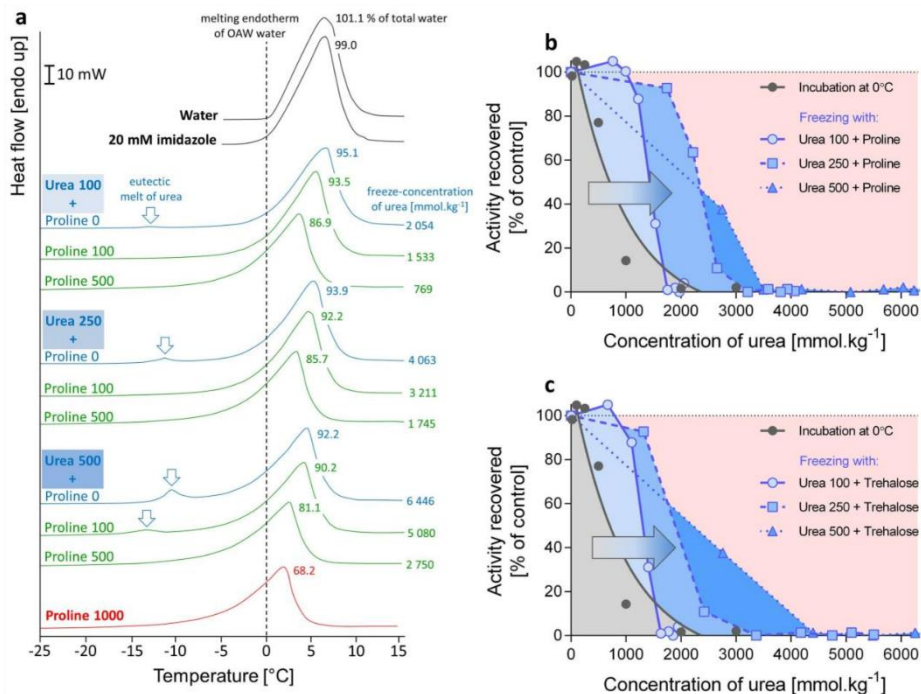
Fig. S7: The freeze-concentration of urea caused by freezing the osmotically active fraction of water (OAW).
(a) Examples of DSC heating curves for the solutions of urea and proline mixed in different concentrations (values show mmol.kg^{-1}) dissolved in 20 mM imidazole (complete dataset is in Table S2). The area under the melt endotherm of bulk water (mJ) corresponds to the fraction of frozen, i.e. osmotically active water (OAW) in the mixture. For pure water, the OAW fraction is 100% in theory (a small deviation from theory, 101.1%, is caused mainly by manually setting the baseline). For 20 mM imidazole, the OAW fraction was close to 100%. Note that gradually increasing concentrations of urea + proline caused the gradual decrease of area under the melt endotherm (a decrease of OAW fraction) and the shift of onset of melting from 0°C (water) to subzero temperatures. The numbers close to peaks of melt endotherms show the measured OAW fraction (% of total water). The smaller the OAW fraction, the lower the freeze-concentration effect on urea; the estimation is shown at the end of each curve. **(b, c)** The effect of urea concentration on activity of G6PDH recovered after either the incubation of total protein extract at 0°C for 1 h (taken from Fig. S4c), or after SLOW freezing to -30°C (taken from Fig. 3e for proline, and from Fig. S6b for trehalose).

Note that concentrations of urea *much higher* than those set by incubation at 0°C experiment (grey area) are tolerated by G6PDH in the -30°C freezing experiment, provided proline (b) or trehalose (c) are added to the solution (arrows from grey to blue areas). These results suggest that proline and trehalose not only help to decrease the freeze-concentration of urea but also directly counteract the chemical disturbance to G6PDH enzyme caused by high urea concentrations. The red area indicates that extremely high concentrations of urea are not tolerable for G6PDH even in the presence of proline or trehalose.

18
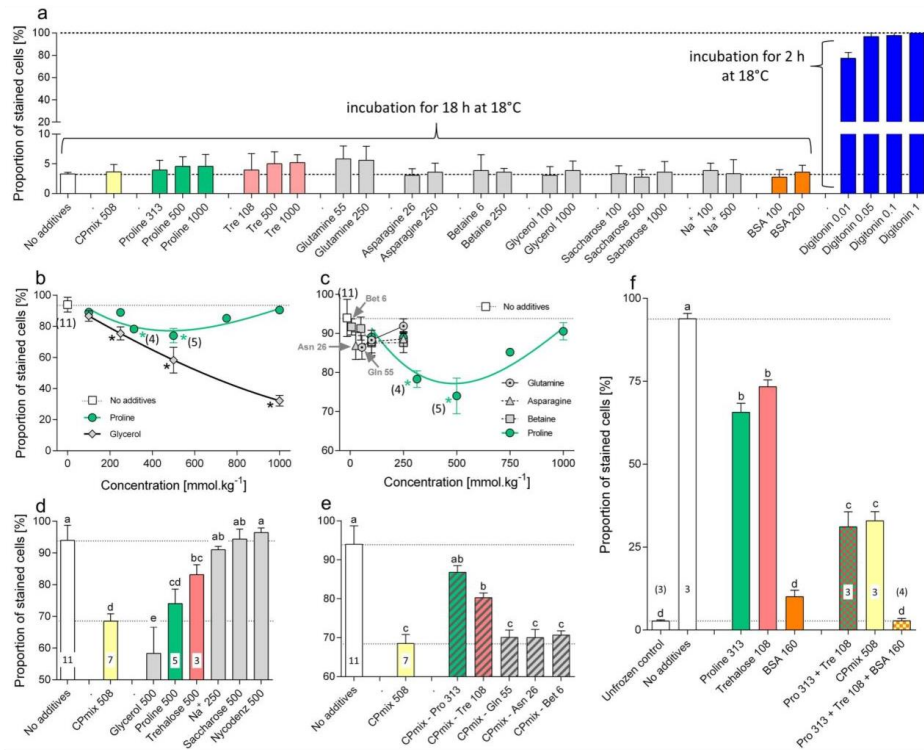
Fig. S8: Effect of additives on plasma membrane integrity of fat body cells during incubation and freezing stress *in vitro*.

The dissected fat body tissues of (**a-e**) freeze-sensitive, or (**f**) freeze-tolerant larval phenotypes of *Chymomyza costata* were either (**a**) incubated at 18°C or (**b-f**) exposed to SLOW inoculative freezing stress *in vitro* in Schneider's solution augmented by different additives at different concentrations (see *x* axes). The control tissues (empty squares in (b, c) or empty columns in (a, d-f) were exposed to incubation or freezing stress without additive. After incubation or melting, the integrity of fat body cell plasma membrane was assessed using the Trypan Blue assay (see *y* axes). For other descriptions, see caption of Fig. 5.

Note:

(**a**) Additives have no effect on membrane integrity of the cells incubated in Schneider's solution at 18°C, while Digitonin at low concentrations permeabilize the membrane for Trypan Blue.

(**b, c**) Glycerol is more effective in membrane integrity protection than proline, while glutamine, asparagine, and betaine are ineffective (data for proline are shown for comparison).

(**d**) Different additives applied in the same osmotic concentration showed different abilities to protect membrane integrity.

(**e**) Excluding proline or trehalose from CPmix caused partial loss of the ability of the reduced-CPmix to protect membrane integrity.

(**f**) Complete rescue of membrane integrity upon *in vitro* freezing stress was achieved in freeze-tolerant phenotype larvae using a mixture of proline, trehalose, and BSA.

19

94
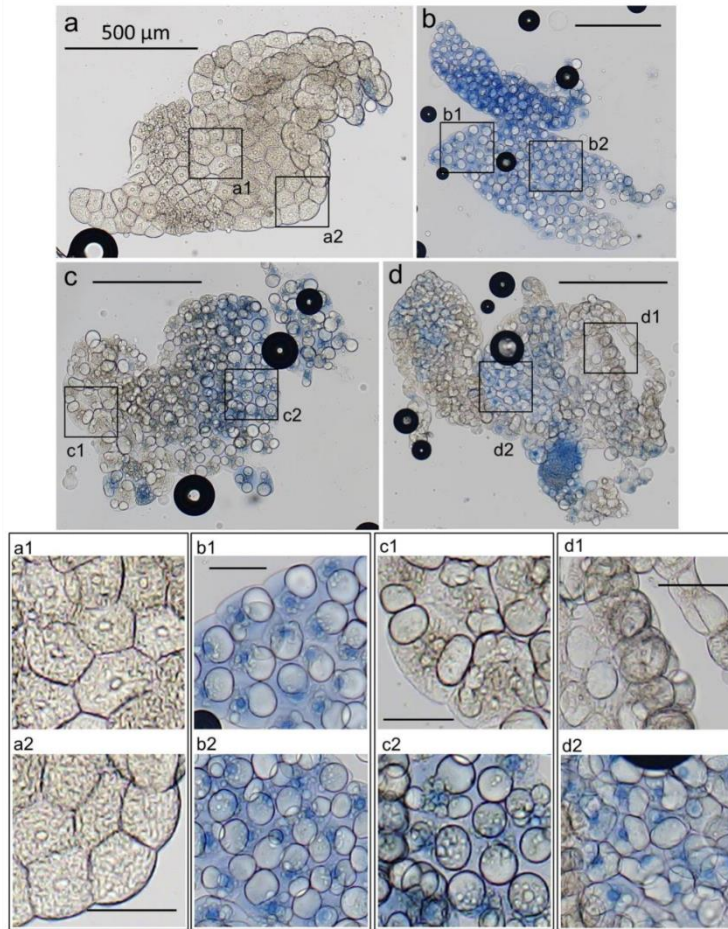
Fig. S9: Examples of Trypan Blue staining of fat body cells.
Fat body tissue was dissected from the freeze-sensitive phenotype of *Chymomyza costata* larvae. Controls (**a**) were not exposed to freezing stress and incubated directly in Trypan Blue. The test tissues were first exposed to SLOW inoculative freezing to -30°C and incubated in Trypan Blue after melting. The cells with compromised membrane integrity stain blue. The test tissues were frozen in: (**b**) plain Schneider's *Drosophila* medium, (**c**) Schneider's medium augmented with CPmix 508 (mixture of proline, trehalose, glutamine, asparagine, and betaine in total concentration of 508 mmol.kg^{-1}), or (**d**) Schneider's medium augmented with BSA, 100 mg.mL^{-1}. All scale bars in (a-d) are 500 μm. The squares delimit two areas in each micrograph that are shown enlarged below.

Note that each piece of tissue shows compact areas with relatively intact cells (no staining), while the cells are stained with Trypan Blue in other areas. All frozen tissues show the characteristic coalescence of initially small lipid droplets (a) into several or single large lipid droplet (b-d) (17).

20

SI Supplementary Discussion

Exact quotations of highly-cited literary sources:

- Storey and Storey, 1988 (18), p. 43 (742 citations in Google Scholar): "… the presence of polyols in freeze-tolerant insects may be key to preserving homeostasis in the frozen state by stabilizing individual enzymes/proteins as well as macromolecular interactions ... against the potential denaturing effects of subzero temperatures and low water content."

- Lee, 2010 (19), p. 17 (389 citations in Google Scholar): "Trehalose and glycerol are commonly produced by insects in response to osmotic challenge due to desiccation and freezing. These compounds serve to stabilize proteins and protect cell membranes."

- Teets and Denlinger, 2013 (20), p. 3 (266 citations in Google Scholar): "The most common cryoprotectants observed in overwintering insects are low molecular weight sugar alcohols such as glycerol, sorbitol and inositol. The functions of these compounds include stabilizing membranes and proteins ..."

- Toxopeus and Sinclair, 2018 (21) (91 citations in Google Scholar), p 9: "Increased osmotic pressure associated with freezing (i.e. freeze concentration) might destabilise proteins and damage cell membranes, causing cell death." p. 13: " ... freeze-tolerant insects must counteract the destabilising effect of dehydration on membranes (including organelle and vesicle membranes) and proteins. These macromolecules can be stabilised by direct or indirect (*via* the hydration shell) interaction with low molecular weight metabolites such as trehalose, proline, and other amino acids."

- The numbers of citations are according to Google Scholar (https://scholar.google.com/) taken on 15 June 2022.

Do proteins in general need stabilization by CPs during freezing stress?
There are several reasons for cautiousness when extending the validity of our hypothesis that the insect *soluble enzymes* are not the primary targets of freezing injury to *all proteins* in general:

First, dissociation of multimeric proteins into subunits was observed to occur in many enzymes at temperatures close to 0°C (22). Similarly, polymeric protein structures such as microtubules, actin filaments, or collagen fibers depolymerize already upon mild cold exposures (23-25). Such dissociation of quaternary structures represents a first step toward protein denaturation and is usually associated with loss of protein function. Nevertheless, spontaneous re-association of mild-cold-dissociated enzymes and polymeric proteins was observed upon incubation at physiological temperatures. Most of the enzymes assessed in this study are dimers or tetramers and their dissociation upon freezing stress *in vivo* (if it occurred at all) must have been fully reversible upon melting and re-warming because no loss of activity was observed. The re-association of larger complexes after severe cold and freeze-dehydration stress, however, might be more problematic as the osmotic shrinkage of cells causes loss of cytoplasmic organization,

21

extensive displacements, or even disintegration of organelles and cytoskeletal structures (10, 17, 26).

Second, severe cold alone (typically around -20°C) is known to cause cold-denaturation of proteins, i.e. unfolding of globular tertiary structure and exposing hydrophobic core domains (22, 27). The occurrence of protein denaturation is theoretically even more probable after freezing due to loss of bulk water and increasing concentrations of chemical perturbants of native protein structure such as protons, metal ions, or urea (28-30). Again, the large polymeric protein complexes might be more sensitive than soluble enzymes to irreversible aggregation of denatured subunits via their exposed hydrophobic domains upon severe freezing stress. Accordingly, the freeze-thaw induced denaturation and aggregation of myofibrilar proteins was often observed in fish muscle (31, 32). We observed irreversible loss of microtubular structure to occur in fat body cells of frozen-thawed larvae of *C. costata* – however, without any apparent loss of larval viability (17).

Third, the thermodynamic theory of protein denaturation by cold and freezing stress, and its prevention by CP-mediated stabilization, has been well established during eighties of the last century by Timasheff and colleagues (33-35) and is accepted until recently (36, 37). That some insect proteins really do denature upon cold and freezing stress *in vivo* is indirectly supported by the observed upregulation of inducible heat shock proteins' expression after the stress (38, 39), as well as by the impaired cold tolerance of insects that had this upregulation response prevented by RNAi targeted against expression of *hsp70* gene (40). We found that the *in vitro* loss of activity of G6PDH caused by heat stress (+45°C or +65°C for 1 h) was not preventable by proline or Ficoll, while the loss of activity caused by freezing stress (-75°C for 1 h) was fully preventable by low concentrations of proline and Ficoll. This result suggests that the nature or extent of the injury to proteins differ between heat and freezing stresses.

Fourth, the accumulated CPs may compensate for the denaturing effects of high concentrations of chemical perturbants (41-43). The concentrations of protein structure denaturants such as urea, arginine, lysine, or inorganic salts may, in theory, exceed toxic limits due to freeze dehydration of biological solutions (29). It has been shown, for instance, that elasmobranch fish accumulating high concentrations of urea (400 mM) protect their pyruvate kinase and ribonuclease against denaturing effects of urea by a mixture of compensating solutes containing TMAO, sarcosine, β-alanine, and betaine (44, 45). Accordingly, we observed that G6PDH activity is protected during freezing stress by proline or trehalose against perturbing effects of urea concentrations exceeding 500 mmol.kg^{-1}. Such high concentrations of urea, however, are unlikely to occur in larvae. We have not measured the concentrations of urea in larvae of *C. costata*; nevertheless, data for larvae of *Drosophila melanogaster* show hemolymph concentrations below 10 mmol.l^{-1} (46).

Fifth, we have studied the acute effects caused by a single freeze-thaw cycle, while the overwintering insects are often exposed to long-term freezing and/or repeated freeze-thaw cycles in the field (47). The increasing time of freeze storage and number of freeze-thaw cycles are well known to aggravate the irreversible denaturation of fish myofibrilar proteins (32).

Collectively, for the reasons specified above, we keep open the question on stability of *proteins in general* upon freezing stress. The stability of large polymeric protein complexes, nucleoprotein

22

multimeric complexes such as ribosomes, or membrane-embedded protein complexes should be attested specifically in independent experiments.

SI References

SI References

1. Riihimaa AJ & Kimura MT (1988) A mutant strain of *Chymomyza costata* (Diptera: Drosophilidae) insensitive to diapause-inducing action of photoperiod. *Physiol Entomol.* 13:441-445.
2. Kostal V, Noguchi H, Shimada K, & Hayakawa Y (1998) Developmental changes in dopamine levels in larvae of the fly Chymomyza costata: comparison between wild-type and mutant-nondiapause strains. *J. Insect Physiol.* 44:605-614.
3. Kučera L, *et al.* (2022) A mixture of innate cryoprotectants is key for freeze tolerance and cryopreservation of a drosophilid fly larva. *J. Exp. Biol.* 225:jeb243934.
4. Rozsypal J, Moos M, Šimek P, & Koštál V (2018) Thermal analysis of ice and glass transitions in insects that do and do not survive freezing. *J. Exp. Biol.* 221:170464.
5. Koštál V, *et al.* (2011) Long-term cold acclimation extends survival time at 0°C and modifies the metabolomic profiles of the larvae of the fruit fly *Drosophila melanogaster*. *PLoS One* 6:e25025.
6. Findsen A, Andersen JL, Calderon S, & Overgaard J (2013) Rapid cold hardening improves recovery of ion homeostasis and chill coma recovery time in the migratory locust, *Locusta migratoria. J. Exp. Biol.* 216:1630-1637.
7. Koštál V, Zahradníčková H, & Šimek P (2011) Hyperprolinemic larvae of the drosophilid fly, Chymomyza costata, survive cryopreservation in liquid nitrogen. *Proc. Natl. Acad. Sci. USA* 108:13041-13046.
8. Smith P, *et al.* (1985) Measurement of protein using bicinchoninic acid. *Anal. Biochem.* 150:76-85.
9. Storey KB, Keefe D, Kourtz L, & Storey JM (1991) Glucose-6-phosphate dehydrogenase in cold hardy insects: kinetic properties, freezing stabilization, and control of hexose monophosphate shunt activity. *Insect Biochem.* 21:157-164.
10. Štětina T, Des Marteaux L, & Koštál V (2020) Insect mitochondria as targets of freezing-induced injury. *Proc. R. Soc. B* 287:20201273.
11. Carpenter JF & Crowe JH (1988) The mechanism of cryoprotection of proteins by solutes. *Cryobiol.* 25:244-255.
12. Laughton AM & Siva-Jothy MT (2011) A standardised protocol for measuring phenoloxidase and prophenoloxidase in the honey bee, *Apis mellifera. Apidologie* 4:140-149.
13. Koštál V, Tollarova M, & Šula J (2004) Adjustments of the enzymatic complement for polyol biosynthesis and accumulation in diapausing cold-acclimated adults of *Pyrrhocoris apterus. J. Insect Physiol.* 50:303-313.
14. Storey KB & Storey JM (2012) Insect cold hardiness: metabolic, gene, and protein adaptation. *Can. J. Zool.* 90:456-475.
15. Strober W (2015) Trypan blue exclusion test of cell viability. *Curr. Protoc. Immunol.* 111:A3. B. 1-A3. B. 3.

23

16. Fiskum G (1985) Intracellular levels and distribution of Ca2+ in digitonin-permeabilized cells. *Cell Calcium* 6:25-37.
17. Des Marteaux LE, Štětina T, & Koštál V (2018) Insect fat body cell morphology and response to cold stress is modulated by acclimation. *J. Exp. Biol.* 221:jeb189647.
18. Storey KB & Storey JM (1988) Freeze tolerance in animals. *Physiol. Rev.* 68:27-84.
19. Lee REJ (2010) A primer on insect cold-tolerance. *Low Temperature Biology of Insects*, eds Denlinger DL & Lee REJ (Cambridge University Press).
20. Teets NM & Denlinger DL (2013) Physiological mechanisms of seasonal and rapid cold-hardening in insects. *Physiol. Entomol.* 38:105-116.
21. Toxopeus J & Sinclair BJ (2018) Mechanisms underlying insect freeze tolerance. *Biol. Rev.* 93:1891-1914.
22. Privalov PL (1990) Cold denaturation of protein. *Crit. Rev. Biochem. Mol. Biol.* 25:281-306.
23. Cottam DM*, et al.* (2006) Non-centrosomal microtubule-organising centres in cold-treated cultured *Drosophila* cells. *Cell Motil. Cytoskeleton* 63:88-100.
24. Belous A (1992) The role of regulatory systems modulating the state of cytoskeletal proteins under the temperature and osmotic effects. *Probl. Cryobiol.* 4:3-14.
25. Fessler J (1960) Some properties of neutral-salt-soluble collagen. *Biochem. J.* 76:463.
26. Des Marteaux LE, Stinziano JR, & Sinclair BJ (2018) Effects of cold acclimation on rectal macromorphology, ultrastructure, and cytoskeletal stability in *Gryllus pennsylvanicus* crickets. *J. Insect Physiol.* 104:15-24.
27. Dias CL*, et al.* (2010) The hydrophobic effect and its role in cold denaturation. *Cryobiology* 60:91-99.
28. Bennion BJ & Daggett V (2003) The molecular basis for the chemical denaturation of proteins by urea. *Proc. Natl. Acad. Sci. USA* 100:5142-5147.
29. Timasheff SN (1993) The control of protein stability and association by weak interactions with water: how do solvents affect these processes? *Annu. Rev. Biophys. Biomol. Struct.* 22:67-97.
30. Hamada H, Arakawa T, & Shiraki K (2009) Effect of additives on protein aggregation. *Curr. Pharm. Biotechnol.* 10:400-407.
31. Zhang Y, Puolanne E, & Ertbjerg P (2021) Mimicking myofibrillar protein denaturation in frozen-thawed meat: Effect of pH at high ionic strength. *Food Chem.* 338:128017.
32. Sikorski ZE, Olley J, Kostuch S, & Olcott HS (1976) Protein changes in frozen fish. *Crit. Rev. Food Sci. Nutr.* 8:97-129.
33. Gekko K & Timasheff SN (1981) Mechanism of protein stabilization by glycerol: preferential hydration in glycerol-water mixtures. *Biochem.* 20:4667-4676.
34. Arakawa T & Timasheff SN (1982) Stabilization of protein structure by sugars. *Biochem.* 21:6536-6544.
35. Arakawa T & Timasheff S (1985) The stabilization of proteins by osmolytes. *Biophys. J.* 47:411-414.
36. Kim NA, Thapa R, & Jeong SH (2018) Preferential exclusion mechanism by carbohydrates on protein stabilization using thermodynamic evaluation. *Int. J. Biol. Macromol.* 109:311-322.
37. Arsiccio A & Pisano R (2017) Stability of proteins in carbohydrates and other additives during freezing: the human growth hormone as a case study. *J. Phys. Chem. B* 121:8652-8660.

24

38. Sinclair B, Gibbs A, & Roberts S (2007) Gene transcription during exposure to, and recovery from, cold and desiccation stress in *Drosophila melanogaster*. *Insect Mol. Biol.* 16:435-443.

39. Teets NM*, et al.* (2019) Changes in energy reserves and gene expression elicited by freezing and supercooling in the Antarctic midge, Belgica antarctica. *Insects* 11:18.

40. Rinehart JP*, et al.* (2007) Up-regulation of heat shock proteins is essential for cold survival during insect diapause. *Proc. Natl. Acad. Sci. USA* 104:11130-11137.

41. Somero G (1986) Protons, osmolytes, and fitness of internal milieu for protein function. *Am. J. Physiol. Regul. Integr. Comp. Physiol.* 251:R197-R213.

42. Yancey PH (2005) Organic osmolytes as compatible, metabolic and counteracting cytoprotectants in high osmolarity and other stresses. *J. Exp. Biol.* 208:2819-2830.

43. Zachariassen KE, Kristiansen E, & Pedersen SA (2004) Inorganic ions in cold-hardiness. *Cryobiol.* 48:126-133.

44. Yancey PH & Somero GN (1979) Counteraction of urea destabilization of protein structure by methylamine osmoregulatory compounds of elasmobranch fishes. *Biochem. J.* 183:317-323.

45. Yancey PH & Somero GN (1980) Methylamine osmoregulatory solutes of elasmobranch fishes counteract urea inhibition of enzymes. *J. Exp. Zool.* 212:205-213.

46. Etienne R, Fortunat K, & Pierce V (2001) Mechanisms of urea tolerance in urea-adapted populations of Drosophila melanogaster. *J. Exp. Biol.* 204:2699-2707.

47. Marshall KE & Sinclair BJ (2015) The relative importance of number, duration and intensity of cold stress events in determining survival and energetics of an overwintering insect. *Funct. Ecol.* 29:357-366.

25

100

3. Discussion

- **Diversity and biosynthesis of cryoprotectants (CPs)**

The first aim of this study was to identify the composition of the natural cryoprotective (CP) mixture within the highly freeze-tolerant *C. costata* larvae. Our mass spectrometry (MS) analysis, which covered 49 metabolites, likely comprehensively represented the most abundant metabolites. We base this assumption on the following arguments:

- The total osmolarity of cold acclimated (SDA) larval hemolymph approximates 700 mOsmol kg^{-1} (Rozsypal et al., 2018). Our MS analysis accounted for 554 mmol l^{-1} of this osmolarity attributed to the 49 metabolites.
- Metal cations, primarily Na^+ and K^+, occupy roughly 80 mmol l^{-1} within the hemolymph (Olsson et al., 2016; Štětina et al., 2018).
- An equivalent concentration of approximately 70 mmol l^{-1} is anticipated for anions, encompassing Cl^-, $HCO3^-$, and proteins, with a 10 mmol l^{-1} allowance to accommodate negatively charged metabolites like aspartate, glutamate, and TCA intermediates.
- Calculations, as follows [700 − 554 − (80 + 70) = -4], indicate no unexplained 'osmotic gap' between the cumulative molar concentrations of the 49 metabolites and the hemolymph osmolality.

The putative components of the CP mixture were identified based on their significant accumulation during larval cold acclimation.The identified composition of this mixture consists of proline, trehalose, glutamine, asparagine, betaine, GPE, GPC, and sarcosine, with concentrations in hemolymph at a ratio of 313:108:55:26:6:4:2.9:0.5 mmol l^{-1}. Notably, this CP mixture exhibits similarities to cocktails found in various organisms exposed to different environmental stressors (Somero, 1986; Yancey, 2005; Choi et al., 2011; Gertrudes et al., 2017). This similarity suggests that the presence of these organic cytoprotectants and compatible osmolytes across different organisms likely results from convergent evolution, favoring the accumulation of polar, water-soluble molecules with high solubility and low toxicity (Hochachka & Somero, 2002).

The CP mixture in *C. costata* likely evolved as a functional adaptation to help larvae survive overwintering in a sub-arctic climate zone. These larvae overwinter in cold yet thermally stable microenvironments under fallen tree bark, often shielded by snow (Band & Band, 1982; Grimaldi, 1986). They are susceptible to external ice crystal formation at temperatures just below 0°C and can survive after the formation of extracellular ice (Rozsypal et al. 2018). Diapause, cold-acclimated larvae (SDA) exhibit significantly higher freeze tolerance compared to non-diapause, warm-acclimated larvae (LD). While LD larvae have lower survival limits at around -5°C, SDA larvae can endure freezing at temperatures as low as -100°C (Shimada & Riihimaa, 1988; Shimada, 1990) and even withstand long-term cryopreservation in liquid nitrogen (Moon et al., 1996, Koštál et al., 2011; Rozsypal et al., 2018).

In our study, we conducted a bioassay, demonstrating that supplementing the larval diet with the major components of the CP mixture, namely proline, trehalose, glutamine, asparagine, and betaine, in their natural stoichiometric ratio, transformed freeze-sensitive LD larvae into freeze-tolerant, cryopreservable larvae within just three days. Moreover, we found that the components of the mixture work in synergy, where the complete mixture's effect surpasses the simple addition of individual component effects. These results suggest that different components may play specific roles, opening avenues for further investigation.

Next, we analyzed the adaptive metabolic modifications that occurred in *C. costata* larvae as they transitioned from a freeze-sensitive to a freeze-tolerant phenotype while entering winter diapause and undergoing subsequent cold acclimation. Our analysis involved the profiling of 56 metabolites, utilizing liquid chromatography and high-resolution mass spectrometry (LC-HRMS), as well as the assessment of the relative expression levels of 95 key genes encoding metabolic enzymes and transport systems. This comprehensive analysis covered metabolic pathways involving all three major chemical groups of potential cryoprotectants (CPs).

We examined changes in 56 metabolites and 95 genes, mapping them onto schematic pathways for proline, trehalose, and betaine (see paper I for figures). It is important to note that these schematic maps do not specify cell types but differentiate between cytosolic and extracellular spaces.

- Proline primarily comes from dietary intake, which contradicts initial expectations. We have also confirmed partial synthesis from precursors like glutamine, glutamate, and ornithine, with a minor contribution from proteins, particularly collagens.
- Trehalose mainly derives from glycogen, a known and confirmed source (Storey & Storey, 2012), and there may be a partial contribution from the diet.
- Betaine sources, including GPC, GPE, DMG, and sarcosine, primarily originate from choline released through phospholipid conversions. Our 13C labeling experiments confirmed that glycine is not a contributing source.

- **Physico-chemical behavior of CPs *in vivo* during slow inoculative freezing**

In our research, we employed the MALDI-MSI technique to explore the distribution of cryoprotectants (CPs) within larval tissues. This application marks a novel addition to cryobiology literature as it allowed us to examine changes in CP localization during gradual extracellular freezing for the first time. Typically, CP concentrations in insects have been reported in whole body samples due to challenges in estimating precise concentrations in small insect tissues and the belief that native CPs move freely across membranes. Our study confirmed that SDA larvae of *C. costata* accumulate putative CPs in all examined tissues, but with the highest concentrations and contents found in the hemolymph. For instance, the pool

of the insect 'blood sugar', trehalose (Thompson, 2003; Mullins, 1985) in cold acclimated larval hemolymph was about 16 times larger than in the fat body or midgut and 64 times larger than in muscle tissue. Other metabolites, however, showed tissue-specific predominance. For instance, maltose was primarily found in the midgut, reflecting the digestion of dietary starch (Applebaum, 1985). Muscles had enriched levels of arginine and arginine phosphate, related to their role as energy stores in insect muscle (Beis & Newsholme, 1975). Aspartate and glutamate were prevalent in all tissues due to their central role in amino acid metabolism (Champe & Harvey, 1994). Tissues also contained abundant glutathione, known for its role in cellular redox balance (Sies, 1999).

One significant finding in our study concerns the behavior of the two main CP components, proline and trehalose, during slow extracellular freezing. The MALDI-MSI analysis revealed that trehalose mainly remains in its original location before freezing, concentrating in partially freeze-dehydrated hemolymph and tissues. In contrast, proline molecules appear to migrate out of the hemolymph and tissues and concentrate in thin layers separating extracellular ice crystals from freeze-dehydrated tissues and hemolymph. The underlying mechanisms behind this delocalization and its functional significance in cryopreserved insects are still hypothetical and speculative. Differences in water solubility, glass transition initiation, and mobility in freeze-concentrated solutions may explain this phenomenon.

Furthermore, our study emphasizes the importance of the glass transition phenomenon during the gradual freezing of SDA larvae. This transition occurred within the temperature range of -20°C to -30°C. Notably, only larvae pre-frozen to temperatures below -30°C, effectively below the glass transition temperature, survived sudden submersion and cryopreservation in liquid nitrogen. This underscores the critical role of the glass transition process in ensuring survival under these conditions.

In contrast to previous research attributing glass formation primarily to high proline concentrations, our investigation using differential scanning calorimetry (DSC) affirmed that proline, even at a concentration of 978 mmol kg^{-1}, does not induce the glass transition (at least not at temperatures down to -60°C) (Rudolph & Crowe, 1986; Rozsypal et al., 2018). Instead, our study recognized trehalose as a potent inducer of the glass transition in *C. costata* tissues, which is in accordance with the knowledge on trehalose glassification in the *in vitro* aqueous systems (Green & Angell, 1989; Chen et al., 2000; Cesaro et al., 2008).

Regarding the viscoelastic properties of proline, it's essential to note that, unlike trehalose, proline does not initiate the glass transition (Rasmussen et al., 1997; Liu et al., 2020) and exhibits extensive solubility in water, potentially exceeding 15 mol kg^{-1} (Held et al., 2014; Qiu et al., 2019). Nonetheless, principles from physical chemistry indicate that proline, when present at high concentrations, can form a viscoelastic liquid (McLain et al., 2007; Troitzsch et al., 2008; de Molina et al., 2017) similar to non-aqueous deep eutectic systems (NADES) (Choi et al., 2011). These liquids are known for their distinctive properties, including a significantly depressed melting point, inhibited ice crystallization, and an enhanced propensity for

amorphous glass formation. The elements within a complex mixture that form NADES are connected to each other through a highly structured three-dimensional network, characterized by optimal interactions involving both intermolecular and intramolecular hydrogen bonding (Dai et al., 2013; Dai et al., 2015).

Our study postulates that within slowly freeze-dehydrating larvae, a proline-dominated viscoelastic solution with properties resembling NADES may form locally at a microscale level. As water molecules migrate from gradually dehydrating hemolymph and tissues toward extracellular ice during extracellular freezing, proline molecules, highly soluble and mobile, may accompany this movement. This phenomenon results in the creation of a thin, highly concentrated layer of proline, observed via MALDI-MSI. This viscoelastic liquid likely contributes to the stabilization of deeply frozen *C. costata* larvae by forming a rubber-like intermediate zone located between extracellular ice crystals and freeze-dehydrated tissues. Consequently, this process aids in alleviating the thermo-mechanical stresses associated with temperature fluctuations during the immersion of larvae in liquid nitrogen and subsequent rewarming.

- **Protective roles of CPs during extracellular freezing and cell freeze dehydration**

Furthermore, we investigated how insects protect their soluble enzymes and cell membranes when exposed to freezing. Our main goal was to determine if the proposed mechanisms for freezing injury and the effectiveness of CPs could be confirmed or disproven. It's worth noting that this idea mainly comes from existing literature, which mainly relies on *in vitro* experiments. Our study, on the other hand, is the first to directly examine these processes using *in vivo* assays.

We began by assessing the *in vivo* response of several distinct soluble enzymes in freeze-sensitive *C. costata* larvae when exposed to freezing temperatures. These enzymes included glucose 6-P dehydrogenase (G6PDH), citrate synthase (CS), lactate dehydrogenase (LDH), phenoloxidase (PO), matrix metalloproteinases (MMPs), amylases and maltases, and glycogen phosphorylase. Our experiments revealed that freezing stress did not lead to complete loss of enzyme activity, with only minor decreases observed in some cases. Specifically, G6PDH in muscle and certain enzymes in the midgut experienced statistically significant reductions in activity. This outcome aligns with the extensive body of literature pertaining to vertebrate (Tamiya et al., 1985; Carpenter & Crowe, 1988; Lippert & Galinski, 1992) and insect enzymes (Storey et. al., 1991) that have shown susceptibility to *in vitro* freezing-induced inactivation. Intriguingly, freezing stress even stimulated the activity of prophenoloxidase in the hemolymph. To validate our findings, we conducted experiments using samples from two other insect species: *D. melanogaster* larvae and *Locusta migratoria* tibial levator muscle. The results aligned with our initial observations, underscoring the preservation of enzymatic activities in soluble enzymes found in various biological solutions within *C. costata*, including hemolymph, alimentary canal, extracellular matrix, cytosol, and

mitochondrial matrix of muscle and fat body cells, during freezing stress *in vivo*. To further investigate the behavior of soluble enzymes during freezing stress, we subjected total protein extracts from *C. costata* larvae to freezing *in vitro*. Soluble enzymes were susceptible to loss of activity upon freezing in vitro in a diluted aqueous solution, often resulting in complete or near-complete inactivity. However, we found that the addition of various CPs and other compounds at low concentrations effectively protected enzyme activity during freezing *in vitro*. These results show that soluble enzymes are more sensitive to freezing stress *in vitro* than in their native biological environment, which is characterized by a crowded milieu of microsolutes and macromolecules.

We explored the protective potential of different additives in preserving enzyme activity during freezing stress *in vitro*. Low concentrations of various CPs and macromolecules were found to be sufficient to shield enzymes from loss of activity during freezing. Notably, five components of the *C. costata* native cryoprotectant mixture displayed protective abilities, with glycerol and bovine serum albumin (BSA) demonstrating similar cryoprotective effects. Urea and potassium (K+) failed to protect enzyme activity at any concentration tested. Furthermore, we examined the interactions between proline and trehalose, two major CPs, and their protective effects under different conditions. Our experiments have illuminated a significant observation: the loss of enzyme activity can be effectively prevented by the addition of low concentrations of various CPs and other microsolutes, including the artificial compound HistoDenz, to the freezing medium. Even at concentrations as low as a few millimolars (mM), these compounds were found to be sufficient to entirely safeguard the enzymes from activity loss upon freezing. This finding closely corresponds to an earlier investigation conducted by Storey et al. (1991), which reported remarkably similar low P50 values (ranging from 7 to 25 mM) for various sugars, polyols, and amino acids in protecting G6PDH from freeze inactivation across different species, including a fly (*Eurosta solidaginis*), a moth (*Epiblema scudderiana*), and yeast.

Furthermore, in addition to these microsolutes, native biological solutions were observed to contain macromolecules – proteins at total concentrations ranging from 50 to 400 mg/mL (Chebotareva et. al. 2004). In our study, we have demonstrated that the inclusion of macromolecules, such as BSA or Ficoll, into the *in vitro* freezing medium at concentrations as low as 4–40 mg/mL sufficed to completely safeguard the insect enzymes from activity loss during freezing.

It is noteworthy that when compared to insect enzymes, purified mammalian enzymes necessitated higher concentrations of CP microsolutes, often in the range of hundreds of mM, to protect against activity loss during *in vitro* freezing (Tamiya et. al., 1985; Carpenter & Crowe, 1988). However, mammalian enzymes were also effectively shielded by extremely low concentrations, typically between 0.02–0.25 mg/mL, of macromolecular compounds such as polyethylene glycol or BSA, or by increasing the concentration of the enzyme itself through self-protection mechanisms. Notably, some vertebrate enzymes were observed to survive freeze-

thaw cycles when frozen within tissues, such as succinate dehydrogenase and cytochrome oxidase in rat heart (Hart et. al., 1972) or sarcoplasmic ATPase and aldolase in fish meat. These enzymes exhibited significant activity loss only upon prolonged frozen storage (Connel, 1966; Yamanaka & Mackie, 1971).

These findings underscore a critical distinction between typical enzymatic assays conducted under low enzyme concentrations within dilute *in vitro* solutions and assays conducted *in vivo* or under conditions simulating "molecular crowding", a characteristic feature of all living organisms (Chebotareva et. al., 2004). Consequently, microsolutes and macromolecules that are ubiquitous in the biological solutions of all organisms may serve as adequate stabilizers for various soluble enzymes during freezing stress. Microsolutes likely operate through the mechanism of "preferential exclusion," (Timasheff, 1992b, 1993, 2002), while macromolecules, whether natural (e.g., BSA) or synthetic (e.g., Ficoll), may stabilize enzymes in their compact native states through the mechanism of nonspecific steric repulsion, often referred to as the "excluded volume effect". This effect arises from the mutual impenetrability of solute molecules (Minton, 2000; Fiorini et. al., 2015).

In summary, our findings suggest that soluble enzymes in insects are sufficiently protected against activity loss when exposed to freezing conditions *in vivo*, within their native biochemical environment, characterized by a biological solution crowded with various microsolutes and macromolecules. However, it is essential to exercise caution when extrapolating the validity of this hypothesis from soluble enzymes to all proteins. Specifically, the stability under freezing stress of large polymeric protein complexes, nucleoprotein multimeric complexes such as ribosomes, or membrane-embedded protein complexes should be further investigated.

Additionally, we assessed the integrity of fat body cell plasma membranes in freeze-sensitive and freeze-tolerant *C. costata* larvae exposed to freezing stress. Our results indicated that freeze-tolerant larvae exhibited significantly better ability to maintain membrane integrity compared to freeze-sensitive larvae when subjected to freezing stress, both *in vivo* and *in vitro*. We also found that the freeze-tolerant hemolymph contained components that effectively preserved membrane integrity during freezing stress. Furthermore, we tested various additives for their ability to protect fat body cell plasma membranes *in vitro*. Proline, trehalose, and BSA displayed partial protection for freeze-sensitive phenotype cells. Freeze-tolerant phenotype cells, on the other hand, showed complete membrane integrity rescue when exposed to a mixture of proline, trehalose, and BSA.

The preservation of membrane integrity through the addition of CPs and proteins has been demonstrated as a crucial process for maintaining cell integrity during freezing stress. In accordance with the widely recognized theory of freezing injury mechanisms, our experimental findings validate that the plasma membranes of freeze-sensitive *C. costata* larval phenotypes lose their barrier function under *in vivo* lethal freezing stress. In contrast, the freeze-tolerant phenotype exhibits almost no loss of membrane integrity. It is worth noting that the plasma

membrane is considered a primary target of cold and freezing injury in plants (Steponkus, 1984) and mammalian cells (Mazur, 1984; Drobnis et. al. 1993).

Another noteworthy observation from this study pertains to the freeze-tolerant *C. costata* larval hemolymph, which appears to contain components essential for preserving plasma membrane integrity during freezing stress. We assessed the cryoprotective capabilities of the micromolecular constituents previously identified within the hemolymph of the freeze-tolerant phenotype, in conjunction with the macromolecular protein, bovine serum albumin (BSA). The combination of three additives in Schneider's medium - proline, trehalose, and BSA - proved sufficient to fully safeguard membrane integrity during *in vitro* freezing stress applied to fat body cells of freeze-tolerant larvae, reducing the incidence of freezing injury from 95% to 3% of cells. These same additives were also effective in partially mitigating freezing injury in freeze-sensitive phenotype cells, reducing it from 94% to 64-68%. These results suggest an interactive effect between cell phenotype and the composition of the freezing medium on membrane integrity. However, the precise mechanisms driving this interaction remain unclear, although acclimation-related changes in the lipid composition of the cell membrane may play a pivotal role (Koštál et. al., 2003).

Among the three additives (proline, trehalose, and BSA), BSA demonstrated the highest efficacy in preserving membrane integrity for both freeze-sensitive and freeze-tolerant phenotypes. We employed BSA to simulate the high concentrations of serum proteins accumulated by many insects prior to metamorphosis (Powell et. al. 1984; Telfer & Kunkel, 1991). Furthermore, late third-instar *C. costata* larvae, as used in this study, exhibit elevated concentrations of serum proteins and total proteins in the hemolymph, measuring 100 and 160 mg/mL for freeze-sensitive and freeze-tolerant phenotypes, respectively. BSA and other nonpermeable compounds like sucrose, Ficoll, polyethylene glycol, and hydroxyethyl starch are frequently added to cryopreservation solutions for mammalian sperm (Hidalgo et. al., 2018). These compounds are believed to indirectly aid in maintaining membrane integrity by influencing thermal transitions in the extracellular medium (including the kinetics of ice crystal growth and morphology and glass transition temperatures) (Oldenhof et. al., 2013; Hornberger et. al., 2021) or by reducing membrane lipid peroxidation caused by reactive oxygen species (Cabrita et. al., 2001). Nevertheless, the precise mechanism underlying BSA's high effectiveness in preserving *C. costata*'s membrane integrity remains unknown. Other nonpermeable compounds, such as sucrose and Ficoll, exhibited little to no cryoprotective effects on *C. costata* fat body cell membranes. Further research is warranted to elucidate how the plasma membrane's permeability to various additives influences their efficacy as cryoprotectants.

Our functional assays provide additional support for earlier studies where insect fat body cells were subjected to freezing stress *in vitro*, followed by the assessment of plasma membrane integrity using vital dyes. For instance, fat body cells of *Eurosta solidaginis* larvae, when frozen to -25 °C in Grace's insect medium, displayed an increase in intact plasma membrane proportions from less than 20% to 80% when the medium was augmented with 1 M

glycerol (Lee et. al., 1993). Similarly, fat body cells of the cricket *Gryllus veletis*, frozen to -12 °C (in warm-acclimated crickets) or -16 °C (in cold-acclimated crickets) in Grace's medium, with or without different CPs, exhibited enhanced survival rates with intact plasma membranes when myo-inositol, trehalose, and glycerol were added to the medium (Toxopeus et al., 2019b). This study also suggested that individual CPs have differential impacts on survival in the frozen state, are not interchangeable, and likely function non-colligatively in insect freeze tolerance. In our present investigation, no single CP or combination of CPs was sufficient to confer high freeze tolerance to warm-acclimated cricket cells. However, in cold-acclimated crickets, the proportion of cells with intact membranes after freezing stress increased to approximately 75% when a combination of myo-inositol plus trehalose or glycerol alone was added (Toxopeus et al., 2019b).

In conclusion, our study shows that membrane integrity plays a crucial role in cell survival during freezing, with proline, trehalose and BSA showing promising cryoprotective effects. Further research is needed to explore the complex interactions between CPs and membrane protection and to understand the downstream effects of membrane integrity loss on cell viability.

4. Conclusions and prospects

- **Diversity and biosynthesis of cryoprotectants (CPs)**

Metabolomics revealed the intricate composition of the naturally accumulated larval cryoprotectant mixture, mainly comprising proline and trehalose, complemented by additional minor components such as glutamine, asparagine, betaine, sarcosine, glycerophospho-choline, and ethanolamine. Our findings emphasize the critical role of food ingestion for direct amino compound assimilation, while glycogen and phospholipids serve as the primary internal sources for cryoprotectant biosynthesis.

Potential avenues for future research include:

- Extending metabolomic analyses to describe the complex cryoprotectant mixtures in various insect species, shedding light on species-specific adaptations.
- Further investigations into the relative importance of dietary intake versus internal sources for cryoprotectant biosynthesis, expanding our understanding of these mechanisms.
- Exploring the roles of diapause and cold acclimation in shaping the composition of cryoprotectants in insects, contributing to a more comprehensive comprehension of seasonal adaptations.

- **Physico-chemical behavior of CPs in vivo during slow inoculative freezing**

The application of MALDI-MSI offered insights into the behavior of cryoprotectants during ecologically relevant gradual extracellular freezing of larvae. Trehalose accumulated in partially dehydrated hemolymph, prompting a transition to the amorphous glass phase, while proline moved to the boundary between extracellular ice and dehydrated hemolymph and tissues, forming a layer of dense viscoelastic liquid.

Potential avenues for future research include:

- Delving into the physical chemistry of these complex cryoprotectant mixtures, aiming to uncover the thermodynamic properties and molecular interactions that govern their unique characteristics.
- Elucidating the thermal behavior of these intricate mixtures, providing insights into their responses to temperature changes, phase transitions, and other relevant thermal phenomena.
- Investigating the potential involvement of Natural Deep Eutectic Solvents (NADES) in cryoprotectant mixtures could provide a deeper understanding of their role in insect cold tolerance and adaptation.

- **Protective roles of CPs during extracellular freezing and cell freeze dehydration**

A combination of in vivo and in vitro assays suggests that cell membranes are susceptible to freezing injury, with their integrity supported by the presence of small cryoprotective molecules and proteins in cold-acclimated *C. costata* larvae. Surprisingly, our assays did not support the hypothesis that proteins, specifically soluble enzymes, require *in vivo* stabilization through cryoprotectant accumulation.

Potential avenues for future research include:

- Exploring the stability of complex assemblages involving proteins, membranes, or proteins with DNA or RNA. These investigations aim to shed light on the interactions and behaviors of other, more complex biological components under freezing conditions.

5. References

Anchordoguy, T. J., Rudolph, A. S., Carpenter, J. F., & Crowe, J. H. (1987). Modes of interaction of cryoprotectants with membrane phospholipids during freezing. Cryobiology 24(4), 324-331.

Applebaum, S. W. (1985). Biochemistry of digestion. In Comprehensive insect physiology, biochemistry and pharmacology, vol. 4, pp. 279-311.

Arakawa, T., & Timasheff, S. (1985). The stabilization of proteins by osmolytes. Biophysical journal 47(3), 411-414.

Asahina, E. (1970). Frost resistance in insects. In Advances in Insect Physiology vol. 6, pp. 1-49: Elsevier.

Bale, J.S., Hansen, T.N., Nishino, M., & Baust, J.G. (1989). Effect of cooling rate on the survival of larvae, pupariation and adult emergence of the gallfly *Eurosta solidaginis*. Cryobiology 21, 285–289.

Ball, P. (2008). Water as an active constituent in cell biology. Chemical reviews 108(1), 74-108.

Band, H. T., & Band, R. N. (1982). Multiple overwintering mechanisms in *Chymomyza amoena* larvae (Diptera: Drosophilidae) and laboratory induction of freeze tolerance. Experientia 38, 1448-1449.

Basden, E. B. (1954). Diapause in *Drosophila* (Diptera: Drosophilidae). In: Proceedings of the Royal Entomological Society of London. Series A, General Entomology (Vol. 29, No. 7-9, pp. 114-118). Oxford, UK: Blackwell Publishing Ltd.

Beis, I., & Newsholme, E. A. (1975). The contents of adenine nucleotides, phosphagens and some glycolytic intermediates in resting muscles from vertebrates and invertebrates. Biochemical Journal 152, 23-32.

Benoit, J. B. (2010). Water management by dormant insects: comparisons between dehydration resistance during summer aestivation and winter diapause. Aestivation 209-229.

Bolen, D. W., & Baskakov, I. V. (2001). The osmophobic effect: natural selection of a thermodynamic force in protein folding. Journal of molecular biology 310(5), 955-963.

Brovchenko, I., & Oleinikova, A. (2008). Which properties of a spanning network of hydration water enable biological functions? ChemPhysChem 9(18), 2695-2702.

Bryant, G., Koster, K. L., & Wolfe, J. (2001). Membrane behaviour in seeds and other systems at low water content: the various effects of solutes. Seed Science Research, 11(1), 17-25.

Cabrita, E., Anel, L., & Herraéz, M. P. (2001). Effect of external cryoprotectants as membrane stabilizers on cryopreserved rainbow trout sperm. Theriogenology 56, 623–635.

Capicciotti, C. J., Doshi, M., & Ben, R. N. (2013). Ice recrystallization inhibitors: from biological antifreezes to small molecules. Recent developments in the study of recrystallization 177, 224.

Carpenter, J. F., & Crowe, J. H. (1988). The mechanism of cryoprotection of proteins by solutes. Cryobiology 25(3), 244-255.

Cesaro, A., De Giacomo, O., & Sussich, F. (2008). Water interplay in trehalose polymorphism. Food Chemistry 106, 1318-1328.

Champe, P., & Harvey, R. (1994). Lippincott's illustrated reviews: biochemistry 2nd ed: Philadelphia: JB Lippincott.

Chebotareva, N. A., Kurganov, B. I., & Livanova, N. B. (2004). Biochemical effects of molecular crowding. Biochemistry (Moscow) 69, 1239–1251.

Chen, T., Fowler, A., & Toner, M. (2000). Literature review: supplemented phase diagram of the trehalose-water binary mixture. Cryobiology 40, 277-282.

Choi, Y. H., van Spronsen, J., Dai, Y., Verberne, M., Hollmann, F., Arends, I. W., Witkamp, G.-J., & Verpoorte, R. (2011). Are natural deep eutectic solvents the missing link in understanding cellular metabolism and physiology? Plant Physiology 156, 1701-1705.

Colinet, H., Lee, S. F., & Hoffmann, A. (2010a). Temporal expression of heat shock genes during cold stress and recovery from chill coma in adult *Drosophila melanogaster*. The FEBS journal 277(1), 174-185.

Colinet, H., Lee, S. F., & Hoffmann, A. (2010b). Knocking down expression of Hsp22 and Hsp23 by RNA interference affects recovery from chill coma in *Drosophila melanogaster*. Journal of Experimental Biology 213(24), 4146-4150.

Colinet, H., Overgaard, J., Com, E., &Sørensen, J. G. (2013). Proteomic profiling of thermal acclimation in *Drosophila melanogaster*. Insect Biochemistry and Molecular Biology 43, 352-365.

Colinet, H., Renault, D., Javal, M., Berková, P., Šimek, P., & Koštál, V. (2016). Uncovering the benefits of fluctuating thermal regimes on cold tolerance of *Drosophila* flies by combined metabolomic and lipidomic approach. Biochimica et Biophysica Acta 1861, 1736-1745.

Cossins, A. R. (1994). Temperature adaptation of biological membranes: Portland Press.

Coulson, S., & Bale, J. (1992). The effect of rapid cold hardening on reproduction and survival of offspring in the housefly *Musca domestica*. J. Journal of Insect Physiology 38, 421–424.

Crowe, J. H. (2007). Trehalose as a "chemical chaperone". Molecular aspects of the stress response: chaperones, membranes, and networks 143-158.

Crowe, J. H., Crowe, L. M., Oliver, A. E., Tsvetkova, N., Wolkers, W., & Tablin, F. (2001). The trehalose myth revisited: introduction to a symposium on stabilization of cells in the dry state. Cryobiology 43(2), 89-105.

Crowe, L. M., Mouradian, R., Crowe, J. H., Jackson, S. A., & Womersley, C. (1984). Effects of carbohydrates on membrane stability at low water activities. Biochimica et Biophysica Acta (BBA)-Biomembranes 769(1), 141-150.

Dai, Y., van Spronsen, J., Witkamp, G.-J., Verpoorte, R., & Choi, Y. H. (2013). Ionic liquids and deep eutectic solvents in natural products research: mixtures of solids as extraction solvents. Journal of Natural Products 76, 2162-2173.

Dai, Y., Witkamp, G.-J., Verpoorte, R., & Choi, Y. H. (2015). Tailoring properties of natural deep eutectic solvents with water to facilitate their applications. Food Chemistry 187, 14-19.

Danks, H. V. (1987). Insect dormancy: an ecological perspective. Biological Survey of Canada (Terrestrial Arthropods).

Das, U., Hariprasad, G., Ethayathulla, A. S., Manral, P., Das, T. K., Pasha, S., Mann, A., Ganguli, M., Verma, A. K., Bhat, R., Chandrayan, S. K., Ahmed, S., Sharma, S., Kaur, P., Singh, T. P., Srinivasan, A., & Srinivasan, A. (2007). Inhibition of protein aggregation: supramolecular assemblies of arginine hold the key. PloS one 2(11), e1176.

Denlinger, D. L. (1991). Relationship between cold hardiness and diapause. In Insects at low temperature (pp. 174-198). Springer, Boston, MA.

Denlinger, D. L. (2002). Regulation of diapause. Annual Review of Entomology 47(1), 93-122.

Des Marteaux, L. E., Štětina, T., & Koštál, V. (2018). Insect fat body cell morphology and response to cold stress is modulated by acclimation. Journal of Experimental Biology 221(21), jeb189647.

Dias, C. L., Ala-Nissila, T., Wong-Ekkabut, J., Vattulainen, I., Grant, M. & Karttunen, M. (2010). The hydrophobic effect and its role in cold denaturation. Cryobiology 60, 91–99.

Drobnis, E. Z., Crowe, L. M., Berger, T., Anchordoguy, T. J., Overstreet, J. W., & Crowe, J. H. (1993). Cold shock damage is due to lipid phase transitions in cell membranes: A demonstration using sperm as a model. J. Exp. Zool. 265, 432–437.

Duman, J. G. (2001). Antifreeze and ice nucleator proteins in terrestrial arthropods. Annual Review of Physiology 63, 327.

Duman, J. G. (2015). Animal ice-binding (antifreeze) proteins and glycolipids: an overview with emphasis on physiological function. The Journal of experimental biology, 218(12) 1846-1855.

Duman, J. G., Walters, K. R., Sformo, T., Carrasco, M. A., Nickell, P. K., Lin, X., & Barnes, B. M. (2010). Antifreeze and ice-nucleator proteins. Low temperature biology of insects 59-90.

Emerson, K. J., Bradshaw, W. E., & Holzapfel, C. M. (2010). Microarrays reveal early transcriptional events during the termination of larval diapause in natural populations of the mosquito, *Wyeomyia smithii*. PLoS One 5(3), e9574.

Enomoto, O. (1982). Larval diapause in *Chymomyza costata* (Diptera: Drosophilidae) I. Effects of temperature and photoperiod on the development. Low temperature science. Proceedings of the Royal Society B: Biological Sciences 39, 21-29.

Etienne, R., Fortunat, K., & Pierce, V. (2001). Mechanisms of urea tolerance in urea-adapted populations of *Drosophila melanogaster*. Journal of Experimental Biology 204, 2699-2707.

Fahy, G. M., & Wowk, B. (2015). Principles of cryopreservation by vitrification. Cryopreservation and freeze-drying protocols 21-82.

Fiorini, E., Börner, R., & Sigel, R. K. (2015). Mimicking the in vivo environment—The effect of crowding on RNA and biomacromolecular folding and activity. Chimia (Aarau) 69, 207–212.

Franks, F., & Hatley, R. H. (1991). Stability of proteins at subzero temperatures: thermodynamics and some ecological consequences. Pure and applied chemistry 63(10), 1367-1380.

Franks, F., & Hatley, R. H. M. (1991). Stability of proteins at subzero temperatures: thermodynamics and some ecological consequences. Pure and Applied Chemistry 63, 1367–1380.

Fraser, L., Strzeżek, J., & Kordan, W. (2011). Effect of freezing on sperm nuclear DNA. Reproduction in Domestic Animals 46, 14–17.

Gehrken, U. (1984). Winter survival of an adult bark beetle *Ips acuminatus* Gyll. Journal of insect physiology 30(5), 421-429.

Gertrudes, A., Craveiro, R., Eltayari, Z., Reis, R. L., Paiva, A., & Duarte, A. R. C. (2017). How do animals survive extreme temperature amplitudes? the role of natural deep eutectic solvents. ACS Sustainable Chemistry & Engineering 5, 9542-9553.

Gilbert, N., & Raworth, D. A. (1996). Insects and temperature – a general theory. The Canadian Entomologist 128, 1–13.

Goto, S. G., & Kimura, M. T. (1998). Heat-and cold-shock responses and temperature adaptations in subtropical and temperate species of *Drosophila*. Journal of Insect Physiology 44, 1233-1239.

Green, J. L., & Angell, C. A. (1989). Phase relations and vitrification in saccharide-water solutions and the trehalose anomaly. The Journal of Physical Chemistry A 93, 2880-2882.

Grimaldi, D. (1986). The *Chymomyza aldrichii* species-group (Diptera: Drosophilidae); relationships, new neotropical species, and the evolution of some sexual traits. Journal of the New York Entomological Society 94, 342-371.

Hackman, W., Lakovaara, S., Saura, A., Sorsa, M., & Vepsalainen, K. (1970). On the biology and karyology of *Chymomyza costata* Zetterstedt, with reference to the taxonomy and distribution of various species of *Chymomyza* (Dipt., Drosophilidae). In Annales Entomologici Fennici (Vol. 36, pp. 1-9).

Hahn, D. A., & Denlinger, D. L. (2007). Meeting the energetic demands of insect diapause: nutrient storage and utilization. Journal of insect physiology 53(8), 760-773.

Hart, R., Ramazzotto, L. J., & Engstrom, R. (1972). Cryoprotection of some rat heart enzymes. Cryobiology 9, 461–464.

Hazel, J. R. (1995). Thermal adaptation in biological membranes: Is homeoviscous adaptation the explanation? Annual Review of Physiology 57, 19–42.

Hemolymph metabolites and osmolality are tightly linked to cold tolerance of *Drosophila* species: a comparative study. The Journal of Experimental Biology 219, 2504-2513.

Hidalgo, M., Consuegra, C., Dorado, J., Diaz-Jimenez, M., Ortiz, I., Pereira, B., Sanchez, R., & Crespo, F. (2018) Concentrations of non-permeable cryoprotectants and equilibration temperatures are key factors for stallion sperm vitrification success. Animal Reproduction Science 196, 91-98.

Hincha, D. K., Oliver, A. E., & Crowe, J. H. (1998). The effects of chloroplast lipids on the stability of liposomes during freezing and drying. Biochimica et Biophysica Acta (BBA)-Biomembranes 1368, 150-160.

Hochachka, P. (1986). Defense strategies against hypoxia and hypothermia. Science 231, 234-241.

Hochachka, P., & Somero, G. (2002). Biochemical Adaptation. Mechanism and Process in Physiological Evolution: Oxford University Press.

Hoekstra, F. A., Golovina, E. A., & Buitink, J. (2001). Mechanisms of plant desiccation tolerance. Trends in plant science 6(9), 431-438.

Holmstrup, M., Bayley, M., & Ramløv, H. (2002). Supercool or dehydrate? An experimental analysis of overwintering strategies in small permeable arctic invertebrates. Proceedings of the National Academy of Sciences 99, 5716-5720.

Hornberger, K., Li, R., Duarte, A. R. C., & Hubel, A. (2020). Natural deep eutectic systems for nature-inspired cryopreservation of cells. AIChE Journal, 67(2), e17085.

Horwath, K. L., & Duman, J. G. (1984). Yearly variations in the overwintering mechanisms of the cold-hardy beetle *Dendroides canadensis*. Physiological Zoology 40-45.

Huang, L. H., Lin, P. H., Tsai, K. W., Wang, L. J., Huang, Y. H., Kuo, H. C., & Li, S. C. (2017). The effects of storage temperature and duration of blood samples on DNA and RNA qualities. PLoS ONE 12, e0184692, 13 pp.

Hutchinson, L., & Bale, J. (1994). Effects of sublethal cold stress on the aphid *Rhopalosiphum padi*. Journal of Applied Ecology 31, 102–108.

Inoue, H., & Timasheff, S. N. (1972). Preferential and absolute interactions of solvent components with proteins in mixed solvent systems. Biopolymers: Original Research on Biomolecules 11(4), 737-743.

Jensen, M. Ø., Mouritsen, O. G., & Peters, G. H. (2004). The hydrophobic effect: Molecular dynamics simulations of water confined between extended hydrophobic and hydrophilic surfaces. The Journal of chemical physics 120(20), 9729-9744.

Joanisse, D., & Storey, K. (1996). Oxidative stress and antioxidants in overwintering larvae of cold-hardy goldenrod gall insects. The Journal of experimental biology 199(7), 1483-1491.

Jovanović-Galović, A., Blagojević, D. P., Grubor-Lajšić, G., Worland, M. R., & Spasić, M. B. (2007). Antioxidant defense in mitochondria during diapause and postdiapause development of European corn borer (*Ostrinia nubilalis*, Hubn.). Archives of Insect Biochemistry and Physiology: Published in Collaboration with the Entomological Society of America 64(3), 111-119.

Kankare, M., Salminen, T., Laiho, A., Vesala, L., & Hoikkala, A. (2010). Changes in gene expression linked with adult reproductive diapause in a northern malt fly species: a candidate gene microarray study. BMC ecology 10(1), 1-9.

Kaul, S., Sharma, S., & Mehta, I. (2008). Free radical scavenging potential of L-proline: evidence from in vitro assays. Amino Acids 34 315-320.

Kaushik, J. K., & Bhat, R. (2003). Why Is trehalose an exceptional protein stabilizer? An analysis of the thermal stability of proteins in the presence of the compatible osmolyte trehalose. Journal of Biological Chemistry 278(29), 26458-26465.

Kelty, J.D., Killian, K.A., & Lee, R.E. (1996). Cold shock and rapid cold-hardening of pharate adult flesh flies (*Sarcophaga crassipalpis*): effects on behaviour and neuromuscular function following eclosion. Physiological Entomology 21, 283–288.

King, A. M., & MacRae, T. H. (2015). Insect heat shock proteins during stress and diapause. Annual Review of Entomology 60, 59-75.

Kobelková, A., Bajgar, A., & Dolezel, D. (2010). Functional molecular analysis of a circadian clock gene timeless promoter from the Drosophilid fly *Chymomyza costata*. Journal of biological rhythms 25(6), 399-409.

Koštál V., Grgac R., & Korbelová J. (2019). Delayed mortality and sublethal effects of cold stress in *Drosophila melanogaster*. Journal of Insect Physiology 113: 24–32.

Koštál, V. (2010). Cell structural modifications in insects at low temperature. Low temperature biology of insects 116-140.

Koštál, V., & Shimada, K. (2001). Malfunction of circadian clock in the non-photoperiodic-diapause mutants of the drosophilid fly, *Chymomyza costata*. Journal of Insect Physiology 47(11), 1269-1274.

Koštál, V., & Tollarová-Borovanská, M. (2009). The 70 kDa heat shock protein assists during the repair of chilling injury in the insect, *Pyrrhocoris apterus*. PloS one 4, e4546.

Koštál, V., Berková, P., & Simek, P. (2003). Remodelling of membrane phospholipids during transition to diapause and cold-acclimation in the larvae of *Chymomyza costata* (Drosophilidae). Comparative Biochemistry and Physiology Part B 135(3):407-19.

Koštál, V., Korbelová, J., Poupardin, R., Moos, M., & Šimek, P. (2016a). Arginine and proline applied as food additives stimulate high freeze tolerance in larvae of *Drosophila melanogaster*. Journal of Experimental Biology 219, 2358-2367.

Koštál, V., Korbelová, J., Rozsypal, J., Zahradníčková, H., Cimlová, J., Tomčala, A., & Šimek, P. (2011b). Long-term cold acclimation extends survival time at 0°C and

modifies the metabolomic profiles of the larvae of the fruit fly *Drosophila melanogaster*. PLoS One 6(9), e25025.

Koštál, V., Mollaei, M., & Schöttner, K. (2016b). Diapause induction as an interplay between seasonal token stimuli and modifying and directly limiting factors: hibernation in *Chymomyza costata*. Physiological Entomology 41(4), 344-357.

Koštál, V., Noguchi, H., Shimada, K., & Hayakawa, Y. (2000). Circadian component influences the photoperiodic induction of diapause in a drosophilid fly, *Chymomyza costata*. Journal of Insect Physiology 46(6), 887-896.

Koštál, V., Šimek, P., Zahradníčková, H., Cimlová, J., & Štětina, T. (2012). Conversion of the chill susceptible fruit fly larva (*Drosophila melanogaster*) to a freeze tolerant organism. Proceedings of the National Academy of Sciences 109(9), 3270-3274.

Koštál, V., Šimůnková, P., Kobelková, A., & Shimada, K. (2009). Cell cycle arrest as a hallmark of insect diapause: changes in gene transcription during diapause induction in the drosophilid fly, *Chymomyza costata*. Insect Biochemistry and Molecular Biology 39, 875-883.

Koštál, V., Štětina, T., Poupardin, R., Korbelová, J., & Bruce, A. W. (2017). Conceptual framework of the eco-physiological phases of insect diapause development justified by transcriptomic profiling. Proceedings of the National Academy of Sciences 114(32), 8532-8537.

Koštál, V., Tollarova, M., & Šula, J. (2004a). Adjustments of the enzymatic complement for polyol biosynthesis and accumulation in diapausing cold acclimated adults of *Pyrrhocoris apterus*. Journal of Insect Physiology 50, 303-313.

Koštál, V., Urban, T., Řimnáčová, L., Berková, P., & Šimek, P. (2013). Seasonal changes in minor membrane phospholipid classes, sterols and tocopherols in overwintering insect, *Pyrrhocoris apterus*. Journal of Insect Physiology 59, 934-941.

Koštál, V., Vambera, J., & Bastl, J. (2004b). On the nature of pre-freeze mortality in insects: water balance, ion homeostasis and energy charge in the adults of *Pyrrhocoris apterus*. Journal of Experimental Biology 207, 1509-1521.

Koštál, V., Yanagimoto, M., & Bastl, J. (2006). Chilling-injury and disturbance of ion homeostasis in the coxal muscle of the tropical cockroach (*Nauphoeta cinerea*). Comparative Biochemistry and Physiology Part B: Biochemistry and Molecular Biology 143(2), 171-179.

Koštál, V., Zahradníčková, H., & Šimek, P. (2011a). Hyperprolinemic larvae of the drosophilid fly, *Chymomyza costata*, survive cryopreservation in liquid nitrogen. Proceedings of the National Academy of Sciences, 108(32), 13041-13046.

Kunugi S. & Tanaka N. (2002). Cold denaturation of proteins under high pressure. - Biochimica et Biophysica Acta 1595: 329-344.

Lakovaara, S., Saura, A., Koref-Santibanez, S. U. S. I., & Ehrman, L. E. E. (1972). Aspects of diapause and its genetics in northern drosophilids. Hereditas 70(1), 89-96.

Lalouette, L., Williams, C., Hervant, F., Sinclair, B. J., & Renault, D. (2011). Metabolic rate and oxidative stress in insects exposed to low temperature thermal fluctuations. Comparative Biochemistry and Physiology A 158, 229-234.

Lange, C., & Rudolph, R. (2009). Suppression of protein aggregation by L-arginine. Current pharmaceutical biotechnology 10(4), 408-414.

Lankinen, P., & Riihimaa, A. (1997). Effects of temperature on weak circadian eclosion rhythmicity in *Chymomyza costata* (Diptera: Drosophilidae). Journal of insect physiology 43(3), 251-260.

Lee, R. E. J. (2010). A primer on insect cold-tolerance. In Denlinger D. L. & Lee R. E. J. (Eds.), Low temperature biology of insects: Cambridge University Press.

Lee, R. E., & Denlinger, D. L. (1991). Insects at low temperature: Chapman and Hall.

Lee, R. E., Costanzo, J. P., & Mugnano, J. A. (1996). Regulation of supercooling and ice nucleation in insects. European Journal of Entomology 93, 405–418.

Lee, R. E., McGrath, J. J., Morason, R. T., & Taddeo, R. M. (1993) Survival of intracellular freezing, lipid coalescence and osmotic fragility in fat body cells of the freeze-tolerant gall fly *Eurosta solidaginis*. Journal of Insect Physiology 39, 445–450.

Lees, A. D. (1955). The physiology of diapause in arthropods. Cambridge Monographs Experimental Biology 4, 1-151.

Linfor, J. J., & Meyers, S. A. (2002). Detection of DNA damage in response to cooling injury in equine spermatozoa using single-cell gel electrophoresis. Journal of Andrology 23, 107–113.

Lippert, K., & Galinski, E. A. (1992). Enzyme stabilization be ectoine-type compatible solutes: Protection against heating, freezing and drying. Applied Microbiology and Biotechnology 37, 61–65.

Lovelock, J. E. (1954). The protective action of neutral solutes against haemolysis by freezing and thawing. Biochemical Journal 56(2), 265.

Lubawy, J., Daburon, V., Chowański, S., Słocińska, M., & Colinet, H. (2019). Thermal stress causes DNA damage and mortality in a tropical insect. Journal of Experimental Biology 222(23), jeb213744.

Lumme, J. (1978). Phenology and Photoperiodic Diapause in Northern Populations of *Drosophila*. In: Dingle, H. (eds) Evolution of Insect Migration and Diapause. Proceedings in Life Sciences. Springer, New York, NY.

MacMillan, H. A. (2019). Dissecting cause from consequence: a systematic approach to thermal limits. Journal of Experimental Biology 222, jeb191593.

MacMillan, H. A., Schou, M. F., Kristensen, T. N., & Overgaard, J. (2016). Preservation of potassium balance is strongly associated with insect cold tolerance in the field: a seasonal study of *Drosophila subobscura*. Biology Letters 12, 20160123.

Macmillan, H.A. (2019). Dissecting cause from consequence: a systematic approach to thermal limits. Journal of Experimental Biology 222, jeb191593, 8 pp.

MacRae, T. H. (2010). Gene expression, metabolic regulation and stress tolerance during diapause. Cellular and Molecular Life Sciences 67(14), 2405-2424.

Marshall, K. E., & Sinclair, B. J. (2010). Repeated stress exposure results in a survival-reproduction trade-off in *Drosophila melanogaster*. Proceedings of the Royal Society B 277, 963–969.

Marshall, K. E., & Sinclair, B. J. (2015). The relative importance of number, duration and intensity of cold stress events in determining survival and energetics of an overwintering insect. Functional Ecology 29, 357–366.

Masters, A. R., Malcolm, S. B., & Brower, L. P. (1988). Monarch butterfly (*Danaus plexippus*) thermoregulatory behavior and adaptations for overwintering in Mexico. Ecology 69, 458-467.

Mazur, P. (1984). Freezing of living cells: mechanisms and implications. American journal of physiology-cell physiology 247(3), C125-C142.

McElhaney, R. N. (1984). The relationship between membrane lipid fluidity and phase state and the ability of bacteria and mycoplasmas to grow and survive at various temperatures. In Membrane fluidity, pp. 249-278: Springer.

Meryman, H. T. (1971). Osmotic stress as a mechanism of freezing injury. Cryobiology 8(5), 489-500.

Minton, A. P. (2000). Implications of macromolecular crowding for protein assembly. Current Opinion in Structural Biology 10, 34–39.

Moon, I., Fujikawa, S., & Shimada, K. (1996). Cryopreservation of *Chymomyza* larvae (Diptera: Drosophilidae) at-196 degrees C with extracellular freezing. Cryo-letters.

Muldrew, K., Acker, J. P., Elliott, J. A., & McGann, L. E. (2004). The water to ice transition: implications for living cells. In Life in the frozen state (pp. 93-134). CRC Press.

Mullins, D. (1985). Chemistry and physiology of hemolymph. In Comprehensive insect physiology, biochemistry and pharmacology, vol. 3, pp. 355-400.

Núñez-Farfán, J., Fornoni, J., & Valverde, P.L. (2007). The evolution of resistance and tolerance to herbivores. Annual Review of Ecology, Evolution, and Systematics 38, 541–566.

Oldenhof, H., Gojowsky, M., Wang, S., Henke, S., Yu, C., Rohn, K., Wolkers, W. F., & Sieme, H. (2013). Osmotic stress and membrane phase changes during freezing of stallion sperm: mode of action of cryoprotective agents. Biology of Reproduction 88(3), 68.

Olsson, T., MacMillan, H. A., Nyberg, N., Staerk, D., Malmendal, A., & Overgaard, J. (2016). Hemolymph metabolites and osmolality are tightly linked to cold tolerance of *Drosophila* species: a comparative study. Journal of Experimental Biology 219 (16): 2504–2513.

Overgaard, J., & Macmillan, H. A. (2017). The integrative physiology of insect chill tolerance. Annual Review of Physiology 79, 187– 208.

Overgaard, J., Sørensen, J. G., Com, E., & Colinet, H. (2014). The rapid cold hardening response of *Drosophila melanogaster*: Complex regulation across different levels of biological organization. Journal of Insect Physiology 62(1): 46-53.

Pavelka, J., Shimada, K., & Koštál, V. (2003). TIMELESS: a link between fly's circadian and photoperiodic clocks? European Journal of Entomology, 100(2), 255-266.

Pittendrigh, C. S. (1960). Circadian rhythms and the circadian organization of living systems. In Cold Spring Harbor symposia on quantitative biology (Vol. 25, pp. 159-184). Cold Spring Harbor Laboratory Press.

Poelchau, M. F., Reynolds, J. A., Elsik, C. G., Denlinger, D. L., & Armbruster, P. A. (2013). Deep sequencing reveals complex mechanisms of diapause preparation in the invasive mosquito, *Aedes albopictus*. Proceedings of the Royal Society B: Biological Sciences 280(1759), 20130143.

Pörtner, H. O. (2002). Climate variations and the physiological basis of temperature dependent biogeography: systemic to molecular hierarchy of thermal tolerance in animals. Comparative Biochemistry and Physiology Part A: Molecular & Integrative Physiology 132(4), 739-761.

Poupardin, R., Schöttner, K., Korbelová, J., Provazník, J., Doležel, D., Pavlinic, D., Beneš, V., & Koštál, V. (2015). Early transcriptional events linked to induction of diapause revealed by RNAseq in larvae of drosophilid fly, *Chymomyza costata*. BMC genomics 16(1), 1-19.

Powell, D., Sato, J. D., Brock, H. W., & Roberts, D. B. (1984). Regulation of synthesis of the larval serum proteins of *Drosophila melanogaster*. Developmental Biology 102, 206–215.

Privalov, P. L. (1990). Cold denaturation of protein. Critical reviews in biochemistry and molecular biology, 25(4), 281-306.

Pullin, A. S., & Bale, J. S. (1988). Cause and effects of pre-freeze mortality in aphids. CryoLetters 9, 101–113.

Qin, W., Neal, S., Robertson, R., Westwood, J., & Walker, V. (2005). Cold hardening and transcriptional change in *Drosophila melanogaster*. Insect Molecular Biology 14, 607-613.

Quinn, P. J. (1985). A lipid-phase separation model of low-temperature damage to biological membranes. Criobiology 22,128–146.

Quinn, P. J. (1988). Effects of temperature on cell membranes. Symposia of the Society for Experimental Biology 42, 237–258.

Råberg, L., Sim, D., & Read, A. F. (2007). Disentangling genetic variation for resistance and tolerance to infectious diseases in animals. Science 318, 812–814.

Ragland, G. J., Denlinger, D. L., & Hahn, D. A. (2010). Mechanisms of suspended animation are revealed by transcript profiling of diapause in the flesh fly. Proceedings of the National Academy of Sciences 107(33), 14909-14914.

Reyes-DelaTorre, A., Peña-Rangel, M. T., & Riesgo-Escovar, J. R. (2012). Carbohydrate metabolism in *Drosophila*: reliance on the disaccharide trehalose. Carbohydrates-comprehensive studies on glycobiology and glycotechnology. Winchester: InTech 317-38.

Richter, K., Haslbeck, M. and Buchner, J. (2010). The heat shock response: life on the verge of death. Molecular Cell 40(2), 253-266.

Riihimaa, A. J., & Kimura, M. T. (1988). A mutant strain of *Chymomyza costata* (Diptera: Drosophilidae) insensitive to diapause-inducing action of photoperiod. Physiological Entomology 13(4), 441-445.

Riihimaa, A. J., & Kimura, M. T. (1989). Genetics of the photoperiodic larval diapause in *Chymomyza costata* (Diptera; Drosophilidae). Hereditas 110(3), 193-200.

Rinehart, J. P., Cikra-Ireland, R. A., Flannagan, R. D., & Denlinger, D. L. (2001). Expression of ecdysone receptor is unaffected by pupal diapause in the flesh fly, *Sarcophaga crassipalpis*, while its dimerization partner, USP, is downregulated. Journal of Insect Physiology 47(8), 915-921.

Rinehart, J. P., Hayward, S. A., Elnitsky, M. A., Sandro, L. H., Lee, R. E. and Denlinger, D. L. (2006). Continuous up-regulation of heat shock proteins in larvae, but not adults, of a polar insect. Proceedings of the National Academy of Sciences 103, 14223-14227.

Rinehart, J. P., Li, A., Yocum, G. D., Robich, R. M., Hayward, S. A., & Denlinger, D. L. (2007). Up-regulation of heat shock proteins is essential for cold survival during insect diapause. Proceedings of the National Academy of Sciences 104(27), 11130-11137.

Rojas, R. R. and Leopold, R. A. (1996). Chilling injury in the housefly: evidence for the role of oxidative stress between pupariation and emergence. Cryobiology 33, 447-458.

Rozsypal, J. (2022). Cold and freezing injury in insects: An overview of molecular mechanisms. European Journal of Entomology 119, Article 43-57.

Rozsypal, J., & Košťál, V. (2018). Supercooling and freezing as eco-physiological alternatives rather than mutually exclusive strategies: A case study in *Pyrrhocoris apterus*. Journal of insect physiology 111, 53-62.

Rozsypal, J., Moos, M., Šimek, P., & Košťál, V. (2018). Thermal analysis of ice and glass transitions in insects that do and do not survive freezing. Journal of Experimental Biology 221(7), jeb170464.

Rubinsky, B., Cravalho, E. G., & Mikic, B. (1980). Thermal stresses in frozen organs. Cryobiology 17, 66-73.

Rudolph, A. S., & Crowe, J. H. (1986). A calorimetric and infrared spectroscopic study of the stabilizing solute proline. Biophysical journal 50(3), 423-430.

Russotti, G., Campbell, J., Toner, M., & Yarmush, M. L. (1997). Studies of heat and PGA1-induced cold tolerance show that HSP27 may help preserve actin morphology during hypothermia. Tissue Engineering 3(2), 135-147.

Salt, R. (1961). Principles of insect cold-hardiness. Annual Review of Entomology 6, 55-74.

Samuel, D., Kumar, T. K. S., Jayaraman, G., Yang, P. W., & Yu, C. (1997). Proline is a protein solubilizing solute. IUBMB Life 41(2), 235-242.

Sanfelice, D., & Temussi, P. A. (2016). Cold denaturation as a tool to measure protein stability. Biophysical chemistry 208, 4-8.

Saunders, D. S. (2002). Insect clocks., 3rd edition, Amsterdam: Elsevier.

Schneider, C. P., Shukla, D., & Trout, B. L. (2011). Arginine and the Hofmeister series: the role of ion–ion interactions in protein aggregation suppression. The Journal of Physical Chemistry B 115(22), 7447-7458.

Seki, S., & Mazur, P. (2008). Effect of warming rate on the survival of vitrified mouse oocytes and on the recrystallization of intracellular ice. Biology of Reproduction 79, 727–737.

Sformo, T., Kohl, F., McIntyre, J., Kerr, P., Duman, J., & Barnes, B. (2009). Simultaneous freeze tolerance and avoidance in individual fungus gnats, *Exechia nugatoria*. Journal of Comparative Physiology B 179, 897-902.

Sformo, T., Walters, K., Jeannet, K., Wowk, B., Fahy, G. M., Barnes, B. M., & Duman, J. G. (2010). Deep supercooling, vitrification, and limited survival to–100 C in the Alaskan beetle *Cucujus clavipes puniceus* (Coleoptera: Cucujidae) larvae. Journal of Experimental Biology 213(3), 502-509.

Shang, Q., Pan, Y., Peng, T., Yang, S., Lu, X., Wang, Z., & Xi, J. (2015). Proteomics analysis of overexpressed plasma proteins in response to cold acclimation in *Ostrinia furnacalis*. Archives of Insect Biochemistry and Physiology 90, 195-208.

Shimada, K. (1990). Cold-induced freezing tolerance in diapausing and non-diapausing larvae of *Chymomyza costata* (Diptera: Drosophilidae) with accumulation of trehalose and proline. Cryo-Letters 11, 243-250.

Shimada, K., & Riihimaa, A. (1988). Cold acclimation, inoculative freezing and slow cooling: essential factors contributing to the freezing-tolerance in diapausing larvae of *Chymomyza costata* (Diptera: Drosophilidae). CryoLetters 9, 5-10.

Sies, H. (1999). Glutathione and its role in cellular functions. Free Radical Biology and Medicine 27, 916-921.

Simms, E. L., & Triplett, J. (1994). Costs and benefits of plant responses to disease: resistance and tolerance. Evolution 48, 1973–1985.

Sinclair, B. J., & Renault, D. (2010). Intracellular ice formation in insects: unresolved after 50 years? Comparative Biochemistry and Physiology Part A: Molecular & Integrative Physiology 155(1), 14-18.

Sinclair, B. J., Addo-Bediako, A., & Chown, S. L. (2003) Climatic variability and the evolution of insect freeze tolerance. Biological Reviews 78:181-195

Sinclair, B. J., Alvarado, C., Litza, E., & Ferguson, L. V. (2015). An invitation to measure insect cold tolerance: Methods, approaches, and workflow. Journal of thermal biology 53, 180-197.

Sinclair, B. J., Gibbs, A. G., & Roberts, S. P. (2007). Gene transcription during exposure to, and recovery from, cold and desiccation stress in *Drosophila melanogaster*. Insect molecular biology 16(4), 435-443.

Sinensky, M. (1974). Homeoviscous adaptation—a homeostatic process that regulates the viscosity of membrane lipids in *Escherichia coli*. Proceedings of the National Academy of Sciences 71, 522-525.

Šlachta, M., Vambera, J., Zahradníčková, H., & Košťál, V. (2002). Entering diapause is a prerequisite for successful cold-acclimation in adult *Graphosoma lineatum* (Heteroptera: Pentatomidae). Journal of Insect Physiology 48, 1031-1039.

Solensky, M. J. (2004). Overview of monarch migration. The monarch butterfly: biology and conservation 79-83.

Somero, G. (1986). Protons, osmolytes, and fitness of internal milieu for protein function. The American Journal of Physiology-Regulatory, Integrative and Comparative Physiology 251, R197-R213.

Sømme, L. (1995). Cold Hardiness in Terrestrial Arthropods. In Invertebrates in Hot and Cold Arid Environments, pp. 177-213: Springer.

Stehlík, J., Závodská, R., Shimada, K., Šauman, I., & Košťál, V. (2008). Photoperiodic induction of diapause requires regulated transcription of timeless in the larval brain of *Chymomyza costata*. Journal of Biological Rhythms 23(2), 129-139.

Steponkus, P. L. (1984). Role of the plasma membrane in freezing injury and cold acclimation. The Annual Review of Plant Biology 35, 543–584.

Štětina, T., Des Marteaux, L. E., & Košťál, V. (2020). Insect mitochondria as targets of freezing-induced injury. Proceedings of the Royal Society B 287(1931), 20201273.

Štětina, T., Hůla, P., Moos, M., Šimek, P., Šmilauer, P., & Košťál, V. (2018). Recovery from supercooling, freezing, and cryopreservation stress in larvae of the drosophilid fly, *Chymomyza costata*. Scientific Reports 8, 4414.

Štětina, T., Košťál, V., & Korbelová, J. (2015). The role of inducible Hsp70, and other heat shock proteins, in adaptive complex of cold tolerance of the fruit fly (*Drosophila melanogaster*). PloS one 10, e0128976.

Storey, J. M., & Storey, K. B. (1985). Freezing and cellular metabolism in the gall fly larva, *Eurosta solidaginis*. Journal of Comparative Physiology B 155, 333-337.

Storey, K. B., & Storey, J. M. (1988). Freeze tolerance in animals. Physiological Reviews 68, 27-84.

Storey, K. B., & Storey, J. M. (1991). Biochemistry of cryoprotectants. In Insects at low temperature, pp. 64-93: Springer.

Storey, K. B., & Storey, J. M. (2010). Oxygen: Stress and adaptation in cold-hardy insects. In D. Denlinger & R. Lee, Jr (Eds.), Low Temperature Biology of Insects (pp. 141-165). Cambridge: Cambridge University Press.

Storey, K. B., & Storey, J. M. (2012). Insect cold hardiness: metabolic, gene, and protein adaptation. Canadian Journal of Zoology 90, 456-475.

Storey, K. B., & Storey, J. M. (2013). Molecular biology of freezing tolerance. Comprehensive Physiology 3(3), 1283-1308.

Storey, K. B., Keefe, D., Kourtz, L., & Storey, J. M. (1991). Glucose-6-phosphate dehydrogenase in cold hardy insects: Kinetic properties, freezing stabilization,

and control of hexose monophosphate shunt activity. Insect Biochemistry 21, 157–164.

Strachan, L. A., Tarnowski-Garner, H. E., Schneider, K. E., & Sinclair, B. J. (2011). The evolution of cold tolerance in *Drosophila* larvae. Physiological and Biochemical Zoology 84, 43-53.

Sunday, J. M., Bates, A. E., & Dulvy, N. K. (2011). Thermal tolerance and the global redistribution of animals. Nature Climate Change 2(9), 686-690.

Sunday, J. M., Bates, A. E., & Dulvy, N. K. (2012). Global analysis of thermal tolerance and latitude in ectotherms. Proceedings of the Royal Society B: Biological Sciences 279(1732), 3121-3127.

Tamiya, T., Okahashi, N., Sakuma, R., Aoyama, T., Akahane, T., & Matsumoto, J. J. (1985). Freeze denaturation of enzymes and its prevention with additives. Cryobiology 22(5), 446-456.

Tatone, C., Di Emidio, G., Vento, M., Ciriminna, R., & Artini, P. G. (2010). Cryopreservation and oxidative stress in reproductive cells. Gynecological Endocrinology 26, 563–567.

Tauber, M. J., Tauber, C. A., & Masaki, S. (1986). Seasonal Adaptations of Insects. Oxford University Press.

Teets, N. M., & Denlinger, D. L. (2013). Physiological mechanisms of seasonal and rapid cold-hardening in insects. Physiological Entomology 38, 105-116.

Telfer, W. H., & Kunkel, J. G. (1991). The function and evolution of insect storage hexamers. Annual Review of Entomology 36, 205–228.

Thompson, S. N. (2003). Trehalose - the insect 'blood' sugar. Advances in insect physiology 31(Supplement C), 205-285.

Timasheff, S. N. (1992a). Water as ligand: preferential binding and exclusion of denaturants in protein unfolding. Biochemistry 31(41), 9857-9864.

Timasheff, S. N. (1992b). A physicochemical basis for the selection of osmolytes by nature. Water and Life (Springer), pp. 70–84.

Timasheff, S. N. (1993). The control of protein stability and association by weak interactions with water: how do solvents affect these processes? Annual Review of Biophysics and Biomolecular Structure 22, 67-97.

Timasheff, S. N. (1998). In disperse solution, "osmotic stress" is a restricted case of preferential interactions. Proceedings of the National Academy of Sciences 95(13), 7363-7367.

Toda, M. J. (1985). Habitat structure of a drosophilid community at Inuvik, NWT, Canada (Diptera: Drosophilidae). The Canadian Entomologist 117(1), 135-137.

Torson, A. S., Yocum, G. D., Rinehart, J. P., Kemp, W. P., & Bowsher, J. H. (2015). Transcriptional responses to fluctuating thermal regimes underpinning differences in survival in the solitary bee *Megachile rotundata*. Journal of Experimental Biology 218, 1060-1068.

Toxopeus, J., & Sinclair, B. J. (2018). Mechanisms underlying insect freeze tolerance. Biological Reviews 93(4), 1891-1914.

Toxopeus, J., Des Marteaux, L. E., & Sinclair, B. J. (2019a). How crickets become freeze tolerant: The transcriptomic underpinnings of acclimation in *Gryllus veletis*. Comparative Biochemistry and Physiology Part D: Genomics and Proteomics 29, 55-66.

Toxopeus, J., Koštál, V., Sinclair, B. J. (2019b). Evidence for non-colligative function of small cryoprotectants in a freeze-tolerant insect. Proceedings: Biological Sciences 27, 286.

Uemura, M., Gilmour, S. J., Thomashow, M. F., & Steponkus, P. L. (1996). Effects of COR6. 6 and COR15am polypeptides encoded by COR (cold-regulated) genes of *Arabidopsis thaliana* on the freeze-induced fusion and leakage of liposomes. Plant Physiology 111, 313-327.

Villeneuve, T. S., Ma, X., Sun, Y., Oulton, M. M., Oliver, A. E., & MacRae, T. H. (2006). Inhibition of apoptosis by p26: implications for small heat shock protein function during *Artemia* development. Cell Stress & Chaperones 11, 71.

Wang, W. (1999). Instability, stabilization, and formulation of liquid protein pharmaceuticals. International journal of pharmaceutics 185(2), 129-188.

Willmer, P. G. (1982). Microclimate and the environmental physiology of insects. In Advances in Insect Physiology, vol. Volume 16 eds. J. E. T. M.J. Berridge and V. B. Wigglesworth), pp. 1-57: Academic Press.

Xie, G., & Timasheff, S. N. (1997). The thermodynamic mechanism of protein stabilization by trehalose. Biophysical chemistry 64(1-3), 25-43.

Yancey, P. H. (2005). Organic osmolytes as compatible, metabolic, and counteracting cytoprotectants in high osmolarity and other stresses. Journal of experimental biology, 208(15), 2819-2830.

Yancey, P. H., & Siebenaller, J. F. (2015). Co-evolution of proteins and solutions: protein adaptation versus cytoprotective micromolecules and their roles in marine organisms. The Journal of experimental biology 218(12), 1880-1896.

Yancey, P. H., & Somero, G. N. (1980). Methylamine osmoregulatory solutes of elasmobranch fishes counteract urea inhibition of enzymes. Journal of Experimental Zoology 212, 205-213.

Yocum, G. D., Rinehart, J. P., Horvath, D. P., Kemp, W. P., Bosch, J., Alroobi, R., & Salem, S. (2015). Key molecular processes of the diapause to post-diapause quiescence transition in the alfalfa leafcutting bee *Megachile rotundata* identified by comparative transcriptome analysis. Physiological Entomology 40(2), 103-112.

Yocum, G.D., Žďárek, J., Joplin, K.H., Lee Jr., R.E., Smith, D.C., Manter, K.D., & Denlinger, D.L. (1994). Alteration of the eclosion rhythm and eclosion behaviour in the flesh fly, *Sarcophaga crassipalpis*, by low and high temperature stress. Journal of Insect Physiology 40, 13–21.

Yoshida, T., & Kimura, M. T. (1995). The photoperiodic clock in *Chymomyza costata*. Journal of Insect Physiology 41(3), 217-222.

Zachariassen, K. E. (1985). Physiology of cold tolerance in insects. Physiological Reviews 65, 799-832.

Zachariassen, K. E., & Kristiansen, E. (2000). Ice nucleation and antinucleation in nature. Cryobiology 41(4), 257-279.

Zetterstedt J. W. (1838). Insecta Lapponica. Dipterologis Scandinaviae. Sect. 3: Diptera. Leopold Voss, Lipsiae, 477–868.

Zhang, J., Marshall, K. E., Westwood, J. T., Clark, M. S., & Sinclair, B. J. (2011). Divergent transcriptomic responses to repeated and single cold exposures in *Drosophila melanogaster*. The Journal of experimental biology 214, 4021-4029.

Rasmussen, P. H., Jørgensen, B., & Nielsen, J. (1997). Aqueous solutions of proline and NaCl studied by differential scanning calorimetry at subzero temperatures. Thermochimica Acta 303, 23-30.

Liu, W., Huang, Z., He, X., Jiang, P., Huo, X., Lu, Z., & Liu, B. (2020). Impacts of trehalose and l-proline on the thermodynamic nonequilibrium phase change and thermal properties of normal saline. Cryobiology 96, 92-98.

Held, C., Reschke, T., Müller, R., Kunz, W., & Sadowski, G. (2014). Measuring and modeling aqueous electrolyte/amino-acid solutions with ePC-SAFT. The Journal of Chemical Thermodynamics 68, 1-12.

Qiu, J., Huang, H., He, H., Liu, H., Hu, S., Han, J., Yi, D., An, M., & Wang, P. (2019). Solubility behavior and data modeling of l-proline in different neat and binary solvent systems. Journal of Chemical & Engineering Data 64, 5920-5928.

McLain, S. E., Soper, A. K., Terry, A. E., & Watts, A. (2007). Structure and hydration of L-proline in aqueous solutions. The Journal of Physical Chemistry A B 111, 4568-4580.

Troitzsch, R. Z., Vass, H., Hossack, W. J., Martyna, G. J., & Crain, J. (2008). Molecular mechanisms of cryoprotection in aqueous proline: light scattering and molecular dynamics simulations. The Journal of Physical Chemistry A 112, 4290-4297.

de Molina, P. M., Alvarez, F., Frick, B., Wildes, A., Arbe, A., & Colmenero, J. (2017). Investigation of the dynamics of aqueous proline solutions using neutron scattering and molecular dynamics simulations. Physical Chemistry Chemical Physics 19, 27739-27754.

6. *Curriculum vitae*

Robert Grgac

Home : Ulica Đure Basaričeka 13, 35000, Slavonski Brod, Croatia

Email: rgrgac@gmail.com   **Phone:** (+385) 0919443830

Date of birth: 23/09/1992   **Nationality:** Croatian

WORK EXPERIENCE

[2019 – 2023]

Physiology research scientist

Biology Centre CAS - Institute of Entomology

City: České Budějovice
Country: Czechia
- research and experimentation
- teaching (university level) and mentorship
- publication and grant proposal writing

[2018 – 2019]

Biology lab technician

Biology Centre CAS - Institute of Entomology

City: České Budějovice
Country: Czechia
- sample preparation and analysis
- operating laboratory instruments, optimization of protocols and data collection
- quality control and laboratory safety

EDUCATION AND TRAINING

[2013 – 2016]

Bachelor's degree, Biology - General

Josip Juraj Strossmayer University of Osijek - Department of Biology   https://www.biologija.unios.hr/about-us/

City: Osijek
Country: Croatia

[02/2017 – 09/2017]

Erasmus+ internship

University of South Bohemia in České Budějovice   https://www.jcu.cz/en/

City: České Budějovice
Country: Czechia
Field(s) of study: Natural sciences, mathematics and statistics: *Biology*
Laboratory of insect diapause

[2016 – 2019]

Master's degree, Biology - General

Josip Juraj Strossmayer University of Osijek - Department of Biology   https://www.biologija.unios.hr/about-us/

City: Osijek
Country: Croatia

[03/2019 – Current]   **Ph.D. - Physiology and Immunology**

University of South Bohemia in České Budějovice   https://www.jcu.cz/en/

City: České Budějovice
Country: Czechia
Thesis: Functional analysis of cryoprotectant system in Chymomyza costata

[03/2022 – 02/2023]   **Erasmus+ internship**

Josip Juraj Strossmayer University of Osijek - Faculty of Medicine Osijek
https://www.mefos.unios.hr/index.php/en/

City: Osijek
Country: Croatia
Field(s) of study: Natural sciences, mathematics and statistics: *Biology*
Department of Medical Biology and Genetics

PUBLICATIONS

[2019]

Delayed mortality and sublethal effects of cold stress in Drosophila melanogaster

[2022]

Cryoprotective Metabolites Are Sourced from Both External Diet and Internal Macromolecular Reserves during Metabolic Reprogramming for Freeze Tolerance in Drosophilid Fly, Chymomyza costata

[2022]

A mixture of innate cryoprotectants is key for freeze tolerance and cryopreservation of a drosophilid fly larva

[2022]

Stabilization of insect cell membranes and soluble enzymes by accumulated cryoprotectants during freezing stress

- first author publication

[2022]

Analysis of Uterine Morphology in Ovariectomized Rats Treated With Alendronate and Hop Extract Using Open-Source Software

[2023]

Retro is the new modern: Contemporary application of gold impregnation staining on brain cryosections for digital image analysis

CONFERENCES AND SEMINARS

[15/03/2022 – 18/03/2022]   **Open Readings 2022**   Vilnius, Lithuania

Presented a poster on the topic of: "Delayed mortality and sublethal effects of cold stress in *Drosophila melanogaster*"

Link: https://openreadings.eu/archive/

Robert Grgac